Universidad de Navarra

“Alquil-lysophospholipids and cancer: development of lipid nanoparticles for oral administration and preclinical studies”

Beatriz Lasa Saracíbar

2013

Universidad de Navarra

Facultad de Farmacia

Departamento de Farmacia y Tecnología Farmacéutica

TESIS DOCTORAL

"Alquil-lysophospholipids and cancer: development of lipid nanoparticles for oral administration and preclinical studies"

Trabajo presentado por **Beatriz Lasa Saracíbar** para obtener el Grado de Doctor

Fdo. Beatriz Lasa Saracíbar

Pamplona, diciembre de 2013

Dña. María J. Blanco Prieto, profesora investigadora de la Universidad de Navarra, informa que:

El presente trabajo, **"Alquil-lysophospholipids and cancer: development of lipid nanoparticles for oral administration and preclinical studies"**, presentado por Dña. BEATRIZ LASA SARACÍBAR para optar al grado de DOCTOR EN FARMACIA, ha sido realizado bajo su dirección en el Departamento de Farmacia y Tecnología Farmacéutica dela Facultad de Farmacia de la Universidad de Navarra y, una vez revisado, no encuentra objeciones para que sea presentado a su lectura y defensa.

Y para que así conste firma el presente informe:

Fdo. Dra. María José Blanco Prieto

Pamplona, 2013

Esta tesis doctoral forma parte de las investigaciones realizadas en el marco de los proyectos:

- "Nanosystems for the oral administration of antitumor alkyl lysophospholipid agents: development of lipidic nanocarriers and preclinical Studies" Ministerio de Educación y Ciencia (SAF2010-15547, SAF2011-30518).
- "Alkyl lysophospholipids and cancer: Development of lipidic nanocarriers for oral administration and preclinical studies" Departamento de Salud del Gobierno de Navarra (ref: 63/09; Premio Ortiz de Landázuri al major proyecto).
- COST Action TD1004 "Theranostics Imaging and Therapy: An Action to Develop Novel Nanosized Systems for Imaging-guided Drug Delivery".
- Caja de Ahorros de Navarra (Programa Tu Eliges Tu Decides).
- Fundación Universidad de Navarra.

Asimismo, se ha llevado a cabo gracias a la ayuda para la formación del personal invetigador de la Asociación de Amigos de la Universidad de Navarra.

A mis padres, Josico y Maribel

AGRADECIMIENTOS

Mi más sincero agradecimiento a la Universidad de Navarra y al Departamento de Farmacia y Tecnología Farmacéutica por toda la formación recibida y por darme la posibilidad de realizar una Tesis Doctoral.

A María, mi directora de tesis, gracias por darme la oportunidad de realizar esta aventura, gracias por contagiarme la pasión por la investigación y gracias por guiarme a lo largo de estos cuatro años.

A mis compañeros del departamento, compañeros de tesis, profesores y empleados:

A las doctoras Tere y Zinni, me alegro de que la vida nos haya juntado. Gracias por vuestra amistad y por tantos buenos momentos.

Hugo, gracias por tu alegría, por tu paciencia y por estar siempre dispuesto a enseñar y ayudar. Gracias por hacer fáciles tantas cosas…

Ander, Fabio, Esther, Edurne, Elisa, Ángela, Cristina, Paula, Eduardo, David Izaskun, Yolanda y Simón, ha sido un placer conoceros y aprender de vosotros cada día. Siempre formaréis una parte muy importante de mis cuatro años de tesis.

Melissa, gracias por compartir conmigo la experiencia "Caco" y tantos ratos en la sala de cultivos.

Gracias a todos los alumnos que han pasado por nuestro grupo, Viktorija, Jessica, Francesca, Adriá y Javi y en especial a Silvia, Chiara y Maria Laura por traer aire fresco italiano a nuestro grupo.

Marije, gracias por ser tan encantadora y gracias por tu cariño.

Felix y Noelia, gracias por vuestra paciencia y vuestras ganas de colaborar, espero que no echéis de menos autoclavar mis jarritas de chupitos…

Juan Luis, gracias por intentar ayudarnos en todo lo que está en tus manos y por todas las charlas compartidas.

Al cima, compañeros, investigadores y personal:

A María Dolores Odero, por abrirme las puertas al apasionante mundo de la citometría y ayudarme en los comienzos de mi doctorado.

A Felipe Prosper, Amaia, Edurne, Xabi, por darme la oportunidad de colaborar y aprender de su trabajo.

Al Dr. Marco Metzger y su grupo de investigación del Fraunhofer Institute gracias por acogerme en vuestro equipo de Wüzburg.

A la Dra. Penélope Bouziotis y todo su grupo de investigación, gracias por invitarme a entrar en el Demokritos, iniciarme en el mundo de la radiofarmacia y darme la oportunidad de disfrutar de Atenas. Y gracias por vuestra hospitalidad.

Gracias a mis amigas,

Adri, Bego, Mayra, Zinni, Tere, Lau, Aranda, Elarre, Ana, gracias por tantos buenos momentos compartidos y gracias por vuestro apoyo y cariño.

Miriam, Paula e Isabel, gracias porque, aunque en estos cinco años habéis incluido cambios muy importantes en vuestra vida, siempre hacéis un esfuerzo por estar ahí. Y gracias por traer pequeñines a nuestras quedadas!

Salena, gracias por escucharme y abrirme siempre las puertas de tu casa. Gracias a ti y a toda tu familia por vuestro cariño y hospitalidad.

A Ignacio,

Gracias por acompañarme en este viaje de la vida. Gracias por tu comprensión, cariño y dedicación. Y gracias por traer sobrinos a mi vida!

A mi familia,

A mi tía Dolores y mi abuela Feli, gracias por ser un ejemplo de vida para todos.

A mis tíos y primos, gracias por tantos buenos ratos familiares.

A mis padres y mis hermanos, gracias por compartir mis momentos de estrés y gracias por vuestro cariño.

TABLE OF CONTENTS

ABBREVIATIONS / ABREVIATURAS

5-FCPal	Capecitabine analog Análogo de Capecitabine
5-FU	5-Fluorouracil 5-Fluorouracilo
% ID	Percentage of initial dose Porcentaje de dosis inicial
^{99m}TC	Technetium-99m Tecnecio-99m
ALB	Albumin Albumina
AFM	Atomic force microscopy Microscopía de fuerza atómica
ALL	Acute lymphoid leukemia Leucemia linfoide aguda
ALPs	Alkyl-lysophospholipids Alquil-lisofosfolípidos
ALT	Aspartate aminotransferase Aspartato aminotransferasa
AML	Acute myeloid leukemia Leucemia mieloide aguda
AMOs	Anti-microRNA oligonucleotides Oligonucleótidos anti-microRNA
AP	Alkalyne phosphatase Fosfatasa alcalina
ASGP	Asialoglycoprotein Asialoglicoproteína
AST	Aspartate aminotransferase Aspartato aminotransferasa

ATP	Adenosine triphosphate Adenosin trifosfato
Blank-LN	Blank lipid nanoparticles Nanopartículas blancas lipídicas
BBB	Blood brain barrier Barrera hematoencefálica
BSA	Bovine serum albumin Albúmina de suero bovino
BUN	Blood urea nitrogen Nitrógeno ureico en sangre
CBSA	Cationic bovine serum albumin Albúmina catiónica de suero bovino
CDRs	Circular dorsal ruffles Volantes dorsales circulares
CFSE	Carboxyfluorescein succinimidyl ester Ester succinimidil de carboxifluoresceína
CIE	Clathrin independent endocytosis Endocitosis independeiente de clatrina
CLL	Chronic lymphocytic leukemia Leucemia linfocítica crónica
CME	Clathrin mediated endocytosis Endocitosis mediada por clatrina
CML	Chronic myeloid leukemia Leucemia mieloide crónica
CML-BC	Chronic myeloid leukemia in blast crisis Lecemia mieloide crónica en crisis blástica
CNS	Central nervous system Sistema nervioso central
CREA	Creatinine Creatinina

CvME	Caveole-mediated endocytosis Endocitosis mediada por caveolina
DOX	Doxorubicin Doxorubicina
DSC	Differential scanning calorimetry Calorimetría diferencial de barrido
DSL	Dynamic light scattering Dispersión de luz dinámica
EGRF	Epidermal growth factor receptor Receptor epidérmico de factor de crecimiento
EPR	Enhanced permeability and retention effect Efecto de permeabilidad y retención aumentadas
ET	Edelfosine Edelfosina
ET-LN	Edelfosine lipid nanoparticles Nanopartículas lipídicas de edelfosina
FAE	Follicle associated epithelium Epitelio asociado al folículo
FBS	Fetal bovine serum Suero fetal bovino
FcR	Fc receptors Receptores Fc
GEMO	Glyceryl-ether monooxygenase Monooxigenasa de ester glicerol
GRAS	Generally recognized as safe Generalmente reconocidos como seguros
HA	Hyaluronan Ácido hialurónico
HCT	Hematocrite Hematocrito

HGB	Hemoglobine Hemoglobina
HMW-HA	High molecular weight hyaluronan Ácido hialurónico de alto peso molecular
HPH	High pressure homogenization Homogenización a alta presión
i.p.	Intraperitoneal Intraperitoneal
i.v.	Intravenous Intravenoso
Ig	Inmunoglobulin Inmunoglobulina
LAL-T	Lymphoid acute leukemia-T Leucemia limfoide aguda-T
LDC	Lipid drug conjugates Conjugados lípido-fármaco
LD50	Lethal dose Dosis letal
LN	Lipid nanoparticles Nanopartículas lipídicas
LMW-HA	Low molecular weight hyaluronan Ácido hialurónico de bajo peso molecular
LysoPC	Lysophosphocholine Lisofosfocolina
M cells	Microfold cells Células de epitelio asociado a folículo
MDR	Multi drug resistance Resistencia multiple a fármacos
MEM	Minimum essential medium Eagle Medio esencial mínimo de Eagle

miR-21	MicroRNA-21
	MicroRNA-21
MTD	Maximum tolerated dose
	Dosis maxima tolerada
MTO	Mitoxantrone
	Mitoxantrona
MWCO	Molecular wight cut-off
	Límite de peso molecular
NLC	Nanostructured lipid carriers
	Vehículos lipídicos de estructura nanométrica
NSCLC	Non-small cell lung cancer
	Cáncer de pulmón de células no pequeñas
O/W	Oil-in-water
	Aceite en agua
PAF	Platelet activating factor
	Factor activador de plaquetas
P_{app}	Aparent permeability percentage
	Porcentage de permeabilidad aparente
PBS	Phosphate buffered saline
	Bufer salino fosfatado
PCS	Photon correlation spectroscopy
	Espectroscopía de correlación de fotones
PDI	Polydispersity index
	Índice de polidispersión
PEG	Polyethylene glycol
	Glicol polietilénico
P-gp	P-glycoprotein
	P-glicoproteína
PI	Propidium iodide
	Ioduro de propidio

PIT	Phase inversion temperature Temperatura de inversion de fases
PIZ	Phase inversion zone Zona de inversion de fases
PLA2	Phospholipase A2 Fosfolipasa A2
PLC	Phosphatidylcholine C Fosfatidilcolina C
PLD	Phosphatidylcholine D Fosfatidilcolina C
PLT	Platelets Plaquetas
PNPP	p-nitrophenyl-phosphate p-nitrofenilfosfato
RBC	Red blood cells Células rojas sanguíneas
RES	Reticuloendothelial system Sistema retículo-endotelial
ROS	Reactive oxygen species Especias reactivas de oxígeno
SEM	Scanning electron microscopy Microscopía electronica de barrido
SPECT	Single photon emission computerized tomography Tomografía computarizada de emisión monofotónica
SLN	Solid lipid nanoparticles Nanopartículas sólidas lipídicas
Starv	Starvation Inanición
STS	Staurosporine Estaurosporina

TBST	Tween tris-buffered saline Bufer salino Tris con Tween
TBSTM	Tween tris-buffered saline 5 % nonfat dry milk TBST suplementado con 5 % leche desnatada
TC	Tamoxifen citrate Citrato de tamoxifeno
TEER	Transepithelial electrical resistance Resistencia eléctrica transepitelial
TEM	Transmission electron microscopy Microscopía electronica de transmisión
Tf	Transferrin Transferrina
UHPLC-MS/MS	Ultra high performance liquid chromatography/mass spectrometry Cromatografía líquida de alta resolución acoplada a espetometría de masas
VB	Vinorelbine bitartrate Bitartrato de vinorelbina
WBC	White blood cells Células balncas sanguíneas
WHO	World health organization Organización mundial de la salud
W/O	Water-in-oil Agua en aceite
W/O/W	Water-in-oil-in-water Agua en aceite en agua
XRD	X-ray diffractometry Difractometría de rayos X

HYPOTHESIS AND OBJECTIVES

Edelfosine (1-O-Octadecyl-2-O-methyl-rac-glycero-3-phosphocholine, ET-18-OCH3) is a synthetic analogue of platelet activating factor that was synthesized in the late 1960's. It is a drug with proven *in vitro* and *in vivo* efficacy against cancer. Numerous *in vitro* studies demonstrate the selectivity of this drug for tumour cells. Besides edelfosine avoids classic antitumor drugs side-effects because its mechanism of action is not linked to a direct targeting of the DNA. However, despite the promising anticancer activity profile of edelfosine, its clinical use is very limited being reduced to purging purposes in leukemia patients. The main reason for this clinical limited use is that edelfosine does not own favourable bioavailability profile and, moreover, it presents severe side effects.

Edelfosine has been previously vehiculized through nanotechnology using lipid nanoparticles in our research group. Lipid nanoparticles of edelfosine, constituted by biodegradable and biocompatible lipids, are produce by an organic solvent free method. These nanoparticles demonstrated several advantages over the free drug such as avoidance of haemolytic toxicity of the free drug. Moreover, they improved oral bioavailability of the drug which seems to be mediated by their absorption through Peyer´s patches in the intestine. Additionally, the oral administration of these systems promoted a 100 % inhibition of extranodal dissemination of a murine mantle cell lymphoma. Finally, edelfosine has shown to be effective in leukemia cell lines.

According to this background, <u>the general hypothesis of this thesis is</u>:

Lipid nanoparticles containing edelfosine might be an alternative therapy in leukemia treatment since these nanosystems could provide better efficacy and higher security profiles. It is expected that the nanoencapsulation of edelfosine could overcome the resistance that some leukemic cells lines show to the free drug.

Based on this premise, the general aim of this project is to study the benefits of the encapsulated edelfosine compared to the free drug in leukemia treatment in terms of efficacy and toxicity as well as to understand the mechanism by which

edelfosine lipid nanoparticles enter the cells and the molecular mechanism implicated in cell death.

The partial objectives are:

1. To evaluate the efficacy of free and nanoencapsulated edelfosine after administration to sensitive and resistant leukemia cell lines.
2. To study the uptake mechanisms of edelfosine and edelfosine lipid nanoparticles in leukemia cells as well as the molecular mechanisms implicated in cell death upon internalization of both the free and nanoencapsulated drug.
3. To assess the permeability of lipid nanoparticles across the intestinal barrier. Caco-2 monoculture and Caco-2/Raji co-culture were used as *in vitro* models of enterocytes and Microfold cells respectively.
4. To investigate the *in vivo* toxicity of free edelfosine, lipid nanoparticles and lipid nanoparticles loaded with edelfosine in mice after oral administration.
5. To study biodistribution of edelfosine lipid nanoparticles and to evaluate their therapeutic efficacy in a xenogeneic mouse model of human acute lymphoblastic leukemia.

CHAPTER 1

INTRODUCTION: Lipid nanoparticles for cancer therapy: state of the art and future prospects

*Beatriz Lasa-Saracibar, Ander Estella-Hermoso de Mendoza, Melissa Guada-Ramírez, Carmen Dios-Vieitez, Maria J. Blanco-Prieto**

Dept. of Pharmaceutics and Pharmaceutical Technology, School of Pharmacy, University of Navarra, Spain

Running title: Lipid nanoparticles and cancer: review

Keywords: Biodegradation, cancer, characterization, colloidal drug carriers, lipid nanoparticles, preparation, release, safety, scaling-up, toxicity

***Corresponding author:** Dra. Maria J. Blanco Prieto, Dept. of Pharmaceutics and Pharmaceutical Technology, School of Pharmacy, University of Navarra, Spain. C/Irunlarrea 1, E-31080, Pamplona, Spain, Office phone: + 34 948 425 600 ext. 6519, Fax: + 34 948 425 649, e-mail: mjblanco@unav.es

Declaration of interest: The authors state no conflict of interest.

Expert Opin Drug Deliv. 2012 Oct;9(10):1245-61

Abstract

Introduction: Cancer is a leading cause of death worldwide and it is estimated that deaths from this disease will rise to over 11 million in 2030. Most cases of cancer can be cured with surgery, radiotherapy or chemotherapy if they are detected at an early stage. However, current cancer therapies are commonly associated with undesirable side effects, as most chemotherapy treatments are cytotoxic and present poor tumor targeting.

Areas covered: Lipid nanoparticles (LN) are one of the most promising options in this field. LN are made up of biodegradable generally recognized as safe (GRAS) lipids, their formulation includes different techniques, and most are easily scalable to industrial manufacture. LN overcome the limitations imposed by the need for intravenous administration, as they are mainly absorbed via the lymphatic system when they are administered orally, which improves drug bioavailability. Furthermore, depending on their composition, LN present the ability to cross the blood brain barrier, thus opening up the possibility of targeting brain tumors.

Expert opinion: The drawbacks of chemotherapeutic agents make it necessary to invest in research to find safer and more effective therapies. Nanotechnology has opened the door to new therapeutic options through the design of formulations that include a wide range of materials and formulations at the nanometer range, which improve drug efficacy through direct or indirect tumor targeting, increased bioavailability and diminished toxicity.

1. Introduction

According to the World Health Organization [1], cancer is one of the leading causes of death worldwide, and cancer deaths are projected to continue rising to over 13.1 million in 2030. The main types of cancer are: lung, stomach, liver, colorectal, breast and cervical cancer; nevertheless, it can affect any part of the body and people of any age. Early detection of this disease through screening prevents the cancer from spreading to other parts of the body (metastasization) and thus improves survival rates. Cancer treatment frequently comprises a combination of surgery, radiotherapy and chemotherapy. Cure rates of surgically removable primary tumors that have not spread to other parts of the body are high (e.g. breast, colorectal). However, even when complete resection of the tumor is possible, chemotherapy is generally required.

Chemotherapy has been used for more than 70 years, since mustard gas was used for the first time in the treatment of lymphomas [2], but it still presents severe side effects and limited efficacy. Most chemotherapeutic drugs act through interaction with DNA that causes irreparable damage or by impeding cell division, which finally leads to cell apoptosis. Chemotherapeutic drugs are generally classified as: alkylating agents (platinums, nitrogen mustard derivates, oxazophosphorines), anti-metabolites (pyrimidine analogues, anti-folates), mitotic inhibitors (vinka alkaloids, taxanes), topoisomerase inhibitors (topoisomerase-I inhibitors, topoisomerase-II inhibitors) and antitumor antibiotics (anthracyclines, bleomycin, mitoxantrone). Even if these drugs present efficacy against the disease, multi drug resistance (MDR) to chemotherapeutic agents complicates cancer treatment. This mechanism is mainly related to P-glycoprotein (P-gp), which extrudes the drug from the cell, decreasing the intracellular drug concentration and thus inhibiting its antitumor action. The group of alkyl lysophospholipids, which are non-DNA affecting molecules, comprises another class of antitumor agents. Edelfosine, the prototype of these new drugs discovered in the late 1980s, presents several advantages over conventional antitumor drugs. It is a drug that can be administered orally, it acts selectively in tumor cells sparing healthy tissues and its mechanism of action is not based on DNA targeting but membrane triggered apoptosis [3]. Chemotherapy is

mainly administered intravenously, a route which is generally associated with poor patient well-being and compliance, and high clinical cost [4]. Moreover, it is also associated with a wide variety of severe side effects (mainly due to the poor targeting of cancer cells) such as myelosupression, gastrointestinal toxicity, alopecia, neuropathy, infertility or cardiac ischemia, among others. Bearing in mind all the drawbacks of chemotherapy, researchers are still investigating into new drugs and new delivery systems to obtain safer and more effective therapies that allow oral administration.

Among drug delivery systems, lipid nanoparticles (LN) are promising drug carriers due to their effectiveness in targeting tumor tissue. They provide higher drug efficacy, as a result of an increased concentration of drug in tumor cells, and lower side effects [5]. LN can be divided into solid lipid nanoparticles (SLN), nanostructured lipid carriers (NLC) and lipid drug conjugates (LDC). In general, they can be defined as nanometer sized solid particles made up of biodegradable generally recognized as safe (GRAS) lipids. Besides the above-mentioned advantages, LN can be administered orally, avoiding all the disadvantages of the intravenous route. Like other nanosystems, LN are passively targeted to the tumor tissue due to the well-known enhanced permeability and retention effect (EPR effect) [6, 7]. Moreover, when given orally, they are absorbed via the lymphatic system avoiding first pass hepatic metabolism and targeting lymph nodes [8, 9]. Depending on their composition, they also have the ability to cross the blood brain barrier (BBB), thus opening up the possibility of targeting brain tumors [10]. Furthermore, active targeting offers the possibility of directing the drug toward different tissues. This review focuses on the most recent advances in the use of LN in the treatment of cancer. Specifically, studies published in the last 5 years will be reviewed and discussed..

2. Lipid Based Nanosystems

The LN concept begins with lipid nanosuspensions. O/W emulsions were first used in clinic in the 1950s to administer parenteral nutrition. Afterwards, Etomidat-Lipuro® and Diazepam-Lipuro® were successfully marketed [11]. At this time, the only purpose of these emulsions was to reduce the side effect of pain after diazepam

injection. Despite the success of the O/W emulsions, the number of products on the market is low due to their physical instability and low drug solubility.

Lipid based nanosystems were first launched on the market in 1986 by the Dior brand [12]. The Dior commercial formula was followed by the first pharmaceutical liposome formulations. Epi-Pevaryl® (antimycotic topical therapy) was introduced in the market in the 1980s, and Alveofact® (pulmonary instillation) and Ambisome® (intravenous injection) in the following decade. One of the major disadvantages of liposomes is their rapid plasma clearance. Consequently, pegylated liposomes (stealth liposomes) were developed by Allen *et al*. in 1994 [13] as a solution to the short half-life of liposomes in plasma as a result of the reticuloendothelial system (RES) clearance. However, the number of commercialized liposomal formulations is low due to disadvantages such as physical instability, insufficient drug solubility and the need for expensive technology. Besides, regardless of the potentiality of these formulations in reducing drug-side effects, their poor controlled release posed a challenging drawback.

In this sense, LN, invented in the 1980s, represent significant progress in the development of lipid based nanosystems.

2.1 Types of lipid Based Nanosystems

2.1.1 Solid Lipid Nanoparticles

SLN were discovered by Speiser [14] and Eldem *et al.* [15] in the 1980s when they formulated SLN by spray drying and nanopellets for peroral administration for the first time. SLN are colloidal carriers composed of lipids that are solid at body temperature. The use of solid lipids prevents the drug from immediate release. The drug is included in a solid matrix that makes the diffusion of the drug to the surface difficult. In addition, the lipids used to form SLN provide low acute and chronic toxicity [5]. In the 1990s, SLN were further developed by Müller *et al*. using high-pressure homogenization (HPH) methods [16, 17] and by Gasco *et al*., who used a warm microemulsion technique [18, 19]. The most important advantages of SLN over liposomes are controlled drug release and the physical stability of the preparations. Nevertheless, they still present some limitations such as limited drug loading and

drug expulsion during storage. Anticancer drugs have been encapsulated into SLN by many different authors [5]. Most of these studies have developed SLN to be administered intravenously, with successful results; nevertheless, SLN can also be a very promising oral drug delivery system. Several studies have demonstrated that these nanocarriers are absorbed via the lymphatic system, improving drug bioavailability [8, 9, 20]. Consequently, the oral administration of antitumor agents might have a large impact on clinical practice both in patient well-being and in treatment costs [4].

2.1.2 Nanostructured Lipid Carriers

NLC are the second generation of LN. They were developed by Müller *et al*. to solve the low drug loading capacity of SLN [21]. The difference between the two formulations is their lipid composition: in NLC the solid lipid is mixed with a liquid lipid in order to obtain a solid structure and to avoid crystallization after particle solidification The applications of NLC are the same as Müller *et al*. described for SLN [17]. Several recent studies endorse the efficacy of NLC in cancer treatment [22-26].

2.1.3 Lipid Drug Conjugates

Although SLN and NLC are able to incorporate hydrophilic drugs, their lipophilic nature makes them more suitable to incorporate lipophilic compounds. LDC were developed in the late 1990s in order to achieve better drug loading rates for hydrophilic drugs [27]. Their manufacture consists of binding the drug to the lipid prior to forming the O/W emulsion. The drug is first conjugated with the lipid by salt formation or by covalent linkage, and afterwards, LDC are formed by homogenizing the drug-lipid complex with a surfactant aqueous solution by HPH.

2.2 Preparation Methods

To date, different methods have been developed to produce LN. Most of them are based on traditional emulsion techniques. The two principal methods used are the HPH, patented by Müller and Lucks in 1993 [17], and microemulsion techniques

patented by Gasco in 1993 [19]. However, several variations of these methods have been proposed in order to optimize the characteristics of LN formulations.

Table I. Examples of drugs incorporated in LN and preparation methods

Preparation method	Drugs loaded	References
Hot high pressure homogenization	Palmityl prodrug analogue of capecitabine, all-trans retinoic acid, chlorambucil, docetaxel, coenzyme Q10	[93, 126-129]
Cold high pressure homogenization	Vinorelbine bitartrate	[84]
Microemulsion technique	Trans-resveratrol, gold (III) porphyrin and camptothecin	[130, 131]
Microemulsion precursor technique	Idarubicin and doxorubicin, paclitaxel, gadolinium	[108, 132, 133]
Coacervation method	Cisplatin, curcumin, methotrexate	[134-136]
Phase inversion temperature method	Etoposide, tripentone 3-(3-hydroxy-4-methoxyphenyl)-8H-thieno[2,3-*b*]pyrrolizin-8-one, paclitaxel	[137-139]
Emulsion formation solvent-evaporation or -diffusion method	Methotrexate, edelfosine, doxorubicin, paclitaxel and siRNA	[8, 36, 53, 140]
Water-in-Oil-in-Water (w/o/w) double emulsion method	Edelfosine, 5-fluorouracil	[36, 87]
Emulsification dispersion followed by ultrasonication	Mitoxantrone, cisplatin	[90, 141]
Hot homogenization by high shear homogenization and/or ultrasonication	Edelfosine, simvastatin and tocotrienol, all-trans retinoic acid, paclitaxel, ɣ-tocotrienol	[10, 142-145]
Solvent injection method	Paclitaxel, 5-fluorouracil	[146, 147]

Table I brings together all these methods and variations along with the drugs used in cancer therapy that have been successfully loaded in these systems. Research efforts have been focused on the improvement of particle stability, surfactants at considerable concentration, particle size control according to the administration routes, functionalization of the particle surface for targeting a specific cell, drug controlled release, minimal mechanical and thermal energy input, risk of organic solvent residues, cost-effective process and industrial scalability, among others. The main advantages and drawbacks of all the production techniques are summarized in Table II.

Table II. Advantages and disadvantages of LN preparation methods

Preparation method	Advantages	Disadvantages
High pressure homogenization (hot and cold)	▪ Good reproducibility ▪ Well established homogenization technology on large scale ▪ Organic solvent free method	▪ High temperature process ▪ High energy input ▪ Complex equipment required ▪ Possible degradation of the components caused by high pressure homogenization
Microemulsion technique	▪ Reduces mean particle size and narrow size distribution ▪ Organic solvent free method ▪ No energy consuming method ▪ Easy to scale up	▪ High concentration of surfactants and co-surfactants ▪ Concentration of final formulation is required
Microemulsion precursor technique	▪ Rapid, reproducible and cost-effective method ▪ Dilution of the final formulation is not needed ▪ Organic solvent free method ▪ Non energy-consuming method	▪ High concentration of surfactants and co-surfactants
Coacervation method	▪ Allows incorporation of thermosensitive drugs ▪ Inexpensive for laboratory and industrial application ▪ Possibility to control shape and size of SLNs by reaction conditions	▪ Possible degradation of the components under acidic conditions

Preparation method	Advantages	Disadvantages
Phase inversion temperature method	▪ Organic solvent free method ▪ Non-energy consuming method ▪ Easy to scale up	▪ Not suitable for thermosensitive molecules like peptides or proteins
Emulsion formation solvent-evaporation or -diffusion method	▪ Allows incorporation of thermosensitive drugs ▪ Reduces mean particle size and narrow size distribution ▪ Good reproducibility	▪ Concentration of final formulation is required ▪ Possible organic solvent residues in the final formulation
Water-in-Oil-in-Water (w/o/w) double emulsion method	▪ Allows incorporation of hydrophilic drugs	▪ Concentration of final formulation is required ▪ Large particle size of the final formulation
Emulsification dispersion followed by ultrasonication	▪ Allows incorporation of thermosensitive drugs	▪ Possible metal contamination
Hot homogenization by high shear homogenization and/or ultrasonication	▪ Easy to handle ▪ No complex equipment is required ▪ High concentration of surfactants and co-surfactants are not required ▪ Organic solvent free method	▪ High energy input ▪ Polydisperse distributions ▪ Possible metal contamination ▪ Concentration of final formulation is required
Solvent injection method	▪ Easy to handle and fast production process	▪ Possible organic solvent residues in the final formulation

3. Scaling-up of LN

After the development and optimization of a formulation on a small scale, the next step is usually to find the way to produce it on a larger scale. However, in most cases, the scaling up of a process implies an increase in problems [28]. In the case of LN production based on HPH, which is the most widely used method in the

pharmaceutical industry, it has been observed that the use of larger scale machines leads to an even better quality of the product with regard to a smaller mean particle size and polydispersity index (PDI) [29].

The most typical devices for lab-scale production are the Avestin C5 (capacity: 5 L/h, batch: 7 mL to 1 L, Avestin Europe) and the Micron LAB 40 (batch: 20–40 mL, APV Deutschland GmbH). In the case of very high-cost drugs, or if there is a limited amount available (e.g., new chemical entities), it is positive to reduce the batch size. Avestin B3 (Avestin Europe) can be employed in order to reduce the batch size, achieving a final volume of 0.5–3.2 mL [30].

The next scaling up step implies a minimum batch size of 2 kg and a maximum of 10 kg. This aim can be achieved using the Micron LAB 60 (APV Deutschland GmbH), which has a homogenization capacity of 60 L/h. The next step in scale-up is the use of a Gaulin 5.5 (APV Deutschland GmbH) with a homogenization capacity of 150 L/h (nearly 150 kg) [31]. In this case, the pre-emulsion is formed in larger containers. The product containers and homogenizer are manufactured from pharmaceutical grade materials. Another feature is that the product containers can be sterilized by autoclaving; formation of the pre-emulsion under protective gas is also feasible. It is noteworthy that a batch size of about 500 kg can be produced in approximately 3-h homogenization time using this machine.

For even larger scales, a Rannie 118 (APV Deutschland GmbH) or an Avestin EmulsiFlex C1000 (Avestin Europe) can be used [30, 31]. Their capacity is much higher than that of the previous machines, ranging from 1,000 to 2,000 L/h at the low pressure required for the production of LN.

4. Physical-chemical characterization of LN

Physical-chemical characterization of the LN is essential due to the fact that these systems present colloidal sized particles [32]. Nevertheless, proper characterization of the formulations is necessary to control the product quality, stability, and release kinetics. The most important parameters of LN to be characterized include particle size and shape, the surface charge, the degree of crystallization and the kind of lipid modification. All these properties must be well characterized because any contact of

the LN dispersion with new surfaces might be able to induce changes in their structure, causing, for example, an alteration in the lipid crystallization or modification leading to the formation of a gel, or to the drug expulsion. Among all the parameters that should be considered for characterization of LN, size is crucial and critical for determining the interactions of nanoparticles with living systems. For instance, particle sizes below 300 nm are suitable for intestinal transport to the thoracic duct [33], while sizes no larger than 5 μm are required in order not to cause embolisms after parenteral administration of LN due to the blocking of the thin capillaries [34]. Besides, particle size also plays a very important role in the clearance of the LN by the RES. A great number of methods are available for determining the size of nanoparticles [35]; however, the most commonly employed techniques are the following. Dynamic light scattering (DLS) is generally used to determine the size distribution profile of LN. Alternatively, electron microscopy and/or atomic force microscopy (AFM) are often used to corroborate the results.

The zeta potential is the overall charge a particle gains in a specific medium, and its value indicates the degree of repulsion between close and similarly charged particles in dispersion. Most authors calculate this value by laser-doppler anemometry [36-40]. Colloids with high zeta potential (negative or positive) are electrically stabilized, while colloids with low zeta potentials tend to coagulate or flocculate. In general, absolute values greater than 30 mV have been found to be enough for good stabilization, and hence indicate good physical stability [41]. In terms of stability, any contact of the LN dispersion with new surfaces might be able to induce changes in their structure, causing, for example, an alteration in the lipid crystallization or modification leading to the formation of a gel or to the drug expulsion [42]. Therefore, the crystallinity and polymorphic behavior of the components of the LN should be studied, as these both influence drug incorporation and release rates to a high degree. Differential scanning calorimetry (DSC) and X-ray diffractometry (XRD) are two of the main tools employed. Bunjes *et al.* [43-46] reported on crystalline properties of lipids and their recrystallization patterns during nanoparticle preparation and the influence of nanoparticle size on recrystallization pattern in a very extensive way.

It is imperative to obtain a dry product to ensure their stability, thus allowing their long-term storage. Lyophilization is one of the most widely used techniques for obtaining dry powders from nanoparticulate suspensions [47-51] and provides an increase in chemical and physical stability over extended periods of time [34]. In general, cryoprotectant agents are used so as not to achieve a final LN aggregated product, which will commonly acquire a rubbery appearance. Saccharides are the most widely employed cryoprotectant agents in the formulation of LN, namely trehalose, sucrose, sorbitol, maltose, glucose and mannose [52-54].

5. Drug release from LN

The solubility of the drug in the aqueous release medium and the lipid component of the formulation, and the partitioning between them, are considered very important factors in predicting the *in vitro* drug release behavior. It is known that increasing the production temperature and surfactant concentration leads to increased drug solubility in the water phase [55]. Cooling the LN suspension again will decrease the water solubility and the repartition to the lipid, forming drug core-enriched or drug shell-enriched LN, depending on the lipid recrystallization temperature [56]. These two drug distribution models lead to too slow and too fast release rates of the drugs, respectively.

In order to study the drug release kinetic profile of drugs from LN, various assays can be performed. The most widely employed assays are based on the use of dialysis membranes, Franz-type diffusion cells and rotating vials.

5.1 Dialysis membranes

Among all assays, dialysis tubes are those that are most widely used to study the drug release kinetics from LN formulations [53, 57-59]. Briefly, a definite amount of prepared LN, free from any unentrapped drug, is separately placed in the dialysis tube of different molecular weight cut-off (MWCO) (usually between 12-14 kDa), tied at both ends and suspended in different beakers (receptor compartment) each containing the appropriate medium to study the release (namely, PBS, gastric or intestinal media). The medium is stirred continuously to favor the crossing of the

membrane, and the whole system is usually assembled at physiologic temperature throughout the experiment (Figure 1). Samples are withdrawn periodically and after each withdrawal of sample the same volume of appropriate medium is added in the receptor compartment so as to maintain a constant volume throughout the study.

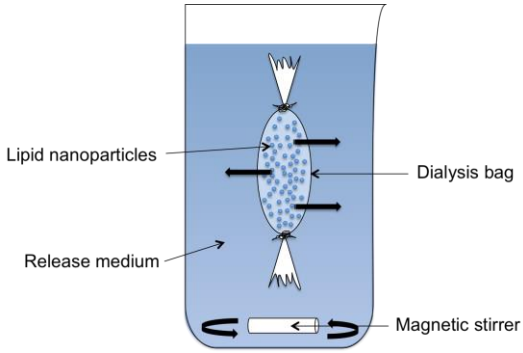

Figure 1. Representative scheme of the determination of drug release by dialysis membrane bag.

5.2 Franz-type diffusion cell

This assay is relatively similar to the method based on dialysis membranes, with the difference of the use of a specific system [52, 60]. A Franz diffusion cell system is composed of a receptor and a donor cell (Figure 2).

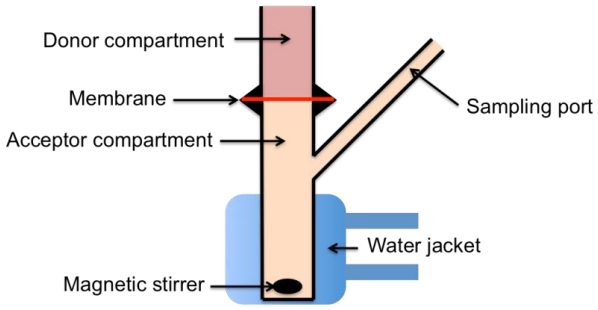

Figure 2. Schematic representation of a Franz diffusion cell system.

This cell has a static receptor solution reservoir with a side-arm sampling port. The membrane (usually of a MWCO of 12 kDa) is mounted between the cell

compartments. The receptor compartment is filled with the appropriate medium to study the release (namely, PBS, gastric or intestinal media). It is kept at physiological temperature by circulating water through an external water jacket. After a certain time of equilibration of the membrane with the receptor solution, a definite amount of the LN formulation is applied in the donor compartment. The donor compartment can then be covered to prevent evaporation of the solvent. The receptor solution is continuously stirred by means of a spinning bar magnet. Receptor solution samples are withdrawn through the sampling port of the receptor compartment at various time intervals and the cells are refilled with receptor solution to keep the volume of receptor solution constant during the experiment.

5.3 Rotating vials

In this method, an amount of LN is placed in small vials contaning the appropriate medium to study the release (PBS, gastric or intestinal media). The vials undergo continuous rotational mixing using a rotating device kept at physiologic temperature throughout the experiment (Figure 3). At the time of sample withdrawal, vials are centrifuged and the supernatant is recovered for analysis [36].

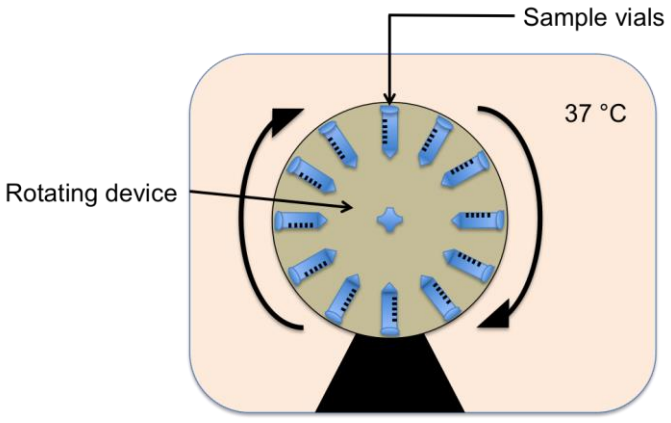

Figure 3. Diagram of a rotating device that can be used to determine drug release from LN formulations by rotating vials.

6. Application in cancer therapy

6.1 Surface modified lipid based nanosystems

Antitumor drugs imply many remarkable side effects as a result of their impaired toxicity. The poor selectivity of these compounds makes them accumulate in healthy tissues causing severe damage. This unspecific drug accumulation also decreases their effectiveness [2]. Nanotechnology has overcome this problem thanks to passive and active targeting of the tumor. Lipid-based nanocarriers are not only able to accumulate in tumor tissues passively, but these systems can also be actively targeted at tumors by attaching different molecules to their surface (Figure 4).

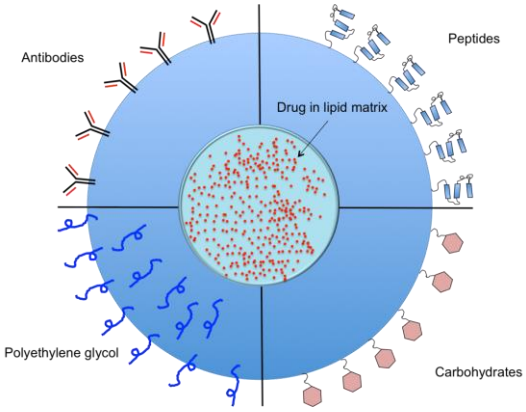

Figure 4. Representation of LN and different surface modifications for active and passive targeting.

6.1.1 Passive targeting

The EPR effect is the principal mechanism of tumor accumulation of nanocarriers [7]. Tumor tissues grow very quickly, promoting special tissue architecture and the development of blood vessels with wide fenestrations between endothelial cells. These particular vessels permit an easier exchange of nutrients and oxygen to support the high demand of this abnormal growth. These wider spaces facilitate the extravasation and accumulation of nanoparticulated systems from the blood vessels into the tumor tissues. Therefore, lipid-based nanosystems are targeted at tumor

tissues in a passive way, which is based on the shape and size and is independent of the surface nature.

In contrast to other nanocarriers, LN offer another possibility in passive targeting when they are administered orally. After oral administration, LN are absorbed via the lymphatic system and the drug is passively targeted at the lymph nodes [20, 61]. This might represent a promising strategy in the treatment of general cancer metastases and in lymph generated tumors (lymphomas) [9].

Another passive targeting approach is the use of certain tensoactive excipients that enable the lipid nanocarriers to penetrate into the central nervous system (CNS). Several studies suggest that LN including tensoactive excipients such as polysorbate 80 (Tween 80) or polyoxyethylene 20-stearyl ether may overcome the BBB, allowing the drug to penetrate into the CNS [10, 62]. Taking into consideration the difficulties of anticancer drugs in crossing the BBB, LN present high potential as therapeutic tools against brain tumors.

6.1.2 Active targeting

Passive targeting is mainly used in nanotechnology to target nanocarriers at the tumor; nevertheless, many authors have developed active targeted LN. In this section we will discuss the main strategies developed to target LN to cancer cells. Efficacy studies will be described and documented in section 6.2 Active targeting consists of attaching molecules to the surface of the nanoparticle. The main strategy in active targeting consists of using ligands that specifically bind to molecules that are selective or over-expressed in tumor cells. However, other approaches like hepatic cell targeting [63] and magnetic targeting [64] are also common.

Among all the molecules used for specific cancer cell targeting, transferrin (Tf) attachment is a widely used strategy [65-67]. Tf receptor is the ubiquitous cell surface glycoprotein related to cell proliferation and is over-expressed in malignant tissues because of the higher iron demand of malignant cells for fast growth and division [65]. Tf binds to its specific receptor on the cell surface and is internalized into the cell by endocytosis.

The attachment of ferritin to the nanoparticle surface is another approach related to the increased iron requirements of cancer cells. Ferritin is an intracellular protein complex, which is intended to store iron in the cell in a non-toxic form. Jain *et a.l* [68] developed ferritin-mediated LN containing 5-fluorouracil (5-FU) to assess their targetability to breast cancer cells.

Mannose has been also used as a ligand in active targeting of lipid nanocarriers [69]. Cancer cells tend to over-express lectin-like receptors with high affinity for polysaccharide molecules on their surface. This occurs as a result of the increased requirement for carbohydrate molecules by tumor tissues. Mannosylated LN containing doxorubicin (DOX) showed enhanced *in vitro* and *in vivo* efficacy compared to non-targeted LN or free drug [58].

Taking advantage of the cancer cell augmented metabolism, another targeted strategy developed is the use of hyaluronan (HA) of different molecular weights [70, 71]. HA is a linear glycosaminoglycan with many biological functions that make it essential in tumor development. HA can be covalently attached to the surface of LN to target epithelial cancer cells and leukocytes over-expressing HA receptors (CD44 and CD168). Mizrahy *et al*. [70] demonstrated that low molecular weight HA might be used as a secure substitute for polyethylene glycol (PEG) if macrophage or complement activation must be avoided. Previous studies demonstrated that low molecular weight HA (LMW-HA) but not high molecular weight HA (HMW-HA) induced inflammatory response [72]; however, Mizrahy *et al*. showed that macrophage activation avoidance was HA molecular weight independent. This could be explained by the low quantity of HA attached to the LN surface compared to preceding studies. Besides, HMW-HA may be used to efficiently target CD44 over-expressing tumors due to the strong binding of HMW-HA to the receptor.

Folate-mediated LN has also been developed to achieve active targeting [73, 74]. Folate receptor has been identified as a useful tumor marker because it is over-expressed in cancer cells. Folate is essential in eukaryotic cells for the biosynthesis of nucleotide bases and, as in the previous cases, its requirement is increased in cancer cells by reason of its accelerated metabolism.

αvβ3 integrins are another target in nanocarrier design. These receptors are over-expressed in angiogenic vessels and in some cancer cells. In a study carried out by Goutayer *et al*. [75], NLC containing a fluorochrome were functionalized with cyclic triad peptide sequence RGD (Arg-Gly-Asp) in order to target αvβ3 integrins. Functionalized LN were shown to have a long half-life in plasma and were distributed widely except for the CNS. Fluorochrome signal was higher in tumor tissues over-expressing target receptors, indicating a targeted distribution of LN.

Apart from this selective targeting of cancer cells, there is another strategy that consists of targeting a specific tissue such as liver or brain. In this sense, selective targeting to hepatic cells is another common approach in nanomedicine. Asialoglycoprotein (ASGP) receptor is commonly used as a therapeutic target in hepatic disease [63]. In contrast to the previous approaches, attaching a hepatic ligand implies targeting of all hepatic cells including healthy tissue. Nevertheless, the EPR effect may help to overcome this drawback, by promoting uptake of nanocarriers by tumor.

CNS has also been targeted through the binding of ligands to the LN surface. Cationic bovine serum albumin (CBSA) promotes transport across the brain capillary endothelial cells [76, 77]. CBSA has recently been used to target LN of DOX to the CNS [78]. In this case, ligand attachment delays *in vitro* drug release from the nanoparticle. Moreover, CBSA-mediated LN were uptaken by cells in a higher rate.

LN can be also targeted through physical approaches using magnetic fields [64]. Besides, drug release from magnetic LN can be controlled when nanoparticles are exposed to an alternating magnetic field [79].

Summarizing, all these possibilities of targeting lead to the conclusion that, although passive targeting has clearly increased antitumor drug efficacy, active targeting clearly improves drug efficacy and security. In fact, active targeting of lipid nanocarriers might be considered an added improvement of passive targeting. LN accumulate in tumor tissue not only due to their physical characteristics but also because of specific binding to cancer cells.

6.2 Cancer therapy using LN

This review is intended to discuss the treatment of cancer with lipid nanocarriers focusing on the past five years. Tumor extirpation combined with radiotherapy, chemotherapy and monoclonal antibodies are conventional treatments in early stages of the disease. However, these therapies are not always effective and entail severe side effects. For this reason, new therapeutic strategies are being investigated. Among all these possibilities, LN are promising drug delivery systems due to the possibility of selectively targeting the nanoparticles at tumor tissues, providing effective and secure therapies.

6.2.1 Lung cancer

Lung cancer is the leading cause of cancer death in the world. This high mortality rates are mainly caused by a late diagnosis of the disease that is associated with non-operable stages. Non-small cell lung cancer (NSCLC) is the most common lung cancer type [80]. NSCLC is composed of heterogeneous aggregates of histologies that include epidermoid or squamous cell carcinoma, adenocarcinoma and large cell carcinoma. Despite improvements in NSCLC therapy, the overall survival at 5 years depends on the cancer stage at diagnosis varying from 49% or 16% to 2% for patients with local, regional, and distant stage, respectively. NSCLC responds badly to radiotherapy and chemotherapy, so patients are frequently included in clinical trials [81]. With this basis in mind, novel formulations are being developed in order to obtain more secure therapies.

In the last five years, different authors have incorporated antitumor drugs into lipid nanocarriers to treat lung cancer [52, 82, 83]. These studies show that lipid vehicles protect labile drugs from degradation, increase drug bioavailability, enhance drug tumor uptake and decrease toxicity. Wan *et al.* [83] studied the *in vitro* efficacy of pegylated-LN containing vinorelbine bitartrate (VB) in A-549 cancer cells. VB is a semi-synthetic vinca alkaloid currently registered for the treatment of NSCLC in many countries. It is a very labile and hydrophilic drug that possesses rapid clearance [84]. Pegylation, coupling of PEG to the surface of the nanocarriers, is a common strategy to avoid macrophage uptake and subsequent LN clearance by the reticuloendothelial

system (RES) [85]. Pegylated-LN containing VB were able to reduce macrophage cell uptake by RAW264.7 cells because of PEG coupling on their surface; furthermore, they were internalized in a higher rate than the free drug in A-549 lung tumor cells. These results might increase *in vivo* efficacy of VB. Another study carried out by Jain *et al*. [58] was based on the use of LN to encapsulate DOX, which is a cytostatic antibiotic with a narrow therapeutic index and severe cardiac toxicity. These authors developed a mannosylated LN formulation of DOX, which was tested *in vitro* in A-549 cells. The hemolytic effect of DOX was avoided when it was encapsulated into LN. *In vivo* studies in male BALB/c mice showed that intravenously administered LN increased biodisponibility of DOX, which is cleared from plasma very quickly when it is administered in its free form. Moreover, vehiculized DOX accumulated in tumor tissue (xenograft A-549) at a higher rate than the free drug, avoiding toxicity in healthy cells.

Gene therapy has also been combined with lipid nanosystems in the treatment of lung cancer. Shi *et al*. [82] investigated the effect of encapsulating anti-microRNA oligonucleotides (AMOs) for suppression of microRNA-21 (miR-21) functions in human lung cancer cells. A-549 human cancer cell line presents over-expression of miR-21, which causes cell proliferation and inhibits apoptosis. These AMOs cannot be administered in their free form due to their labile nature, and therefore LN constitute a promising drug delivery system in gene therapy. The *in vitro* results of the study clearly indicate that AMOs transfection efficacy is enhanced when it is encapsulated into LDC. Besides, this is the first time that AMOs is encapsulated instead of complexed. The high rate of transfection in A-549 cells inhibited cell proliferation and promoted apoptosis; moreover, cell motility was also inhibited.

6.2.2 Colon cancer

Colon cancer is one of the most common cancers worldwide. The prognosis of the disease is directly related to the penetration of the cancer through the bowel wall. Bowel localized cancer is removed by surgery and is curable in only 50% of the cases because recurrence is very frequent. Moreover, as in most cancer types, tumors are detected at an advanced stage and so radiotherapy and chemotherapy are the only feasible treatments [86].

Antitumor drugs against colon cancer have been encapsulated into LN by several authors lately [87, 88]. 5-FU is an antimetabolite widely used in colorectal cancer treatment but it presents large individual variability in pharmacokinetics and its toxicity is closely related to this variability. Yassin *et al*. [87] incorporated this drug into LN successfully; however, they did not test the efficacy of the formulation either *in vitro* or *in vivo*.

6.2.3 Breast cancer

Breast cancer is the second leading cause of cancer death in women after lung cancer. It causes death in about 3% of the cases. The decline in death rates since 1990 is mainly a result of early detection programs. These preventive measures have allowed the complete elimination of most tumors by surgical resection. This measure is commonly associated with local radiotherapy, systemic chemotherapy, hormone therapy or targeted therapy [89].

Many drugs have been vehiculized through lipid nanocarriers to achieve better drug efficacy and decrease toxicity in breast cancer treatment [58, 65, 68, 75, 83, 90-94].

Capecitabine is a prodrug of 5-FU that must be converted by enzymes that are mainly restricted to the liver and tumor site. In this sense, capecitabine and its analogues have fewer side effects than 5-FU; nevertheless, its rapid plasma clearance requires frequent dose regimens. LN are a promising tool due to their ability to provide controlled drug release and, subsequently, improved dose regimens. Capecitabine analog (5-FCPal) was encapsulated by Gong *et al*. in LN [93]. The *in vitro* results in MCF-7 breast cancer cells showed that encapsulated 5-FCPal was as effective as capecitabine and less toxic than 5-FU. *In vivo* study on a mouse breast cancer model in female BALB/c mice did not show any significant differences between free capecitabine and encapsulated 5-FCPal analog administered via orogastric gavage; however, a tendency to higher efficacy was observed in the LN group. The authors also postulate that LN containing 5-FCPal might be administered on an intermittent basis obtaining similar efficacy due to controlled drug release. More studies are required in order to demonstrate that LN administered intermittently could provide similar efficacy to the free drug administered daily.

Lu *et al*. [90] encapsulated the antitumor drug mitoxantrone (MTO) in LN. Heart toxicity, myelosupression and local toxicity at injection site are reported frequently when using this drug against breast cancer. Authors efficiently overcame these drug drawbacks by using LN to vehiculize the drug. A breast cancer model in BALB/c-nu nude mice was established and MTO-LN were subcutaneously injected. Not only were LN containing MTO more effective in restricting the action of the drug to the tumor site, but additionally, they were also able to avoid macrophage uptake by using the PEG derivated surfactant S-40. Local injection of MTO-LN avoided hepatonecrosis and interstitial pneumonia that is caused by the free drug. The breast tumor model was not satisfactory in all animals and, therefore statistically significant results were not obtained. Preliminary histopathological results showed more necrotic areas and thinner overgrown tumor layer when mice were treated with the encapsulated drug.

Wan *et al*. [83] evaluated the *in vitro* efficacy of including the antitumor drug VB in LN. As in the preceding study, these authors also aimed to protect LN from macrophage uptake, and so they decided to cover the LN surface with PEG. The increment in PEG percentage on the surface of the LN increases its hydrophilicity, thus avoiding macrophage uptake. *In vitro* efficacy in MCF-7 cells of nanoencapsulated VB was enhanced about 6.5 fold compared to the free drug.

Another approach in breast cancer therapy is the use of hormonal therapy. Most breast cancers need estrogen to grow, and estrogen-receptor antagonists are therefore used to block the receptor and hamper cancer development. Tamoxifen citrate (TC) is a nonsteroidal estrogen antagonist commonly used after mastectomy or in early breast cancer stages. One study from Reddy *et al*. [91] incorporated TC in LN to evaluate the *in vivo* pharmacokinetics of the encapsulated drug in rats. They showed that nanoencapsulation of the drug produced higher plasma concentrations of TC and slower clearance, thus demonstrating again the potential use of LN as a secure and efficient drug delivery system in breast cancer.

Tumor targeting improvement through functionalized LN has been demonstrated in a wide variety of studies. In the last few years, many studies have focused on the treatment of breast cancer with lipid nanocarriers possessing active targeting. Goutayer *et al*. [75] investigated the *in vivo* distribution of LN and the effect of

functionalizing them in their biodistribution. They targeted the nanoparticles to αvβ3 integrins, over-expressed on angiogenic vessels and tumor tissues, achieving longer nanoparticle plasma circulation time. Nanoparticles were accumulated mainly in tumor tissue followed by uterus, ovarian and adrenal glands. Tumor targeting was achieved in the case of a cell line over-expressing the target: in this case, functionalized nanoparticles accumulate in tumor tissue in a higher rate than non-targeted LN. Another study conducted by Jain *et al*. [58], in which LN were labeled with mannose, affirmed that functionalized lipid nanocarriers are more effective than free drug in inhibiting proliferation in breast cancer cells. Besides, *in vivo* bioavailability and tumor accumulation were enhanced when using LN, especially when they were coupled with mannose. Tf mediated LN has also been utilized to target antitumor drugs at breast cancer cells [65]. In this study, curcumin efficacy in MCF-7 cells was enhanced due to the use of functionalized nanoparticles. Curcumin is a physically labile antitumor drug that presents a low bioavailability profile. LN were effective in protecting the drug from degradation. Non-targeted LN were also effective but at a lower rate than Tf mediated LN.

5-FU is one of the most commonly used drugs in the treatment of breast cancer due to its effectiveness against several solid tumors; however, it presents serious drawbacks due to a lack of specificity for tumor cells [95]. Jain *et al*. [68] studied the possible advantages of using LN to target the drug towards the tumor tissue while avoiding its toxic effects. This also included the targeting of the LN with ferritin. *In vitro* results demonstrated that ferritin mediated LN containing 5-FU were internalized at a significant rate by breast cancer cells (MDA-MB-468) through a saturable mechanism. Furthermore, drug half-life in plasma was significantly enhanced when the drug was encapsulated in nanoparticles. 5-FU accumulates in the tumor 7.7 times more than drug included in non-targeted LN or free drug.

6.2.4 Brain cancer

Nowadays brain diseases remain one of the most challenging pathologies to treat. Many circumstances make treatment of cerebral tumors particularly complicated. They are in many cases inoperable due to their location, and the BBB prevents drugs from crossing into the brain. BBB consists of physical (tight junctions)

and metabolic (enzymes) barriers, which hamper the passing of drugs and toxins from circulation blood to the extracellular fluid of the brain. Lastly, the broad heterogeneity of brain malignancies makes the individual response to the treatment very unpredictable. Brain tumors are associated with high mortality rates despite their low incidence compared to other tumors. The pharmacology of brain cancer is always difficult but LN have provided a new insight in its treatment alternatives [10, 59, 78, 96-98].

Several active and passive strategies have been used to enhance targeting of LN at the CNS. The inclusion of certain tensioactive agents has been demonstrated to be an effectively passive targeting strategy to bypass the BBB. Tensioactives such as Tween 80 enhance the binding of plasma proteins, with specificity for the BBB, to the LN surface [99]. Moreover, Tween 80 temporarily inhibits the MDR effect mediated by P-gp protein avoiding drug efflux [10]. Estella-Hermoso de Mendoza *et al*. investigated the *in vitro* efficacy and *in vivo* biodistribution of edelfosine-LN. Edelfosine is an antitumor drug with *in vitro* activity against several cancer cells [5, 10, 100, 101]. This study demonstrated that LN are able to inhibit P-gp *in vitro* and that they can thus revert the C6 cell line resistance to the free drug. Moreover, biodistribution studies showed drug accumulation in brain tissue after oral administration of the nanoencapsulated drug.

Active targeting to the brain was also carried out by Agarwal *et al*. [78]. In this study they conjugated DOX LN with CBSA. They based their strategy on previous studies that demonstrated that CBSA promotes transport of nanoparticles across the BBB [76, 77]. The results of the study showed that CBSA conjugated LN provided slower drug release rates than empty-LN; this effect is commonly seen in lipid nanocarriers with attached ligands on their surface, which might happen because these added molecules act as extra barriers. Drug targeting was successfully achieved *in vitro* and *in vivo* through intravenous administration. CBSA conjugated-LN were able to target DOX to the CNS improving its brain concentration and avoiding side effects in healthy tissues. Kuo and Liang [59, 97] also applied active targeting attaching anti-EGFR to the nanoparticle surface, and since EGFR is normally expressed in glioma, the attachment of an antibody against this receptor can certainly improve drug efficacy. These authors have published two studies in which

they encapsulate DOX and carmustine into EGFR-targeted LN. Both studies evaluated the *in vitro* efficacy on U87MG cells, and showed that the efficacy of chemotherapy was enhanced as a result of the EGFR targeting.

6.2.5 Ovarian cancer

According to the American Cancer Society [102], ovarian cancer accounts for about 3% of all cancers in women and causes more deaths than any other cancer of the female reproductive system. It mainly affects older women, half of the diagnosed women being older than 60 years. As in other tumors, surgical removal of the tumor is the first option. Nevertheless, chemotherapy and radiotherapy must be administered in many cases if the main tumor cannot be removed or it has metastasized to other parts of the body. Chemotherapy in ovarian cancer is usually administered in combination therapy using a platinum compound, such as cisplatin or carboplatin, and a taxane, such as paclitaxel (Taxol®) or docetaxel (Taxotere®). Encapsulating, for example, docetaxel, into LN increased their efficacy compared to the commercial formulation (Taxotere®) [92].

Many researchers are investigating new drug delivery systems that may overcome MDR to common chemotherapy drugs. Among these new strategies, LN have been successfully evaluated in ovarian cancer [62, 70, 92, 103-105].

As we have seen before, MDR can be overcome by using LN that include specific surfactants in their formulation. On this basis, one study developed by Dong *et al*. [62] confirmed that polyoxyethylene 20-stearyl ether (Brij 78) can also inhibit P-gp efflux pump and, consequently, increase not only drug internalization but also drug retention inside the cells. The study, which consists of LN containing DOX and paclitaxel, showed that both, blank-LN and LN containing the antitumor drugs were able to inhibit the P-gp mechanism in P-gp over-expressing human ovarian carcinoma cell line NCI/ADR-RES. This inhibition is followed by a transitory ATP depletion, which induces mitochondria stress and swelling as a desperate mechanism to obtain energy and supply ATP depletion. This study proves that LN containing certain tensioactive agents have an effect on the MDR mechanism that helps to achieve higher intracellular drug accumulation. In fact, the addition of free DOX after treating the

cells with non-loaded LN produced an *in vitro* cytotoxic effect similar to the drug loaded nanocarriers, probably due to the transitory P-gp inhibition.

6.2.6 Hematological cancer

Blood cancer includes leukemia, lymphoma and myeloma. Leukemia develops in the bone marrow and affects white blood cells; it has different subtypes depending on its speed of development and the subtype of white cells involved. Childhood leukemia is the most common cancer in children. Lymphoma is a blood cancer that appears as a solid tumor and is commonly located in the lymph nodes. It causes the production of abnormal lymphocytes. There are two types of lymphoma: non-Hodgkin (more common) and Hodgkin. Non-Hodgkin lymphoma is the most common blood cancer in teenagers and young people. Myeloma affects the plasma cells on the blood unbalancing the immune system. Myeloma mainly occurs in people over the age of 40.

As has been mentioned before, lymphomas develop in lymph nodes, and so LN might be an appropriate tool to fight this cancer. Several studies support the theory that LN are absorbed by a lymphatic route after oral administration [8, 20, 61, 106]. LN can passively target lymph nodes by concentrating unmetabolized drug at the cancer origin. So far, the only study of orally administered LN to treat hematological cancers was performed by Estella-Hermoso de Mendoza *et al.* [9]. In this work, very promising results were obtained after the oral administration of edelfosine loaded LN to mantle cell lymphoma bearing mice. These authors proved that the administration of drug loaded LN every four days was as effective as the daily free drug in decreasing tumor growth. Moreover, while the daily administration of the free drug was able to reduce the metastases by a half, the administration of drug loaded LN orally every four days completely eradicated the metastatization process. This study offers new hopes in orally administered chemotherapy to treat this kind of cancer.

In another study Reddy *et al*. [107] demonstrated that LN containing etoposide were more effective than the free drug after intraperitoneal administration in Dalton's lymphoma ascites bearing mice. Controlled release of etoposide in this kind of intraperitoneal tumors is essential due to the necessity of prolonged exposure to the drug to obtain a cytotoxic effect. LN remains in the peritoneal cavity after

intraperitoneal administration, providing sustained release of the drug and thus increasing its antitumor efficacy. Antitumor drug encapsulation into LN has been carried out by several authors for treating hematological tumors [9, 66, 108, 109]. Idarubicin and DOX were encapsulated into LN by Ma *et al*. [108] in order to avoid P-gp mediated MDR in leukemia patients and subsequent disease relapses. The results of the study showed that idarubicin inclusion into LN did not increase its efficacy. This could be explained because idarubicin uptake rate is much higher than its P-gp mediated efflux because of its lipophilic properties. DOX-LN were, in contrast, more effective than the free drug, probably due to the P-gp inhibition mechanism mediated by the surfactants (Brij 78 and Vitamin E TPGS) included in the formulation.

Gene therapy has also been combined with LN in the treatment of leukemia leading to protection from serum nucleases, longer blood circulation and increased tumor concentration of oligodeoxyribonucleotides [109]. In addition, the coupling of these LN with Tf improves its targeting to leukemia cells over-expressing Tf-receptor. Moreover, targeting can be enhanced with a pretreatment with defeoxamine, a clinically used iron chelator which is known to up-regulate Tf-receptor expression in cells.

6.2.7 Other cancer types

Many other studies have been performed in relation to other cancer types such as prostate, tongue, hepatocellular cancer, melanoma and sarcoma [57, 62, 63, 74, 92, 110-113]. In these studies, antitumor drugs and genetic material are encapsulated into LN.

As in other approaches, genetic material is protected from plasma nuclease degradation and LN show higher *in vitro* transfection efficiency than commercially available gene carriers [110, 111]. Besides, an *in vivo* study carried out by Bauman *et al*. [110] with oligonucleotides that down-regulate Bcl-x (an anti-apoptotic member of the Bcl-2 family) demonstrated that they are able to induce splicing modification in tumor cells.

Radiotherapy has also been combined with nanotechnology in the treatment of head and neck cancers. Some studies show that β-emitting radionuclides that are

included in LN better accumulate and localize radiation in the tumor, sparing healthy tissues after intratumor administration [112].

LN are also a good strategy for topical oral delivery of poorly water soluble drugs used in oral cancer chemoprevention strategy [113]. Moreover, LN can reach connective tissue and, therefore, they could be used for systemic therapeutics through the oral mucosa. It is remarkable that this study also showed that LN must be in a high concentration in the treatment site to avoid MDR efflux; at a low concentration they conjugate with glutathione and are effluxed by cell proteins.

The taxanes, including paclitaxel and docetaxel, have broad activity and are extensively used in clinical practice in the treatment of cancer. As explained before, several authors have vehiculized them into LN to treat ovarian and colorectal cancer; however, prostate, hepatocellular or sarcoma, among others, have also been investigated [57, 62, 63, 92]. As major antitumor drugs, taxanes comprise severe side effects because of their poor targeting and high toxicity; moreover, they exhibit poor water solubility. The studies mentioned above demonstrated that, in all cases, encapsulated drug effects were more potent and toxic effects were avoided due to a lower accumulation in healthy tissues.

7. Biodegradation, safety and toxicity aspects

Over the past years, the development of lipid drug delivery systems has entailed a wide range of tasks such as the development of nanosystems that are suitable to specific applications, the type of release kinetics (pulsatile, fast, slow) and proof of efficacy. Furthermore, it is very important to prove the systems' safety, which implies at least two major entities: the biocompatibility of the delivery system and the safety of the systemically distributed drug [114]. The control of the systemic drug distribution can be a relatively simple matter of engineering release kinetics so that blood levels are lower. Being in the solid state, the lipid components of LN will be degraded more slowly providing a longer lasting exposure to the immune system. Degradation can be slowed down even more when using sterically stabilizing surfactants that hinder the anchoring of enzyme complexes. Reducing biocompatibility problems can be much harder, involving drug-tissue interactions and

material properties that are still not well understood. However, LN are biocompatible and biodegradable and have been used for controlled drug delivery and specific targeting. Furthermore, in terms of safety issues, one clear advantage of the use of LN as drug carrier systems is the fact that the matrix is composed of physiological components, that is, excipients with generally recognized as safe (GRAS) status for oral, topical and intravenous administration [5, 29, 101, 115, 116], which decreases the possible cytotoxicity. LN have been already tested as site-specific carriers mainly for drugs that present a relatively fast metabolism and are quickly cleared from the blood, that is, peptides and proteins [117, 119]. LN are generally well tolerated, and as stated above they are mainly formulated using biocompatible or physiological compounds that can be included in different metabolic pathways after degradation [120, 121].

The biodegradation velocity of nanoparticles affects their toxicological acceptance (e.g. concentration of degradation products). As a result, many studies have been focused on the toxicology of LN, including genotoxicity and cytotoxicity studies [122]. It was observed that these effects usually occur at rather high concentrations, but the effects that happen at lower concentrations, without necessarily causing cell death, also should be taken into consideration..

8. Concluding remarks

LN have been shown to be effective carriers in cancer. The inclusion of anticancer drugs in LN improves drug efficacy and decreases side effects. Among all the advantages that these carriers offer, it is noteworthy that they protect labile drugs from degradation or rapid RES clearance. This is particularly relevant in the case of gene therapy or in antitumor drugs that have short plasma half-lives. Besides, they not only decrease toxicity but they also generally provide longer circulation times and higher concentration of the drug in tumor tissue. This proved efficacy is mainly based on passive and active targeting. Apart from these general considerations, LN present some particularly relevant advantages. First of all, they can be administered orally avoiding the tedious intravenous route in chemotherapy. When administered by this route, they are mainly absorbed via the lymphatic system, thus opening a new window in treatment of cancer metastases and lymphomas. Secondly, they can be

targeted to the brain due to its capacity to cross the BBB when specific tensioactive (Tween 80, Brij 78) compounds are used in the formulation. *In vitro* studies have demonstrated that these molecules inhibit MDR by inhibiting P-gp efflux pump. LN can easily be scaled up, even obtaining improved results over those produced in the laboratory.

9. Expert opinion

Nowadays, LN are widely being investigated in the field of pharmaceutical technology. LN formulations are based on traditional emulsion techniques and a broad spectrum of manufacturing methods are currently available. Production methods for LN have been widely modified since their invention by Speiser [14] in the 1980s. Most of these methods are based on the HPH and warm microemulsion technique developed respectively by Müller and Lucks [17] and Gasco [19] in the 1990s. The investigations carried out in this field have led to improved nanoparticles due to the avoidance of degradation of thermolabille compounds, non-energy consuming methods, reproducibility, and low surfactant concentrations, among other factors. Most of them can be easily scaled up, HPH-based procedures being the most suitable for this purpose, as homogenizers have been used for a long time in the pharmaceutical industry. Indeed, nanoparticles produced on a large scale have been seen to present better size quality [29]. Regarding safety issues, LN present the advantage of being composed by GRAS lipids for oral, topical and intravenous administration. Therefore, LN matrix composition would not be potentially toxic unless large non-ionic surfactant or organic solvent quantities are used in the formulation. Several *in vivo* studies demonstrate that the intravenous administration of LN lower than 5 μm does not produce macroscopic toxicity [57, 58, 75, 110]. Besides, *in vitro* toxicity experiments have shown that LN do not affect Caco-2 cell viability [123], which makes this system suitable for oral administration. However, regardless of the potential safety of these nanosystems, further research is necessary in order to elucidate nanoparticle behavior after *in vivo* administration, emphasizing the study of LN barrier crossing (e.g. intestinal barrier or BBB) and cell interaction. The knowledge of this basis would enable us to anticipate possible toxic effects.

The antitumor activity of these nanosystems loaded with antitumor drugs has been widely demonstrated since their discovery. Studies carried out in the last five years show that antitumor drug toxicity is dramatically reduced when the drug is encapsulated into LN [63, 92, 124]. Besides, LN provide higher bioavailability rates and prolonged plasma circulation times, thus improving drug efficacy [10, 58, 78, 125]. The advantages of LN over the administration of free drugs can be mainly explained by the passive and active targeting of the tumor tissue, mediated by the lipid vehicle. Another important improvement in these systems is that when some tensioactive molecules are used in the formulation, LN are able to overcome MDR [10, 62]. This benefit is due to the ability of LN to inhibit P-gp protein, which mediates the efflux of antitumor drugs from the cell and thus enhances intracellular drug concentration. Targeting anticancer drugs at the tumor avoids severe chemotherapy side-effects. Although most studies in cancer treatment with LN are based on intravenous route, some authors have considered the oral route [9, 10], which is better tolerated in terms of patient welfare. These studies suggest that LN are absorbed via the lymphatic system after oral administration, achieving high drug concentration in lymph nodes. This fact might be very relevant in the avoidance of metastases and in lymphoma treatment. Bearing in mind the benefits of orally administrated LN, current research efforts should be focused on this route. Further studies are required in order to fully characterize their lymphatic absoption. Besides, intracellular uptake and interactions between cells and LN must be evaluated with the aim of clarifying the biodegradation, safety and toxicity aspects of these vehicles. Despite the need for further research concerning these aspects of the field, and considering all the reviewed studies, in our opinion LN should provide more secure and effective antitumor treatments in the near future.

10. Article highlights

- Lipid nanoparticles (LN) have been widely studied since their discovery in the 80's. The broad spectrum of fabrication methods and targeting strategies have improved nanoparticles efficacy in tumor treatment.

- Their composition based on generally recognized as safe (GRAS) lipids for oral administration, guarantees less potential toxicity than other nanovehicles and their scaling-up is currently feasible.
- LN reduce drug toxicity and enhance antitumor activity mainly due to: i) passive and active targeting and ii) multi-drug resistance MDR overcoming (P-glycoprotein (P-gp) inhibition).
- Current investigations suggest two relevant advantages of LN in cancer treatment: i) the oral administration and further absorption through the lymphatic system and ii) BBB penetration due to certain formulation components.

11. References

Papers of special note have been highlighted as either of interest (*) or of considerable interest (**) to readers.

[1] WHO: Cancer, 2012. Available at: http://www.who.int/mediacentre/ factsheets/fs297/en/ [Last accessed 15 May 2012].

[2] Bhosle J, Hall G. Principles of cancer treatment by chemotherapy. Surgery (Oxford) **2009**; *27*:173-177.

[3] Principe P, Braquet P. Advances in ether phospholipids treatment of cancer. Crit Rev Oncol **1995**; *18*:155-178.

[4] Banna GL, Collovà E, Gebbia V, et al. Anticancer oral therapy: Emerging related issues. Cancer Treat Rev **2010**; *36*:595-605.

[5] Estella-Hermoso de Mendoza A, Campanero MA, Mollinedo F, et al. Lipid nanomedicines for anticancer drug therapy. J Biomed Nanotechnol **2009**; *5*:323-343.

[6] Peer D, Karp JM, Hong S, et al. Nanocarriers as an emerging platform for cancer therapy. Nat Nanotechnology **2007;** *2*:751-760.

[7] Torchilin V. Tumor delivery of macromolecular drugs based on the EPR effect. Adv Drug Deliv Rev **2011**; *63*:131-135.

[8] Paliwal R, Rai S, Vaidya B, et al. Effect of lipid core material on characteristics of solid lipid nanoparticles designed for oral lymphatic delivery. Nanomedicine **2009**; 5:184-191.

[9] Estella-Hermoso de Mendoza A, Campanero MA, Lana H, et al. Complete inhibition of extranodal dissemination of lymphoma by edelfosine-loaded lipid nanoparticles. Nanomedicine **2012**; 7:679-690 ****Research work that shows effectiveness of orally administered LN loaded with the antitumoral drug edelfosine in inhibiting metastases.**

[10] Estella-Hermoso de Mendoza A, Preat V, Mollinedo F, et al. In vitro and in vivo efficacy of edelfosine-loaded lipid nanoparticles against glioma. J Control Release **2011**; *156*:421-426 ****Research work showing that LN are able to cross the BBB and are effective against glioma.**

[11] Altmayer P, Grundmann U, Ziehmer M, et al. Comparative effectiveness and tolerance study of a new galenic etomidate formula. Anasthesiol Intensivmed Notfallmed Schmerzther **1993**; *28*:415-419.

[12] Müller RH, Petersen RD, Hommoss A, et al. Nanostructured lipid carriers (NLC) in cosmetic dermal products. Adv Drug Deliv Rev **2007**; *59*:522-530.

[13] Allen TM. Long-circulating (sterically stabilized) liposomes for targeted drug delivery. Trends Pharmacol Sci **1994**; *15*:215-220.

[14] Speiser P. Lipid nanopellets als tragersystem fur arzneimittel zur peroralen anwendung. EP 0167825 (**1990**).

[15] Eldem T, Speiser P, Hincal A. Optimization of spray-dried and -congealed lipid micropellets and characterization of their surface morphology by scanning electron microscopy. Pharm Res **1991**; *8*:47-54.

[16] Schwarz C, Mehnert W, Lucks JS, et al. Solid lipid nanoparticles (SLN) for controlled drug delivery. I. Production, characterization and sterilization. J Control Release **1994**; *30*:83-96.

[17] Müller RH, Lucks JS. Medication vehicles made of solid lipid particles (solid lipid nanospheres - SLN). EP0605497 (**1993**).

[18] Gasco MR. Solid lipid nanospheres from warm microemulsions. Pharm Tech Eur **1997**; *9*:52-58.

[19] Gasco MR. Method for producing solid lipid microspheres having a narrow size distribution. US188837 (**1993**).

[20] Cai S, Yang Q, Bagby TR, et al. Lymphatic drug delivery using engineered liposomes and solid lipid nanoparticles. Adv Drug Deliv Rev 2011;*63*:901-908. ****This review discusses recent advances in the field of lymphatic drug delivery and imaging and focuses specifically on the development of liposomes and solid lipid nanoparticles.**

[21] Müller RH, Radtke M, Wissing SA. Nanostructured lipid matrices for improved microencapsulation of drugs. Int J Pharm **2002**; *242*:121-128.

[22] Liu D, Liu Z, Wang L, et al. Nanostructured lipid carriers as novel carrier for parenteral delivery of docetaxel. Colloids Surf B Biointerfaces **2011**; *85*:262-269.

[23] Sharma P, Dube B, Sawant K. Development and evaluation of nanostructured lipid carriers of cytarabine for treatment of meningeal leukemia. J Nanosci Nanotechnol **2011**; *11*:6676-6682.

[24] Zhao X, Zhao Y, Geng L, et al. Pharmacokinetics and tissue distribution of docetaxel by liquid chromatography-mass spectrometry: Evaluation of folate receptor-targeting amphiphilic copolymer modified nanostructured lipid carrier. J Chromatogr B Analyt Technol Biomed Life Sci **2011**; *879*:3721-3727.

[25] Li F, Weng Y, Wang L, et al. The efficacy and safety of bufadienolides-loaded nanostructured lipid carriers. Int J Pharm **2010**; *393*:203-211.

[26] Zhang XG, Miao J, Dai YQ, et al. Reversal activity of nanostructured lipid carriers loading cytotoxic drug in multi-drug resistant cancer cells. Int J Pharm **2008**; *361*:239-244

[27] Müller, R.H., Olbrich, C. Lipid matrix-drug conjugates particle for controlled release of active ingredients. US 6770299 (**2002**).

[28] Muchow M, Maincent P, Muller RH. Lipid nanoparticles with a solid matrix (SLN, NLC, LDC) for oral drug delivery. Drug Dev Ind Pharm **2008**; *34*:1394-405 ***This paper describes the scaling up proccess od SLN.**

[29] Muller RH, Radtke M, Wissing SA. Solid lipid nanoparticles (SLN) and nanostructured lipid carriers (NLC) in cosmetic and dermatological preparations. Adv Drug Deliv Rev **2002**; *54*:S131-55.

[30] Avestin. Available at: www.avestin.com [Last accessed 15 May **2012**].

[31] APV®. Available at: www.apv.com [Last accessed 15 May **2012**].

[32] Mader K. Solid lipid nanoparticles as drug carriers. In: Torchilin V, editor. Nanoparticulates as Drug Carriers. Imperial College Press; **2006**.

[33] Charman WN, Stella VJ. Lymphatic transport of drugs. CRC Press; **1992.**

[34] Zimmermann E, Muller RH, Mader K. Influence of different parameters on reconstitution of lyophilized SLN. Int J Pharm **2000**; *196*:211-213.

[35] Brown SC, Palazuelos M, Sharma P, et al. Nanoparticle characterization for cancer nanotechnology and other biological applications. Methods Mol Biol **2010**; *624*:39-65.

[36] Estella-Hermoso de Mendoza A, Rayo M, Mollinedo F, et al. Lipid nanoparticles for alkyl lysophospholipid edelfosine encapsulation: Development and in vitro characterization. Eur J Pharm Biopharm **2008**; *68*:207-213.

[37] Patel MR, San Martin-Gonzalez MF. Characterization of ergocalciferol loaded solid lipid nanoparticles. J Food Sci **2012**; *77*:N8-13.

[38] Zaucha M, Adamczyk Z, Barbasz J. Zeta potential of particle bilayers on mica: A streaming potential study. J Colloid Interface Sci **2011**; *360*:195-203.

[39] Thielbeer F, Donaldson K, Bradley M. Zeta potential mediated reaction monitoring on nano and microparticles. Bioconjug Chem **2011**; *22*:144-50.

[40] Freire JM, Domingues MM, Matos J, et al. Using zeta-potential measurements to quantify peptide partition to lipid membranes. Eur Biophys J **2011**; *40*:481-487

[41] Freitas C, Muller RH. Effect of light and temperature on zeta potential and physical stability in solid lipid nanoparticles (SLN) dispersion. Int J Pharm **1998**; *168*:221-229.

[42] Souto EB, Mehnert W, Muller RH. Polymorphic behaviour of Compritol888 ATO as bulk lipid and as SLN and NLC. J Microencapsul **2006**; 23:417-433.

[43] Bunjes H, Koch MH. Saturated phospholipids promote crystallization but slow down polymorphic transitions in triglyceride nanoparticles. J Control Release **2005**; *107*:229-243.

[44] Bunjes H, Koch MH, Westesen K. Effect of surfactants on the crystallization and polymorphism of lipid nanoparticles. Prog Colloid Polym Sci **2002**; *121*:7-10.

[45] Bunjes H, Koch MH, Westesen K. Influence of emulsifiers on the crystallization of solid lipid nanoparticles. J Pharm Sci **2003**; *92*:1509-1520.

[46] Bunjes H, Steiniger F, Richter W. Visualizing the structure of triglyceride nanoparticles in different crystal modifications. Langmuir **2007**; *23*:4005-4011.

[47] Kramer T, Kremer DM, Pikal MJ, et al. A procedure to optimize scale-up for the primary drying phase of lyophilization. J Pharm Sci **2009**; *98*:307-318.

[48] Yadava P, Gibbs M, Castro C, et al. Effect of lyophilization and freeze-thawing on the stability of siRNA-liposome complexes. AAPS Pharm Sci Tech **2008**; *9*:335-341.

[49] Bensouda Y, Laatiris A. The lyophilization of dispersed systems: Influence of freezing process, freezing time, freezing temperature and RBCs concentration on RBCs hemolysis. Drug Dev Ind Pharm **2006**; *32*:941-945.

[50] Seetharam R, Wada Y, Ramachandran S, et al. Long-term storage of bionanodevices by freezing and lyophilization. Lab Chip **2006**; *6*:1239-1242.

[51] Cavalli R, Caputo O, Gasco MR. Preparation and characterization of solid lipid nanospheres containing paclitaxel. Eur J Pharm Sci **2000**; *10*:305-309.

[52] Souza LG, Silva EJ, Martins AL, et al. Development of topotecan loaded lipid nanoparticles for chemical stabilization and prolonged release. Eur J Pharm Biopharm **2011**; *79*:189-196.

[53] Subedi RK, Kang KW, Choi HK. Preparation and characterization of solid lipid nanoparticles loaded with doxorubicin. Eur J Pharm Sci **2009**; *37*:508-513.

[54] del Pozo-Rodriguez A, Solinis MA, Gascon AR, et al. Short- and long-term stability study of lyophilized solid lipid nanoparticles for gene therapy. Eur J Pharm Biopharm **2009**; *71*:181-189.

[55] zur Muhlen A, Schwarz C, Mehnert W. Solid lipid nanoparticles (SLN) for controlled drug delivery--drug release and release mechanism. Eur J Pharm Biopharm **1998**; *45*:149-155.

[56] Battaglia L, Gallarate M. Lipid nanoparticles: state of the art, new preparation methods and challenges in drug delivery. Expert Opin Drug Deliv **2012**; *9*:497-508.

[57] Wu L, Tang C, Yin C. Folate-mediated solid-liquid lipid nanoparticles for paclitaxel-coated poly(ethylene glycol). Drug Dev Ind Pharm **2010**; *36*:439-448.

[58] Jain A, Agarwal A, Majumder S, et al. Mannosylated solid lipid nanoparticles as vectors for site-specific delivery of an anti-cancer drug. J Control Release **2010**; *148*:359-367.

[59] Kuo YC, Liang CT. Catanionic solid lipid nanoparticles carrying doxorubicin for inhibiting the growth of U87MG cells. Colloids Surf B Biointerfaces **2011**; *85*:131-137.

[60] Huang ZR, Hua SC, Yang YL, et al. Development and evaluation of lipid nanoparticles for camptothecin delivery: A comparison of solid lipid nanoparticles, nanostructured lipid carriers, and lipid emulsion. Acta Pharmacol Sin **2008**; *29*:1094-1102.

[61] Aji Alex MR, Chacko AJ, Jose S, et al. Lopinavir loaded solid lipid nanoparticles (SLN) for intestinal lymphatic targeting. Eur J Pharm Sci **2011**; *42*:11-8.

[62] Dong X, Mattingly CA, Tseng MT, et al. Doxorubicin and paclitaxel-loaded lipid-based nanoparticles overcome multidrug resistance by inhibiting P-glycoprotein and depleting ATP. Cancer Res **2009**; *69*:3918-3926.

[63] Xu Z, Chen L, Gu W, et al. The performance of docetaxel-loaded solid lipid nanoparticles targeted to hepatocellular carcinoma. Biomaterials **2009**; *30*:226-232.

[64] Ying XY, Du YZ, Hong LH, et al. Magnetic lipid nanoparticles loading doxorubicin for intracellular delivery: Preparation and characteristics. J Magn Magn Mater **2011**; *323*:1088-1093.

[65] Mulik RS, Monkkonen J, Juvonen RO, et al. Transferrin mediated solid lipid nanoparticles containing curcumin: Enhanced in vitro anticancer activity by induction of apoptosis. Int J Pharm **2010**; *398*:190-203.

[66] Yang X, Koh CG, Liu S, et al. Transferrin receptor-targeted lipid nanoparticles for delivery of an antisense oligodeoxyribonucleotide against bcl-2. Mol Pharm **2009**; *6*:221-230.

[67] Gupta Y, Jain A, Jain SK. Transferrin-conjugated solid lipid nanoparticles for enhanced delivery of quinine dihydrochloride to the brain. J Pharm Pharmacol **2007**; *59*:935-940.

[68] Jain SK, Chaurasiya A, Gupta Y, et al. Development and characterization of 5-FU bearing ferritin appended solid lipid nanoparticles for tumour targeting. J Microencapsul **2008**; *25*:289-297.

[69] Nimje N, Agarwal A, Saraogi GK, et al. Mannosylated nanoparticulate carriers of rifabutin for alveolar targeting. J Drug Target **2009**; *17*:777-787.

[70] Mizrahy S, Raz SR, Hasgaard M, et al. Hyaluronan-coated nanoparticles: The influence of the molecular weight on CD44-hyaluronan interactions and on the immune response. J Control Release **2011**; *156*:231-238.

[71] Rivkin I, Cohen K, Koffler J, et al. Paclitaxel-clusters coated with hyaluronan as selective tumor-targeted nanovectors. Biomaterials **2010**; *31*:7106-7114.

[72] Scheibner KA, Lutz MA, Boodoo S, et al. Hyaluronan fragments act as an endogenous danger signal by engaging TLR2. J Immunol **2006**; *177*:1272-1281.

[73] Liu Z, Zhong Z, Peng G, et al. Folate receptor mediated intracellular gene delivery using the charge changing solid lipid nanoparticles. Drug Deliv **2009**; 16:341-347

[74] Schroeder JE, Shweky I, Shmeeda H, et al. Folate-mediated tumor cell uptake of quantum dots entrapped in lipid nanoparticles. J Control Release **2007**; *124*:28-34

[75] Goutayer M, Dufort S, Josserand V, et al. Tumor targeting of functionalized lipid nanoparticles: Assessment by in vivo fluorescence imaging. Eur J Pharm Biopharm **2010**; *75*:137-147.

[76] Shimon-Hophy M, Wadhwani KC, Chandrasekaran K, et al. Regional blood-brain barrier transport of cationized bovine serum albumin in awake rats. Am J Physiol **1991**; *261*:R478-83.

[77] Wadhwani KC, Shimon-Hophy M, Rapoport SI. Enhanced permeabilities of cationized-bovine serum albumins at the blood-nerve and blood-brain barriers in awake rats. J Neurosci Res **1992**; *32*:407-414.

[78] Agarwal A, Agrawal H, Tiwari S, et al. Cationic ligand appended nanoconstructs: A prospective strategy for brain targeting. Int J Pharm **2011**; *421*:189-201.

[79] Hsu MH, Su YC. Iron-oxide embedded solid lipid nanoparticles for magnetically controlled heating and drug delivery. Biomed Microdevices **2008**; *6*:785-793.

[80] Bareschino MA, Schettino C, Rossi A, et al. Treatment of advanced non small cell lung cancer. J Thorac Dis **2011**; *3*:122-133.

[81] National cancer institute; general information about non-small cell lung cancer treatment, **2012**. Available at: http://www.cancer.gov/cancertopics/pdq /treatment/non-small-cell-lung/healthprofessional [Last accessed 14 May 2012].

[82] Shi SJ, Zhong ZR, Liu J, et al. Solid lipid nanoparticles loaded with anti-microRNA oligonucleotides (AMOs) for suppression of MicroRNA-21 functions in human lung cancer cells. Pharm Res **2012**; *29*:97-109.

[83] Wan F, You J, Sun Y, et al. Studies on PEG-modified SLNs loading vinorelbine bitartrate (I): Preparation and evaluation in vitro. Int J Pharm **2008**; *359*:104-110

[84] You J, Wan F, de Cui F, et al. Preparation and characteristic of vinorelbine bitartrate-loaded solid lipid nanoparticles. Int J Pharm **2007**; *343*:270-276.

[85] Amoozgar Z, Yeo Y. Recent advances in stealth coating of nanoparticle drug delivery systems. Wiley Interdiscip Rev Nanomed Nanobiotechnol **2012**; *4*:219-233.

[86] National cancer institute; general information about colon cancer, **2012**. Available at: http://www.cancer.gov/cancertopics/pdq/treatment/colon/Health Professional/page1 [Last accessed 14 May 2012].

[87] Yassin AE, Anwer MK, Mowafy HA, et al. Optimization of 5-flurouracil solid-lipid nanoparticles: A preliminary study to treat colon cancer. Int J Med Sci **2010**; *7*:398-408.

[88] Minelli R, Serpe L, Pettazzoni P, et al. Cholesteryl butyrate solid lipid nanoparticles inhibit the adhesion and migration of colon cancer cells. Br J Pharmacol **2011**; *166*:587-601.

[89] American cancer society; breast cancer, **2012**. Available at: http://www.cancer.org/Cancer/BreastCancer/DetailedGuide/breast-cancer-treating-general-info [Last accessed 14 May 2012].

[90] Lu B, Xiong SB, Yang H, et al. Solid lipid nanoparticles of mitoxantrone for local injection against breast cancer and its lymph node metastases. Eur J Pharm Sci **2006**; *28*:86-95.

[91] Reddy LH, Vivek K, Bakshi N, et al. Tamoxifen citrate loaded solid lipid nanoparticles (SLN): Preparation, characterization, in vitro drug release, and pharmacokinetic evaluation. Pharm Dev Technol **2006**; *11*:167-177.

[92] Zhigaltsev IV, Winters G, Srinivasulu M, et al. Development of a weak-base docetaxel derivative that can be loaded into lipid nanoparticles. J Control Release **2010**; *144*:332-340.

[93] Gong X, Moghaddam MJ, Sagnella SM, et al. Lamellar crystalline self-assembly behaviour and solid lipid nanoparticles of a palmityl prodrug analogue of capecitabine--a chemotherapy agent. Colloids Surf B Biointerfaces **2011**; *85*:349-359.

[94] Hrycushko BA, Gutierrez AN, Goins B, et al. Radiobiological characterization of post-lumpectomy focal brachytherapy with lipid nanoparticle-carried radionuclides. Phys Med Biol **2011**; *56*:703-719.

[95] Alvarez P, Marchal JA, Boulaiz H, et al. 5-fluorouracil derivatives: A patent review. Expert Opin Ther Pat **2012**; *22*:107-123.

[96] Venishetty VK, Komuravelli R, Kuncha M, et al. Increased brain uptake of docetaxel and ketoconazole loaded folate grafted solid lipid nanoparticles. Nanomedicine **2013**; *9*: 111-121.

[97] Kuo YC, Liang CT. Inhibition of human brain malignant glioblastoma cells using carmustine-loaded catanionic solid lipid nanoparticles with surface anti-epithelial growth factor receptor. Biomaterials **2011**; *32*:3340-3350.

[98] Brioschi A, Zara GP, Calderoni S, et al. Cholesterylbutyrate solid lipid nanoparticles as a butyric acid prodrug. Molecules **2008**; *13*:230-254.

[99] Goppert TM, Muller RH. Plasma protein adsorption of tween 80- and poloxamer 188-stabilized solid lipid nanoparticles. J Drug Target **2003**; *11*:225-231.

[100] Mollinedo F, de la Iglesia-Vicente J, Gajate C, et al. In vitro and in vivo selective antitumor activity of edelfosine against mantle cell lymphoma and chronic lymphocytic leukemia involving lipid rafts. Clin Cancer Res **2010**; *16*:2046-2054.

[101] Estella-Hermoso de Mendoza A, Campanero MA, de la Iglesia-Vicente J, et al. Antitumor alkyl ether lipid edelfosine: Tissue distribution and pharmacokinetic behavior in healthy and tumor-bearing immunosuppressed mice. Clin Cancer Res **2009**; *15*:858-864.

[102] American cancer society: Ovarian cancer, **2010**. Available at: http://www.cancer.org/Cancer/OvarianCancer/DetailedGuide/ovarian-cancer [Last accessed 20 May 2012].

[103] Siddiqui A, Patwardhan GA, Liu YY, et al. Mixed backbone antisense glucosylceramide synthase oligonucleotide (MBO-asGCS) loaded solid lipid nanoparticles: In vitro characterization and reversal of multidrug resistance in NCI/ADR-RES cells. Int J Pharm **2010**; *400*:251-259.

[104] Zhang P, Chen L, Zhang Z, et al. Pharmacokinetics in rats and efficacy in murine ovarian cancer model for solid lipid nanoparticles loading docetaxel. J Nanosci Nanotechnol **2010**; *10*:7541-7544.

[105] Lee MK, Lim SJ, Kim CK. Preparation, characterization and in vitro cytotoxicity of paclitaxel-loaded sterically stabilized solid lipid nanoparticles. Biomaterials 2007; 28:2137-2146.

[106] Sanjula B, Shah FM, Javed A, et al. Effect of poloxamer 188 on lymphatic uptake of carvedilol-loaded solid lipid nanoparticles for bioavailability enhancement. J Drug Target **2009**; *17*:249-256.

[107] Reddy LH, Adhikari JS, Dwarakanath BS, et al. Tumoricidal effects of etoposide incorporated into solid lipid nanoparticles after intraperitoneal administration in dalton's lymphoma bearing mice. AAPS J **2006**; *8*:E254-262.

[108] Ma P, Dong X, Swadley CL, et al. Development of idarubicin and doxorubicin solid lipid nanoparticles to overcome pgp-mediated multiple drug resistance in leukemia. J Biomed Nanotechnol **2009**; *5:*151-161.

[109] Pan X, Chen L, Liu S, et al. Antitumor activity of G3139 lipid nanoparticles (LNPs). Mol Pharm **2009***; 6*:211-220.

[110] Bauman JA, Li SD, Yang A, et al. Anti-tumor activity of splice-switching oligonucleotides. Nucleic Acids Res **2010**; *38*:8348-8356.

[111] de Jesus MB, Ferreira CV, de Paula E, et al. Design of solid lipid nanoparticles for gene delivery into prostate cancer. J Control Release **2010**; *148*:e89-90.

[112] French JT, Goins B, Saenz M, et al. Interventional therapy of head and neck cancer with lipid nanoparticle-carried rhenium 186 radionuclide. J Vasc Interv Radiol **2010**; *21*:1271-1279.

[113] Holpuch AS, Hummel GJ, Tong M, et al. Nanoparticles for local drug delivery to the oral mucosa: Proof of principle studies. Pharm Res **2010**; *27*:1224-1236.

[114] Kohane DS, Langer R. Biocompatibility and drug delivery systems. Chem Sci **2010**; 1:441-446.

[115] Joshi MD, Muller RH. Lipid nanoparticles for parenteral delivery of actives. Eur J Pharm Biopharm **2009**; *71*:161-172.

[116] Severino P, Andreani T, Macedo AS, et al. Current state-of-art and new trends on lipid nanoparticles (SLN and NLC) for oral drug delivery. J Drug Deliv **2012**, doi:10.3109/10837450.2011.591804.

[117] Almeida AJ, Souto E. Solid lipid nanoparticles as a drug delivery system for peptides and proteins. Adv Drug Deliv Rev **2007**; *59*:478-490.

[118] Fangueiro JF, Gonzalez-Mira E, Martins-Lopes P, et al. A novel lipid nanocarrier for insulin delivery: Production, characterization and toxicity testing. Pharm Dev Technol **2013**; 18:545-549.

[119] Liu J, Gong T, Fu H, et al. Solid lipid nanoparticles for pulmonary delivery of insulin. Int J Pharm **2008**; *356:333*-344.

[120] Rawat MK, Jain A, Singh S. In vivo and cytotoxicity evaluation of repaglinide-loaded binary solid lipid nanoparticles after oral administration to rats. J Pharm Sci **2011**; *6:*2406-2407.

[121] Wissing SA, Kayser O, Muller RH. Solid lipid nanoparticles for parenteral drug delivery. Adv Drug Deliv Rev **2004**; *56*:1257-1272.

[122] Smijs TG, Bouwstra JA. Focus on skin as a possible port of entry for solid nanoparticles and the toxicological impact. J Biomed Nanotechnol **2010**; *6*:469-484.

[123] Spada G, Gavini E, Cossu M, et al. Solid lipid nanoparticles with and without hydroxypropyl-beta-cyclodextrin: A comparative study of nanoparticles designed for colonic drug delivery. Nanotechnology **2012**; published on line 6 Feb 2012, doi: doi:10.1088/0957-4484/23/9/095101.

[124] Estella-Hermoso de Mendoza A, Calvo P, Bishop A, et al. Comparison of pharmacokinetic profiles of PM02734 loaded lipid nanoparticles and cyclodextrins: In vitro and in vivo characterization. J Biomed Nanotechnol **2012**; *8*:723-728.

[125] Feng L, Wu H, Ma P, et al. Development and optimization of oil-filled lipid nanoparticles containing docetaxel conjugates designed to control the drug release rate in vitro and in vivo. Int J Nanomedicine **2011**; *6:*2545-2556.

[126] Lim S, Lee M, Kim C. Altered chemical and biological activities of all-trans retinoic acid incorporated in solid lipid nanoparticle powders. J Control Release **2004**; *100*:53-61.

[127] Song H, Nie S, Yang X, et al. Characterization and in vivo evaluation of novel lipid-chlorambucil nanospheres prepared using a mixture of emulsifiers for parenteral administration. Int J Nanomedicine **2010**; *5*:933-942.

[128] Wang L, Liu Z, Liu D, et al. Docetaxel-loaded-lipid-based-nanosuspensions (DTX-LNS): Preparation, pharmacokinetics, tissue distribution and antitumor activity. Int J Pharm **2011**; *413*:194-201.

[129] Piao H, Ouyang M, Xia D, et al. In vitro–in vivo study of CoQ10-loaded lipid nanoparticles in comparison with nanocrystals. Int J Pharm **2011**; *419*:255-259.

[130] Teskac K, Kristl J. The evidence for solid lipid nanoparticles mediated cell uptake of resveratrol. Int J Pharm **2010**; *390*:61-69.

[131] Lee P, Zhang R, Li V, et al. Enhancement of anticancer efficacy using modified lipophilic nanoparticle drug encapsulation. Int J Nanomedicine **2012**; *7*:731-737.

[132] Dong X, Mattingly CA, Tseng M, et al. Development of new lipid-based paclitaxel nanoparticles using sequential simplex optimization. Eur J Pharm Biopharm **2009**; *72*:9-17.

[133] Oyewumi MO, Mumper RJ. Gadolinium-loaded nanoparticles engineered from microemulsion templates. Drug Dev Ind Pharm **2002**; *28*:317-328.

[134] Gallarate M, Trotta M, Battaglia L, et al. Cisplatin-loaded SLN produced by coacervation technique. J Drug Deliv Sci Tech **2010**; *20*:343-347.

[135] Chirio D, Gallarate M, Peira E, et al. Formulation of curcumin-loaded solid lipid nanoparticles produced by fatty acids coacervation technique. J Microencapsul **2011**; *28*:537-548.

[136] Battaglia L, Serpe L, Muntoni E, et al. Methotrexate-loaded SLNs prepared by coacervation technique: In vitro cytotoxicity and in vivo pharmacokinetics and biodistribution. Nanomedicine **2011**; *6*:1561-1573.

[137] Lamprecht A, Benoit J. Etoposide nanocarriers suppress glioma cell growth by intracellular drug delivery and simultaneous P-glycoprotein inhibition. J Control Release **2006**; *112*:208-213.

[138] Malzert-Fréon A, Vrignaud S, Saulnier P, et al. Formulation of sustained release nanoparticles loaded with a tripentone, a new anticancer agent. Int J Pharm **2006**; *320*:157-164.

[139] Lacoeuille F, Hindre F, Moal F, et al. In vivo evaluation of lipid nanocapsules as a promising colloidal carrier for paclitaxel. Int J Pharm **2007**; *344*:143-149.

[140] Yu YH, Kim E, Park DE, et al. Cationic solid lipid nanoaprticles for co-delivery of paclitaxel and siRNA. Eur J Pharm Biopharm **2012**; *80*:268-273.

[141] Tian J, Pang X, Yu K, et al. Preparation, characterization and in vivo distribution of solid lipid nanoparticles loaded with cisplatin. Pharmazie **2008**; *63*:593-597.

[142] Ali H, Shirode AB, Sylvester PW, et al. Preparation, characterization, and anticancer effects of simvastatin-tocotrienol lipid nanoparticles. Int J Pharm **2010**; *389*:223-231.

[143] Das S, Ng WK, Kanaujia P, et al. Formulation design, preparation and physicochemical characterizations of solid lipid nanoparticles containing a hydrophobic drug: Effects of process variables. Colloids Surf B Biointerfaces **2011**; *88*:483-489.

[144] Videira M, Almeida AJ, Fabra A. Preclinical evaluation of a pulmonary delivered paclitaxel-loaded lipid nanocarrier antitumor effect. Nanomedicine **2012**; 8:1208-1215.

[145] Abuasal BS, Lucas C, Peyton B, et al. Enhancement of intestinal permeability utilizing solid lipid nanoparticles increases gamma-tocotrienol oral bioavailability. Lipids **2012**; *47*:461-469.

[146] Pandita D, Ahuja A, Velpandian T, et al. Characterization and in vitro assessment of paclitaxel loaded lipid nanoparticles formulated using modified solvent injection technique. Pharmazie **2009**; *64*:301-310.

[147] Wang T, Wang N, Zhang Y, et al. Solvent injection-lyophilization of tert-butyl alcohol/water cosolvent systems for the preparation of drug-loaded solid lipid nanoparticles. Colloids Surf B Biointerfaces **2010**; *79*:254-261.

CHAPTER 2

Edelfosine lipid nanosystems overcome drug resistance in leukemic cell lines

---

*Beatriz Lasa-Saracíbar[1], Ander Estella-Hermoso de Mendoza[1], Faustino Mollinedo[2], María D. Odero[3], María J. Blanco-Príeto[1]**

[1]Dept. of Pharmaceutics and Pharmaceutical Technology, School of Pharmacy, University of Navarra, E-31080 Pamplona, Spain

[2]Instituto de Biología Molecular y Celular del Cáncer-Centro de Investigación del Cáncer, CSIC-Universidad de Salamanca, Campus Miguel de Unamuno, E-37007 Salamanca, Spain

[3]Division of Oncology, Center for Applied Medical Research (CIMA), University of Navarra, E-31080 Pamplona, Spain

Keywords: Alkyl-lysophospholipids, edelfosine, lipid nanoparticles, leukemia

***Corresponding author:** Dra. Maria J. Blanco Prieto, Dept. of Pharmaceutics and Pharmaceutical Technology, School of Pharmacy, University of Navarra, Spain. C/Irunlarrea 1, E-31080, Pamplona, Spain, Office phone: + 34 948 425 600 ext. 6519, Fax: + 34 948 425 649, e-mail: mjblanco@unav.es

Declaration of interest: The authors state no conflict of interest

Cancer Letters. 2013 Jul;334(2):302-10

Abstract

Although current therapies have improved leukemia survival rates, adverse drug effects and relapse are frequent. Encapsulation of edelfosine (ET) in lipid nanoparticles (LN) improves its oral bioavailability and decreases its toxicity. Here we evaluated the efficacy of ET-LN in myeloid leukemia cell lines. Drug-loaded LN were as effective as free ET in sensitive leukemia cell lines. Moreover, the encapsulated drug overcame the resistance of the K562 cell line to the drug. LN containing ET might be used as a promising drug delivery system in leukemia due to their capacity to overcome the *in vivo* pitfalls of the free drug and their efficacy *in vitro* in leukemia cell lines.

1. Introduction

Cancer is one of the leading causes of death worldwide, and the World Health Organization (WHO) estimates that it will cause 13.1 million deaths in 2030 [1]. Among all cancer types, leukemia represents 3% of total cancer cases [2]. Acute myeloid leukemia (AML) is a heterogeneous clonal disease that disrupts normal hematopoiesis. Leukemic cells are characterized by a block in differentiation and apoptosis, together with an enhanced proliferation. Despite progressive advances in our understanding of the molecular biology of AML, patient outcomes are still very poor. Complete remission occurs in up to half of these patients; however, relapse is generally expected and prognosis is dismal [3]. Therefore, it is necessary to develop more effective treatment strategies to improve the survival of these patients [4]. Among these new therapies, treatment with ether lipids has emerged as a potential alternative to the current ones. Edelfosine (ET) (1-O-octadecyl-2-O-methyl-sn-glycero-3-phosphocholine) is the prototype of a promising class of anticancer drugs known as synthetic alkyl-lysophospholipids (ALPs), which selectively target tumor cells sparing healthy ones [5]. ET is active against several tumor cell lines [5-7]. The exact mechanism of action of ET still remains to be fully elucidated, but it has been proved that it accumulates in membrane lipid rafts by recruiting and promoting clustering of Fas/CD95 receptors [6,8-10]. Moreover, other apoptotic mechanisms involving mitochondria and endoplasmic reticulum have also been hypothesized [11]. Previous studies have demonstrated that ET induces a rapid apoptotic response in leukemia cells [6]; nevertheless, Tidwell et al. showed that the cell line K562, established from a patient with chronic myeloid leukemia in blast crisis (CML-BC), presents resistance to the action of the drug [12]. Another work by Tsutsumi et al. demonstrated that ET was internalized at a slower rate in ET resistant cells (K562) than in ET sensitive cells (HL-60) [13].

Regardless of promising *in vitro* results, ET presents some drawbacks when it is administered *in vivo*, such as gastrointestinal and hemolytic toxicity and low oral bioavailability [6,14]. These *in vivo* disadvantages led to the vehiculization of the drug using nanotechnology [15]. This technology has been widely used in an attempt to

improve the therapeutic index of drugs by improving their bioavailability, lowering toxic effects and achieving targeted localization [16]. Among the nanoparticulate systems, lipid nanoparticles (LN) are colloidal carriers that can be produced by an organic solvent free method. Furthermore, these systems have been able to avoid the *in vivo* drawbacks of ET, diminishing its side effects and increasing its oral bioavailability [17]. Taking this into consideration, the aim of this research was to evaluate the *in vitro* intracellular uptake and efficacy of drug-loaded LN after administration to sensitive and resistant cell lines.

2. Material and methods

2.1 Chemicals

ET was purchased from APOINTECH (Salamanca, Spain). Precirol® ATO 5 was a gift from Gattefossé (France). Tween® 80 was purchased from Roig Pharma (Barcelona, Spain). Chloroform was from Panreac (Madrid, Spain), formic acid 99% for mass spectroscopy was obtained from Fluka (Barcelona, Spain), and methanol was purchased from Merck (Barcelona, Spain). All solvents employed for the chromatographic analysis were of analytical grade; all other chemicals were of reagent grade and used without further purification. Amicon Ultra-15 10,000 MWCO centrifugal filter devices were purchased from Millipore (Cork, Ireland). Bovine serum albumin (BSA), trehalose, propidium iodide (PI), RNase, paraformaldehyde and nile red (NR) were acquired from Sigma (Barcelona, Spain). RPMI 1640 and DMEM cell culture media, heat-inactivated fetal bovine serum (FBS) and penicillin/streptomycin antibiotics were purchased from Life Technologies, Invitrogen (Barcelona, Spain). DAPI was obtained from Invitrogen (Madrid, Spain). Fluorescence mounting medium was obtained from Dako (Barcelona, Spain).

2.2 Preparation and characterization of LN loaded with ET

LN were prepared by the hot homogenization method consisting of high shear homogenization and ultrasonication [18]. ET (15 mg) and Precirol® (300 mg) were

melted at approximately 5ºC above the melting point of the lipid (60ºC). A 2% Tween® 80 aqueous solution (10 mL) previously heated at the same temperature was added and dispersed in the molten lipid with the help of a Microson™ ultrasonic cell disruptor (NY, USA) for 1 min at an effective power of 10W. The preformed emulsion was then homogenized with an Ultraturrax® (IKA-Werke, Germany) for 1 min at 24,000 rpm and sonicated again with a Microson™ ultrasonic cell disruptor (NY, USA) for 1 min at 10W. The emulsion was removed from heat and placed in an ice bath to obtain LN by lipid solidification. In order to remove the excess of surfactant and non-incorporated drug, the LN suspension was centrifuged using Amicon® Ultra-15 10,000 MWCO filters at 4500 × g for 30 min and washed twice with distilled water. Afterwards, 10% (w/v) trehalose was added as cryoprotectant agent to the LN suspension, which was then kept at -80ºC and freeze-dried to obtain a nanoparticulate powder.

Particle size and polydispersity index (PDI) were evaluated by photon correlation spectroscopy (PCS) using a Zetasizer Nano (Malvern Instruments, UK). Each formulation was diluted 30-fold in distilled water in order to avoid multiscattering events. The measurements were carried out three times. Surface charge was measured using the same Zetasizer Nano equipment combined with laser Doppler velocimetry. For the ET loading determination, 5 mg of nanoparticles were dissolved in 1 ml of chloroform and mixed with 4 ml of methanol. The mixture was vortexed for 1 min and then centrifuged at 20,000 × g for 10 min. The supernatant was analyzed by a previously validated ultra-high-performance liquid chromatography tandem mass spectrometry (UHPLC-MS/MS) method [19].

2.3 Morphology of ET LN

Morphology of ET LN was observed by transmission electron microscopy (Philips CM120 TEM). Briefly, 5 µL of the sample were put on carbon film supported by a copper grid previously submitted to glow discharge and blotted with filter paper to obtain a thin liquid film on the grid. The sample-loaded grid was stained with uranyl acetate for 60 seconds and blotted with filter paper afterwards. The images were recorded with a digital camera (Morada, Olympus).

2.4 Cell culture

Four AML cell lines (HL-60, HEL, OCI-AML-2 and MOLM-13) and one CML-BC cell line (K562) were used in this study. HL-60, HEL, MOLM-13 and K562 cell lines were grown in RPMI 1640 culture medium supplemented with 10% FBS, 100 units/mL penicillin and 100 µg/mL streptomycin at 37ºC in humidified 95% air and 5% CO2. OCI-AML2 was grown in DMEM culture medium supplemented with 10% FBS, 100 units/mL penicillin and 100µg/mL streptomycin at 37ºC in humidified 95% air and 5% CO2.

2.5 Cell proliferation and viability assays

Cell proliferation and viability were assessed by MTS, included in the CellTiter 96® Aqueous One Solution Cell Proliferation Assay (Promega, Madrid, Spain). Cells were treated with culture medium containing various concentrations of free ET, empty nanoparticles (blank-LN) or drug-loaded LN and seeded (100 µL, 4•104 cells per well) in 96-well culture plates. Plates were incubated at 37ºC in 5% CO2. After different incubation times (0, 24, 48 and 72 hours), MTS reagent solution was added to culture plate (20 µL in each well), the mixture was incubated for 2 hours and the formazan production was measured by a microplate spectrophotometer (Labsystems, Helsinki, Finland) at 490 nm with a reference wavelength of 690 nm.

2.6 Apoptosis and cell cycle assays

Apoptosis Staining with Annexin-V-Fluos Kit (Roche, Madrid, Spain) was used for these experiments. Cells were treated with culture medium containing various concentrations of free-ET, blank-LN or drug-loaded LN and seeded in 12-well culture plates (4 mL, 1.6•106 cells per well).

Quantification of apoptotic cells after each treatment was performed by flow cytometry using Annexin-V-FLUOS Staining Kit® following the manufacturer's instructions. Cells were harvested (500 µL), centrifuged at 200 × g for 5 min at 20ºC and washed with PBS. Afterwards, they were suspended in 100 µL of Annexin-V-

FLUOS labeling solution. This solution was incubated for 15 min at room temperature, 300 µL of the incubation buffer were added to each cytometer tube after the incubation time and samples were analyzed on a FacsCalibur flow cytometer (Becton Dickinson, NJ, USA).

For the cell cycle analysis, cells were harvested (500 µL), centrifuged at 200 × g for 5 min at 20°C and washed twice with PBS. Cells were then treated with ice-cold ethanol 70% in order to fix them and permeabilize their membrane; samples were then washed with PBS and suspended in a mixture of 445 µL of PBS, 50 µL of PI and 5 µL of RNase per sample. Finally, cells were incubated in darkness for 1 hour and analyzed by flow cytometry.

2.7 LN uptake

NR-loaded LN were formulated by adding the fluorochrome (0.34% w/w) to the lipid phase (method described in section 2.2). HL-60 and K562 cells were treated with culture medium containing various concentrations of free-ET, blank-LN or NR-LN and seeded in 24-well culture plates (500 µL, 3•105 cells per well). After different incubation times, cells were collected by centrifugation, washed twice with PBS and analyzed in a flow cytometer. For the microscopy studies, cells were fixed with p-formaldehide 4% (300 µl, 5 min). They were then stained with DAPI for 5 min. Samples were then placed on 24-well plates with a cover glass on the surface of the wells. Cells were adhered to the surface of the cover glass by centrifugation of the plate at 260 × g for 5 min. Finally, cover glasses were extracted and placed on microscope slides with fluorescence mounting media. Samples were examined on a fluorescence microscope (Zeiss, 120 Libra).

2.8 Caspase-3/8/9 detection

Caspase 9 and 3 activities were detected by CaspGlowTM Red Active Caspase-9 Staining Kit and CaspGlowTM Fluorescein Active Caspase-3 Staining Kit, respectively (BD Biosciences, Madrid, Spain). Caspase 8 activity was detected by cleaved Caspase-8 (Asp 391) (18C8) (Cell Signaling, Barcelona, Spain). HL-60 and K562 cells were

treated with culture medium containing various concentrations of free-ET, blank-LN or drug-loaded LN and seeded in 24-well culture plates (500 µL, 5•105 cells per well). After different incubation times, cells were incubated with the antibody (caspase-3/9) provided in the kits following the manufacturer's instructions. For the caspase-8 assay, cells were fixed with p-formaldehyde, permeabilized with methanol (90%) and washed twice with a solution of BSA (0.5%). Antibody was then added and incubated for 1 hour at room temperature. Samples were then washed twice with incubation buffer and analyzed by flow cytometry.

2.9 Statistical analysis

Each experiment was repeated three times (n = 3) and the average of the three values was used for statistical calculations. Each experimental value was expressed as mean ± standard deviation (SD). Statistical analyses were performed using GraphPad Prism 5. Groups that are significantly different from control are indicated in the figures as *$p < 0.05$, **$p < 0.01$ and ***$p < 0.001$.

3. Results and discussion

Nanotechnology applications in medicine have improved the therapeutic efficacy of many anticancer drugs [16]. The encapsulation of the ether lipid ET into LN has led to a reduction of its *in vivo* toxicity and to an increase in its oral bioavailability [17]. These promising *in vivo* results, along with the great efficacy of the free drug shown *in vitro* in myeloid leukemia [5], opened up the possibility of applying this formulation to this disease. This study aimed to investigate the *in vitro* antitumor effect of ET in LN versus the free drug in myeloid leukemia cells (HL-60, HEL, OCI-AML-2, MOLM-13 and K562).

3.1 LN containing ET: physicochemical characterization.

The average size was close to 100 nm, suitable for oral administration with a PDI index less than 0.3 in all cases, suggesting homogenous distribution of the nanoparticulate suspension (Table 1). Blank-LN presented a size 20 nm over drug-

loaded LN. This difference may be attributed to the tensoactive properties of the drug given by its amphiphilic nature. LN charge was negative and enough to maintain nanoparticle stability [20].

Table 1. Physicochemical characteristics of the developed LN (mean ± SD)

Formulation	Size (nm)	PDI	ζ-potential (mV)	EE (%)	Drug loading (µg drug/mg formulation)
Blank-LN	123.80 ± 9.02	0.260 ± 0.015	-28.1 ± 2.4	--	--
Drug-loaded LN	104.83 ± 3.40	0.248 ± 0.006	-26.5 ± 5.6	75.75 ± 10.26	13.02 ± 0.99
NR-LN	117.53 ± 1.58	0.246 ± 0.010	-21.5 ± 0.4	--	--
Drug-loaded NR-LN	103.27 ± 1.65	0.260 ± 0.010	-14.9 ± 0.5	91.86 ± 9.11	11.87 ± 1.52

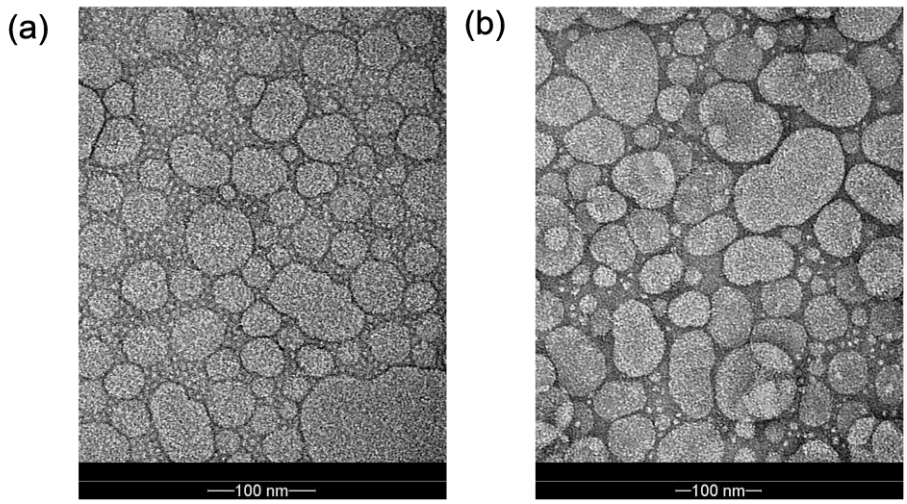

Figure 1. TEM images of blank-LN (a) and Drug-loaded LN (b).

TEM images (Fig. 1) confirmed the size of LN previously measured by PCS. The LN obtained showed good encapsulation efficiency of 75%, presenting a drug loading of 13 µg ET per mg of formulation.

3.2 ET antitumor effect in sensitive cell lines is preserved when using encapsulated drug, while drug activity in the resistant cell line is enhanced when it is included in LN.

Previous *in vitro* studies have shown that leukemia cells have different sensitivities to the antitumor action of ET [5]. Hence, we aimed to classify the cell lines used in this work into sensitive and resistant cells, in order to reveal the advantage of encapsulating the drug. MTS proliferation assay was used to obtain the IC_{50} of free and encapsulated drug in the different leukemia cells. Comparison of IC_{50} values of free ET and drug-containing LN (Table 2) led to the classification of the cell lines in two groups based on their sensitivity to the free drug: sensitive cell lines (HL-60, OCI-AML-2, MOLM-13 and HEL) and resistant (K562). HL-60, MOLM-13, HEL and OCI-AML-2 showed similar low IC_{50} values that were, in all cases, less than 5 µM when treated with free drug, OCI-AML-2 being the most sensitive to the action of the free drug with an IC_{50} of 0.64 µM. LN were more efficient in OCI-AML-2 and MOLM-13 and less efficient in HL-60 and HEL. Nevertheless, IC_{50} values of nanoencapsulated drug were less than 9 µM in all sensitive cell lines.

Table 2. IC_{50} values of leukemia cell lines alter 72 h of incubation with free-ET and Drug-loaded LN.

Cell type	Cell name	Free-ET (µM)	Loaded LN (µM)
Human acute myeloid leukemia	**HL-60**	3.48	8.64
Human acute myeloid leukemia	**OCI-AML-2**	0.64	0.22
Human acute myeloid leukemia	**MOLM-13**	3.64	3.41
Human erythroleukemia	**HEL**	4.42	7.96
Human chronic myeloid leukemia	**K562**	57.70	20

To further clarifyied theseis results, Figure 2 shows dose-responses curves of ET and ET-LN of in MOLM-13, selected as representative sensitive cell lines, and in K-562 resistant cell line. As it can be seen, the dose- response curves for the sensitive cell line isare similar showing similarcomparable IC_{50} values for ET and ET-LN. In contrast for to the resistant sensitive cell lines, ET-LN were able to produce a pronounced cell growth inhibition in the resistant K562 cell line compared to free ET. Indeed, the IC_{50}

of ET in this cell line, was 20 µM for the drug-loaded LN compared to 57.50 µM of the free ET (Figure 2 and Table 2).

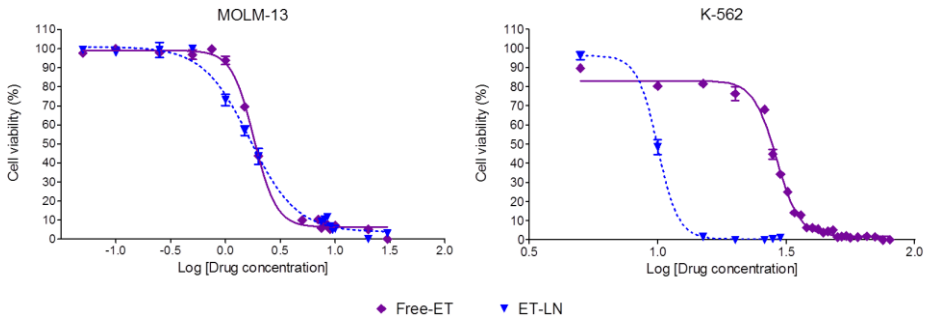

Figure 2. Dose- reponse curve in sensitive (MOLM-13) and resistant (K-562) cells at 72 hours of incubation with different doses of free ET or drug-loaded LN.

Cell proliferation was measured by MTS reagent, which is bioreduced by metabolically active cells. Proliferation studies were carried out in all the cell lines at different drug concentrations over a period of 72 h. The efficacy of drug-loaded LN in inhibiting cell growth was similar to the free drug in sensitive cell lines (HL-60, MOLM-13, OCI-AML-2 and HEL). Both treatments showed fast and potent inhibition of cell proliferation, achieving in some cases a complete inhibition of cell viability after 72 hours of incubation. In these cell lines, free and drug-loaded LN were effective at the lowest dose (5 µg/ml, 9.5 µM) used in the study. The initial effect of the free drug is faster in sensitive cell lines probably due to the time needed by the encapsulated drug to be internalized and released into the cell; indeed, the antitumor effect is similar at the end of the treatment with both treatments. In resistant cell line K562, free ET showed a slight inhibition effect, whereas encapsulated drug was able to inhibit proliferation from the first 24 hours of incubation at a LN dose equivalent to 10 µg/ml (19 µM) of free drug. This overcoming of resistance might be related to an increased ET concentration inside the cell after LN uptake; it also could be associated with an enhanced apoptotic mechanism due to the different intracellular localization of the drug. These results prove that

encapsulating the drug in LN does not affect drug activity in sensitive leukemia cells; moreover, nanoencapsulated ET was able to overcome the resistance to the free drug in the case of resistant cells.

Cytotoxicity of LN containing ET versus the free drug was analyzed by flow cytometry. Viable, early apoptotic, late apoptotic and necrotic cells can be distinguished by flow cytometric analysis using dual staining with annexin V-FITC and PI dyes. Viable cells are negative for both stains; early apoptotic cells bind annexin due to the expression of phosphatidylserine in the outer-leaflet of cell membrane and late apoptotic cells bind both stains because PI only binds DNA when the cell membrane losses its integrity. Our data showed that ET induced cell death in a dose- and time-dependent manner. As in proliferation studies, free ET was able to induce apoptosis earlier than the encapsulated drug in sensitive cell lines; Fig. 3 shows the induction of apoptosis by the different treatments in OCIAML-2 cells after 24 and 72 hours of incubation. However, the percentages of apoptotic cells produced by both treatments were equivalent after 72 hours of incubation, being the percentage of viable cells in OCI-AML-2 less than 10 % (Fig. 3).

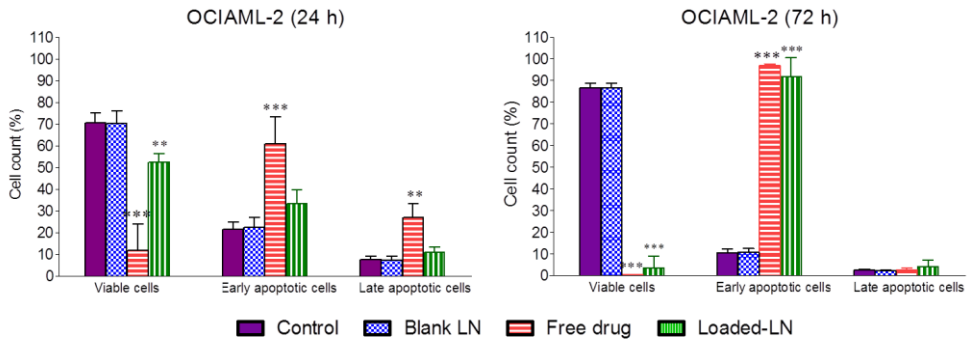

Figure 3. Apoptosis induced in OCI-AML-2 (sensitive cells) by the different treatments (9.5 µM of ET) after 24 h and 72 h of incubation. **p < 0.01; ***p < 0.001 vs. control by two-way ANOVA (Bonferroni post-test).

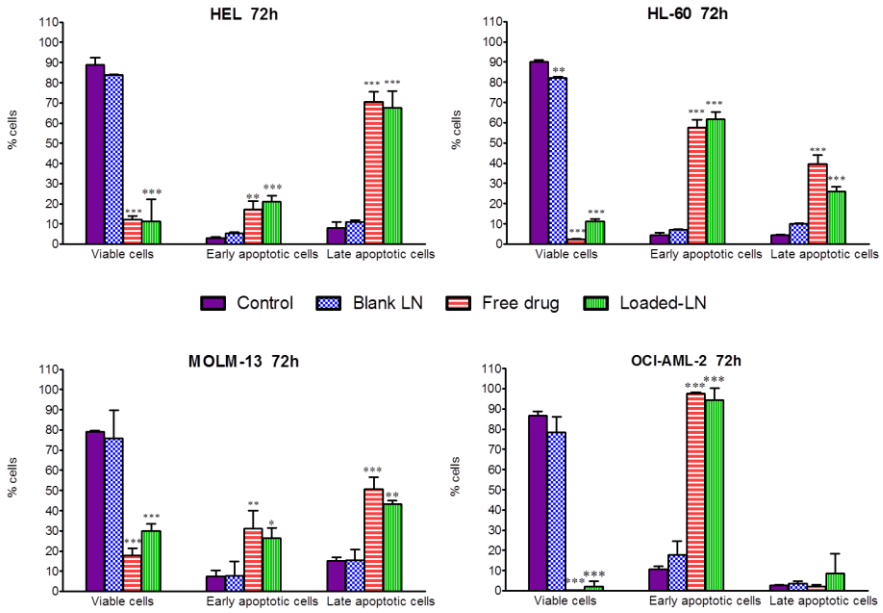

Figure 4. Apoptosis induced in sensitive cell lines by the different treatments (19 µM of ET) after 72 h of incubation. *p < 0.05; **p < 0.01; ***p < 0.001 vs. control by two-way ANOVA (Bonferroni post-test).

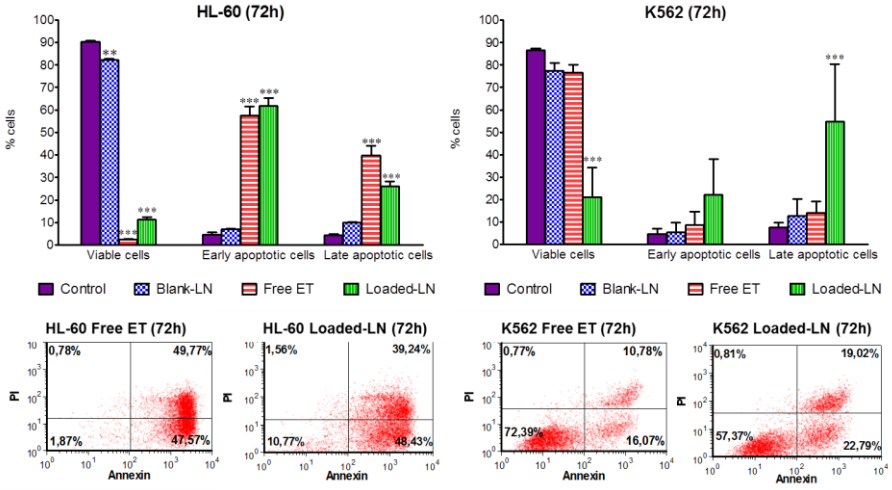

Figure 5. Flow cytometry graphs of apoptosis induced in HL-60 and K562 cells after 72 hours of incubation with medium, blank-LN, free ET and drug-loaded LN at a dose equivalent to 19 µM (HL-60) and 28.6 µM (K562) of free ET. *p < 0.05; **p < 0.01; ***p < 0.001 vs. control by two-way ANOVA (Bonferroni post-test).

Figure 4 shows the percentage of apoptotic cells in sensitive cells after 72 hours of incubation with both treatments (free and nanoencapsulated drug); these results

prove that encapsulating the drug in LN does not affect its apoptotic effect. In K562 cells, free ET did not show any apoptotic effect; in contrast, drug-loaded LN were able to diminish the number of living cells at a dose equivalent to 15 µg/ml (28.6 µM) of ET. Figure 5 shows that drug-loaded LN were able to decrease significantly the percentage of viable cells with respect to the untreated cells after 72 hours of incubation with the treatment.

The cell cycle is a tightly regulated process in normal cells and cancer is closely related to cell cycle abnormalities. Cell cycle steps are deregulated due to mutations in proto-oncogenes and tumor suppressor genes [21]. In cancer cells, cell cycle checkpoints are altered and cells undergo uncontrolled growth. Many antitumor drugs act at this level inducing cell arrest and preventing cell division. As a result, cell cycle analysis was performed to examine whether the inhibition of cell proliferation and apoptosis induction involved cell cycle changes. The results obtained are in accordance with previous studies that affirm that ET inhibits cell division leading to the accumulation of cells into G2/M [22]. ET induces a G2/M cell cycle arrest increase percentage of dead cells in sensitive cells (Fig. 6).

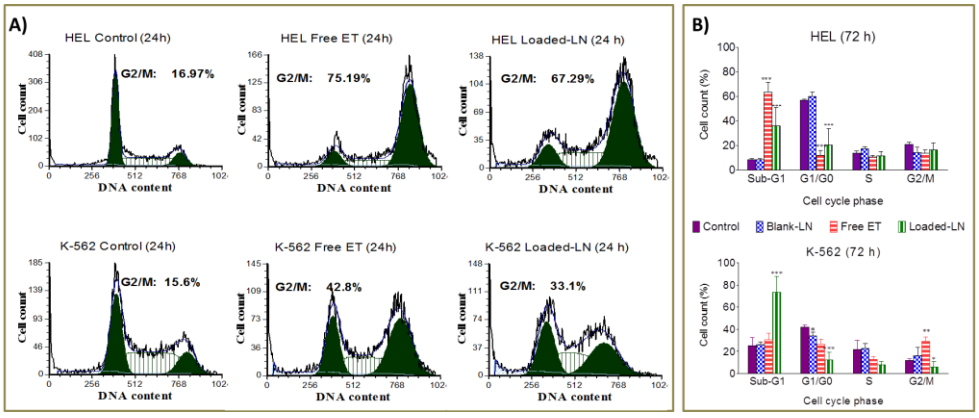

Figure 6. (A) Free and nanoencapsulated drug effect in cell cycle distribution in sensitive (HEL) and resistant (K562) cells after 24 (A) and 72 (B) hours of incubation. Cells were treated with medium, blank-LN, free ET and drug-loaded LN at a dose equivalent to 9.5 µM of ET (HEL) and 28.6 µM of ET (K562). *p < 0.05; **p < 0.01; ***p < 0.001 vs. control by two-way ANOVA (Bonferroni post-test).

As it was observed in apoptosis studies, free drug effect was faster but both treatments achieved similar death rates at the end of the treatment in sensitive cells (Fig. 7). The analysis of K562 cell cycle revealed that, again, drug-loaded LN were

effective inducing cell cycle arrest in G2/M phase (Fig. 6). Free-ET also induces this phase arrest; however, cell cycle arrest might not be enough to induce apoptosis and cell cycle analysis also shows that only loaded LN increase the percentage of cells in Sub G1 peak (dead cells) in resistant cells. This led to the conclusion that only the encapsulated drug is able to trigger the whole machinery of apoptotic mechanisms in resistant cells.

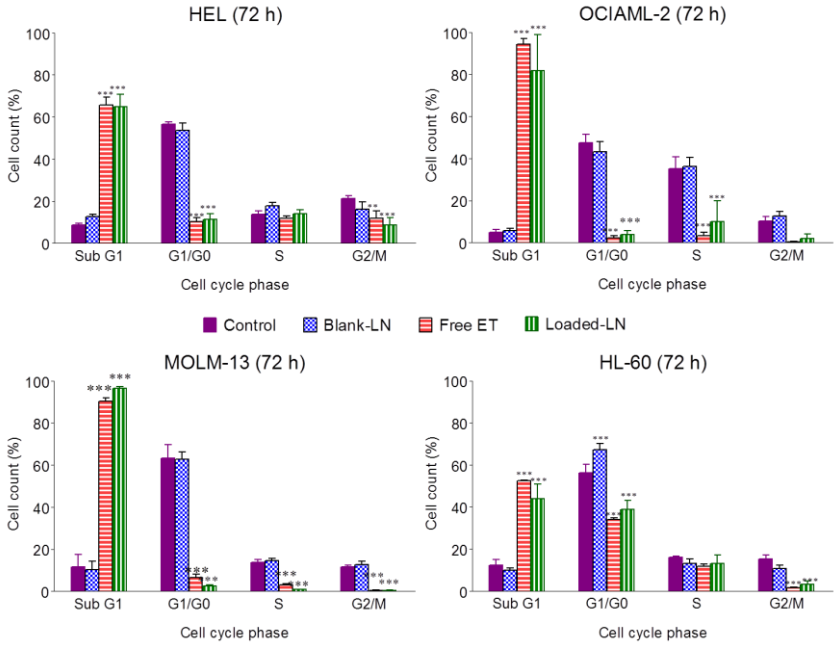

Figure 7. Analysis of cell cycle distribution in sensitive cell lines by the different treatments (at a dose corresponding to 19 µM of ET) after 72 h of incubation. *p < 0.05; **p < 0.01; ***p < 0.001 vs. control by two-way ANOVA (Bonferroni post-test)

3.3 NR-LN are internalized quickly and in a time-dependent manner in sensitive and resistant cell lines.

In contrast to free ET, which interacts with the cell membrane and accumulates in lipid rafts [23], LN require endocytosis to release the drug inside the cell [24]. This process might change the antitumor activity of the drug because ET LN might target the drug to a different intracellular localization. ET cell entry occurs through membrane lipid rafts [23]; however, drug-loaded LN might have a different

intracellular localization after nanoparticle entry. Nanoparticle uptake by leukemia cells was studied incorporating a lipophilic fluorochrome into the LN. NR was added to the lipid phase and LN were formulated following the same method as for ET-loaded LN. NR-LN showed similar size, PDI and charge to drug-loaded LN. Drug-loaded NR-LN were also formulated confirming that NR does not affect ET encapsulation. However, drug-loaded NR-LN charge was -14.9 mV and, therefore, blank-LN were used to study nanoparticle internalization on the basis of their similarity to the original formulation (Table 1). To evaluate LN uptake, HL-60 (sensitive) and K562 (resistant) cells were incubated with NR-LN for different times. The NR-LN internalization was analyzed by fluorescence microscopy and flow cytometry (Fig. 8 and 9).

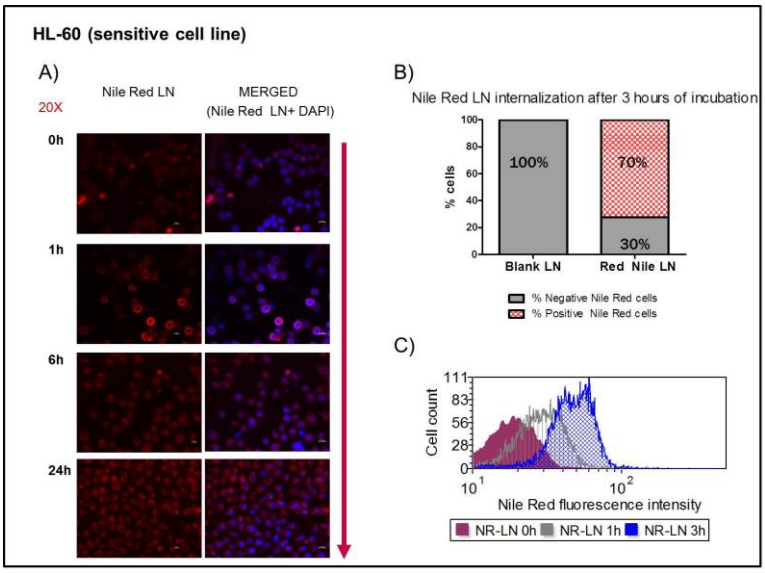

Figure 8. (A) Fluorescence images of HL-60 cells cultured with NR-LN for different incubation times. (B) Flow cytometry graph corresponding to NR-LN uptake by HL-60 cells after 3 hours of incubation with NR-LN. (C) Flow cytometry analysis of NR-LN uptake within the time (3 hours) after incubation of HL-60 cells with NR-LN.

The data reported here show that LN were internalized into leukemia cancer cells very rapidly and in a time-dependent manner in both cell lines. This internalization might be independent of cell sensitivity to the free drug since it is incorporated in the LN. This could mean that, in contrast to free ET [13], encapsulated drug might easily

be incorporated into K562 cells enhancing its intracellular concentration, which could trigger a major response to the drug. Interestingly, Fig. 8 shows how LN accumulate in the cell membrane after one hour of incubation indicating a strong interaction between the particles and cells. Furthermore, red fluorescence was all over the cytoplasm avoiding the nucleus at later incubation times. Unfortunately, the extended diffusion of the fluorochrome avoided the colocalization inside the cytoplasm with different organelle labels, thus hampering the determination of the exact localization the nanoparticles inside the cell. These results are consistent with previous uptake studies of LN by Teskac and Kristl [25] that show the rapid internalization and diffuse localization of LN containing 6-coumarin dye in keratinocytes. Nanoparticle uptake was quantified by flow cytometry to obtain a quantitative analysis of NR-LN internalization. The results showed accordance with fluorescence microscopy studies. Nanoparticles were internalized in a time-dependent manner achieving 70% of cells containing fluorescent nanoparticles after 3 hours of incubation (Fig. 8). This internalization pattern was also observed in resistant cells (Fig. 9) confirming the microscopy results.

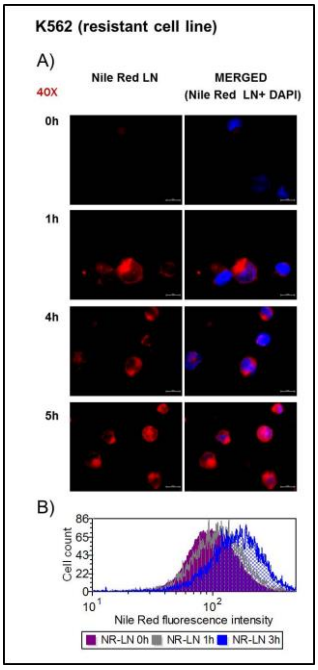

Figure 9. (A) Fluorescence images of K562 cells cultured with NR-LN for different incubation times. (B) Flow cytometry graph corresponding to NR-LN uptake by K562 cells within the time (3 h).

3.4 Free and encapsulated ET induce Caspases-3, 8 and 9 only in sensitive cells.

The exact mechanism of action of ET still remains remains to be fully elucidated; however, it has been seen that there are many different mechanisms implicated. Intrinsic and extrinsic apoptotic signaling pathways are considered the major programmed mechanisms of cell death. Both processes are mediated by cysteine proteases named caspases. The intrinsic apoptosis pathway is mediated by mitochondria, and caspase-9 is considered the predominant initiator caspase. The extrinsic pathway is triggered from the cell membrane and it is mediated by death receptors, such as Fas/CD95 receptor. In this case, signaling cascade is mainly initiated by caspase-8 cleavage. Both apoptotic mechanisms converge in the induction of caspases-3/7 [26].

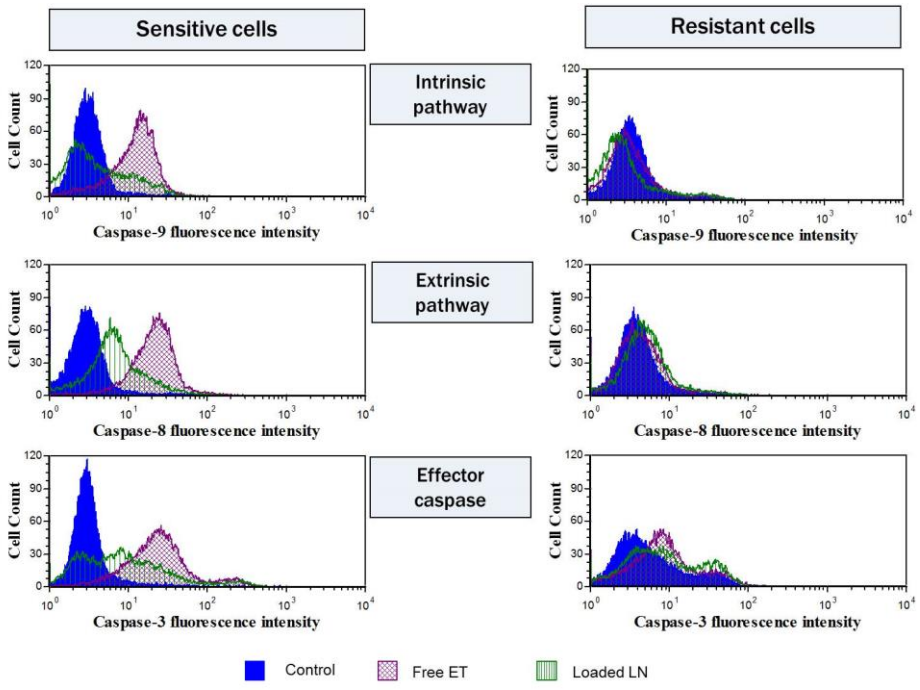

Figure 10. Caspase-9, 8 and 3 activation in HL-60 (sensitive) and K562 (resistant) cells by flow cytometry. Cells were untreated (control), treated with free ET (Free-ET) or drug-loaded LN (Loaded-LN) with a dose equivalent to 19 µgM free ET and analyzed after 72 hours of incubation.

Recent studies suggest that ET mainly accumulates in membrane lipid rafts and triggers the extrinsic apoptotic pathway throughout Fas/CD95 death receptor

[9,10,23,27]. However, this mechanism might be diminished in the case of encapsulated drug, as it could be directed to different cell targets once inside the cell, promoting other drug actions and therefore overcoming resistance to the drug. In fact, it has also been described that ET also triggers the intrinsic apoptotic signaling pathway [23,28]. Besides, there are more mechanisms implicated such as endoplasmic reticulum stress and the production of reactive oxygen species [29,30].

To gain further insight into mechanisms for apoptosis induction, HL-60 and K562 cells were incubated with free and drug-loaded LN and samples were analyzed after different incubation times by flow cytometry to detect activated caspases. Free ET and LN containing the drug induced the cleavage of caspase-8 and 9 and, subsequently, also induced caspase-3 in HL-60 cells (Fig. 10). This caspase induction in sensitive leukemia cells occurs with free and encapsulated drug but it is faster when cells are treated with free ET. Caspase induction was time-dependent becoming more pronounced after 72 hours of incubation. However, no caspase induction was observed in K562 cells regardless of the treatment. Bearing in mind that drug-loaded LN induce apoptosis mediated death as was demonstrated by flow cytometry analysis; these data suggest the existence of caspase independent apoptosis pathways triggered by encapsulated ET. In fact, other mechanisms such as oxygen reactive species production have already been described as ET antitumor mechanism [29,30]. Drug-loaded LN might be able to overcome the resistance of K562 cells to the entrance of the free drug. This increased influx of drug into the cell increases its apoptotic mechanism overcoming drug resistance. Among the apoptotic mechanisms that might be involved in the loaded LN effect, we have demonstrated that encapsulated drug triggers a G2/M peak arrest in cell cycle. Although free-ET also induces a cell cycle arrest, this effect is not able to induce apoptosis by itself. Therefore, loaded LN might be able to induce multiple apoptotic mechanisms that finally overcome free drug resistance.

4. Conclusions

The present research allows us to conclude that LN are potential vehicles of ET in myeloid leukemia. LN are internalized in sensitive and resistant leukemia cells

possibly overcoming the difficulties of the free ET in being internalized in K562 cells. LN preserve the potent apoptotic effect that free ET has in sensitive leukemia cells by means of caspase activation. Nanoparticles could be triggering other pathways of programmed cell death that appear to be independent from caspase activation in edelfosine-resistance cells.

5. References

[1] WHO: Cancer, **2012**. Available at: http://www.who.int/mediacentre/ factsheets/fs297/en/ [last accessed 09 October 2012].

[2] Iarc: Globocan **2008** fast stats. Available at: http://globocan.iarc.fr/factsheets /populations/factsheet.asp?uno=900 [last accessed 09 October 2012].

[3] J.M. Rowe, Optimal induction and post-remission therapy for AML in first remission. Hematology, Am Soc Hematol Educ Program. 1 (**2009**) 396–405.

[4] T. Haferlach, Molecular genetic pathways as therapeutic targets in acute myeloid leukemia, Hematology Am Soc Hematol Educ Program 1 (**2008**) 400–411.

[5] F. Mollinedo, J.L. Fernández-Luna, C. Gajate, B. Martín-Martín, A. Benito, R. Martinez-Dalmau, M. Modolell, Selective induction of apoptosis in cancer cells by the ether lipid ET-18-OCH3 (edelfosine): Molecular structure requirements, cellular uptake, and protection by bcl-2 and bcl-X(L), Cancer Res. 57 (**1997**) 1320-1328.

[6] F. Mollinedo, J. de la Iglesia-Vicente, C. Gajate, A. Estella-Hermoso de Mendoza, J.A. Villa-Pulgarín, M. de Frias, G. Roué , J. Gil , D. Colomer, M.A. Campanero, M.J. Blanco-Prieto, In vitro and in vivo selective antitumor activity of edelfosine against mantle cell lymphoma and chronic lymphocytic leukemia involving lipid rafts, Clin. Cancer Res. 16 (**2010**) 2046-2054.

[7] F. Mollinedo, J. de la Iglesia-Vicente, C. Gajate, A. Estella-Hermoso de Mendoza, J.A. Villa-Pulgarin, M.A. Campanero, M.J. Blanco-Prieto, Lipid raft-targeted therapy in multiple myeloma, Oncogene 26 (**2010**) 3748-3757.

[8] F. Mollinedo, C. Gajate, Fas/CD95 death receptor and lipid rafts: New targets for apoptosis-directed cancer therapy, Drug Resist Updat. 9 (**2006**) 51-73.

[9] C. Gajate, F. Mollinedo, The antitumor ether lipid ET-18-OCH3 induces apoptosis through translocation and capping of Fas/CD95 into membrane rafts in human leukemic cells, Blood. 98 (**2001**) 3860-3863.

[10] C. Gajate, E. del Canto-Jañez, A.U. Acuña, F. Amat-Guerri, E. Geijo, A.M. Santos-Beneit, R.J. Veldman, F. Mollinedo, Intracellular triggering of Fas aggregation and recruitment of apoptotic molecules into Fas-enriched rafts in selective tumor cell apoptosis, J Exp Med 200, (**2004**) 353-365.

[11] C. Gajate, M. Matos-da-Silva, E.L. Dakir, R.I. Fonteriz, J. Alvarez, F. Mollinedo, Antitumor alkyl-lysophospholipid analog edelfosine induces apoptosis in pancreatic cancer by targeting endoplasmic reticulum, Oncogene 31 (**2012**) 2627-2639.

[12] T. Tidwell, G. Guzman, W.R. Vogler, The effects of alkyl-lysophospholipids on leukemic cell lines. I. Differential action on two human leukemic cell lines, HL60 and K562, Blood. 57 (**1981**) 794-797.

[13] T. Tsutsumi, A. Tokumura, S. Kitazawa, Undifferentiated HL-60 cells internalize an antitumor alkyl ether phospholipid more rapidly than resistant K562 cells, Biochim. Biophys. Acta. 1390 (**1998**) 73-84.

[14] C. Gajate, F. Mollinedo, Biological activities, mechanisms of action and biomedical prospect of the antitumor ether phospholipid ET-18-OCH3 (edelfosine), a proapoptotic agent in tumor cells, Curr Drug Metab 3, (**2002**) 491-525.

[15] A. Estella-Hermoso de Mendoza, M. Rayo, F. Mollinedo, M.J. Blanco-Prieto, Lipid nanoparticles for alkyl lysophospholipid edelfosine encapsulation: Development and in vitro characterization, Eur. J. Pharm. Biopharm. 68 (**2008**) 207-213.

[16] A. Estella-Hermoso de Mendoza, B. Lasa-Saracíbar, M.A, Campanero, M.J. Blanco-Prieto, Lipid Nanoparticles in Biomedicine, Encyclopaedia of Nanoscience and Nanotechnology, American Scientific Publishers, USA, **2010**, pp 455-478.

[17] A. Estella-Hermoso de Mendoza, M.A. Campanero, H. Lana, J.A. Villa-Pulgarin, J. de la Iglesia-Vicente, F. Mollinedo, M.J. Blanco-Prieto, Complete inhibition of extranodal dissemination of lymphoma by edelfosine-loaded lipid nanoparticles, Nanomedicine UK. 7 (**2012**) 679-690.

[18] A. Estella-Hermoso de Mendoza, V. Preat, F. Mollinedo, M.J. Blanco-Prieto, In vitro and in vivo efficacy of edelfosine-loaded lipid nanoparticles against glioma, J. Control. Release. 3 (**2011**) 421-426.

[19] A. Estella-Hermoso de Mendoza, M. A. Campanero, F. Mollinedo, M. J. Blanco-Prieto, Comparative study of a HPLC-MS assay versus an UHPLC-MS/MS for anti-tumoral alkyl lysophospholipid edelfosine determination in both biological samples and in lipid nanoparticulate systems, J. Chromatogr. B. Analyt Technol. Biomed. Life. Sci. 877 (**2009**) 4035-4041.

[20] S. Das, A. Chaudhury, Recent advances in lipid nanoparticle formulations with solid matrix for oral drug delivery, AAPS PharmSciTech. 12 (**2011**) 62-76.

[21] F. McLaughlin, P. Finn, N.B. La Thangue, The cell cycle, chromatin and cancer: Mechanism-based therapeutics come of age, Drug Discov. Today. 8 (**2003**) 793-802.

[22] K. P. Boggs, C. O. Rock, S. Jackowski, Lysophosphatidylcholine attenuates the cytotoxic effects of the antineoplastic phospholipid 1-O-octadecyl-2-O-methyl-rac glycero-3- phosphocholine, J Biol Chem 270 (**1995**) 270-11612.

[23] C. Gajate, F. Mollinedo, Edelfosine and perifosine induce selective apoptosis in multiple myeloma by recruitment of death receptors and downstream signaling molecules into lipid rafts, Blood. 109 (**2007**) 711-719.

[24] G. Sahay, D.Y. Alakhova, A.V. Kabanov, Endocytosis of nanomedicines, J. Control. Release. 145 (**2010**) 182-195.

[25] K. Teskac, J. Kristl, The evidence for solid lipid nanoparticles mediated cell uptake of resveratrol, Int. J. Pharm. 390 (**2010**) 61-69.

[26] B. Favaloro , N. Allocati1, V. Graziano, C. Di Ilio, V. De Laurenzi, Role of Apoptosis in disease, Aging 4 (**2012**) 330-349.

[27] C. Gajate, F. Mollinedo, Lipid rafts and Fas/CD95 signaling in cancer chemotherapy, Recent. Pat. Anticancer Drug Discov. 6 (**2011**) 274-283.

[28] C. Gajate, A. M. Santos-Beneit, A. Macho, M. Lazaro, A. Hernandez-De Rojas, M. Modolell, E. Muñoz, F. Mollinedo, Involvement of mitochondria and caspase-3 in

ET-18-OCH(3)-induced apoptosis of human leukemic cells, Int. J. Cancer. 86 (**2000**) 208-218.

[29] H. Zhang, C. Gajate, L.P. Yu, Y.X. Fang, F. Mollinedo, Mitochondrial-derived ROS in edelfosine-induced apoptosis in yeasts and tumor cells, Acta Pharmacol Sin. 28 (**2007**) 888-894.

[30] V.A. Selivanov, P. Vizán, F. Mollinedo, T.W. Fan, P.W. Lee, M. Cascante, Edelfosine-induced metabolic changes in cancer cells that precede the overproduction of reactive oxygen species and apoptosis, BMC Syst Biol. 4 (**2010**) 135.

CHAPTER 3

Edelfosine Lipid Nanoparticles overcome MDR in K-562 leukemia cells by caspase-independent mechanism

---

*Beatriz Lasa-Saracíbar‡-María Ángela Aznar‡, Maria J. Blanco-Prieto**

Dept. of Pharmaceutics and Pharmaceutical Technology, School of Pharmacy, University of Navarra, Pamplona, Spain

Key words: Apoptosis, autophagy, edelfosine, endocytosis, leukemia, lipid nanoparticles

***Corresponding author:** Dr. María J. Blanco-Prieto, Department of Pharmaceutics and Pharmaceutical Technology, School of Pharmacy, University of Navarra, C/Irunlarrea 1, E-31080 Pamplona, Spain, Office phone: + 34 948 425 600 ext. 6519, Fax: + 34 948 425 649, e-mail: mjblanco@unav.es

Author Contributions: ‡These authors contributed equally.

Declaration of interest: The authors state no conflict of interest.

Submitted to Molecular Pharmaceutics

Abstract

The anti-tumor ether lipid edelfosine is the prototype of a novel generation of promising anticancer drugs that has been shown as an effective anti-tumor agent in numerous malignancies. However, several cancer types display resistance to different antitumor compounds due to multi-drug resistance (MDR). Thus, MDR is a major drawback in anticancer therapy.

In that sense, the leukemic cell line K-562 shows resistance to edelfosine due to MDR. This resistance can be overcome by the use of nanotechnology. The present paper describes the rate and mechanism of internalization of free and nano-encapsulated edelfosine. The molecular mechanisms underlying cell death is described in the present paper by characterization of several molecules implied in the apoptotic and autophagic pathways (PARP, LC3IIB, Caspases-3, -9 and -7) and its pattern of expression is compared with the cell induction in a cell line HL-60 sensitive to edelfosine.

Our results showed different internalization patterns in HL-60 and K-562 cells. Clathrin and lipid rafts mediated endocytosis were observable in edelfosine uptake whereas these mechanisms were not visible in the uptake of lipid nanoparticles which might suffer phagocytosis and macropinocytosis. Both treatments endorsed caspase-mediated apoptosis in HL-60 cells, whereas this cell death mechanism was not noticeable in K-562 cells. Moreover, an important increase in autophagic vesicles was visible in K-562 cells, so this mechanism might be implicated in overcoming K-562's resistance to edelfosine by using lipid nanoparticles.

1. Introduction

Therapeutic systems based on the nanometric scale, known as nanomedicines, are currently at the cutting edge of drug development. Among all nanomedicines, lipid nanoparticles (LN) have been shown to be effective vehicles for overcoming MDR in cancer cells [1]. Edelfosine (ET) is an antitumor drug of the alkylphospholipid (ALP) family with proven antitumor efficacy [2, 3]. Previous studies developed by our research group have shown that LN containing ET (ET-LN) are as effective as free drug and prevent severe side-effects of ET such as hemolysis and gastrointestinal toxicity [4, 5]. Furthermore, ET-LN are able to overcome MDR in leukemia [4] and breast cancer cells [6]. These results might be explained by the different mechanisms of entry by which the free and the encapsulated drug enter the cell. Different mechanisms of drug incorporation could influence/boost the intracellular concentration of ET or might change its intracellular trafficking, promoting different death mechanisms. Despite the increase in research in the field of LN, the uptake mechanism of these nanosystems by cells is not clear, although it seems to be dependent on the nanoparticle material and the cell type [7].

LN may interact with the plasmatic membrane and be internalized into the cell being delivered to different intracellular compartments. The uptake mechanism might entail a location of the nanoparticles different from that of the free drug. Mammalian cells accomplish different uptake pathways that promote the delivery of the cargos into different subcellular compartments. Nanoparticles might enter the cell either by endocytosis or, to a lesser extent, by passive transport [8, 9]. Endocytic pathways are typically classified into two subtypes: phagocytosis and pinocytosis. Phagocytosis is characteristic of specialized cells (with Fc receptors and complement receptors) such as macrophages, monocytes, neutrophils and dendritic cells, whereas pinocytosis occurs in all kind of mammalian cells.

ET uptake by cancer cells has been shown to be dependent on the cell type [10]. Raft-mediated endocytosis seems to be the major entry mechanism in leukemia cells whereas an energy-dependent mechanism involving a lipid transporter/translocase (flippase) has been found in carcinoma cells [11-13]. Flippases are membrane

proteins that translocate phospholipids from one leaflet of the bilayer to the opposing one in order to assure the assembly and maintenance of the lipid bilayer structure of cellular membranes [14]. Phospholipid flip-flop in plasmatic membrane of eukaryotic cells is highly regulated and energy-dependent. Lipid translocation from the outer to inner membrane leaflet promotes endocytic vesicle formation and accelerates endocytosis by stabilization of the vesicles with coating proteins such as clathrin CDE [14].

The uptake mechanism of a toxic compound into a cell would influence the pathway of cell demise. In general, cell death can be achieved by different intracellular mechanisms (apoptosis, necrosis, autophagic cell death). Thus, the diverse cell death mechanisms can be distinguished according to their morphological and molecular features [15, 16].

Several studies have described apoptosis induction in response to drug-loaded nanoparticles in cancer cell lines [4, 6, 17], pointing towards the potential of lipid nanoparticles as anticancer agents [1]. On the other hand, autophagy and autophagic cell death are reported to be induced as a response to different classes of nanoparticles such as quantum dots, gold nanoparticles, and iron oxide nanoparticles [18-21]. However, the role of LN in autophagic cell death induction remains unclear.

It has been previously demonstrated that ET-LN induces greater cell death than the free drug in several leukemic cell lines, overcoming the resistance of K-562 to ET [4]. Besides, previous flow cytometry studies revealed cell death induction in response to the ET-LN treatment that was caused by apoptosis activation in the sensitive cell line HL-60 but not in K-562 [4].

For these reasons, this study was focused on the uptake mechanisms of ET and ET-LN in HL-60 and K-562 leukemia cells. In addition, the molecular mechanisms implicated in cell death upon internalization of both the drug and the ET-LN in the cells was examined.

2. Material and methods

2.1 Chemicals

ET was purchased from APOINTECH (Salamanca, Spain). Precirol® ATO 5 was a gift from Gattefossé (France). Tween® 80 was purchased from Roig Pharma (Barcelona, Spain). Chloroform was from Panreac (Madrid, Spain), formic acid 99% for mass spectroscopy was obtained from Fluka (Barcelona, Spain), and methanol was purchased from Merck (Barcelona, Spain). Ultra-purified water was used throughout and all solvents employed for the chromatographic analysis were of analytical grade; all other chemicals were of reagent grade and used without further purification. Amicon Ultra-15 10,000 MWCO centrifugal filter devices were purchased from Millipore (Cork, Ireland). RPMI 1640 culture media, Heat-inactivated Fetal Bovine Serum (FBS), Glutamax, MEM Non-Essential Amino Acids and Penicillin/Streptomycin antibiotics were purchased from Life Technologies, (Barcelona, Spain). M-PER Mammalian Protein Extraction Reagent was purchased from Thermo Fisher Scientific (Madrid, Spain). Protease inhibitor cocktail was from Roche (Madrid, Spain). Genistein was purchased from LC Laboratories (Massachusetts, USA). Chlorpromazine, Methyl-β-cyclodextrin, Triton-X-100, DTT and Phosphate-buffered saline (PBS; 10 mM phosphate, 0.9% NaCl) were obtained from Sigma Aldrich Quimica (Madrid, Spain). The antibodies anti-PARP1 (9542), anti-caspase-3 (9662), anti-caspase-7 (9492), anti-caspase-9 (9508), and anti-LC3 I/II (4108) were purchased from Cell Signaling (Izasa, Barcelona, Spain), and anti-β-actin antibody was from Sigma Aldrich (Madrid, Spain).

2.2 Preparation and characterization of lipid nanoparticles

LN were prepared by the hot homogenization method consisting of high shear homogenization and ultrasonication [5]. ET (30 mg) and Precirol® (300 mg) were melted at approximately 5ºC above the melting point of the lipid (60ºC). A 2% Tween® 80 aqueous solution (10 mL) previously heated at the same temperature was added and dispersed in the molten lipid with the help of a Microson™ ultrasonic cell

disruptor (NY, USA) and an Ultraturrax® (IKA-Werke, Germany). The emulsion was removed from heat and placed in an ice bath to obtain LN by lipid solidification. Then, the LN suspension was centrifuged and washed twice with distilled water. Afterwards, 150 % (w/w of lipid weight) trehalose was added as cryoprotectant agent to the LN suspension, which was then kept at -80ºC and freeze-dried to obtain a nanoparticulate powder. Particle size and polydispersity index (PDI) were evaluated by photon correlation spectroscopy (PCS) using a Zetasizer Nano (Malvern Instruments, UK). Surface charge was measured using the same Zetasizer Nano equipment combined with laser Doppler velocimetry. ET loading determination was carried out after ET extraction from LN by a previously validated ultra-high-performance liquid chromatography tandem mass spectrometry (UHPLC-MS/MS) method [22].

2.3 Cell culture

Human cell lines HL-60 and K-562 (American Type Culture Collection, Manassas, VA, USA) were cultured at 5 x 105 cells/ml in RPMI supplemented with 20% (v/v) FBS, 100 units/mL penicillin and 100 µg/mL streptomycin at 37ºC in a humidified incubator supplemented with 5% carbon dioxide. Cells were split 1:3-1:5 every 3-4 days.

2.4 Study of endocytic pathways in leukemia cells

2.4.1 Quantification of internalized ET by UPLC-MS/MS

HL-60 and K-562 cells were incubated with the different treatments: i) free ET; ii) ET-LN at a dose equivalent to 5 µg/ml (9.55 µM) of the free drug. For the study of the involvement of energy in the endocytosis, cells were incubated for 3 h at 37ºC or at 4ºC. For the inhibition of the internalization pathways, cells were pre-incubated with medium (control), Genistein (200 µM, 120 minutes), Methyl-β-cyclodextrin (5 mM, 60 minutes) and Chlorpromazine (30 µM, 60 minutes). Afterwards, cells were washed three times with PBS, treatments were added and cells were incubated for 5 h. Next, cells were harvested, washed three times with PBS and lysed. The total amount of

proteins per sample was quantified using the Bradford assay and internalized ET was quantified by UPLC-MS/MS [22].

2.4.2 Visualization of endocytosis vesicles by transmission electron microscope (TEM)

HL-60 and K-562 cells were treated with culture medium containing i) free ET; ii) ET-LN at a dose equivalent to 10 µg/ml (19.1 µM) of the free drug and seeded in flask (500 µL, 5*105 cells per sample). After different incubation times (30 min. and 4 h.), cells were harvested and washed twice with PBS. Afterwards, cells were analyzed by a Zeiss EM10CR transmission electron microscope (TEM) following the method described elsewhere [23].

2.5 Study of cell death mechanisms

In brief, 4 X 106 cells were grown in the presence of ET, non-loaded LN (Blank-LN) and ET-LN in 25 cm2 culture flasks at 37ºC. According to the IC_{50} of both cell lines determined in our previous studies [4], 5 and 10 µg/mL (9.55 and 19.1 µM) of ET or equivalent concentrations of Blank-LN and ET-LN were selected for HL-60 and K-562 respectively. Afterwards, cells were collected to perform Western blot analysis.

Cells treated only with culture medium served as negative control for the experiment and cultures grown with EBSS starving medium and normal culture medium containing 1 µM of staurosporine served as positive controls for autophagy and apoptosis experiments respectively.

2.5.1 Western Blot Analysis

Cells were collected by centrifugation at 1500 rpm for 5 min, and were washed in PBS followed by detergent lysis (1% TRITON X-100, 1mM DTT), containing protease inhibitor cocktail. Protein concentration was determined by BRADFORD protein assay (Bio-Rad, Madrid, Spain).

Equal protein amounts of each sample were resolved in 15% SDS polyacylamide gel for LC3 I/II detection, and 12% SDS polyacrylamide gel for the detection of the

rest of proteins studied. Afterwards proteins were transferred to polyvinylidene difluoride membranes, washed with Tris buffered saline containing Tween (TBST) and blocked 1 h at RT with TBST containing 5% nonfat dry milk (TBSTM). Eventually, proteins of interest were detected by incubating overnight at 4ºC overnight in TBSTM with the following primary antibody dilutions: anti-PARP1 (1:2000), anti-caspase-3 (1:2000), anti-caspase-7 (1:5000), caspase-9 (1:5000), and LC3 I/II (1:5000); as loading control, membranes were then incubated with anti-β-actin antibody (1:10000). Afterward, membranes were incubated with the corresponding anti-mouse or anti-rabbit secondary antibody (Sigma Aldrich, Madrid, Spain) in a 1:5000 dilution for 1 h at room temperature. Proteins were visualized by using enhanced chemiluminescence detection reagents (Amersham Biosciences, Barcelona, Spain). Band intensities were detected and quantified using a GE Healthcare ImageQuant ECL system with IQuant Capture ECL software (GE Healthcare, Madrid, Spain). Experiments were performed in triplicate

For apoptosis detection, cells were collected at 24, 48 and 72 h after adding treatments and for autophagy detection, immunoblot of LC3 I/II was performed in samples of 24 and 48 h. LC3 I refers to the unconjugated form of LC3 protein and LC3 II is the form of the protein which is present in autophagosomal membranes. Both forms differ in molecular weight (14 and 12 KDa for LC3 I and LC3 II respectively), which allows their detection by western blot. Besides, LC3 II is rapidly degraded by lysosomal activity in autophagosomes. Thus lysosome degradation was blocked by adding 40mM of the lysosomotropic chemical NH_4Cl, a V-ATPase-independent neutralyzer of lysosomal pH to the culture medium 4 h before cells were collected [24, 25].

LC3 protein conversion was used as a marker of autophagy induction [26]. Autophagy was measured by LC3 immunoblotting and quantification of LC3 II/LC3 I ratio as previously described [27].

2.6 Statistical analysis

Data are presented as a mean of three or more independent experiments, with error bars indicating the standard deviation. Statistical comparisons were performed by analysis of variance, and further post-hoc testing was conducted using the statistical software GraphPad Prism 5 (GraphPad Software, Inc., San Diego, CA, USA). Groups that are significantly different from control are indicated in the figures as *$p < 0.05$, **$p < 0.01$; ***$p < 0.001$.

3. Results and discussion

3.1 Lipid Nanoparticles characterization

The hot homogenization method consisting of high shear homogenization and ultrasonication provided LN with a size of 127.89 ± 9.95 nm and negative surface charge (-28.42 ± 1.39). ET-LN loading was 22.677 ± 2.262 μg ET/mg.

3.2 Uptake of ET and ET-LN, an energy-dependent mechanism?

Phospholipids can be internalized in the cells by a passive transport consisting of a spontaneous or a facilitated (mediated by flippase) trans-bilayer movement from the outer to the inner leaflet of the cell membrane or by an active transport mediated either by a translocator protein (ATP-dependent flippase), or via an endocytic mechanism [10]. These mechanisms seem to be present in cell lines to a greater or lesser extent depending on the cell type. To assess the importance of endocytosis in ET and ET-LN uptake, leukemic cells were incubated with both treatments at 4ºC and at 37ºC. Results showed that ET and ET-LN uptake was energy-dependent and, therefore, it was inhibited at 4ºC (Fig. 1).

Comparing ET uptake in both cells, Fig. 1 shows that ET was internalized in a higher quantity (1.9 times higher) in HL-60 leukemia cells than in K-562 cells in normal culture conditions (37ºC). Results confirmed that an energy-dependent mechanism was involved in this uptake; in fact, ET uptake was decreased when cells

were incubated under 4ºC in both cell lines. Conversely, low temperature did not entirely prevent ET internalization, suggesting the implication of an energy-independent mechanism (passive transport) that seemed to be independent on the cell line as there were no significant differences in ET uptake in both cells lines at 4ºC. These results demonstrated that there might be a similar passive entry of ET in both cell lines and that, therefore, the differences in ET internalization in HL-60 and K-562 cells were due to the entry of the drug into the cells by an energy-dependent mechanism that predominate in HL-60 leukemia cells.

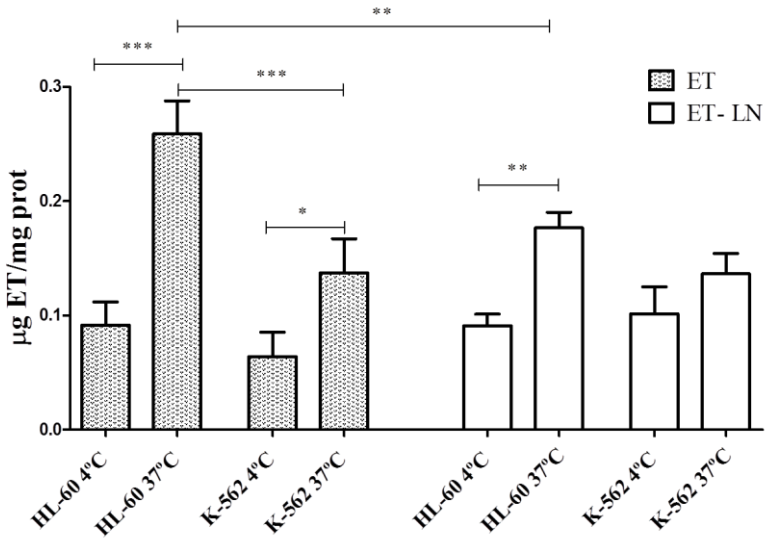

Figure 5. Graphic representation of edelfosine (ET) and lipid nanoparticles containing ET (ET-LN) internalization in HL-60 and K-562 cells after 3 h of incubation under different temperatures (4ºC and 37ºC). Values are means of triplicates ± SD. *P < 0.05; **P < 0.01; ***P < 0.001. One-way ANOVA (Bonferroni post-test).

LN internalization also seemed to involve passive and active (endocytosis) transport [7]. Results showed a higher internalization of drug (statistically significant in case of HL-60 cells) when cells were incubated at 37ºC. Besides, ET-LN were also incorporated at a similar rate by both cell lines at 4ºC. Previous studies have described the internalization of nanoparticles from 4 to 600 nm by passive membrane penetration in red blood cells [8, 28]. Although large nanoparticles may produce local membrane deformation with subsequent hemolysis, Zhao et al.[28]

showed that nanoparticles of 100 nm do not disturb the erythrocyte cell membrane. As the diameter of ET-was around 100 nm, this uptake mechanism should be further studied, since to our knowledge, there are no studies referring to LN passive transport in cells. The results obtained also indicated that encapsulating the drug in LN did not enhance its internalization in comparison to the free drug in both leukemia cell lines. Encapsulated ET was internalized to a lesser extent by HL-60 cells than free drug whereas it did not show differences with respect to the free drug in K-562 cells. Besides, ET-LN were incorporated at similar rates by both cell lines.

3.3 Effect of endocytosis inhibitors in ET and ET-LN uptake

ET uptake mechanisms seem to be dependent on the cell line. Lipid raft internalization is common in leukemic cells whereas spontaneous flipping (at a minor rate) or an energy-dependent mechanism which involves a lipid transporter/translocase (flippase) is found in other cancer cells [10]. In this sense, recent studies carried out by Rui Chen et al. [13] reported the involvement of the transmembrane protein subunit CD50a (TMEM30a) in the endocytosis of ET in mammalian cells. They demonstrated that ET endocytosis is an energy-dependent process mediated by TMEM30a in complex with a transmembrane phospholipid flippase (P4-ATPase).

To obtain deeper insights into the mechanisms implied in ET and ET-LN uptake, cells were pre-incubated with different endocytosis inhibitors: chlorpromazine, methyl betha cyclodextrin (MβCD) and genistein. Afterwards, cells were grown in medium containing either the free or nanoencapsulated drug (5 μg/ml; 9.55 μM) and internalized drug was quantified and normalized with respect to the total amount of protein.

Fig. 2 shows the results of the internalization of ET and ET-LN after pre-incubation of the cells with the inhibitors. Concerning the ET uptake, the internalization of the free drug in HL-60 cells was reduced by pre-incubating the cells with MβCD and Chlorpromazine suggesting an implication of lipid rafts and clathrin-mediated endocytosis respectively. These results were in agreement with previous

studies that refer to an accumulation of ET in lipid rafts in lymphoma and multiple myeloma cells and subsequent endocytosis [29-31]. Clathrin-mediated endocytosis of ET has also been described in lymphoma and epidermal carcinoma cells [12]. Although other authors have reported a passive uptake mechanism (not affected by endocytosis inhibitors) of ET in HL-60 cells [32], the present study showed a minor involvement of this ATP-independent entry of ET in HL-60 cells (Fig. 1). This energy-independent uptake might be mediated by ATP-independent flippases that non-specifically flip-flop phospholipids across the plasmatic membrane [14, 33].

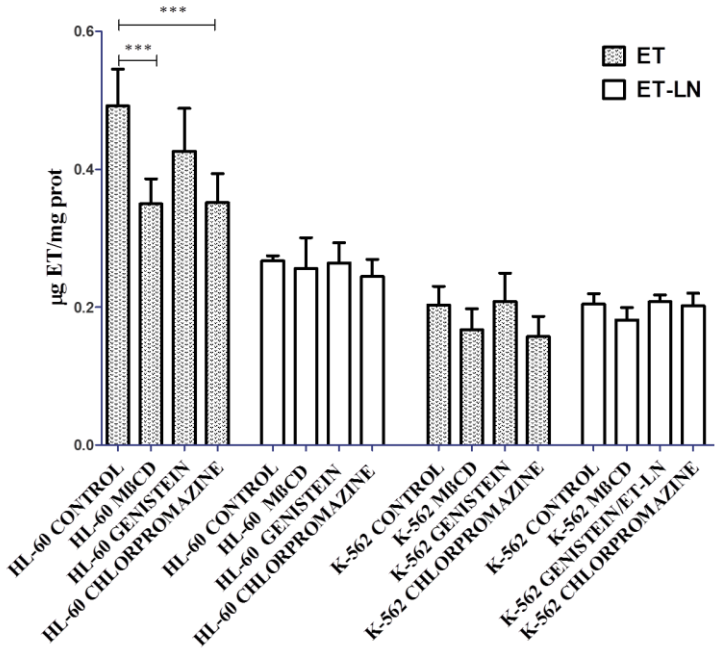

Figure 2. Uptake of edelfosine (ET) and lipid nanoparticles containing edelfosine (ET-LN) in HL-60 and K-562 cells after pre-incubation of the cells with different endocytosis inhibitors for 5 h. Values are means of triplicates ± SEM. ***P < 0.001. One-way ANOVA (Bonferroni post-test).

Regarding ET-resistant cell line K-562, the inhibition of endocytosis mechanisms induced a slight but not significant decrease in ET internalization suggesting a minor role of CME and lipid rafts endocytosis in this cell line. Therefore, ET uptake mechanisms such as spontaneous flipping from the outer to the inner leaflet [10] might be responsible for the free drug uptake in K-562 resistant cells.

Blocking CvME with genistein did not induce significant differences in free or encapsulated ET internalization in any of the two cell lines. Moreover, endocytosis inhibitors did not have any apparent effect in the internalization of ET-LN. Even though endocytosis of LN by caveolin [34] and clathrin [35] have been reported by other authors, we did not detect LN internalization via these routes in the present study. In case of these cells, absence of CvME endocytosis might be due to a lack of caveolae protein in the plasmatic membrane of these cells, since, as stated by some authors, the expression and/or distribution of this protein might be dependent on the activation and/or maturation state of immune cells [36]. The caveolae-mediated pathway should, therefore, not be discarded in other cancer cells.

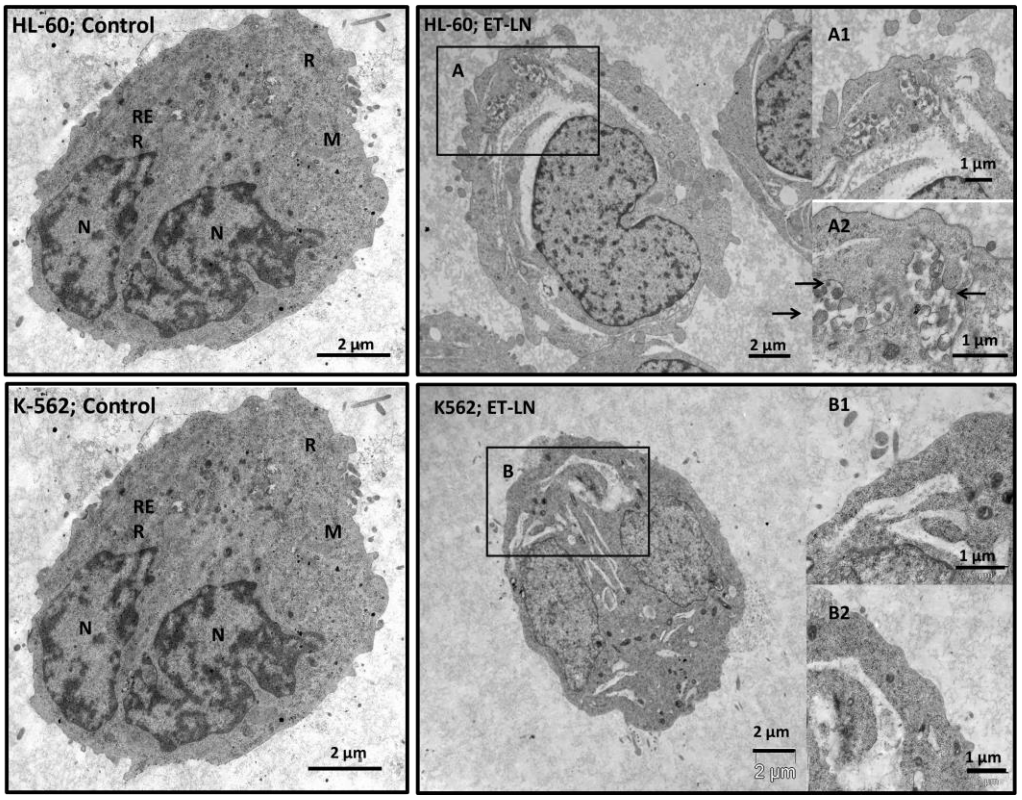

Figure 3. TEM images of HL-60 and K-562 cells after incubation with ET-LN. Control cells (upper and lower left) exhibited characteristic ultrastructural morphology of a control cell. N: nucleus; RER: rough endoplasmic reticulum; M: mitochondria; R: ribosomes and polyribosomes. Phagocytic like structures (arrows; A, A1, A2; B, B1, B2) were visible.

On the other hand, Guilleron et al [35] have recently showed that LN can be internalized via CME followed by macropinocytosis, suggesting that macropinocytosis

could be the major endocytic process involved in LN uptake, once it is activated after LN uptake by CME. Although we did not observe a CME of LN in this study, Guilleron et al. stated that the implication of CME in LN endocytosis accounted for less than 1% of total endocytic nanoparticles. Therefore, CME might be also occurring in our experiments even though it was not possible to detect it. Macropinocytosis might be, therefore, the major endocytosis mechanism involved in ET-LN internalization. Nevertheless, phagocytosis might be also a reliable endocytic mechanism in these cells; indeed, HL-60 and K-562 are reported to express Fc receptors (FcR) [37], a heterogeneous group of cell membrane receptors involved in phagocytosis due to its binding to immunoglobulins (Ig). In addition, LN could be opsonized by several opsonic factors such as IgG [38] and, therefore, ET-LN might be being phagocytized by HL-60 cells. This phagocytic activity might be more remarked in case of HL-60 cells due to their neutrophilic origin [39]. Nevertheless, it might be also feasible in K-562 cells; indeed, this cell line is characterized by their multipotential profile and their capacity to spontaneously differentiate into recognizable progenitors of the erythrocytic, granulocytic and monocytic series [40]. In this regard, TEM images showed phagocytic like structures filled with 100 nm spherical nanoparticles in HL-60 cells (Fig. 3). Similar structures were observed in K-562 cells (Fig. 3).

3.4 K-562 from HL-60 exhibit different molecular mechanisms that contribute to cell death in response to ET and ET-LN treatments

As has been previously described by flow cytometry studies, both K-562 and HL-60 cell lines presented massive cell demise when grown in presence of ET-LN, and therefore the viability of cells was significantly reduced. In the case of the ET-sensitive HL-60 cell line, comparable levels of cell death were induced with the nanoencapsulated and the free drug. However, the IC_{50} of K-562 cell line was considerably reduced with the treatment with encapsulated drug, inhibiting its proliferation from the first 24 h of incubation at a ET-LN dose equivalent to 10 µg/ml of free drug [4]. This reversion of resistance to ET in K-562 could be attributed to an increased intracellular ET concentration after nanoparticle uptake or to an enhanced cell death mechanism due to the different intracellular localization of the drug.

Higher intracellular accumulation of the drug with the ET-LN was discarded on the basis of the above results and different sensitivity to the treatments might thus depend on the death mechanisms triggered by the two treatments.

To gain further insights into mechanisms for apoptosis induction, caspase activation was studied at protein level in both cell lines. Thus, cells were grown in medium containing ET or ET-LN (5 and 10 µg/mL of ET or equivalent concentrations of Blank-LN and ET-LN for HL-60 and K-562 respectively) at several time points and proteins were subsequently obtained from cell lysates. Western blots were performed to detect effector caspase activation, which would entail apoptosis induction. One of the first identified substrates of caspases, PARP1 was also inspected. The processing of both effector caspases -7 and -3 and its substrate, PARP1 were detected in ET- and ET-LN-treated HL-60 cells (Fig. 4), thereby indicating the same apoptotic cell induction of both treatment groups. These results might be explained due to the fact that HL-60 is ET-sensitive. Besides, the encapsulated drug might be rapidly internalized in HL-60 and released into the cell. Due to its sensitivity, low concentrations of ET might be enough to induce apoptosis. The abovementioned uptake studies indicate that ET may be internalized by other mechanisms apart from lipid rafts and that those mechanisms may be different from those involved in the uptake of ET-LN. Among all these internalization pathways, the diffusion facilitated could be considerable due to its capacity of delivering ET directly in the cytoplasm avoiding lysosomes.

On the other hand, K-562 did not display caspase-mediated apoptosis when treated with either ET or drug-loaded LN, as processed forms of inductor caspase-9 and effector caspases-3 and -7 were not detected in protein extracts (Fig. 4).

The K-562 cell line was derived from a CML blast crisis patient [41] and therefore it presents several characteristics of this stage of the disease, such as hyperproliferation and apoptosis resistance. For this reason, the resistance of K-562 to apoptosis induction has been extensively reported [42-45]. This resistance may be attributed to Bcr-Abl expression. Besides, low ganglioside levels in cell membrane and ERK/MAPK overactivation among others may have an important role in the

resistance of this cell line [46, 47]. These molecular particularities would explain the absence of caspase-mediated cell death in K-562 in response to the treatments.

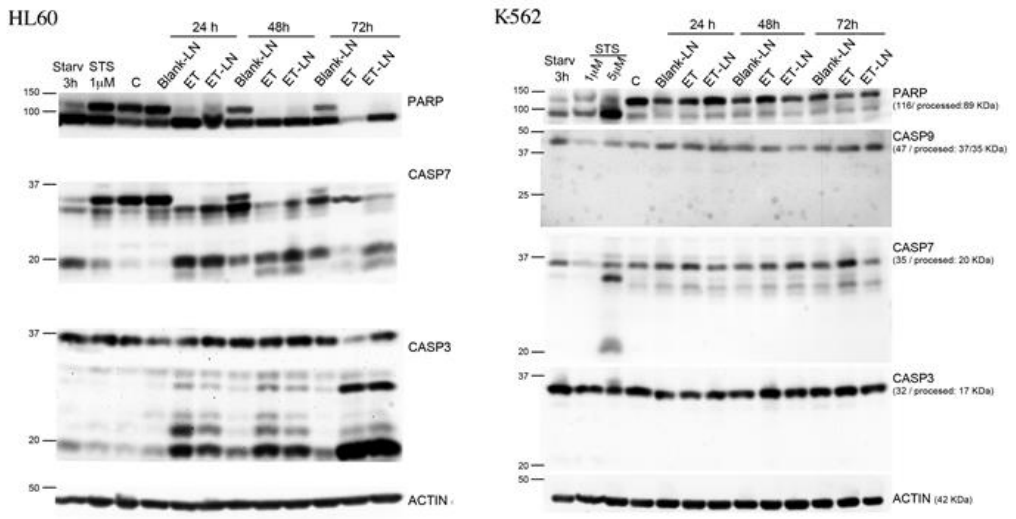

Figure 4. Characterization of caspase activation status of HL-60 and K-562 after incubation with medium, free edelfosine (ET) and drug-loaded LN (ET-LN) at a dose equivalent of 5 and 10 μg/mL of ET respectively. Caspase activation was inspected by western blot. Protein extracts of cells grown in starvation EBSS medium (Starv 3h), Staurosporine (STS), untreated control cells (C) and unloaded nanoparticles (Blank-LN) were included as controls.

The abovementioned results indicate that HL-60 cell line induced caspase-mediated cell death in response to free and nanoencapsulated ET treatments whereas K-562 exhibited an enhanced resistance in inducing the processing and activation of pro-caspases and therefore in inducing apoptosis via caspase activation. These findings confirm our previous observations using flow cytometry that showed absence of caspase activation in K-562 cells after treatment with either ET or ET-LN [4]. Therefore, mechanisms different from caspase activation may have a role in cell induction in the K-562 cell line.

3.5 Increase of autophagy-associated LC3 II protein in response to ET and ET-LN treatments

We have previously hypothesized that this different induction of cell death by ET-LN might be related to a distinct entry route of the drug into the cell when it is encapsulated [4], causing a different intracellular location of ET. In the above uptake studies we showed that ET endocytosis in K-562 cells was low, suggesting the major implication of passive flip-flop of ET in these cells. This uptake would promote direct delivery of the drug in the cytoplasm, whereas we hypothesize that the encapsulated ET intracellular traffic might be mediated by macropinosomes and phagosomes. Then, vesicles might directly fuse with lysosomes or be engulfed by into double-membrane vesicles called autophagosomes which will later fuse with lysosomes. In addition, the aforementioned absence of caspase activation would indicate that K-562 cells might undergo a caspase-independent cell death mechanism. Hence, autophagic cell death could have a role in the cell demise induced by ET-LN in K-562 cells. To gain a better insight, LC3 I and LC3 II protein levels were inspected via western blot and subsequent band quantification. LC3 is an ubiquitin-like protein that can be detected unconjugated (LC3 I) or associated with autophagosomal membranes (LC3 II). Thus, LC3 II levels are augmented during autophagy. Accordingly, an increase in the ratio of LC3 II to LC3 I reflects the accumulation of autophagic vesicles in cells, and therefore autophagy induction. For that reason, the status of autophagy was inspected in order to detect an increase in LC3 II/LC3 I ratio (Fig. 5). In both cell lines, the ratio increased in all the groups after 24 h of treatment. This could be explained as a response to cell stress produced for the change of the culture conditions (that is, the presence of the nanoparticles or the free drug in the cellular media) [48]. At 48 h after treatment, the Blank-LN control group was found to have similar expression levels to the untreated control whereas those of the treated cells rose. This increase reached statistical significance at 48 h in K-562 cells, indicating an increase of LC3 II compared to LC3 I in nanoparticle-treated cells, which in turn entails a higher presence of autophagosomes in treated cells [4].

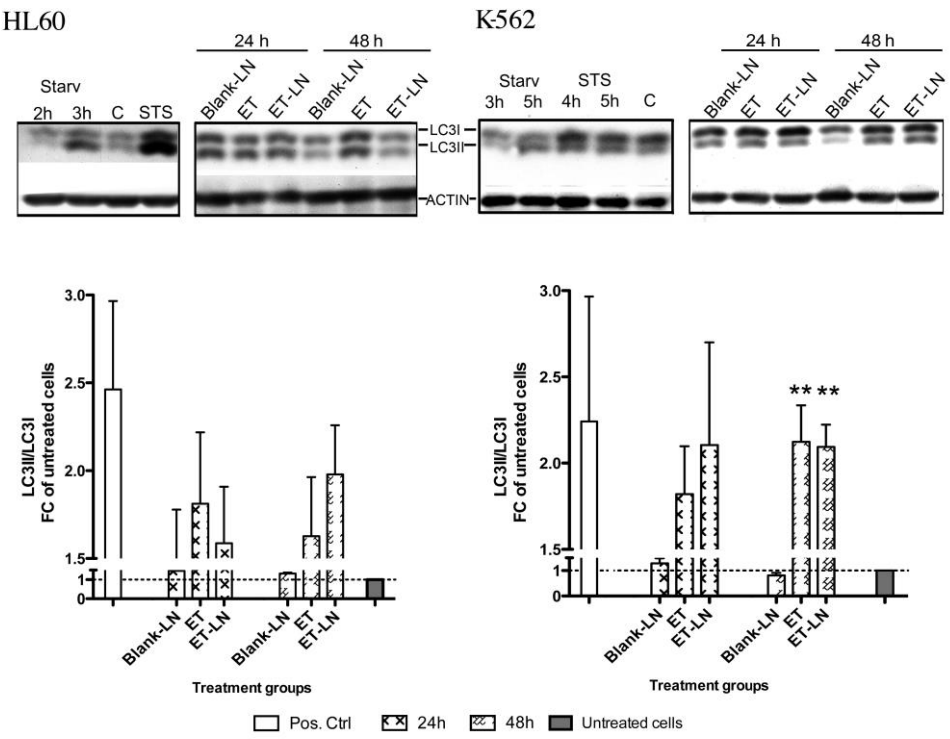

Figure 5. LC3 protein expression in HL-60 and K-562 cells after 24 and 48 h of treatment with edelfosine (ET) and lipid nanoparticles containing edelfosine (ET-LN) at a dose equivalent of 5 and 10 μg/mL of ET respectively. LC3I and LC3II were detected by western blot. Protein extracts of cells grown in starvation EBSS medium (Starv 3h), Staurosporine (STS), untreated control cells (C) and unloaded nanoparticles (Blank-LN) were included as controls. Graphs depict the fold increase of LC3 II/LC3 I ratio relative to untreated control cells. Values are means of triplicates ± SEM. **P<0.01 vs. Blank-LN control by one-way ANOVA (Bonferroni post-test).

Hence, both K-562 ET and ET-LN-treated cells presented high levels of LC3 II/LC3 I at 48 h, although cultures treated with encapsulated drug underwent a strong cell death induction not detected with the free drug.

On the other hand, ET-LN would alter the autophagic machinery in cells (Fig. 6). Ma et al.[51] reported that gold nanoparticles induced an accumulation of autophagic vacuoles through lysosomal impairment. The authors described that autophagosome accumulation was induced by a blockage of the autophagic flux rather than induction of autophagy. Such an effect would also explain the results observed with K-562. Such interference with lysosomal function might also eventually lead to cell death.

In addition, many efforts are being made to further understand the crosstalk between necrosis, autophagy and apoptosis [52, 53]. For this reason, the novel autophagic induction described in the present study in response to ET-LN treatment could induce a caspase-independent cell death mechanism (i.e caspase independent apoptosis or necrosis). To our knowledge this study represents the first report of the possible role of autophagy in the cellular response to LN. In that sense, more experiments (i.e microscopy studies with LC3-GFP transfectants or characterization of the cell death response to ET and ET-LN in presence of autophagic flux inhibitors) should be performed in order to ascertain the role of the observed autophagic induction in cell death.

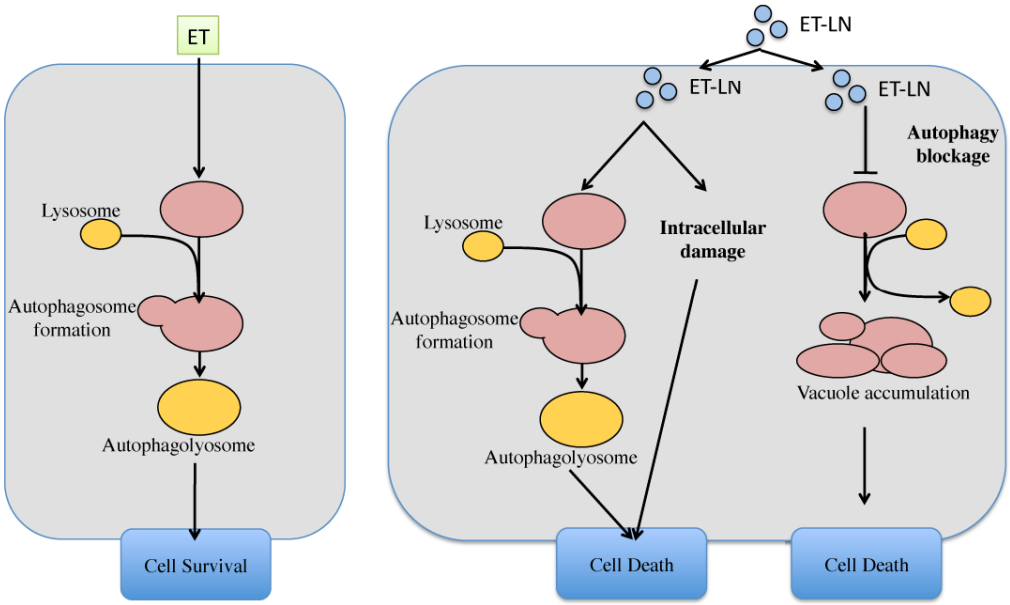

Figure 6. Graphic representation mechanisms that main explain the increase of LC3 II/LC3 I ratio and therefore, the autophagic flux in K-562 cells. Both the free drug (ET) and the encapsulated drug (ET-LN) would induce autophagy in response to the cytotoxic agent ET. However, as LN may be incorporated by transport mechanisms different from those for ET, it may induce toxic effects in unknown organelles that together with autophagy would lead eventually to cell death. On the other hand, ET-LN may induce an accumulation of autophagic vacuoles through blockage of the autophagic flux thereby triggering cell death. Such an effect would also explain the results observed.

4. Conclusions

The data presented above provide evidence that ET and ET-LN intracellular incorporation is prompted by different uptake mechanisms. Endocytic and facilitated

diffusion appear to be major uptake mechanisms in free drug uptake; whereas, in case of ET-LN, passive diffusion, phagocytosis and macropinocytosis are the most likely uptake mechanism. LN do not enhance the intracellular concentration of the drug in both leukemic cell lines despite the different uptake mechanism of ET-LN. Besides, both treatments activate caspase-mediated cell death in the ET-sensitive cell line HL-60, conversely in K-562 caspases were not activated. Moreover, an important increase of lipidated LC3 II was detected after both treatments, pointing towards an increase of autophagic vesicles in K-562 cells. Importantly, as ET-LN overcome the resistance of K-562 cells, autophagic cell death could be involved in the cell demise process caused by the toxic effects of ET when it is incorporated in the nanoparticles at a subcellular location different from the free drug.

5. References

[1] Lasa-Saracibar, B.; Estella-Hermoso de Mendoza, A.; Guada, M.*, et al.* Lipid nanoparticles for cancer therapy: state of the art and future prospects. Expert Opin Drug Deliv **2012**, *9*: 1245-1261.

[2] Gajate, C.; Mollinedo, F. The antitumor ether lipid ET-18-OCH(3) induces apoptosis through translocation and capping of Fas/CD95 into membrane rafts in human leukemic cells. Blood **2001**, *98*: 3860-3863.

[3] Castro, B. M.; Fedorov, A.; Hornillos, V.*, et al.* Edelfosine and Miltefosine Effects on Lipid Raft Properties: Membrane Biophysics in Cell death by Anti-Tumor Lipids. J Phys Chem B **2013**, *117*: 7929–7940.

[4] Lasa-Saracíbar, B.; Estella-Hermoso de Mendoza, A.; Mollinedo, F.; *et al.* Edelfosine lipid nanosystems overcome drug resistance in leukemic cell lines. *Cancer Lett.* **2013**, 334, 302-310.

[5] Estella-Hermoso de Mendoza, A.; Blanco-Prieto, M. J.; Campanero, M. A., *et al*. Development and use of lipidic nanoparticles loaded with edelfosine and ether phospholipids in antitumoral and antiparasitic therapy. **2011**. P201130433.

[6] Aznar, M. A.; Lasa-Saracibar, B.; Estella-Hermoso de Mendoza, A.*, et al.* Efficacy of edelfosine lipid nanoparticles in breast cancer cells. Int J Pharm **2013**, *454*: 720-726.

[7] Treuel, L.; Jiang, X.; Nienhaus, G. U. New views on cellular uptake and trafficking of manufactured nanoparticles. J R Soc Interface **2013**, *10*: 20120939.

[8] Wang, T.; Bai, J.; Jiang, X.*, et al.* Cellular uptake of nanoparticles by membrane penetration: a study combining confocal microscopy with FTIR spectroelectrochemistry. ACS Nano **2012**, *6*: 1251-1259.

[9] Hillaireau, H.; Couvreur, P. Nanocarriers' entry into the cell: relevance to drug delivery. Cell Mol Life Sci **2009**, *66*: 2873-2896.

[10] van Blitterswijk, W. J.; Verheij, M. Anticancer mechanisms and clinical application of alkylphospholipids. Biochim Biophys Acta **2013**, *1831*: 663-674.

[11] Small, G. W.; Strum, J. C.; Daniel, L. W. Characterization of an HL-60 cell variant resistant to the antineoplastic ether lipid 1-O-octadecyl-2-O-methyl-rac-glycero-3-phosphocholine. Lipids **1997**, *32*: 715-723.

[12] Vink, S. R.; van der Luit, A. H.; Klarenbeek, J. B.*, et al.* Lipid rafts and metabolic energy differentially determine uptake of anti-cancer alkylphospholipids in lymphoma versus carcinoma cells. Biochem Pharmacol **2007**, *74*: 1456-1465.

[13] Chen, R.; Brady, E.; McIntyre, T. M. Human TMEM30a promotes uptake of antitumor and bioactive choline phospholipids into mammalian cells. J Immunol **2011**, *186*: 3215-3225.

[14] Pomorski, T.; Menon, A. K. Lipid flippases and their biological functions. Cell Mol Life Sci **2006**, *63*: 2908-2921.

[15] Galluzzi, L.; Vitale, I.; Abrams, J. M.*, et al.* Molecular definitions of cell death subroutines: recommendations of the Nomenclature Committee on Cell Death 2012. Cell Death Differ **2012**, *19*: 107-120.

[16] Kroemer, G.; Galluzzi, L.; Vandenabeele, P.*, et al.* Classification of cell death: recommendations of the Nomenclature Committee on Cell Death 2009. Cell Death Differ **2009**, *16*: 3-11.

[17] Wang, P.; Zhang, L.; Peng, H.*, et al.* The formulation and delivery of curcumin with solid lipid nanoparticles for the treatment of on non-small cell lung cancer both in vitro and in vivo. Mater Sci Eng C Mater Biol Appl **2013**, *33*: 4802-4808.

[18] Andon, F. T.; Fadeel, B. Programmed cell death: molecular mechanisms and implications for safety assessment of nanomaterials. Acc Chem Res **2013**, *46*: 733-742.

[19] Halamoda Kenzaoui, B.; Chapuis Bernasconi, C.; Guney-Ayra, S.*, et al.* Induction of oxidative stress, lysosome activation and autophagy by nanoparticles in human brain-derived endothelial cells. Biochem J **2012**, *441*: 813-821.

[20] Li, H.; Li, Y.; Jiao, J.*, et al.* Alpha-alumina nanoparticles induce efficient autophagy-dependent cross-presentation and potent antitumour response. Nat Nanotechnol **2011**, *6*: 645-650.

[21] Yu, K. N.; Yoon, T. J.; Minai-Tehrani, A.*, et al.* Zinc oxide nanoparticle induced autophagic cell death and mitochondrial damage via reactive oxygen species generation. Toxicol In Vitro **2013**, *27*: 1187-1195.

[22] Estella-Hermoso de Mendoza, A.; Campanero, M. A.; Mollinedo, F.*, et al.* Comparative study of A HPLC-MS assay versus an UHPLC-MS/MS for anti-tumoral alkyl lysophospholipid edelfosine determination in both biological samples and in lipid nanoparticulate systems. J Chromatogr B Analyt Technol Biomed Life Sci **2009**, *877*: 4035-4041.

[23] Lecaroz, C.; Blanco-Prieto, M. J.; Burrell, M. A.*, et al.* Intracellular killing of Brucella melitensis in human macrophages with microsphere-encapsulated gentamicin. J Antimicrob Chemother **2006**, *58*: 549-556.

[24] Rubinsztein, D. C.; Cuervo, A. M.; Ravikumar, B.*, et al.* In search of an "autophagomometer". Autophagy **2009**, *5*: 585-589.

[25] Seglen, P. O.; Reith, A. Ammonia inhibition of protein degradation in isolated rat hepatocytes. Quantitative ultrastructural alterations in the lysosomal system. Exp Cell Res **1976**, *100*: 276-280.

[26] Mizushima, N.; Levine, B. Autophagy in mammalian development and differentiation. Nat Cell Biol **2010**, *12*: 823-830.

[27] He, B.; Lin, P.; Jia, Z*., et al.* The transport mechanisms of polymer nanoparticles in Caco-2 epithelial cells. Biomaterials **2013**, *34*: 6082-6098.

[28] Zhao, Y.; Sun, X.; Zhang, G*., et al.* Interaction of mesoporous silica nanoparticles with human red blood cell membranes: size and surface effects. ACS Nano **2011** *5*: 1366-1375.

[29] van der Luit, A. H.; Vink, S. R.; Klarenbeek, J. B*., et al.* A new class of anticancer alkylphospholipids uses lipid rafts as membrane gateways to induce apoptosis in lymphoma cells. Mol Cancer Ther **2007**, *6*: 2337-2345.

[30] Mollinedo, F.; de la Iglesia-Vicente, J.; Gajate, C*., et al.* Lipid raft-targeted therapy in multiple myeloma. Oncogene **2010**, *29*: 3748-3757.

[31] Gajate, C.; Gonzalez-Camacho, F.; Mollinedo, F. Involvement of raft aggregates enriched in Fas/CD95 death-inducing signaling complex in the antileukemic action of edelfosine in Jurkat cells. PLoS One **2009**, *4*: e5044.

[32] Tsutsumi, T.; Tokumura, A.; Kitazawa, S. Undifferentiated HL-60 cells internalize an antitumor alkyl ether phospholipid more rapidly than resistant K562 cells. Biochim Biophys Acta **1998**, *1390*: 73-84.

[33] Gummadi, S. N.; Kumar, K. S. The mystery of phospholipid flip-flop in biogenic membranes. Cell Mol Biol Lett **2005**, *10*: 101-121.

[34] Sahay, G.; Alakhova, D. Y.; Kabanov, A. V. Endocytosis of nanomedicines. J Control Release **2010**, *145*: 182-195.

[35] Gilleron, J.; Querbes, W.; Zeigerer, A*., et al.* Image-based analysis of lipid nanoparticle-mediated siRNA delivery, intracellular trafficking and endosomal escape. Nat Biotechnol **2013**, *31*: 638-646.

[36] Harris, J.; Werling, D.; Hope, J. C*., et al.* Caveolae and caveolin in immune cells: distribution and functions. Trends Immunol **2002**, *23*: 158-164.

[37] van de Winkel, J. G.; Anderson, C. L. Biology of human immunoglobulin G Fc receptors. J Leukoc Biol **1991**, *49*: 511-524.

[38] Uner, M.; Yener, G. Importance of solid lipid nanoparticles (SLN) in various administration routes and future perspectives. Int J Nanomedicine **2007**, *2*: 289-300.

[39] Gallagher, R.; Collins, S.; Trujillo, J.*, et al.* Characterization of the continuous, differentiating myeloid cell line (HL-60) from a patient with acute promyelocytic leukemia. Blood **1979**, *54*: 713-733.

[40] Lozzio, B. B.; Lozzio, C. B.; Bamberger, E. G.*, et al.* A multipotential leukemia cell line (K-562) of human origin. Proc Soc Exp Biol Med **1981**, *166*: 546-550.

[41] Lozzio, B. B.; Lozzio, C. B. Properties of the K562 cell line derived from a patient with chronic myeloid leukemia. Int J Cancer **1976**, *18*: 421-431.

[42] Chang, M. P.; Bramhall, J.; Graves, S.*, et al.* Internucleosomal DNA cleavage precedes diphtheria toxin-induced cytolysis. Evidence that cell lysis is not a simple consequence of translation inhibition. J Biol Chem **1989**, *264*: 15261-15267.

[43] Kaufmann, S. H.; Desnoyers, S.; Ottaviano, Y.*, et al.* Specific proteolytic cleavage of poly(ADP-ribose) polymerase: an early marker of chemotherapy-induced apoptosis. Cancer Res **1993**, *53*: 3976-3985.

[44] Martins, L. M.; Mesner, P. W.; Kottke, T. J.*, et al.* Comparison of caspase activation and subcellular localization in HL-60 and K562 cells undergoing etoposide-induced apoptosis. Blood **1997**, *90*: 4283-4296.

[45] McGahon, A.; Bissonnette, R.; Schmitt, M.*, et al.* BCR-ABL maintains resistance of chronic myelogenous leukemia cells to apoptotic cell death. Blood **1994**, *83*: 1179-1187.

[46] Tringali, C.; Lupo, B.; Cirillo, F.*, et al.* Silencing of membrane-associated sialidase Neu3 diminishes apoptosis resistance and triggers megakaryocytic differentiation of chronic myeloid leukemic cells K562 through the increase of ganglioside GM3. Cell Death Differ **2009**, *16*: 164-174.

[47] Kang, C. D.; Yoo, S. D.; Hwang, B. W.*, et al.* The inhibition of ERK/MAPK not the activation of JNK/SAPK is primarily required to induce apoptosis in chronic myelogenous leukemic K562 cells. Leuk Res **2000**, *24*: 527-534.

[48] Kroemer, G.; Marino, G.; Levine, B. Autophagy and the integrated stress response. Mol Cell **2010**, *40*: 280-293.

[49] Kroemer, G.; Levine, B. Autophagic cell death: the story of a misnomer. Nat Rev Mol Cell Biol **2008**, *9*: 1004-1010.

[50] Maiuri, M. C.; Zalckvar, E.; Kimchi, A*., et al.* Self-eating and self-killing: crosstalk between autophagy and apoptosis. Nat Rev Mol Cell Biol **2007**, *8*: 741-752.

[51] Ma, X.; Wu, Y.; Jin, S*., et al.* Gold nanoparticles induce autophagosome accumulation through size-dependent nanoparticle uptake and lysosome impairment. ACS Nano **2011**, *5*: 8629-8639.

[52] Nikoletopoulou, V.; Markaki, M.; Palikaras, K*., et al.* Crosstalk between apoptosis, necrosis and autophagy. Biochim Biophys Acta **2013,** *1833*: 3448–3459 .

[53] Strasser, A.; Cory, S.; Adams, J. M. Deciphering the rules of programmed cell death to improve therapy of cancer and other diseases. EMBO J **2011**, *30*: 3667-3683.

CHAPTER 4

In vitro intestinal co-culture cell model to evaluate intestinal absorption of edelfosine lipid nanoparticles

Beatriz Lasa-Saracíbar[1], Melissa Guada[1], Victor Sebastián[2], Maria J. Blanco-Prieto[1]*

[1] Dept. of Pharmaceutics and Pharmaceutical Technology, School of Pharmacy, University of Navarra, Pamplona, Spain

[2] Chemical & Environmental Engineering Department & Nanoscience Institute of Aragon (INA) University of Zaragoza, Zaragoza, Spain

Keywords: Caco-2, Edelfosine, Lipid nanoparticles, Permeabiltity, Raji, Transport

***Corresponding author:** Dr. María J. Blanco-Prieto, Department of Pharmaceutics and Pharmaceutical Technology, School of Pharmacy, University of Navarra, C/Irunlarrea 1, E-31080 Pamplona, Spain, Office phone: + 34 948 425 600 ext. 6519, Fax: + 34 948 425 649, e-mail: mjblanco@unav.es

Declaration of interest: The authors state no conflict of interest.

Submitted to Current Topics in Medicinal Chemistry

Abstract

Nanotechnology is providing a new therapeutic paradigm by enhancing drug efficacy and preventing side-effects. Edelfosine is a synthetic ether lipid analogue of platelet activating factor with high antitumor activity. The encapsulation of this potent antitumor drug in lipid nanoparticles increases its oral bioavailability; moreover, it prevents the hemolytic and gastrointestinal side-effects of the free drug. The literature points towards lymphatic absorption of lipid nanoparticles after oral administration, and previous *in vitro* and *in vivo* studies stress the protection against toxicity that these nanosystems provide. The present study is intended to assess the permeability of lipid nanoparticles across the intestinal barrier. Caco-2 monoculture and Caco-2/Raji co-culture were used as *in vitro* models of enterocytes and Microfold cells respectively. Results showed that free drug is internalized and possibly metabolized in enterocytes. These results do not correlate with those observed *in vivo* when edelfosine-lipid nanoparticles were administered orally in mice, which suggests that the microfold model is not a good model to study the absorption of edelfosine-lipid nanoparticles across the intestinal barrier *in vitro*.

1. Introduction

Edelfosine (ET) is a synthetic ether lipid analogue of platelet activating factor (PAF) with proved *in vitro* and *in vivo* antitumor activity [1]. However, it presents some drawbacks such as hemolysis after intravenous administration and gastrointestinal toxicity and poor bioavailability after oral administration [2]. These drawbacks can be overcome through nanotechnology [3]. Lipid nanoparticles (LN) prevent ET toxicity [4] and improve its oral bioavailability [2]. Moreover, they can be formulated by an organic solvent free method using biodegradable lipids [5]. Due to their physicochemical characteristics, LN containing ET (ET-LN) can be administered orally, intravenously and intraperitoneally [3]. Bearing in mind the importance of oncological patient well-being, the possibility of administering therapy by oral route is a challenge. Several *in vivo* studies report accumulation of the drug in the lymph nodes, endorsing lymphatic intestinal absorption after LN oral administration [3]. In order to obtain further insight into the evaluation of drug absorption in the gastrointestinal tract, several *in vitro* models have been developed since the 1980s [6]. Among all these models, Caco-2 monoculture is one of the most commonly used due to its ability to simulate the intestinal epithelium. The human epithelial colorectal adenocarcinoma cell line Caco-2 differentiates to enterocyte-like cells under specific culture conditions [6]. In addition, the hypothesis of lymphatic oral absorption of LN has promoted the development of intestinal *in vitro* models that simulate microfold cells (M cells) of Peyer`s patches in the intestinal follicle-associated epithelium (FAE). M cells specialize in transporting soluble macromolecules, small particles and entire microorganisms from the intestinal lumen to the immune system. These cells have unique morphological features including the presence of a reduced glycocalyx, irregular brush border and reduced microvilli [7]. Previous authors have developed numerous strategies to obtain M-cell like *in vitro* models [8-12]. This work includes the development of an *in vitro* model of M cells based on the strategy of co-cultivating Caco-2 cells with Raji cells (B lymphocytes derived from Burkitt cell lymhoma) [9]. ET and ET-LN transport across mono and co-culture models are evaluated in the present study.

2. Material and methods

2.1 Materials

ET was purchased from APOINTECH (Salamanca, Spain). Precirol® ATO 5 was a gift from Gattefossé (France). Tween® 80 was purchased from Roig Pharma (Barcelona, Spain). Chloroform was obtained from Panreac (Madrid, Spain), formic acid 99% for mass spectroscopy was obtained from Fluka (Barcelona, Spain), and methanol was purchased from Merck (Barcelona, Spain). All solvents employed for the chromatographic analysis were of analytical grade; all other chemicals were reagent grade and used without further purification. Amicon Ultra-15 10,000 MWCO centrifugal filter devices and Millicell Cell Culture Inserts were purchased from Millipore (Cork, Ireland). RPMI 1640 and MEM cell culture media, Heat-inactivated Fetal Bovine Serum (FBS), Glutamax, MEM Non-Essential Amino Acids, Penicillin/Streptomycin antibiotics, ZO-1 Monoclonal Antibody, Villin-1 Polyclonal Antibody, Alexa Fluor®594 Goat Anti-Rabbit IgG (H+L), Topro-3 Iodide and CellTrace CFSE Cell Proliferation Kit were purchased from Life Technologies, (Barcelona, Spain). DAPI was obtained from Invitrogen (Madrid, Spain). Fluorescence mounting medium was obtained from Dako (Barcelona, Spain). SIGMAFAST™ p-Nitrophenyl phosphate Tablets, rhodamine 123 and fluorescein sodium were obtained by Sigma Aldrich Química S.A. (Madrid, Spain). M-PER Mammalian Protein Extraction Reagent and Silicone tubing were purchased from Thermo Fisher Scientific (Madrid, Spain).

2.2 Preparation and characterization of lipid nanoparticles

LN were prepared by the hot homogenization method consisting of high shear homogenization and ultrasonication [13]. ET (30 mg) and Precirol® (300 mg) were melted at approximately 5ºC above the melting point of the lipid (60ºC). A 2% Tween® 80 aqueous solution (10 mL) previously heated at the same temperature was added and dispersed in the molten lipid with the help of a Microson™ ultrasonic cell disruptor (NY, USA) for 1 min at an effective power of 10W. The preformed emulsion was then homogenized with an Ultraturrax® (IKA-Werke, Germany) for 1 min at

24,000 rpm and sonicated again with a Microson™ ultrasonic cell disruptor (NY, USA) for 1 min at 10W. The emulsion was removed from heat and placed in an ice bath to obtain LN by lipid solidification. Then, the LN suspension was centrifuged using Amicon® Ultra-15 10,000 MWCO filters at 4500 × g for 30 min and washed twice with distilled water. Afterwards, 150 % (w/w of lipid weight) trehalose was added as cryoprotectant agent to the LN suspension, which was then kept at -80ºC and freeze-dried to obtain a nanoparticulate powder. Particle size and polydispersity index (PDI) were evaluated by photon correlation spectroscopy (PCS) using a Zetasizer Nano (Malvern Instruments, UK). The measurements were carried out three times. Surface charge was measured using the same Zetasizer Nano equipment combined with laser Doppler velocimetry. For the ET loading determination, 5 mg of nanoparticles were dissolved in 1 ml of chloroform and mixed with 4 ml of methanol. The mixture was vortexed for 1 min and then centrifuged at 20,000 × *g* for 10 min. The supernatant was analyzed by a previously validated ultra-high-performance liquid chromatography tandem mass spectrometry (UHPLC-MS/MS) method [14].

ET-LN morphology was evaluated by transmission electron microscopy (TEM). Images were taken on a FEI Tecnai T20 microscope at INA-LMA(Zaragoza). To prepare ET-LN samples for TEM observation, lyophilized NPs were dispersed in milli-Q water. After 30 s in an ultrasonic bath, a drop of this suspension was applied to a copper grid (200 mesh) coated with carbon film, and allowed to dry in air. The microscope was operated at 80 kV to preserve the ET-LN morphology and diminish radiation damage.

2.3 Cell culture

Caco-2 cells were culture in MEM supplemented with 20% (v/v) fetal bovine serum, 1% v/v non-essential aminoacids and 1% (v/v) Glutamax at 37ºC under a 5% CO_2 water saturated atmosphere. Cells were harvested with trypsin/EDTA every 3-4 days and subcultured at 12 x 10^3 cells/cm^2. Raji cells were cultured at 0.5 x 10^6 cells/ml in RPMI supplemented with 20% (v/v) fetal bovine serum, and 1% (v/v) penicillin and streptomycin, at 37ºC in a humid atmosphere with 5% CO_2. Cells were split 1:3-1:5 every 3-4 days.

2.4 Enterocyte and M-cell like: *in vitro* models of gastrointestinal barrier

2.4.1 Development

In vitro models were developed following a previous experiment by des Rieux *et al.* [9]. The human colon adenocarcinoma cell line Caco-2 cells were seeded at a density of 9 x 10^4 cells on the apical chamber of Transwell inserts (3-mm pore PET Transwell filters; 12-well) in MEM supplemented with 20% (v/v) fetal bovine serum, 1% v/v non-essential aminoacids, 1% (v/v) Glutamax and 1% penicillin and streptomycin. Cultures were maintained at 37ºC, 5% CO_2 for up to 21 days. The medium was replaced every 2-3 days (0.5 ml in the apical compartment and 1.5 ml in the basolateral compartment). In case of the M-cell *in vitro* model, inserts were inverted after 14 days of culture and a piece of silicon (12.8 mm diameter) was placed on the basolateral side of each insert. The silicon piece was filled with a suspension of 5 x 10^5 Raji cells in 1 ml of supplemented MEM. Co-culture was maintained for 4 days. Afterwards, Raji cells and silicon tubes were removed and inserts were placed in their original orientation. Transport experiments in both models were performed after 21 days of Caco-2 seeding.

2.4.2 Assessment of cell monolayer integrity

Cell monolayer integrity was assessed in both models by measurement of trans-epithelial electrical resistance (TEER) [15]. Prior to measuring TEER, culture media was replaced by MEM without supplements. Inserts were placed at room temperature for 15 minutes and TEER was measured with a Millicell ERS-2 Voltohmmeter (Merck Millipore, Germany). The resistance is expressed as Ω/cm^2. Cell monolayer confluence was analyzed weekly. TEER measurement was also used to assess cell monolayer integrity during permeation experiments.

2.4.3 Characterization of the *in vitro* intestinal models

a. Inmunofluorescence

After 21 days of culture, cell monolayers were washed carefully with PBS, fixed with 4% paraformaldehyde (w/v) and permeabilized with Triton X-100 0.5 % (v/v).

Monolayers were blocked with a 1% BSA solution in TBS. Then cells were incubated with Anti-ZO-1 Alexa Fluor 488 (1:100) and Anti-villin (1:100) antibodies in TBS 1%BSA o.n. Later, cells labelled with Villin antibody were incubated with Alexa Fluor®594 Goat Anti-Rabbit IgG (H+L) (1:500). Samples were stained with Topro-3 Iodide or Dapi and visualized under fluorescence and confocal microscopy.

b. Carboxyfluorescein succinimidyl ester (CFSE) labeling

Raji cells were incubated with CellTrace CFSE for 15 minutes at 37 ºC (10 µM for flow cytometry and 25 µM for fluorescence microscopy). Afterwards, cells were incubated in culture media for 30 minutes and washed twice with PBS. Three days later, Caco-2 monolayers were co-cultured with the stained Raji cells as described above (section 2.4.1). After 21 days, cells monolayers were observed under fluorescence and confocal microscopy. Cells were fixed with 4% paraformaldehyde and nuclei were stained with Topro-3 Iodide or Dapi. In addition, the presence of Raji cells in the culture was quantified by flow cytometry.

c. P-Nitrophenyl Phosphate (PNPP) Activity

After 21 days of incubation, cells were carefully washed with PBS 0.05% Tween 20 and incubated with 500 µl of PNPP substrate for 30 minutes and protected from light. Afterwards, the supernatant was collected and absorbance was measured by a microplate spectrophotometer (Labsystems, Helsinki, Finland) at 405 nm.

2.4.4 Transport studies

TEER was measured before and after the experiments. Only cell monolayers with TEER values over 250 Ω were used. All transport studies were conducted under agitation at 37ºC in transport medium (MEM without supplements). Total experiment volumes were 0.5 ml in the apical compartment and 0.6 ml in the basolateral compartment. The different treatments were added to the donor compartments: Free ET (ET) and LN containing ET (ET-LN) at a final dose equivalent to 30 µg/ml of free drug. ET transport was studied from the apical compartment to the basolateral compartment (A→B) and vice versa (B→A). Fluorescein and rhodamine 123 were used as control substances in the transport experiments. Low permeable

substance fluorescein free acid was added to the apical compartment at a final concentration of 100 μg/ml. The p-glycoprotein substrate rhodamine 123 was added to the apical compartment (A→B) and to the basolateral compartment (B→A) at a concentration of 5 μg/ml. The experiment lasted 2 hours and donor samples were collected at the beginning and at the end of the experiment. Samples were analyzed using UHPLC-MS/MS (ET and ET-LN) and fluorescence spectrometry (fluorescein and rhodamine). The permeability (apparent permeability coefficient; P_{app}) was calculated according to the following equation [16]:

$P_{app}= dQ/dt*1/A*C_0$ [cm/s]

'dQ/dt' is the rate of appearance of drugs on the acceptor compartment (μmol/s); C_0 is the initial drug concentration on the donor side (mM); 'A' is the surface area of the monolayer (cm^2).

2.5 Statistical analysis

Data analysis and graphic presentations were done using Prism version 5.00 software for Windows (GraphPad Software, San Diego, CA). Data are presented as a mean of three or more independent experiments, with error bars indicating the standard deviation. The statistical significance level was defined as a P value of <0.05.

3. Results and discussion

3.1 Lipid nanoparticle formulation

The hot homogenization method consisting of high shear homogenization and ultrasonication provided LN with a size of 127.89 ± 9.95 nm suitable for oral, intravenous and intraperitoneal administration [3]. LN charge was negative and enough to maintain formulation stability (-28.42 ± 1.39). This method of LN formulation has been previously developed and used by our research group [13, 17, 18]. The formulation used in this study was slightly modified in order to increase drug loading capacity. ET-LN loading was 22.677 ± 2.262 μg ET/mg formulation. In comparison to LN prepared in the above-mentioned previous studies, increasing the

amount of drug that was initially added to the nanoparticles (from 15 to 30 mg) allowed us to obtain a higher loading capacity (from 13 µg ET/mg formulation to 22.677 µg ET/mg of formulation). Despite the increase in drug loading capacity, ET-LN maintained their homogeneous morphology and round shape as is shown in TEM images (Fig. 1).

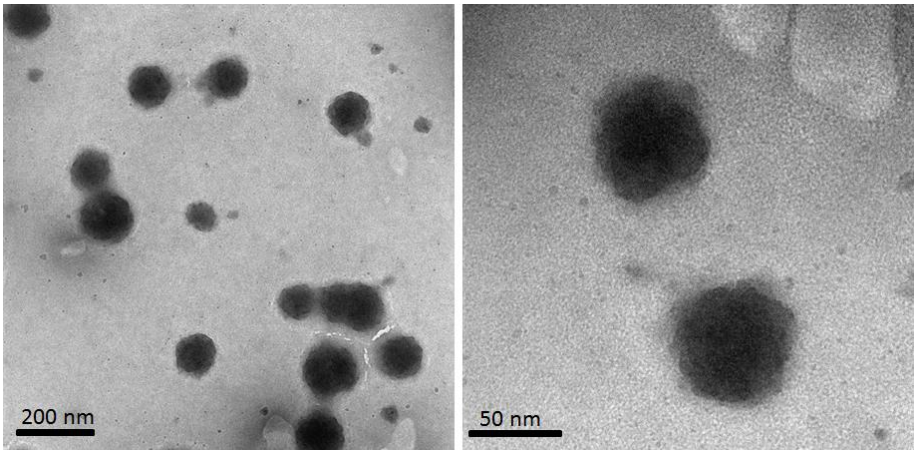

Figure 1. TEM images of LN containing edelfosine at different magnifications. ET-LN nanoparticles are not aggregated, which is in agreement with the polydispersity index obtained by PCS characterization.

3.2 *Transport experiments*

Several adapted *in vitro* models based on colorectal adenocarcinoma Caco-2 cells have been developed in the last decade to test drug permeability across the intestinal barrier [8, 9, 16, 19]. Among all these models, Caco-2 monoculture and co-culture of Caco-2 cells with Burkitt lymphoma B cells (Raji cells) are being widely used to simulate enterocytes and intestinal M cells respectively. As many researchers have reported significant accumulation of LN in the lymphatic system after oral administration [3], M-cell *in vitro* models have been developed in order to assess the absorption of these nano-systems by this route and compare it with the absorption by enterocytes (mono-culture of Caco-2 cells).

3.2.1 In vitro models of intestinal barrier: characterization

a. Cell monolayer integrity

Caco-2 monoculture and Caco-2/Raji co-culture presented similar TEER values after 21 days of culture (Fig. 2). As previously described, TEER values decreased after the co-culture with Raji cells for four days [9]. However, our results showed that, after removing Raji cells from the culture, TEER values recovered and achieved the monoculture values at day 21 (Fig. 2). Caco-2 monoculture and Caco-2/Raji co-culture showed TEER values of 480.2 ± 11.56 Ω/cm^2 and 502.8 ± 23.50 Ω/cm^2 respectively with no statistically significant differences between them. All monolayers reached TEER values above 200 Ω/cm^2 at the time of the transport experiment, indicating the formation of a cell monolayer with maintenance of tight junction integrity [16].

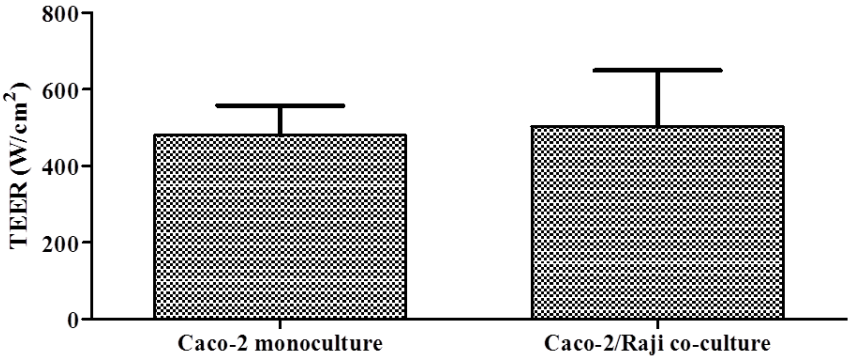

Figure 2. TEER values of Caco-2 monoculture and Caco-2/Raji co-culture after 21 days of incubation (Ω/cm2). Monoculture of Caco-2 and co-culture with Raji cells did not show differences in TEER values.

b. Immunofluorescence characterization

The formation of a monolayer containing cells phenotypically similar to enterocytes and M cells was monitored by immunofluorescence. Tight junctions were labeled with ZO-1 antibody [20]. ZO-1 is a protein that is present in the cytoplasmic membrane of cells with tight intercellular junctions. Both intestinal models showed the presence of this protein (Fig. 3). However, Caco-2 monoculture presented a more homogenous and structured monolayer architecture than Caco-2/Raji co-culture, indicating the formation of M-cells (Fig. 3).

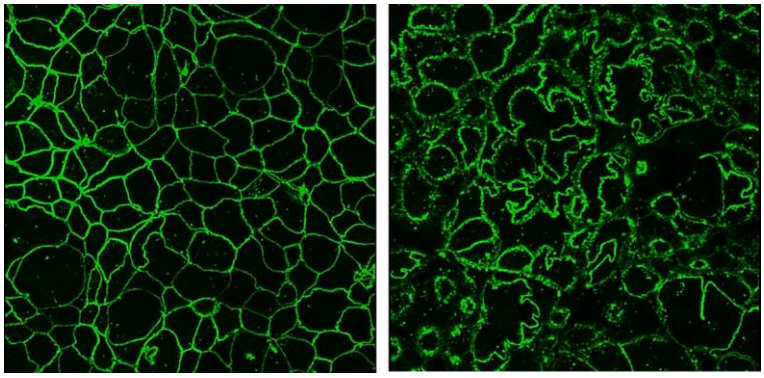

Figure 3. Confocal images of Caco-2 monoculture (left) and Caco-2/Raji co-culture (right) stained with ZO-1 antibody.

Presence of villin, a component of brush border assembly, was also assessed in both cultures. M cells are characterized by an irregular brush border and reduced microvilli to facilitate contact with particles and microorganisms [7]. Conversely, villin is present in M cells but its distribution is different, being located mainly in the cytoplasmic region [11, 21]. Such expression patterns were reproduced in our experiments (Fig. 3).

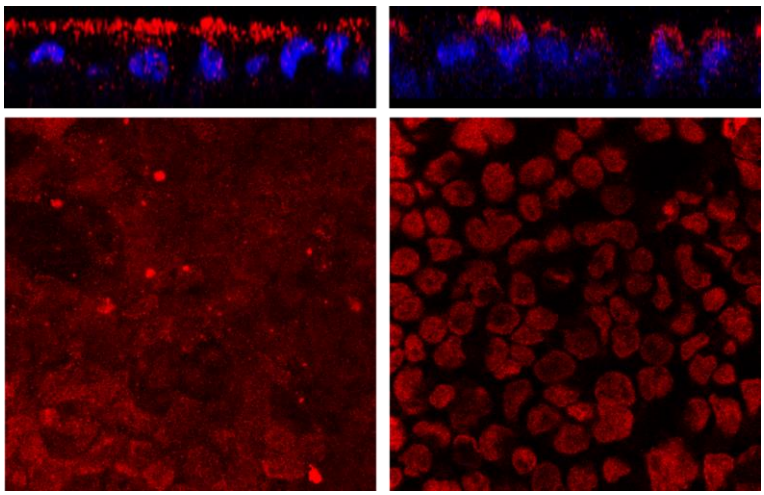

Figure 4. Confocal images of Caco-2 monoculture (left) and Caco-2/Raji co-culture (right) stained with Villin antibody (red) and Topro-3 Iodide (blue). Caco-2 monoculture showed a homogeneous layer of villin on the cell surface whereas it was partially distributed in the cell surface of the co-culture model.

Fig. 4 shows that Caco-2 monocultures presented a homogenous layer of villin on the surface of the cells, indicating the development of a brush border typically

present in enterocytes. Villin was also visible in Caco-2/Raji co-cultures but with a different distribution pattern; in this culture, some cells expressed villin in their surface but the protein did not cover the cell monolayer. The imperfect layer of villin indicates the differentiation of some Caco-2 cells into M-like cells with their typical reduced brush border.

c. Alkaline phosphatase activity

Alkaline phosphatase (AP) is an enzyme that is present in the brush border of the enterocytes. A lower activity of this enzyme in the co-culture model might be related to microvilli degeneration due to the differentiation of Caco-2 cells into M-like cells [19]. Fig. 5 shows that AP activity was significantly reduced in the co-culture model with respect to the Caco-2 monoculture model. However, there was also a significant decrease in alkaline phosphatase activity when the Caco-2 monoculture model is culture-inverted during the same days as the co-culture model. Other studies demonstrate that AP activity is reduced in the co-culture models but they compare it with the AP monoculture activity [19].

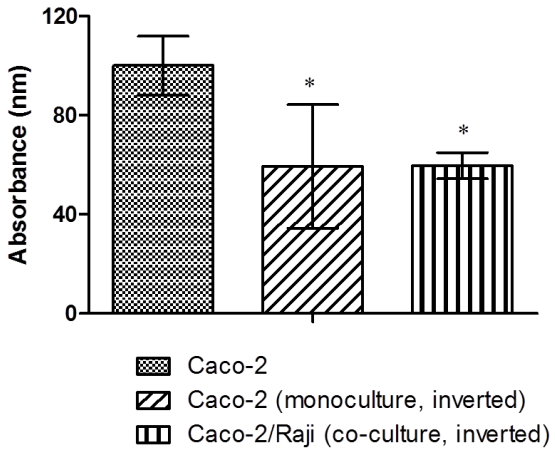

Figure 5. Alkaline phosphatase activity in Caco-2 monoculture, Caco-2 monoculture (inverted) and Caco-2/Raji co-culture. Both inverted monoculture and co-culture produced a decrease in alkaline phosphatase activity of the cells with respect to the conventional monoculture of Caco-2. *p<0.05; **p<0.01; ***p<0.001 vs. control by two-way ANOVA (Dunnet post-test).

d. Localization and quantification of Raji cells in Caco-2/Raji co-culture (CFSE labeling)

In order to localize Raji cells, we stained them with carboxyfluorescein diacetate succinimidyl ester (CFSE). This reagent passively diffuses into cells and turns into a fluorescent compound that is retained in the cell [22]. The developed model of co-culture is based on the direct contact of Raji cells with Caco-2 cells. At day 14, inserts were inverted and Raji cells were placed in the basolateral side of the membrane. Most authors support the need for direct contact between both cell lines in order to obtain a more reliable M-cell model [9, 11]. In the inverted culture model, Raji cells are expected to migrate through the pores of the insert membrane and, therefore, to be incorporated into the Caco-2 cell monolayer. Presence of Raji cells within the monolayer was visualized by fluorescence microscopy and quantified by flow cytometry.

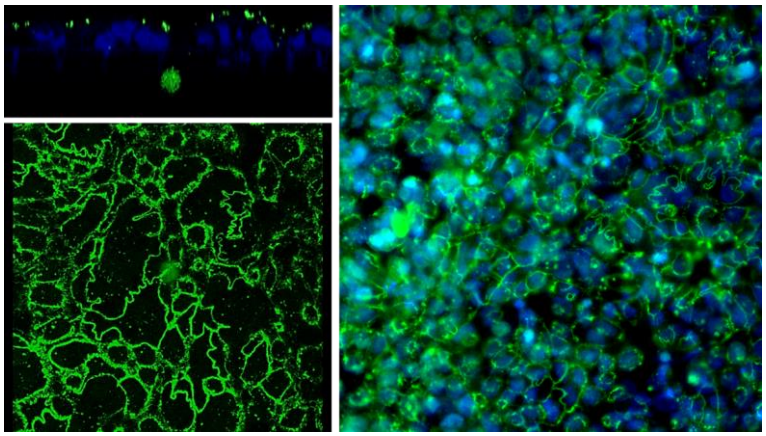

Figure 6. Confocal images (upper and lower left) and fluorescence microscopy image (right) of Caco-2/Raji co-culture. Raji cells were stained with CFSE prior to incubation with Caco-2 cells. Raji cells were detectable below the inserts.

The percentage of Raji cells in the culture assessed with flow cytometry was about 27 % of all cells; these data were consistent with the results published by Rieux *et al.* [9], who obtained a percentage between 17 and 30% of total number of cells. Confocal images showed presence of CFSE labeled cells below the inserts (Fig. 6). Raji cells were not detected within the monolayer by fluorescence microscopy and the

total proportion of fluorescent cells observable by fluorescence microscopy appeared to be lower than 30%. This discrepancy might be explained due to the higher sensitivity of flow cytometry technique. Besides, Raji cells integrated into the cell monolayer might display lower fluorescence intensity, only detectable by flow cytometry. In conclusion, enterocyte and M-cell like *in vitro* culture models were successfully developed in our laboratory [9].

3.3 Transport studies

Transport studies were performed in order to compare the transport of free drug and LN containing ET in the Caco-2 monoculture and Caco-2/Raji co-culture. Integrity of the cell monolayer was evaluated by measuring TEER values before and after transport experiments. TEER values showed that LN did not alter tight junctions; in contrast, ET produced a significant decrease of the TEER if it is incubated for four hours.

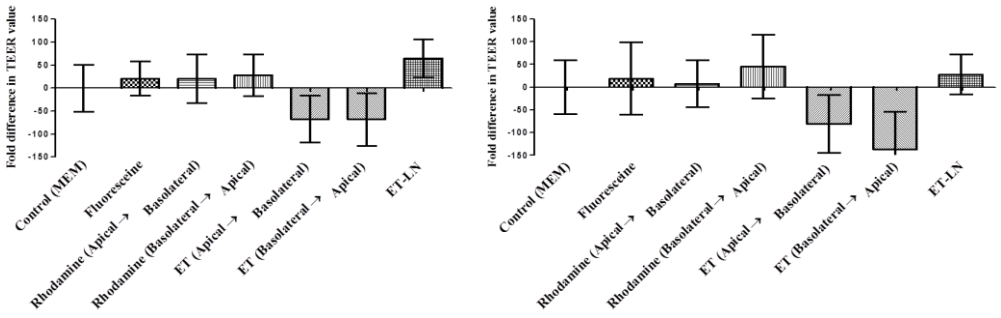

Figure 7. Fold increase/decrease in TEER value of Caco-2 monolayer (left) and Caco-2/Raji co-culture (right) after 2 hours of incubation with the different treatments. Free drug was the only treatment that produced a slight decrease in TEER values.

Fig. 7 shows the changes in TEER values after two hours of incubation with the different treatments. As can be observed, free ET was the only treatment that produced a decrease in the transepithelial resistance. Our results led us to conclude that transport experiments could not last for more than two hours due to the high disruption of the cell culture, measurable by the TEER value, which was caused by the free drug. Although LN were not harmful for the insert cultures over longer times,

transport experiments were performed up to 2 hours in order to compare ET and ET-LN transport in both *in vitro* models.

Rhodamine 123 and fluorescein were used as controls for the transport study. Rhodamine is a P-glycoprotein (P-gp) substrate, a multidrug efflux transporter that avoids the absorption of potentially risk molecules in the intestine [23]. As ET is also a P-gp substrate [17], rhodamine 123 was used to assess the P-gp function in Caco-2 *in vitro* intestinal model in order to further evaluate P-gp efflux transporter. Rhodamine 123 transport is performed by paracellular transport from the apical side while it is internalized by the transcellular route and eluded to the apical side by the P-gp in case of secretory transport [24]. Fluorescein is transported via paracellular route and is a common marker used in transport studies to assess the integrity of the tight junctions. Due to its size, fluorescein presents very low permeability in Caco-2 monolayers because of the presence of tight junctions. Table 1 shows the apparent permeabilities (P_{app}) of both markers in the intestinal models studied. P_{app} coefficients showed differences between the two culture models in case of secretory transport of rhodamine (from the basal to the apical compartment).

Table 1. Apparent permeability coefficient (Papp x 10-6 (cm/s) of fluorescein and rhodamine in Caco-2 and Caco-2/Raji B cultures **p < 0.01; ***p < 0.001 vs. corresponding control group by two-way ANOVA (Bonferroni post-test).

	Caco-2 monoculture	Caco-2/Raji B co-culture
Fluorescein	5.25 ± 0.10	6.05 ± 4.38
Rhoamine 123 (Apical)	2.59 ± 0.26	9.04 ± 3.49
Rhodamine 123 (Basal)	29.93 ± 2.15 ***	19.83± 0.53 **

As has been previously explained, the transport of both substances across Caco-2 monolayer occurs via the paracellular route, which is consistent with the low P_{app} absorptive coefficients of fluorescein and rhodamine. It means that tight junctions between cells prevented the crossing of these molecules. Regarding the differences in rhodamine transport in each culture, rhodamine secretory transport (from the basolateral to the apical side) was about 11.5 (Caco-2 monoculture) and 2.2 (Caco-2/Raji B co-culture) times higher than absorptive transport. This difference in

transport rates has been previously described by other authors [24]. The difference in rhodamine secretory transport was clearer in the case of the monoculture due to the larger presence of enterocyte-like cells which express the P-gp transporter.

LN have been shown to increase the oral bioavailability of many different drugs including ET [3], and therefore many researchers have shown an interest in *in vitro* models of the intestinal barrier that make it easier to assess the absorption of these nanosystems at the intestinal level [10, 25]. Roger et al. [25] studied the permeability of Paclitaxel across Caco-2 monolayers, concluding that LN were able to increase drug uptake up to 3.5 times. Beloqui *et al*. [10] also conclude that LN enhance the absorption of saquinavir; however, they report a lower drug permeability of LN across Caco-2/Raji B co-culture than in the enterocyte-like model. With these premises we expected to observe increased permeability of ET-LN compared to the free ET in the Caco-2 *in vitro* intestinal model. Fig. 8 shows the amount of drug after the experiment in each compartment (apical and basolateral sides and cells) at the end of the experiment (2 hours).

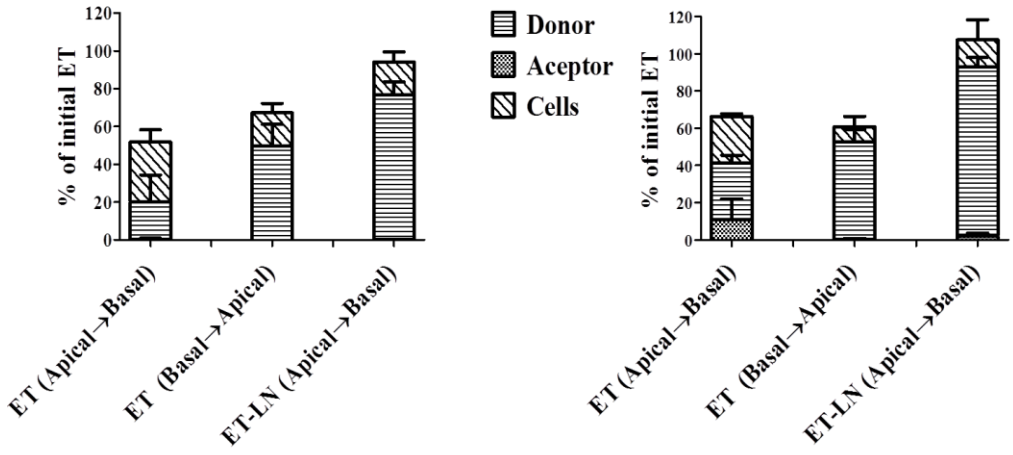

Figure 8. Edelfosine (% of initial drug quantity on the donor compartment) present in the donor, acceptor and cell samples at the end of the transport experiment (2 hours of incubation) in Caco-2 monoculture (left) and Caco-2 co-culture (right). Free drug was not detectable in the basolateral chamber. It can also be observed that ET is internalized more rapidly than ET-LN in both culture models.

As can be observed, there was no ET in the basolateral side. This drawback did not allow us to calculate P_{aap} of each treatment. Considering that only part of the ET

quantity that decreases from the apical compartment is quantified inside the cells, ET might suffer some metabolic process inside Caco-2 cells. ET is a synthetic PAF analog which contains a methyl group, attached by an ether linkage, at the sn-2 position. This change in the molecule is related to a longer *in vivo* half-life because it prevents the degradation by the Phospholipase A_2 (PLA_2). However, ET is susceptible of being degraded by three pathways: i) cleavage of the alkyl group by glyceryl-ether monooxygenase (GEMO), ii) hydrolysis by Phospholipase C (PLC), and iii) Phospholipase D (PLD) hydrolysis [26]. Nowadays, ET degradation by GEMO has been discarded [26]. Wilcox *et al* [27] showed that ET is metabolized in MDCK, K-562 and HL-60 cells at very slow rates; however, hepatocytes metabolize up to half the administered ET after 24 hours of incubation [28]. In conclusion, as has been demonstrated in hepatocytes, ET might be absorbed and metabolized in enterocytes. This process could be one of the causes of its poor oral bioavailability [2], and so the fate of ET in enterocytes should be further studied.

Nevertheless, in spite of being unable to calculate P_{app}`s coefficients, we were able to compare the internalization rates of ET and ET-LN in both *in vitro* intestinal models. ET was internalized into the cells very quickly in both culture models; besides, its internalization was higher from the apical than from the basolateral side. This might be explained by the lipid nature of ET; actually, hydrophobic compounds are taken up more efficiently by Caco-2 cells than hydrophilic molecules [10, 29]. This could mean that the concentration of ET used in the transport studies is high enough to saturate the P-gp efflux system. This saturation process, dependent on the drug concentration, has been previously demonstrated with other drugs [30]. Besides, the apical enterocyte membrane is enriched with lipid rafts, microdomains enriched with cholesterol and glycolipids [31, 32] where ET accumulates in cells [33]. This high proportion of lipid rafts in the apical enterocyte membrane might also induce high absorption of the drug by the cells. Comparing both models, ET was internalized at a higher rate in both *in vitro* models: in fact, 76% and 90.96% of LN remained in the apical side of Caco-2 monoculture and Caco-2/Raji co-culture respectively at the end of the transport experiment. These results are in agreement with results obtained by *Roger et al*. [25] who did not observe an increment in LN transport in the Caco-2/Raji

B model in comparison with Caco-2 monoculture model. Taking into consideration that previous *in vivo* studies show an accumulation of drugs in the lymphatic system after their oral administration in LN [3], Caco-2/Raji co-culture might be not comparable to Peyer's patch follicle-associated epithelium (FAE) in the intestine. In this sense, the importance of three dimensional models for the development of more realistic intestinal models has been pointed out [16].

4. Conclusions

ET is internalized at a higher rate in its free form in both *in vitro* intestinal models (Caco-2 and Caco-2/Raji). In fact, about 76% and 90% of the initial LN quantity remains in the donor compartment in Caco-2 monoculture and Caco-2/Raji co-culture respectively after 2 hours of incubation These results do not correlate with those observed *in vivo* when edelfosine-lipid nanoparticles were administered orally in mice, which suggests that the microfold model is not a good model to study the absorption of edelfosine-lipid nanoparticles across the intestinal barrier *in vitro*. Indeed, our results suggest that ET might suffer some metabolic process upon being internalized in Caco-2 and Caco-2/Raji intestinal models. The absence of drug in the acceptor compartment and its poor oral bioavailability might be explained by a similar metabolic process in enterocytes. Finally, the rapid ET internalization in the culture monolayers (about 80% of the initial ET in two hours) might be related to the hydrophilic nature of the drug, the elevated presence of lipid rafts in the apical surface of enterocytes and the saturation of the P-gp transporter.

5. References

[1] van Blitterswijk, W. J.; Verheij, M. Anticancer mechanisms and clinical application of alkylphospholipids. *Biochim Biophys Acta*, **2013,** 1831(3), 663-674.

[2] Estella-Hermoso de Mendoza, A.; Campanero, M. A.; de la Iglesia-Vicente, J.; Gajate, C.; Mollinedo, F.; Blanco-Prieto, M. J. Antitumor alkyl ether lipid edelfosine: tissue distribution and pharmacokinetic behavior in healthy and tumor-bearing immunosuppressed mice. *Clin Cancer Res*, **2009,** 15(3), 858-864.

[3] Lasa-Saracibar, B.; Estella-Hermoso de Mendoza, A.; Guada, M.; Dios-Vieitez, C.; Blanco-Prieto, M. J. Lipid nanoparticles for cancer therapy: state of the art and future prospects. *Expert Opin Drug Deliv*, **2012,** 9(10), 1245-1261.

[4] Mollinedo, F.; de la Iglesia-Vicente, J.; Gajate, C.; Estella-Hermoso de Mendoza, A.; Villa-Pulgarin, J. A.; Campanero, M. A.; Blanco-Prieto, M. J. Lipid raft-targeted therapy in multiple myeloma. *Oncogene*, **2010,** 29(26), 3748-3757.

[5] Estella-Hermoso de Mendoza, A.; Rayo, M.; Mollinedo, F.; Blanco-Prieto, M. J. Lipid nanoparticles for alkyl lysophospholipid edelfosine encapsulation: development and *in vitro* characterization. *Eur J Pharm Biopharm*, **2008,** 68(2), 207-213.

[6] Sambuy, Y.; De Angelis, I.; Ranaldi, G.; Scarino, M. L.; Stammati, A.; Zucco, F. The Caco-2 cell line as a model of the intestinal barrier: influence of cell and culture-related factors on Caco-2 cell functional characteristics. *Cell Biol Toxicol*, **2005,** 21(1), 1-26.

[7] Mabbott, N. A.; Donaldson, D. S.; Ohno, H.; Williams, I. R.; Mahajan, A. Microfold (M) cells: important immunosurveillance posts in the intestinal epithelium. *Mucosal Immunol*, **2013,** 6(4), 666-677.

[8] Antunes, F.; Andrade, F.; Araujo, F.; Ferreira, D.; Sarmento, B. Establishment of a triple co-culture in vitro cell models to study intestinal absorption of peptide drugs. *Eur J Pharm Biopharm*, **2012,** 83(3), 427-435.

[9] des Rieux, A.; Fievez, V.; Theate, I.; Mast, J.; Preat, V.; Schneider, Y. J. An improved in vitro model of human intestinal follicle-associated epithelium to study nanoparticle transport by M cells. *Eur J Pharm Sci*, **2007,** 30(5), 380-391.

[10] Beloqui, A.; Solinis, M. A.; Gascon, A. R.; del Pozo-Rodriguez, A.; des Rieux, A.; Preat, V. Mechanism of transport of saquinavir-loaded nanostructured lipid carriers across the intestinal barrier. *J Control Release*, **2012,** 166(2), 115-123.

[11] Kerneis, S.; Bogdanova, A.; Kraehenbuhl, J. P.; Pringault, E. Conversion by Peyer's patch lymphocytes of human enterocytes into M cells that transport bacteria. *Science*, **1997,** 277(5328), 949-952.

[12] Lo, D.; Tynan, W.; Dickerson, J.; Scharf, M.; Cooper, J.; Byrne, D.; Brayden, D.; Higgins, L.; Evans, C.; O'Mahony, D. J. Cell culture modeling of specialized tissue: identification of genes expressed specifically by follicle-associated epithelium of Peyer's patch by expression profiling of Caco-2/Raji co-cultures. *Int Immunol*, **2004,** 16(1), 91-99.

[13] Ander Estella-Hermoso de Mendoza, M. J. B.-P., Miguel Angel Campanero, Faustino Mollinedo, Janny Villa-Pulgarín, Rubén Varela. Development and use of lipidic nanoparticles loaded with edelfosine and ether phospholipids in antitumoral and antiparasitic therapy. Spain. **2011**. P201130433.

[14] Estella-Hermoso de Mendoza, A.; Campanero, M. A.; Mollinedo, F.; Blanco-Prieto, M. J. Comparative study of A HPLC-MS assay versus an UHPLC-MS/MS for anti-tumoral alkyl lysophospholipid edelfosine determination in both biological samples and in lipid nanoparticulate systems. *J Chromatogr B Analyt Technol Biomed Life Sci*, **2009,** 877(31), 4035-4041.

[15] Millicell® ERS-2 User Guide. http://www.millipore.com/userguides.nsf/a73664f9f981af8c852569b9005b4eee/a5708d8207d7accf85257609005c7c5f/$FILE/00108103.pdf (Accesed Sept 11, **2013**).

[16] Pusch, J.; Votteler, M.; Gohler, S.; Engl, J.; Hampel, M.; Walles, H.; Schenke-Layland, K. The physiological performance of a three-dimensional model that mimics the microenvironment of the small intestine. *Biomaterials*, **2011,** 32(30), 7469-7478.

[17] Estella-Hermoso de Mendoza, A.; Preat, V.; Mollinedo, F.; Blanco-Prieto, M. J. In vitro and in vivo efficacy of edelfosine-loaded lipid nanoparticles against glioma. *J Control Release*, **2011,** 156(3), 421-426.

[18] Lasa-Saracibar, B.; Estella-Hermoso de Mendoza, A.; Mollinedo, F.; Odero, M. D.; Blanco-Prieto, M. J. Edelfosine lipid nanosystems overcome drug resistance in leukemic cell lines. *Cancer Lett*, **2013,** 334(2), 302-310.

[19] Gullberg, E.; Leonard, M.; Karlsson, J.; Hopkins, A. M.; Brayden, D.; Baird, A. W.; Artursson, P. Expression of specific markers and particle transport in a new human intestinal M-cell model. *Biochem Biophys Res Commun*, **2000,** 279(3), 808-813.

[20] Stevenson, B. R.; Siliciano, J. D.; Mooseker, M. S.; Goodenough, D. A. Identification of ZO-1: a high molecular weight polypeptide associated with the tight junction (zonula occludens) in a variety of epithelia. *J Cell Biol*, **1986,** 103(3), 755-766.

[21] Kerneis, S.; Bogdanova, A.; Colucci-Guyon, E.; Kraehenbuhl, J. P.; Pringault, E. Cytosolic distribution of villin in M cells from mouse Peyer's patches correlates with the absence of a brush border. *Gastroenterology*, **1996,** 110(2), 515-521.

[22] Weston, S. A.; Parish, C. R. New fluorescent dyes for lymphocyte migration studies. Analysis by flow cytometry and fluorescence microscopy. *J Immunol Methods*, **1990,** 133(1), 87-97.

[23] Xue, X.; Liang, X. J. Overcoming drug efflux-based multidrug resistance in cancer with nanotechnology. *Chin J Cancer*, **2012,** 31(2), 100-109.

[24] Troutman, M. D.; Thakker, D. R. Rhodamine 123 requires carrier-mediated influx for its activity as a P-glycoprotein substrate in Caco-2 cells. *Pharm Res*, **2003,** 20(8), 1192-1199.

[25] Roger, E.; Lagarce, F.; Garcion, E.; Benoit, J. P. Lipid nanocarriers improve paclitaxel transport throughout human intestinal epithelial cells by using vesicle-mediated transcytosis. *J Control Release*, **2009,** 140(2), 174-181.

[26] Gajate, C.; Mollinedo, F. Biological activities, mechanisms of action and biomedical prospect of the antitumor ether phospholipid ET-18-OCH(3) (edelfosine), a proapoptotic agent in tumor cells. *Curr Drug Metab*, **2002,** 3(5), 491-525.

[27] Wilcox, R. W.; Wykle, R. L.; Schmitt, J. D.; Daniel, L. W. The degradation of platelet-activating factor and related lipids: susceptibility to phospholipases C and D. *Lipids*, **1987,** 22(11), 800-807.

[28] Magistrelli, A.; Villa, P.; Benfenati, E.; Modest, E. J.; Salmona, M.; Tacconi, M. T. Fate of 1-O-octadecyl-2-O-methyl-rac-glycero-3-phosphocholine (ET18-OME) in malignant cells, normal cells, and isolated and perfused rat liver. *Drug Metab Dispos*, **1995,** 23(1), 113-118.

[29] Gaumet, M.; Gurny, R.; Delie, F. Interaction of biodegradable nanoparticles with intestinal cells: the effect of surface hydrophilicity. *Int J Pharm*, **2009,** 390(1), 45-52.

[30] Jang, S. H.; Wientjes, M. G.; Au, J. L. Kinetics of P-glycoprotein-mediated efflux of paclitaxel. *J Pharmacol Exp Ther*, **2001,** 298(3), 1236-1242.

[31] Danielsen, E. M.; Hansen, G. H. Lipid rafts in epithelial brush borders: atypical membrane microdomains with specialized functions. *Biochim Biophys Acta*, **2003,** 1617(1-2), 1-9.

[32] Kunding, A. H.; Christensen, S. M.; Danielsen, E. M.; Hansen, G. H. Domains of increased thickness in microvillar membranes of the small intestinal enterocyte. *Mol Membr Biol*, **2010,** 27(4-6), 170-177.

[33] Ausili, A.; Torrecillas, A.; Aranda, F. J.; Mollinedo, F.; Gajate, C.; Corbalan-Garcia, S.; de Godos, A.; Gomez-Fernandez, J. C. Edelfosine is incorporated into rafts and alters their organization. *J Phys Chem B*, **2008,** 112(37), 11643-11654.

CHAPTER 5

In vivo toxicity evaluation of lipid nanoparticles loaded with edelfosine

*Beatriz Lasa-Saracíbar[1], María Ángela Aznar[1], Hugo Lana[1], Ismael Aizpún[2], Ana Gloria Gil[2], Maria J. Blanco-Prieto[1]**

[1] *Department of Pharmacy and Pharmaceutical Technology, School of Pharmacy, University of Navarra, Pamplona, Spain*

[2] *Laboratory of Toxicology, Center of Research in Applied Pharmacobiology (CIFA), University of Navarra, Pamplona, Spain*

KEYWORDS: Edelfosine, *in vivo*, lipid nanoparticles, toxicity

***Corresponding author:** Dr. María J. Blanco-Prieto, Department of Pharmaceutics and Pharmaceutical Technology, School of Pharmacy, University of Navarra, C/Irunlarrea 1, E-31080 Pamplona, Spain, Office phone: + 34 948 425 600 ext. 6519, Fax: + 34 948 425 649, e-mail: mjblanco@unav.es

Declaration of interest: The authors state no conflict of interest.

Submitted to Nanotoxicology

Abstract

Despite the large number of studies regarding the use of lipid nanoparticles as vehicles for drug administration, toxicity studies are very limited. The lipid nanoparticles used in the present paper are made of lipids recognized as safe by the Food and Drug Administration (FDA) and, therefore, these systems are generally considered as nontoxic vehicles. Nevertheless, the particular physicochemical characteristics of these systems, due to their nanometric scale, might cause interactions with the biological systems and lead to undesirable effects. Hence, toxicity studies are needed in order to ensure the safety of these nanomedicines. Edelfosine, an alkyl-lysophospholipid antitumor drug with severe side-effects, has previously been encapsulated into lipid nanoparticles with the purpose of improving their toxicity profile. In the present study we investigated the *in vivo* toxicity of free edelfosine, lipid nanoparticles and lipid nanoparticles loaded with edelfosine in mice after oral administration. Our results showed that oral administration of the free drug at 4 times higher than the therapeutic dose caused the death of the animals within 72 hours. Moreover, histopathology revealed gastrointestinal toxicity and an immunosuppressive effect. In contrast, lipid nanoparticles were completely safe and showed a protective effect against edelfosine toxicity even at the higher dose. Lipid nanoparticles are, therefore, a safe vehicle for the administration of edelfosine by the oral route. The nanosystems developed could be further used for the administration of other drugs.

1. Introduction

Lipid nanoparticles (LN) were developed in the late 1980s, and since then they have become a cornerstone in the nanomedicine field [1]. Several studies confirm the advantages of using LN to encapsulate antitumor drugs, demonstrating several benefits over the administration of the free drugs in terms of bioavailability and pharmacokinetic profiles [2]. Edelfosine (ET) is a member of a family of drugs known as alkyl lysophospholipids (ALPs). ET has proved antitumor effects *in vitro* and *in vivo*; nevertheless, its poor oral bioavailability and severe side effects prevent therapeutic use of ET in clinical practice [3-5]. To overcome these drawbacks, Estella et al. [6] developed nanoparticles containing edelfosine (ET-LN) which showed improved bioavailability and pharmacokinetic profiles and enhanced antitumor efficacy compared to the free drug [7, 8].

Despite the large number of LN formulations existing in the literature, few toxicity studies have been carried out [9-14]. The anticipated biocompatibility of these nanosystems due to their lipid composition may explain the lack of toxicity studies. However, the interaction of nanoparticles with biological systems might trigger biological effects that are not observed with traditional drugs. In this paper, we evaluate the *in vivo* toxicity profile of free ET, LN and ET-LN after their oral administration in mice.

2. Material and methods

2.1 Materials

ET was purchased from APOINTECH (Salamanca, Spain). Precirol® ATO 5 was a gift from Gattefossé (France). Tween® 80 was purchased from Roig Pharma (Barcelona, Spain). Chloroform was obtained from Panreac (Madrid, Spain), formic acid 99% for mass spectroscopy was obtained from Fluka (Barcelona, Spain), and methanol was purchased from Merck (Barcelona, Spain). All solvents employed for the chromatographic analysis were of analytical grade; all other chemicals were

reagent grade and used without further purification. Amicon Ultra-15 10,000 MWCO centrifugal filter devices were purchased from Millipore (Cork, Ireland).

2.2 Preparation of LN

LN were prepared by the hot homogenization method consisting of high shear homogenization and ultrasonication [6]. Briefly, ET (30 mg) and Precirol® (300 mg) were place in a vial and heated at 5ºC above the lipid melting point. Then, an aqueous solution of Tween 80 (2%), previously heated at the same temperature, was poured onto the lipid phase. Emulsion was formed and homogeneized by a Microson™ ultrasonic cell disruptor (NY, USA) and an Ultraturrax® (IKA-Werke, Germany). The emulsion was removed from heat and placed in an ice bath to obtain LN by lipid solidification. Afterwards, 150 % (w/w of lipid weight) trehalose was added as cryoprotectant agent to the LN suspension, which was then kept at -80ºC and freeze-dried to obtain a nanoparticulate powder. Particle size and polydispersity index (PDI) were evaluated by photon correlation spectroscopy (PCS) using a Zetasizer Nano (Malvern Instruments, UK). The measurements were carried out three times. Surface charge was measured using the same Zetasizer Nano equipment combined with laser Doppler velocimetry. ET loading was analyzed by a previously validated ultra-high-performance liquid chromatography tandem mass spectrometry (UHPLC-MS/MS) method [15].

2.3 *In vivo* toxicity studies

2.3.1 Animal handling

BALB/c mice of each sex (20-22 g) were obtained from Harlan Interfauna Ibérica (Barcelona, Spain). Animals were housed at room temperature under a 12-h light/dark cycle with water and food provided *ad libitum*. The experimental protocol was revised and approved by the Animal Experimentation Ethics Committee of the University of Navarra (protocol number CEEA: 054-13).

2.3.2 Experimental design

Mice were divided into 7 groups (n=20; 10 females and 10 males). Two different doses were used in the study: the therapeutic dose (equivalent to 30 mg/kg of ET) and a dose 4 times higher (equivalent to 120 mg ET/kg of body weight). The higher dose was the maximum feasible dose (MFD) for adequate nanoparticle resuspension. Animals received for 1 month (i) ET (30 mg/kg); ii) ET (120 mg/kg); iii) ET-LN (30 mg/kg), iv) ET-LN (120 mg/kg); (v) Blank-LN (30 mg/kg); (vi) Blank-LN (120 mg/kg) (vii) physiological serum. All treatments were administered orally. ET was administered daily while ET-LN and Blank-LN were administered every three days. Physiological serum was administered daily to the control group.

2.3.3 Evaluation of the treatments regarding animal health and survival

Cage-side clinical observations were performed daily on all animals; an additional afternoon check was performed daily for dead or moribund animals. Body weights were recorded at study day 0, weekly during the study, and at schedule necropsy. Food and water consumption was assessed on a daily basis and expressed as grams per mice per day. At the end of the experiment, blood samples were collected from the eye vein for biochemical and hematological assays. Biochemical parameters, aspartate aminotransferase (AST), alanine aminotransferase (ALT), albumin (ALB), creatinine (CREA) and blood urea nitrogen (BUN), were inspected in serum sample by using a Roche semiautomatic analyzer (Hitachi 911). The hemogram, red blood cells (RBC), white blood cells (WBC), hemoglobin (HGB), hematocrit (HCT) and platelets (PLT), were investigated by using a Roche hematology analyzer (Sysmex XT1800i). Finally, all surviving test and control animals were euthanized with CO_2 in an appropriate chamber. External appearance, internal organs and tissues were observed macroscopically. Organs were weighed using an electronic balance Mettler FX-300i. Relative organ weights were calculated from the body weight on the day of gross pathology. The organs (stomach, intestines, spleen, liver, kidneys, lung, heart and brain) were carefully removed and fixed with 10% formalin for histological studies.

2.4 Statistical analysis

Statistical analysis was performed with the SPSS v15.0 program (IBM, Spain). The statistical significance level was defined as a P value of <0.05.

3. Results and discussion

3.1 Lipid nanoparticle formulation

The use of a hot homogenization method developed previously [6] provided LN with a size of 127.89 ± 9.95 nm suitable for oral administration [1]. LN charge was negative and enough to maintain formulation stability (-28.42 ± 1.39).

3.2 *In vivo* toxicity studies

3.2.1 Clinical signs and mortality

After administration of ET at the higher dose, all mice died in the first 72 hours. Moreover, half of the animals were found dead in the first 24 hours after the first administration. Animals presented anorexia, diarrhea and action retardation. In contrast, no mice treated with the lower dose of free drug died during the experiment. Additionally, Blank-LN and ET-LN did not induce animals' death at any of the administered doses and animals' behavior and general physical appearance was normal during the course of the experiment.

3.2.2 Body weight gain, food and water consumption

Body weight gain, food and water consumption were similar to the control group in all the animal groups (data not shown). These results were not applied to the animals treated with ET at the higher dose. These animals presented severe anorexia and died within the first 72 hours after the first administration.

3.2.3 Biochemistry, hematology and histopathology (organ appearances and coefficients)

Animals treated with ET at the higher dose were found dead or sacrificed (due to their moribund appearance) in the first 72 hours of the experiment. Necropsy of these animals showed gastrointestinal tract obstruction with accumulation of food in the stomach, swelling, fluid accumulation and thickness of the stomach and intestine walls (Fig. 1). Histopathology revealed degeneration, necrosis and peeling of superficial cells in the stomach and the small intestine (Fig. 2). These findings were accompanied by moderate inflammatory infiltration of the *lamina propia* of the intestinal mucosa, which suggest an irritant effect of ET at the higher dose over the gastric and duodenal mucosa. In addition, the treatment produced a clear lymphoid depletion with size decrease, disorganization and loss of the general structure of the lymphoid tissue of Peyer`s patches, mesenteric lymph nodes and spleen (Fig. 3).

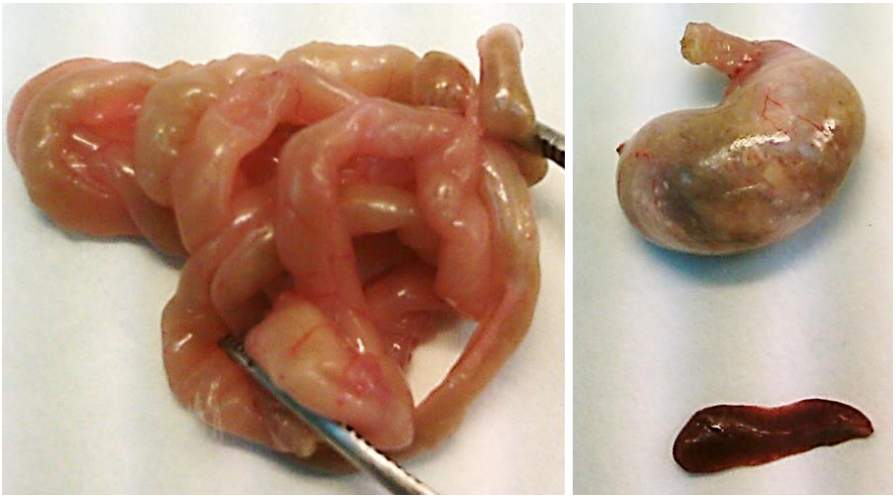

Figure 1. Stomach and small intestine. Paraffin embedded tissues stained with hematoxylin and eosin; X200 (stomach/free-ET; X400). ET (120 mg/kg) caused gastrointestinal toxicity with degeneration, necrosis and peeling of the stomach and intestine walls.

The rest of the animals were sacrificed 30 days from the beginning of the experiment. None of the animals presented any macroscopic organ changes with respect to the control group.

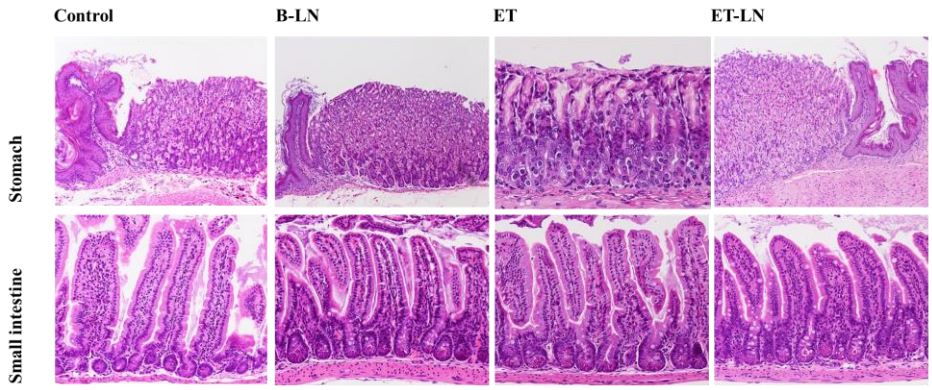

Figure 2. Stomach and small intestine. Paraffin embedded tissues stained with hematoxylin and eosin; X200 (stomach/free-ET; X400). ET (120 mg/kg) caused gastrointestinal toxicity with degeneration, necrosis and peeling of the stomach and intestine walls.7

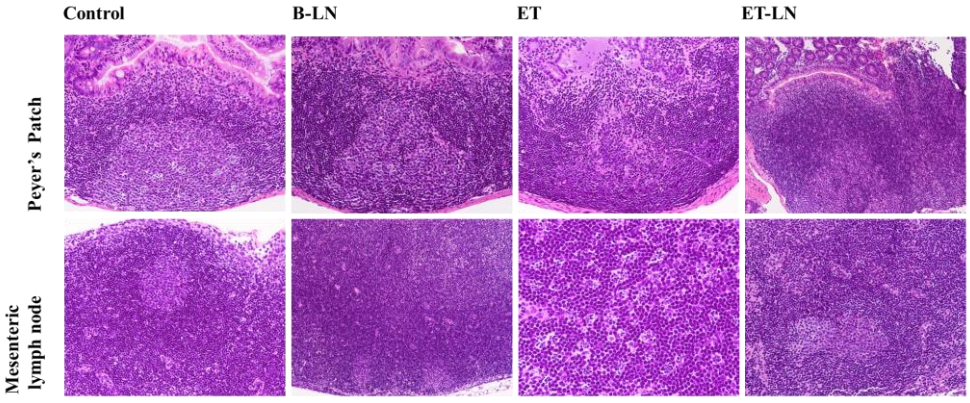

Figure 3. Peyers`patches and mesenteric lymph nodes. Paraffin embedded tissues stained with hematoxylin and eosin; X200. ET (120 mg/kg) had an immunosuppressant effect characterized by size decrease, disorganization and loss of the general structure of the lymphoid tissue of Peyer´s patches, mesenteric lymph nodes and spleen.

Organ coefficients (Table 1) showed some slight differences especially in the group of animals treated with the higher dose of ET-LN; Biochemical and hematological parameters (Table 2) also showed some variations with respect to the control group. Nevertheless, none of these observations followed any specific pattern. Moreover, they were not related to any histologic pathology and therefore

they should be considered common variations in the blood parameters present in the murine species.

Table 1. Organ coefficients of treated mice (Mean ± S.D., n=5)[a]. *p < 0.05;p < 0.01; ***p < 0.001 vs. corresponding control group by Wilcoxon–Mann–Whitney statistical test.**

Sex	Treatment	Dose (µg/kg)	Heart	Spleen	Liver	Kidneys
Male	**Saline**		0.70 ± 0.11	0.32 ± 0.05	5.10 ± 0.17	0.90 ± 0.02
	BLANK-LN	**30**	0.78 ± 0.12	0.27 ± 0.07	5.31 ± 0.49	0.83 ± 0.09
		120	0.74 ± 0.16	0.25 ± 0.02*	4.98 ± 0.46	0.69 ± 0.09**
	ET	**30**	0.73 ± 0.12	0.29 ± 0.10	5.12 ± 0.38	0.87 ± 0.02
		120	†	†	†	†
	ET-LN	**30**	0.65 ± 0.11	0.49 ± 0.20	5.12 ± 0.30	0.77 ± 0.08
		120	0.70 ± 0.23	0.28 ± 0.05	5.36 ± 0.28	0.91 ± 0.03
Female	**Saline**		0.63 ± 0.08	0.37 ±0.03	4.96 ± 0.26	0.75 ±0.02
	BLANK-LN	**30**	0.67 ± 0.15	0.34 ± 0.07	5.32 ± 0.06	0.81 ± 0.01
		120	0.67 ± 0.08	0.54 ± 0.29	5.30 ± 0.42	0.80 ± 0.03
	ET	**30**	0.70 ± 0.16	0.36 ± 0.66	5.24 ± 0.37	0.75 ± 0.01
		120	†	†	†	†
	ET-LN	**30**	0.98 ± 0.13*	0.33 ± 0.14	5.55 ± 0.32*	0.80 ± 0.15
		120	0.72 ± 0.08	0.48 ± 0.79*	5.36 ± 0.23*	0.80 ± 0.02

a: Values expressed as g tissue/g body weight x 100

These results are in agreement with previous findings that demonstrate that LN provide a potent protective effect against drug toxicity [9, 11]. Edelfosine gastrointestinal toxicity has been previously reported as the main toxic effect of edelfosine administered by the oral route [16]; however, these studies report a DL50 of 250 mg/kg of body weight in mice, and the present study showed that the dose of 120 mg/kg was lethal for half of the animals in the first 24 hours after the first oral administration. Nevertheless, the results obtained are in agreement with previous *in vivo* toxicity studies that describe a lack of toxicity on doses below 40 mg/kg of body weight [16, 17]. On the other hand, to our knowledge, this is the first time that an immunosuppressant effect has been observed after oral administration of ET. In fact, previous studies proved that ET does not induce bone marrow toxicity [16]. Myelotoxicity was not observed in the present work either (blood cell counts were normal in mice treated with ET at 120 mg/kg). The immunosuppressant effect seems to be caused by direct action of the drug in the lymph nodes and the lymphatic nodules (Peyers´patches and spleen). Besides, both side effects were only observable after the administration of the free drug at the higher dose. In conclusion, ET is lethal by the oral route at doses 4-times superior to the therapeutic dose (30

mg/kg). It causes severe gastrointestinal irritation and immunodepression. On the other hand, it is safe at a therapeutic dose. Furthermore, ET-LN are safe at both doses, evidencing the protective effect that LN provides over the administration of the free-drug. On the other hand, no toxic effects were detected after the oral administration of blank-LN. LN are, therefore a safe vehicle for the administration of drugs by the oral route.

Table 2. Biochemical and hematological parameters of treated mice ((Mean ± S.D., n=5). *p < 0.05;p < 0.01; ***p < 0.001 vs. corresponding control group by Wilcoxon–Mann–Whitney statistical test.**

Sex	Treatment	Dose (mg/kg)	AST (U/L)	ALT (U/L)	ALB (g/dL)	CREA (mg/dL)	Urea (mg/dL)
Male	Saline		74.80 ± 16.75	69.60 ± 18.73	3.39 ± 1.13	0.07 ± 0.02	77.40 ± 10.40
	BLANK-LN	30	141.00 ± 129.39	71.00 ± 51.97	2.91 ± 0.75	0.12 ± 0.01*	74.67 ± 9.07
		120	214.50 ± 185.73*	106.00 ± 83.76	4.05 ± 0.30	0.12 ± 0.01*	59.75 ± 18.59
	ET	30	116.40 ± 19.63*	91.60 ± 45.93	2.48 ± 1.67	0.09 ± 0.01	70.80 ± 20.89
		120	†	†	†	†	†
	ET-LN	30	161.25 ± 78.46*	149.75 ± 96.80	4.09 ± 0.55	0.13 ± 0.04*	70.25 ± 18.39
		120	84.40 ± 54.85	26.40 ± 7.40**	2.45 ± 1.62	0.14 ± 0.04*	69.60 ± 19.51
Female	Saline		131.00 ± 37.56	57.80 ± 13.86	2.79 ± 1.65	0.10 ± 0.23	68.20 ± 1.79
	BLANK-LN	30	78.75 ± 21.33*	46.00 ± 6.98	3.55 ± 1.562	0.14 ± 0.01	69.50 ± 9.43
		120	91.00 ± 24.90*	53.00 ± 13.51	3.67 ± 1.65	0.09 ± 0.01	60.60 ± 3.97*
	ET	30	145.00 ± 106.54	54.00 ± 23.89	2.79 ± 1.86	0.13 ± 0.12	66.00 ± 7.16
		120	†	†	†	†	†
	ET-LN	30	99.60 ± 46.01	39.80 ± 12.64	3.60 ± 1.50	0.13 ± 0.02*	58.60 ± 10.36
		120	266.60 ± 54.10**	95.00 ± 39.48	3.50 ± 1.75	0.10 ± 0.02	75.80 ± 22.92
Sex	**Treatment**	**Dose (mg/kg)**	**AST (U/L)**	**ALT (U/L)**	**ALB (g/dL)**	**CREA (mg/dL)**	**Urea (mg/dL)**
Male	Saline		10.90 ± 0.30	3.67 ± 2.22	16.08 ± 0.50	47.02 ± 1.00	745.00 ± 257.52
	BLANK-LN	30	10.84 ± 0.12	2.26 ± 0.80	15.92 ± 0.16	47.60 ± 0.31	720.60 ± 30.92
		120	10.54 ± 0.54	1.85 ± 0.41	15.38 ± 0.78	47.10 ± 2.23	739.60 ± 67.51
	ET	30	9.75 ± 2.21	1.85 ± 0.70	14.20 ± 3.20	42.24 ± 8.82	755.40 ± 117.49
		120	12.23 ± 0.27	4.26 ± 0.10	18.40 ± 0.56	49.85 ± 1.77	553.00 ± 16.971
	ET-LN	30	10.72 ± 0.42	2.16 ± 0.76	16.04 ± 0.67	46.58 ± 2.13	921.60 ± 67.80*
		120	10.96 ± 0.31	3.52 ± 1.01	16.18 ± 0.34	46.68 ± 1.20	901.60 ± 74.63
Female	Saline		10.89 ± 0.16	7.25 ± 1.03	16.34 ± 0.17	46.92 ± 0.99	859.40 ± 8.65
	BLANK-LN	30	10.78 ± 0.35	4.65 ± 1.22*	16.20 ± 0.59	46.54 ± 1.13	788.00 ± 49.73**
		120	10.82 ± 0.55	5.91 ± 3.84	15.76 ± 1.15	46.86 ± 3.78	807.60 ± 180.28
	ET	30	10.79 ± 0.24	3.54 ± 0.55**	16.04 ± 0.29	45.74 ± 1.10	888.20 ± 78.00
		120	11.90 ± 2.23	10.85 ±15.82	18.96 ± 2.95*	50.52 ± 6.33	586.50 ± 150.69
	ET-LN	30	10.29 ± 0.25**	2.60 ± 0.62**	15.54 ± 0.48*	44.36 ± 1.35*	875.00 ± 70.24
		120	10.55 ± 0.25	4.39 ± 0.81**	15.86 ± 0.23**	45.36 ± 0.57*	1058.40 ± 72.84**

4. Conclusions

In vivo toxicity studies demonstrate that LN provide a protective effect against toxicity of the free drug. LN protect recipients from the severe acute toxicity of the higher dose of ET which induced the death of the animals within the first 72 hours of the experiment. Besides, ET at the higher dose provoked gastrointestinal toxicity and triggered an immunosuppressive effect. Free drug (30 mg/kg), blank-LN and ET-LN (30 and 120 mg/kg) did not induce any side-effects. Besides, blank-LN showed no toxicity effects at any of the administered doses. These results show that ET-LN do not present toxicity effects *in vivo* and, therefore, they might be used safely by the oral route.

5. References

[1] Lasa-Saracibar, B.; Estella-Hermoso de Mendoza, A.; Guada, M.; Dios-Vieitez, C.; Blanco-Prieto, M. J. Lipid nanoparticles for cancer therapy: state of the art and future prospects. *Expert Opin Drug Deliv*, **2012,** *9*, 1245-1261.

[2] Guo, S.; Huang, L. Nanoparticles containing insoluble drug for cancer therapy. *Biotechnol Adv*, **2013**, *13*:S0734-9750

[3] Reis-Sobreiro, M.; Roue, G.; Moros, A.; Gajate, C.; de la Iglesia-Vicente, J.; Colomer, D.; Mollinedo, F. Lipid raft-mediated Akt signaling as a therapeutic target in mantle cell lymphoma. *Blood Cancer J*, **2013,** *3*, e118.

[4] Gajate, C.; Matos-da-Silva, M.; Dakir el, H.; Fonteriz, R. I.; Alvarez, J.; Mollinedo, F. Antitumor alkyl-lysophospholipid analog edelfosine induces apoptosis in pancreatic cancer by targeting endoplasmic reticulum. *Oncogene*, **2011,** *31*, 2627-2639.

[5] van Blitterswijk, W. J.; Verheij, M. Anticancer mechanisms and clinical application of alkylphospholipids. *Biochim Biophys Acta*, **2013,** *1831*, 663-674.

[6] Estella-Hermoso de Mendoza, A.; Blanco-Prieto, M.J., Campanero, M.A.; Mollinedo F.; Villa-Pulgarín, J.; Varela, R. Development and use of lipidic

nanoparticles loaded with edelfosine and ether phospholipids in antitumoral and antiparasitic therapy. **2011**. P201130433.

[7] Estella-Hermoso de Mendoza, A.; Campanero, M. A.; Lana, H.; Villa-Pulgarin, J. A.; de la Iglesia-Vicente, J.; Mollinedo, F.; Blanco-Prieto, M. J. Complete inhibition of extranodal dissemination of lymphoma by edelfosine-loaded lipid nanoparticles. *Nanomedicine (Lond)*, **2012,** *7*, 679-690.

[8] Estella-Hermoso de Mendoza, A.; Preat, V.; Mollinedo, F.; Blanco-Prieto, M. J. In vitro and in vivo efficacy of edelfosine-loaded lipid nanoparticles against glioma. *J Control Release*, **2011,** *156*, 421-426.

[9] Xie, S.; Wang, F.; Wang, Y.; Zhu, L.; Dong, Z.; Wang, X.; Li, X.; Zhou, W. Acute toxicity study of tilmicosin-loaded hydrogenated castor oil-solid lipid nanoparticles. *Part Fibre Toxicol*, **2011,** *8*, 33.

[10] Aillon, K. L.; Xie, Y.; El-Gendy, N.; Berkland, C. J.; Forrest, M. L. Effects of nanomaterial physicochemical properties on in vivo toxicity. *Advanced Drug Delivery Reviews*, **2009,** *61*, 457-466.

[11] Xue, M.; Jiang, Z.-z.; Wu, T.; Li, J.; Zhang, L.; Zhao, Y.; Li, X.-j.; Zhang, L.-Y.; Yang, S.-y. Anti-inflammatory effects and hepatotoxicity of Tripterygium-loaded solid lipid nanoparticles on adjuvant-induced arthritis in rats. *Phytomedicine*, **2012,** *19*, 998-1006.

[12] Xue, M.; Zhao, Y.; Li, X.-j.; Jiang, Z.-z.; Zhang, L.; Liu, S.-h.; Li, X.-m.; Zhang, L.-Y.; Yang, S.-y. Comparison of toxicokinetic and tissue distribution of triptolide-loaded solid lipid nanoparticles vs free triptolide in rats. *European Journal of Pharmaceutical Sciences*, **2012,** *47*, 713-717.

[13] Blasi, P.; Schoubben, A. l.; Traina, G.; Manfroni, G.; Barberini, L.; Alberti, P. F.; Cirotto, C.; Ricci, M. Lipid nanoparticles for brain targeting III. Long-term stability and in vivo toxicity. *International Journal of Pharmaceutics*, **2013,** *454*, 316-323.

[14] Silva, A. H.; Locatelli, C.; Filippin-Monteiro, F. B.; Zanetti-Ramos, B. G.; Conte, A.; Creczynski-Pasa, T. B. Solid lipid nanoparticles induced hematological changes and inflammatory response in mice. *Nanotoxicology*, **2013.**

[15] Estella-Hermoso de Mendoza, A.; Campanero, M. A.; Mollinedo, F.; Blanco-Prieto, M. J. Comparative study of A HPLC-MS assay versus an UHPLC-MS/MS for anti-tumoral alkyl lysophospholipid edelfosine determination in both biological samples and in lipid nanoparticulate systems. *J Chromatogr B Analyt Technol Biomed Life Sci*, **2009,** *877*, 4035-4041.

[16] Gajate, C.; Mollinedo, F. Biological activities, mechanisms of action and biomedical prospect of the antitumor ether phospholipid ET-18-OCH(3) (edelfosine), a proapoptotic agent in tumor cells. *Curr Drug Metab*, **2002,** *3*, 491-525.

[17] Mollinedo, F.; Gajate, C.; Morales, A. I.; del Canto-Janez, E.; Justies, N.; Collia, F.; Rivas, J. V.; Modolell, M.; Iglesias, A. Novel anti-inflammatory action of edelfosine lacking toxicity with protective effect in experimental colitis. *J Pharmacol Exp Ther*, **2009,** *329*, 439-449.

CHAPTER 6

In vivo biodistribution of edelfosine radio-labeled lipid nanoparticles and efficacy in xenogeneic mouse model of human acute lymphoblastic leukemia

---

*Beatriz Lasa-Saracíbar, Stavros Xanthopoulos, Tsotakos Theodore, Amaia Vilas-Zornoza, Edurne San José, Xabier Agirre, Felipe Prosper, Penelope Bouziotis, Maria J. Blanco-Prieto**

Department of Pharmacy and Pharmaceutical Technology, School of Pharmacy, University of Navarra, Pamplona, Spain

***Corresponding author**

Dr. María J. Blanco-Prieto, Department of Pharmaceutics and Pharmaceutical Technology, School of Pharmacy, University of Navarra, C/Irunlarrea 1, E-31080 Pamplona, Spain, Office phone: + 34 948 425 600 ext. 6519, Fax: + 34 948 425 649, e-mail: mjblanco@unav.es

Declaration of interest: The authors state no conflict of interest.

Abstract

Acute lymphoblastic leukemia (ALL) is an aggressive blood cancer with high frequency or relapse in adults; current treatments still present side-effects and thus novel treatments are required. In these regard, many authors support the advantages of nanomedicines in cancer therapy. Previous studies state the efficacy of lipid nanoparticles containing an antitumor drug known as edelfosine (ET-LN) in leukemia cells. Edelfosine (ET) is a potent antitumor agent but it provokes severe side effects that have limited its use in clinical practice. For this reason, ET-LN are advantageous as they protect from ET side-effects. Moreover, they allow oral administration of antitumor agents, thus increasing their bioavailability. This study was aimed to evaluate the efficacy of ET-LN in a xenogeneic mouse model of human acute lymphoblastic leukemia. This *in vivo* model allows blood, spleen and bone marrow engraftment. However, it was carried out in a specific immunosuppressed strain of mice that are not likely to absorb LN delivered orally. Considering this, biodistribution studies were performed in order to select a suitable route of administration in these mice. ET-LN were labeled with Technetium-99m ($_{99m}$Tc) and administered by the oral, intravenous (i.v.) and intraperitoneal (i.p.) route in mice. ET-LN were successfully labeled and results led us to select the i.p. route due to the lower accumulation in reticulo-endothelial system (RES) organs and its capacity to maintain sustained levels of drug in the blood. However, efficacy studies exhibited a problem of overdosing. Animals were administered a dose that is consider safe given orally but that was toxic by the i.p. route. Therefore, although the efficacy study has to be optimized, preliminary results were encouraging as both ET and ET-LN were able to decrease the percentage of human leukemia cells in mice with respect to the control group.

1. Introduction

Acute lymphoblastic leukemia (ALL), also known as acute lymphocytic leukemia, is an aggressive blood cancer characterized by an excessive production by the bone marrow of abnormal lymphoblasts, B lymphocytes or T lymphocytes. Leukemia may cause infection, anemia, and easy bleeding due to the quick blood invasion. The cancer can also spread to lymph nodes, liver, spleen and to the central nervous system (brain and spinal cord); without treatment it usually progresses quickly. This disease can affect either children or adults and it is the most common cancer in children [1]. Prognosis and survival depend on several factors: i) age; ii) CNS involvement; iii) cellular morphology and iv) chromosomal abnormalities. Treatment is divided into different phases: i) remission induction; ii) CNS prophylaxis and iv) post-remission; and includes chemotherapy, biological treatments, targeted therapy, radiation and stem cell transplant. Almost 80 % of children diagnosed with ALL are cured with modern risk-adapted therapies. However, more than 60 % of adult patients will eventually relapse and most of them will succumb to their disease [2]. As a result, new therapies are required and, among all these, the use of nanotherapy such as lipid nanoparticles (LN) provides benefits in the treatment of the disease [3]. LN have been widely used to encapsulate antitumor drugs and, among all these formulations, LN containing edelfosine (ET-LN) have shown improved bioavailability and pharmacokinetics profile, high antitumor efficacy and decreased toxicity in comparison to the free drug [4-6]. ET and ET-LN have proven *in vitro* and *in vivo* efficacy against several kinds of cancer and both treatments are effective in blood cancers [4, 7-9]. Despite the effectiveness of ET in some of these studies, as has been mentioned above, LN provide multiple advantages over it and allow for a more effective and safe therapy [3]. Considering this background, this study aim to take a step forward evaluating the efficacy of ET nanosystems in a xenogeneic mouse model of human acute lymphoblastic leukemia. This model is developed by injecting intravenously human leukemia cells in immune-deficient mice and allowing blood, spleen and bome marrow engraftment [2]. Previous efficacy studies include xenograft models [9] and therefore, the use of this model is advantageous due to its

similarities to the real disease. ET-LN have been administered orally in previous studies [4, 5]. This administration responds to an accurate oral bioavailability that arranges for less future patient discomfort and, thus, subsequent improvement in therapy compliance. However, this pre-clinical leukemia model did not allow oral administration of the drug. The literature points towards lymphatic absorption of LN mediated by Peyer´s patches in the gut [10]. The development of the disease model involves the use of a specific strain of immune-deficient mice named BALB/cA-RAG2-/-γc-/-. The absence of the ɣ-channel in these animals prevents IL-7 production and this cytokine seems to be related to a deficient development of the Peyer`s patches of the gut [11-15]. Therefore, in order to ensure an efficient absorption of the drug, oral route was discarded. In this regard, as previous biodistribution data only refers to oral and intravenous administration of ET-LN [4, 5] and there are no data regarding intraperitoneal administration of these nanosystems, an additional objective of this work to characterized the intraperitoneal biodistribution of the particles labeled with a radioactive tracer (technetium-99m, 99mTc). As it was the first time that ET-LN were radio-labeled, oral and intravenous routes were also examined.

2. Material and methods

2.1 Material

ET was purchased from APOINTECH (Salamanca, Spain). Precirol® ATO 5 was a gift from Gattefossé (France). Tween® 80 was purchased from Roig Pharma (Barcelona, Spain). Chloroform was from Panreac (Madrid, Spain), formic acid 99 % for mass spectroscopy was obtained from Fluka (Barcelona, Spain), and methanol was purchased from Merck (Barcelona, Spain). All solvents employed for the chromatographic analysis were of analytical grade; all other chemicals were of reagent grade and used without further purification. Amicon Ultra-15 10,000 MWCO centrifugal filter devices were purchased from Millipore (Cork, Ireland).

2.2 Preparation of lipid nanoparticles

LN were prepared by the hot homogenization method consisting of high shear homogenization and ultrasonication [6]. ET (30 mg) and the lipid (Precirol® ATO 5 , 300 mg) were heated 5ºC above the lipid melting point. Then, an aqueous solution of Tween 80 (2 %), previously heated at the same temperature, was poured onto the lipid phase and the mixture was dispersed and homogeneized by a Microson™ ultrasonic cell disruptor (NY, USA) and an Ultraturrax® (IKA-Werke, Germany). Afterwards, 150 % (w/w of lipid weight) of trehalose was used as cryoprotectant agent to the LN suspension, which was then kept at -80ºC and freeze-dried to obtain a nanoparticulate powder. Particle size and polydispersity index (PDI) were evaluated by photon correlation spectroscopy (PCS) using a Zetasizer Nano (Malvern Instruments, UK). Surface charge was measured using the same Zetasizer Nano equipment combined with laser Doppler velocimetry. For the ET loading determination, the formulation was analyzed by a previously validated ultra-high-performance liquid chromatography tandem mass spectrometry (UHPLC-MS/MS) method [16].

2.3 Radiolabeling of lipid nanoparticles

99mTechnetium, in the form of Na99mTcO4 in 0.9% NaCl, was eluted from a commercial 99Mo-99mTc generator (Mallinckrodt Medical B.V.).

2.3.1 Intravenous administration

The nanoparticles were radiolabeled with $_{99m}$Tc by direct labeling method using SnCl2 as reducing agent. 30 µL of an acidic, aqueous solution containing SnCl2 (10 mg dissolved in 500 µL HCl 37 %, diluted to 10 mL, 1mg/mL) was added to 100 µL pertechnetate eluate ($^{99m}TcO_4^-$). The pH was adjusted to the range of 6-7 with an aqueous solution of NaHCO3 0.5M (~22 µL). 20 µl of aliquot containing 30 mg/ml of LN were added and the mixture was shaken horizontally at RT for 30 min.

2.3.2 Intraperitoneal/oral administration

The nanoparticles were radiolabeled with 99mTc by direct labeling method using SnCl2 as reducing agent. 30 µL of an acidic, aqueous solution containing SnCl2 (10 mg dissolved in 500 µL HCl 37 %, diluted to 10 mL, 1mg/mL) was added to 100 µL pertechnetate eluate (99m TcO4-). The pH is adjusted to the range of 6-7 with an aqueous solution of NaHCO3 0.5M (~22 µL). 50 µl of an aliquot containing 540 mg of LN/ml were added and the mixture was shaken horizontally at RT for 30 min.

2.4 Radioanalysis

Quality control of radiolabeling was performed using acetone and a mixture of pyridine: acetic acid: water (3:5:1.5) as mobile phases and ITLC-SA sheets as stationary phase. Using acetone as mobile phase, free pertechnetate is expected to migrate to the front, while radiolabeled LN and potentially formed reduced/hydrolyzed $_{99m}$Tc (^{99m}TcO2) are expected to remain at the spot. Using the pyridine: acetic acid: water mixture all radiolabeled forms are expected to migrate to the front, except large radiocolloids, consisting primarily of ^{99m}TcO2, which are expected to remain at the spot.

2.4.1 Labeling stability

Stability of the radiolabeled nanoparticles was assessed in the reaction mixture, in serum and in simulated gastric and intestinal medium. Radioanalysis was performed using acetone and a mixture of pyridine: acetic acid: water (3:5:1.5) as mobile phases and ITLC-SA sheets (a layer chromatography medium with salicylic acid) as stationary phase.

2.4.2 Stability in serum

For the serum study, 20 µL of the radiolabeled-LN were challenged against 180 µL of serum at 37ºC for 1, 2 and 4 hours.

2.4.3 Stability in gastric medium and in intestinal medium

Stability in gastric and intestinal medium was assessed by incubating 50 µl of radiolabeled-LN with 450 µl of simulated gastric medium (0.1M HCl in PBS; pH= 1.5) or intestinal medium (0.05M Potassium phosphate monobasic in water; pH=6.8)at 37ºC for 1, 2 and 4 hours.

2.5 Imaging and biodistribution studies

Female normal Swiss and SCID mice (average weight of 20–25 g) of the same colony and age (approximately 6 weeks) were purchased from the Breeding Facilities of NCSR 'Demokritos'

2.5.1 Oral administration

Mice (n=1) received one single oral dose of labeled-LN (200 µl; 1350 mg ET-LN/Kg; 320 µCi) or of free pertechnetate (320 µCi). Afterwards, PET images were captured at different time points after administration (1.5, 3 and 5.5 hours post-administration). Mice were fixed on animal fixing tray board and imaging was performed with Single Photon Emission Computed Tomography (SPECT) gamma camera.

2.5.2 Intravenous administration (i.v.)

Mice (n=1) received one single i.v. dose of labeled-LN (100 µl; 30 mg ET-LN/Kg; 320 µCi). Afterwards, PET images were captured at different time points after administration (1, 4 and 24 hours post-administration). Mice were fixed on animal fixing tray board and imaging was performed with Single Photon Emission Computed Tomography (SPECT) gamma camera. For the biodistribution studies, Mice (n=3; 3 groups) received one single i.v. dose of labeled-LN (100 µl; 30 mg ET/Kg). Then, animals were sacrificed at 6, 24 and 48 hours post-administration. Organs were extracted and weighed and radioactivity measurements were conducted in an automated well-typed γ-counter (NaI(Tl) crystal Canberra-Packard,auto-gamma 5000

series model) calibrated for 99mTc. Radioactivity was interpreted as percentage of injected dose (% ID) per gram of organ/tissue.

2.5.3 Intraperitoneal administration (i.p.)

Mice (n=1) received one single ip dose of labeled-LN (200 µl; 1350 mg ET-LN/Kg; 320 µCi). Afterwards, PET images were captured at different time points after administration (2 and 4 hours post-administration). Mice were fixed on animal fixing tray board and imaging was performed with Single Photon Emission Computed Tomography (SPECT) gamma camera. For the biodistribution studies, Mice (n=3) received one single i.p. dose of labeled-LN (100 µl; 30 mg ET/Kg). Then, animals were sacrificed at 6, 24 and 48 hours post-administration. Organs were extracted, weighed and radioactivity measurements were conducted in an automated well-typed γ-counter NaI (Tl) crystal (Packard). Radioactivity was interpreted as % of injected dose (% ID) per gram of organ/tissue.

2.6 Efficacy in human acute lymphoblastic leukemia

2.6.1 *In vitro* efficacy of ET in acute lymphoblastic leukemia

a. Human samples and cell lines

Two ALL-derived cell lines NALM-20 and MOLT-4 were purchased from the DSMZ (German Collection of Microorganisms and Cell Cultures). Cell lines were maintained in culture in RPMI 1640 medium supplemented with 10 % fetal bovine serum and with 1% penicillin-streptomicin and 2% HEPES (Gibco-BRL) at 37ºC in a humid atmosphere containing 5% CO2. To generate the mouse model, bone marrow or peripheral blood mononuclear cells (CEMO-1, LAL-CUN-2) were obtained at diagnosis from patients with ALL after signed informed consent, obtained from the patient or the patient's guardians, in accordance with the Declaration of Helsinki.

b. Proliferation assay

MOLT-4 and NALM-20 (acute lymphoblastic leukemia) cells were seeded at a density of $4*10^5$ cells/well in 96-well-plates. CEMO-1 AND LAL-CUN-2 were seeded at

1 x 10^6 cells/ml. Then, treatments (ET) was added at different concentrations from 0 to 50 µg/ml. Plates were incubated at 37ºC in 5 % CO_2 for 72 hours. Finally, 20 µl of CellTiter 96® Aqueous One Solution Cell Proliferation Assay (Promega, Madrid, Spain) were added to each well. The mixture was incubated for 1 hours and the formazan production was measured by a microplate spectrophotometer (Labsystems, Helsinki, Finland) at 490 nm with a reference wavelength of 690 nm.

CEMO-1 AND LAL-CUN-2 (cells from the Universidad de Navarra clinic) were seeded at 1 x 10^6 cells/ml. Then, treatments (ET) were added at different concentrations from 0 to 50 µg/ml. Plates were incubated at 37ºC in 5 % CO_2 for 72 hours. Finally, 20 µl of CellTiter 96® Aqueous One Solution Cell Proliferation Assay (Promega, Madrid, Spain) were added to each well. The mixture was incubated for 4 hours and the formazan production was measured by a microplate spectrophotometer (Labsystems, Helsinki, Finland) at 490 nm with a reference wavelength of 690 nm.

2.6.2 *In vivo* efficacy of ET and ET-LN in a xenogeneic mouse model of human acute lymphoblastic leukemia

a. Development of an xenogeneic mouse model of human acute lymphoblastic leukemia

All animal studies had previous approval from the Animal Care and Ethics Committee of the University of Navarra. Animals were housed at room temperature under a 12-h light/dark cycle with water and food provided *ad libitum*. Experiments that used patient samples were approved by the Human Research Ethics Committees of University of Navarra. ALL-T human xenograft model was developed following a protocol developed by Vilas-Zornoza *et al.* [2]. Briefly, 10x106 human primary cells diluted in 100 µl of saline solution in the tail vein of 6-week old female BALB/cA-RAG2-/-γc-/- mice. After primary engraftment in mice, human blasts from mice spleen were isolated (>97 % of human blasts) by Ficoll-Paque plus (GE healthcare) and transplanted into the tail vein of new BALB/cA-RAG2-/-γc-/- mice.

b. Treatment

Mice were divided in 4 treatment groups (n=3 in each group): i) Control (saline); ii) Blank-LN; iii) ET; iv) ET-LN. Treatments were administered daily by i.p. route at a dose corresponding to 30 mg ET/kg of weight. Clinical symptoms were observed daily. At day 10, blood samples were collected in EDTA surface-coated tubes and animals were sacrificed by cervical dislocation.

c. FACS analysis

100 µl of collected peripheral blood were labeled for 15 minutes with the following antibodies: rat anti-mouse CD45-PE (BD pharmingen), mouse anti-human CD5-APC (BD pharmingen) mouse anti-human CD45-PerCP (BD pharmingen), mouse anti-human CD22-PE (BD pharmingen) followed by 10 minutes incubation with 2 ml of FACS lyses solution (1:10)(Becton Dickinson). Cells were washed with saline solution and centrifuged at 600 x g. for 7 minutes. The supernatant was decanted and cells were fixed in 400 µl of 4 % paraformaldehide. The analysis was done with FACSCalibur cytometer and Paint-A- Gate software (Bencton Dickinson).

3. Results and discussion

3.1 Lipid Nanoparticles characterization

ET-LN were prepared by the hot homogenization method consisting of high shear homogenization and ultrasonication [6]. This technique yielded LN with a size of 127.89 ± 9.95 nm and negative surface charge (-28.42 ± 1.39). ET-LN loading was 22.677 ± 2.262 µg ET/mg.

3.2 Radiolabeling of lipid nanoparticles

ET-LN were radiolabeled with ^{99m}Tc yielding high labeling efficiency (>97 %) and with minimal amounts of pertechnetate and/or radiocolloids formed during both labeling procedures (oral; i.p.; i.v.). Stability in the reaction mixture after 2.5 hours of preparation was evaluated. Results showed that the sample remained intact with

only 3.0 percent of colloids. These results confirm the feasibility of using $_{99m}$Tc to effectively label LN as has been previously stated by other authors [17].

3.3 Stability of radiolabeling in media

3.3.1 Serum

The technetium was not dissociated; no re-oxidation to pertechnetate took place after 4 hours of incubation with serum. However, stability studies showed that larger radiocomplexes are formed as shown by the pyridine: acetic acid: water mixture quality control. This might be caused due to the interaction with serum proteins. After 30 minutes of incubation only 7.8 % of the radiolabeled-LN remained intact. This percentage was maintained also after 2 and 4 hours of incubation with serum. These results might promote higher uptake by reticulo-endothelial system (RES) organs due to a larger nanoparticle size [18].

3.3.2 Gastric Medium and intestinal medium

The technetium was not dissociated; no reoxidation to pertechnetate took place after 4 hours of incubation with gastric medium. Nevertheless larger radiocomplexes are formed as shown by the pyridine: acetic acid: water mixture quality control. After 1 hour of incubation only 12.6 % of the radiolabeled-LN remained intact. This percentage was lower after 4 hours (7.3 %) of incubation. The formation of large radiocomplexes might influence oral absorption of the complexes because it is believed that nanoparticles smaller than 300 nm are better absorbed by the oral route [18].

Concerning the intestinal medium, the technetium was not dissociated; no reoxidation to pertechetate took place after 4 hours of incubation with gastric medium. However larger radiocomplexes were formed as shown by the pyridine: acetic acid: water mixture quality control. After 1 hour of incubation only 9.5 % of the radiolabeled-LN remained intact. This percentage was similar after 4 hours of incubation. The formation of larger radiocomplexes in gastric and intestinal media

might be caused by the coagulation of labeled LN or by the formation of reduced/hydrolyzed ^{99m}TcO2.

3.4 Oral administration of free pertechnetate radiolabeled-LN

The results showed that free pertechnetate ^{99m}TcO4- was absorbed in the stomach after its oral administration and it was concentrated in thyroid area, lungs, stomach and bladder (Figure 1: A-B). In contrast, labeled ET-LN were not distributed through the body after oral administration (Figure 1:C-D). In fact, after 7 hours post-administration, the radioactive signal was still concentrated in the intestines and stomach indicating that radiolabeled ET-LN were not absorbed.

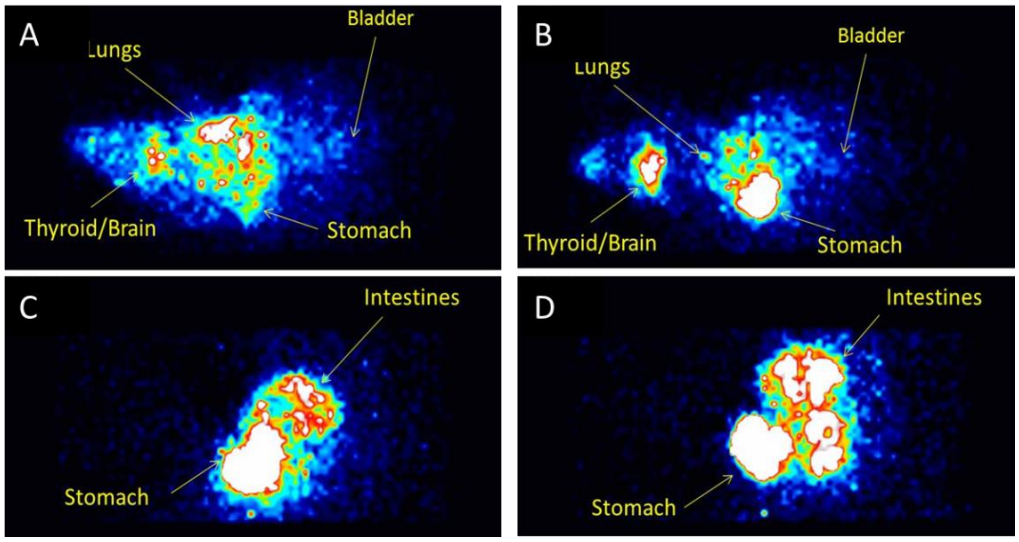

Figure 1. A-B: dynamic 2 minute images of mice after oral administration of free pertechnetate TcO4- (320 µCi) 12 min. post administration (A) and 190 min. post-administration (B). C-D: dynamic 2 minute images of mice after oral administration of radiolabeled-LN (320 µCi) 145 min. post administration (C) and 181 min. post-administration (D). Brain area is not noticeable since its area is overlaid by the corresponding thyroid area.

These results do not correlate with previous biodistribution results that show oral ET absorption when it is encapsulated into LN [5]. Nevertheless, the observed gastrointestinal accumulation of radiolabeled-LN might be due to large radio-complexes formation in acid media (as it has been mentioned in the stability section).

As intestinal absorption requires nanoparticles sizes below 300 nm, radio-complexes would not be absorbed and, therefore, accumulated in the gastrointestinal tract. In view of these results, this technique did not seem to be adequate to observe oral trafficking of LN. Thus, in view of these results, further biodistribution studies were not performed.

3.5 Intravenous administration of radiolabeled-LN

Results of biodistribution after i.v. administration are consistent with LN physicochemical characteristics. Figure 2. and Table 1 show that LN were mainly accumulated in liver, lungs, spleen and kidneys/bladder.

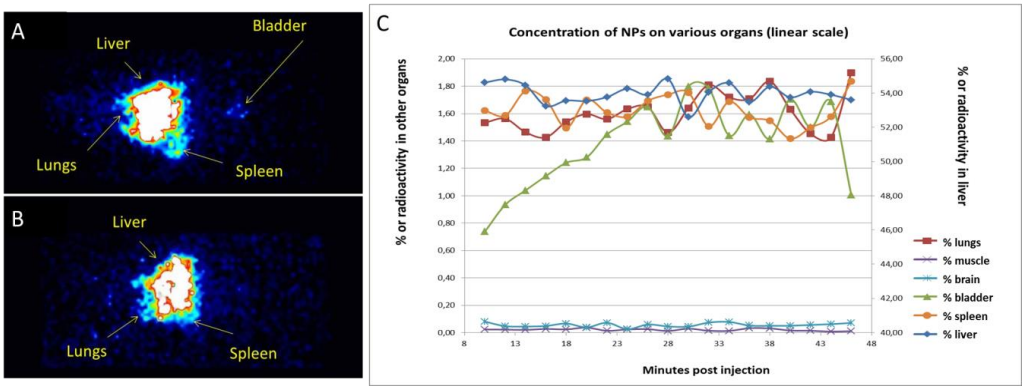

Figure 2. Dynamic 2 minute images of mice after intravenous administration of radiolabeled-LN (320 µCi) 10 min. (A) and 24 hours (B) post administration and concentration of radioactive signal in various organs 10-45 min. post-administration (C).

RES clearance is associated to nanoparticles with sizes larger than 200 nm [18]; ET-LN have a size around 120 nm and, thus, large radiocomplexes might be uptaken by the kupffer cells in the lymphatic organs such as spleen and liver. The splenic uptake of radiolabeled ET-LN was high initially (22.13 % ID at 3 h), but decreased with time whereas % ID in liver and lungs was maintained or even increased after 24 and 48 hours. Besides, very low uptake by thyroid and stomach ($_{99m}$Tc usually accumulates in these organs [19]), indicating that technetium remained associated to the nanoparticles. Estella et al. [4] not only described a similar pattern of distribution but also stated an ET-LN accumulation in stomach, intestine and kidneys. They

explained these accumulations in elimination organs as a result of sacrificing the mice 9 days post-administration. As our experiments lasted only for 48 hours, due to 99mTc half-life, both studies are not comparable.

3.6 Intraperitoneal administration of radiolabeled-LN

Radiolabeled ET-LN were more widely distributed than in case of i.v. route. Radioactive signal was accumulated in stomach, pancreas, intestines, spleen and bladder/kidneys (Fig. 3 and Table 1). The radioactive signal in these organs was almost null at 24 and 48 hours post administration except on kidneys where the signal was maintained for 48 hours. In view of these results, we can conclude that biodistribution of radiolabeled ET-LN after i.v. route differs from the i.v. route. In general, after i.p. administration, labeled ET-LN are more widely distributed throughout the different organs avoiding the high accumulation of nanoparticles in liver, lungs and spleen after i.v. administration. These data are in agreement with previous studies regarding 99mTc labeled LN biodistribution after i.p. and intravenous injection [17]. The intestines and stomach radioactive signal might be explained by the direct delivery of the radiolabeled nanoparticles in the peritoneum.

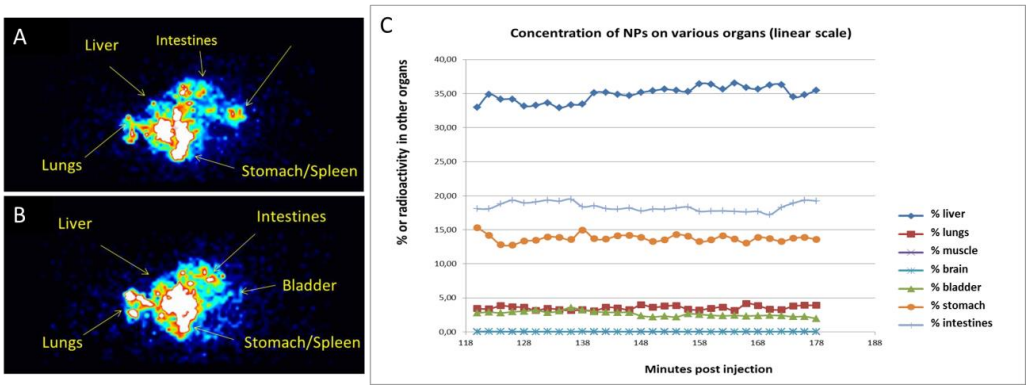

Figure 3. Dynamic 2 minute images of mice after intraperitoneal administration of radiolabeled-LN (320 µCi) 120 min. (A) and 284 min. (B) post administration and concentration of radioactive signal in various organs 118-178 min. post-administration (C).

Table 1. Biodistribution of radiolabelled-LN in mice (6, 24 and 48 hours post administration) after intravenous (IV) and intraperitoneal (IP) administration. (Percent of injected dose per gm of organ/tissue ± SD) The animals were intravenously (IV) or intraperitoneally (IP) administered with radiolabeled ET-LN and were sacrificed at 6 h, 24 and 48 h post-injection. Radioactivity was counted in each organ and expressed as percent of injected dose per gm of organ/tissue. Each value is the mean ± SD of 3 mice.

	6 h		24 h		48 h	
	IV	IP	IV	IP	IV	IP
Blood	1,02 ± 1.05	0,18 ± 0.11	0,39 ± 0.04	0.15 ± 0.01	0.37 ± 0.06	0.19 ± 0.06
Liver	22,15 ± 2.58	0,61 ± 0.92	28,54 ± 2.50	0.07 ± 0.02	27.06 ± 4.9	0.10 ± 0.04
Heart	0,25 ± 0.01	0,06 ± 0.02	0,31 ± 0.18	0.05 ± 0.02	0.30 ± 0.05	0.10 ± 0.03
Kidneys	1,97 ± 0.06	0,72 ± 0.44	1,89 ± 0.12	0.64 ± 0.13	1.79 ± 0.24	0.74 ± 0.19
Stomach	1,22 ± 1.12	2,89 ± 2.86	0,68 ± 0.17	0.17 ± 0.06	0.70 ± 0.15	0.27 ± 0.07
Intestines	0,50 ± 0.27	1,19 ± 0.86	0,33 ± 0.11	0.11 ± 0.05	0.32 ± 0.17	0.10 ± 0.03
Spleen	22,13 ± 5.42	0,79 ± 1.29	13,53 ± 3.76	0.03 ± 0.01	7.93 ± 0.96	0.09 ± 0.02
Muscles	0,17 ± 0.08	0,32 ± 0.39	0,10 ± 0.05	0.07 ± 0.05	0.14 ± 0.08	0.29 ± 0.32
Lungs	8,60 ± 1.39	0,24 ± 0.28	5,95 ± 2.17	0.09 ± 0.02	8.48 ± 5.24	0.10 ± 0.03
Bones	0,63 ± 0.12	0,13 ± 0.05	0,49 ± 0.12	0.10 ± 0.02	0.44 ± 0.14	0.16 ± 0.06
Pancreas	0,27 ± 0.21	1,90 ± 3.14	0,09 ± 0.03	0.05 ± 0.02	0.12 ± 0.03	0.09 ± 0.04
Thyroid	0,14 ± 0.02	0,15 ± 0.14	0,14 ± 0.01	0.07 ± 0.02	0.15 ± 0.02	0.06 ± 0.01
Brain	0,03 ± 0.00	0,04 ± 0.03	0,04 ± 0.03	0.01 ± 0.01	0.03 ± 0.00	0.02 ± 0.01

Results of biodistribution after i.p. administration showed that the total measured radioactivity in the organs/tissues was lower than after i.v. administration (Table 1). Since the initial amount of radioactivity administered in both routes was the same; this lower amount of total radioactivity might be explained by a faster elimination of the $_{99m}$TC or by an accumulation of the radiolabeled ET-LN in organs/tissues different from those that were analysed in the study. Radioactive signal in kidneys was maintained after 24 and 48 hours (suggesting sustained elimination of labeled ET-LN, and was lower after i.p. administration than after i.v. administration; thus, faster elimination of labeled ET-LN after i.p. administration does not seem to be a likely phenomenon. Therefore, the remaining radioactivity might be located in other organs/tissues such as peritoneal adipose tissue or lymph nodes (radioactivity in this tissue was not measured). In this regard, previous studies [17] refer to biphasic absorption of LN labeled with $_{99m}$Tc in blood after i.p. administration due to an initial faster distribution followed by a slow disposition from the peritoneum. This pattern was also observed in this study; blood concentration of $_{99m}$Tc decreased within time

after i.v. administration whereas it was constant after i.p. administration. These blood and kidney results might support the hypothesis of a depot compartment from which labeled ET-LN are released to the blood in a sustained manner. Considering these results, i.p. route seems to be an adequate route of administration in the leukemia model developed in the present study. It might provide lower accumulation of the LN in RES organs and more constant blood ET-LN levels.

3.7 Efficacy in human acute lymphoblastic leukemia

The efficacy of ET-LN was evaluated in a in a xenogeneic mouse model of human acute lymphoblastic leukemia in mice. Previously, ET efficacy was assessed *in vitro* in commercial leukemia cells as in leukemia cells obtained from patients in order to evaluate the sensitivity of these cells to the free drug.

3.7.1 *In vitro* proliferation

ET antitumor effect was evaluated by measuring the IC_{50} of the drug in leukemia cells by means of cells proliferation activity measured by MTS® assay. Cells (NALM-20, MOLT-4, CEMO-1 and LAL-CUN-2) were incubated with increasing concentrations of ET and proliferation activity was measured after 72 hours of incubation. ET antitumor efficacy was expressed based on the IC_{50} of the drug in the different cells. As it can be observed in Fig. 4, leukemia cell lines obtained from patients (CEMO-1 and LAL-CUN-2) showed slightly higher IC_{50} values than DSMZ cells (NALM-20 and MOLT-4). Nevertheless, all the cell lines exhibited IC_{50} values between 3 and 7.5 µg ET/ml (5.73 and 14.32 µM). Comparing these results with previous work by our research group [7], we can conclude that all the tested cell lines showed sensitivity to the effect of the free drug. In view of these results, we could assume good antitumor activity of both free drug (ET) and LN containing edelfosine (ET-LN), in the *in vivo* mouse model of acute lymphoblastic leukemia.

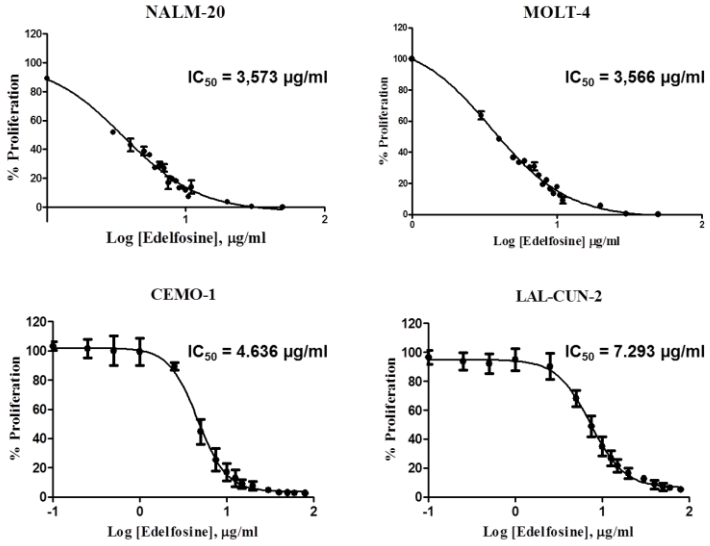

Figure 4. IC_{50} values of ET after treatment of different leukemia cell lines with increasing concentrations of ET

3.7.2 *In vivo* efficacy of ET and ET-LN in a xenogeneic mouse model of human acute lymphoblastic leukemia

Animals were administered a daily i.p. dose of Blank-LN, ET or ET-LN equivalent to 30 mg ET/kg of animal weight. Previous studies revealed by our work demonstrated that this is a non-toxic dose in case of oral administration. These data and the fact that this animal model of leukemia is very aggressive led us to administer the same dose intraperitoneally. Although LN present the great advantage of possible oral administration over other chemotherapeutic agents [3], we decided to administer the treatment i.p. This decision was based on the special immunologic characteristics of the mice that are used to develop the disease model. The gamma chain, supressed in BALB/cA-RAG2-/-γc-/- mice is essential in IL-7 production [12, 14]. This cytokine seems to be directly related to the formation of Peyer´s patches [11, 13]. In consequence, these mice would not absorb ET-LN orally because it is believed that these nanosystems are mainly absorbed by the lymph system in the intestine. In this regard, although the oral route was preferable, it was decided to administer the treatments intraperitoneally in order to assure therapeutic drug concentrations. Intraperitoneal route was thought to be more suitable than i.v. based on above

mentioned biodistribution studies. Unfortunately, i.p. administration seemed to have a lower toxicity threshold. Animals treated with ET and ET-LN showed severe toxicity symptoms and were sacrificed 10 days after the induction of the disease. ET provoke loose of weight, gastrointestinal symptoms (diahorrea) and anorexia. Animals treated with ET-LN presented similar symptoms. Moreover, 3 animals treated with ET and 4 animals treated with ET-LN died during the experiment. Necropsy of animals showed evidence of excessive LN dosing. Animals treated with Blank-LN presented severe ascites indicating liver disease; white patches of LN were observable in the whole abdominal cavity; besides, spleen weight was higher than control animals ratifying the biodistribution results that showed accumulation of these nanosystems in liver and spleen. ET-LN also provoked this pathological sign but in a minor degree. Bearing all these data in mind, the first conclusion of this pilot experiment is that dose regimen should be review in order to be adjusted to the therapeutic window of the free and nanoencapsulated drug. Nevertheless, blood samples were taken after animals sacrifice at day 10. Then, blood was stained with antibodies against human and mouse cells in order to detect percentage of human cells (LAL-T cells) in mice blood and infer a possible antileukemic activity of the treatments. These results showed a low percentage of human leukemic cells engraftment due to the early stage of the disease. ET-LN treatment showed 0.1 % of human cells in contrast to 1.12 % in the control group. ET was also efficient (0.303 %) which is consistent with the proven efficacy in other *in vivo* models of blood cancer [9]. Surprisingly, Blank-LN also produced a decrease in human cells engraftment in blood (0.47 %). These data might be explained by the toxicity of the overdosed system which seems to be accumulated in liver and spleen inducing cell toxicity death. However these results are not concluding because the percentage of human blasts in mouse blood is maintained at a very low quantity for some days after disease induction and it begins to grow exponentially reaching quantities superior to 40 % after 19 days [2]. In view of these results, an optimized ET-LN dose regimen might probably lead to optimal antitumor efficacy.

4. Conclusions

ET-LN were successfully radiolabeled (>97%) with minimal amounts of pertechnetate and/or radiocolloids formed in both labeling procedures (oral/i.p. and i.v.). In addition, the technetium was not dissociated; no reoxidation to pertechetate took place after 4 hours of incubation with serum, gastric or intestinal media; however large radiocomplexes are formed after incubation with all the different media. This could be the cause of absence of oral absorption of radiolabeled ET-LN. Intravenous administrations led to a quick biodistribution of the labeled ET-LN with a major accumulation of the nanosystems in the RES organs such as liver, spleen and lungs. In contrast, the i.p. route showed very slow biodistribution with the peculiarity of avoidance of accumulation of the nanoparticles in RES organs. Besides, the lower total quantity of radioactivity signal in comparison to i.v. administration suggested accumulation of the radiolabeled ET-LN in other tissues different from those that were analyzed in the study. In fact, the sustained radioactive signal in blood and kidneys suggests biphasic absorption of the radiolabeled ET-LN which in turn, might provide a controlled release of the drug over time. *In vitro* efficacy studies demonstrated that cells were sensitive to the action of the free drug. However, *in vivo* efficacy studies revealed an overdose and therefore, this study could be considered only a proof of concept. Nevertheless, both treatments, ET and ET-LN showed a slight decrease in human leukemia cells engraftment in the blood.

5. References

[1] NIH National Cancer Institute. http://www.cancer.gov/cancertopics/wyntk/leukemia [Last accesed 30 Oct 2013].

[2] Vilas-Zornoza, A.; Agirre, X.; Abizanda, G.; Moreno, C.; Segura, V.; De Martino Rodriguez, A.; Jose-Eneriz, E. S.; Miranda, E.; Martin-Subero, J. I.; Garate, L.; Blanco-Prieto, M. J.; Garcia de Jalon, J. A.; Rio, P.; Rifon, J.; Cigudosa, J. C.; Martinez-Climent, J. A.; Roman-Gomez, J.; Calasanz, M. J.; Ribera, J. M.; Prosper, F. Preclinical activity of LBH589 alone or in combination with chemotherapy in a xenogeneic mouse model of human acute lymphoblastic leukemia. Leukemia **2012**, *26*: 1517-1526.

[3] Lasa-Saracibar, B.; Estella-Hermoso de Mendoza, A.; Guada, M.; Dios-Vieitez, C.; Blanco-Prieto, M. J. Lipid nanoparticles for cancer therapy: state of the art and future prospects. Expert Opin Drug Deliv **2012**, *9*: 1245-1261.

[4] Estella-Hermoso de Mendoza, A.; Campanero, M. A.; Lana, H.; Villa-Pulgarin, J. A.; de la Iglesia-Vicente, J.; Mollinedo, F.; Blanco-Prieto, M. J. Complete inhibition of extranodal dissemination of lymphoma by edelfosine-loaded lipid nanoparticles. Nanomedicine (Lond) **2012**, *7*: 679-690.

[5] Estella-Hermoso de Mendoza, A.; Preat, V.; Mollinedo, F.; Blanco-Prieto, M. J. In vitro and in vivo efficacy of edelfosine-loaded lipid nanoparticles against glioma. J Control Release **2011**, *156*: 421-426.

[6] Estella-Hermoso de Mendoza, A.; Blanco-Prieto, M.J.; Campanero M.A.; Mollinedo F.; Villa-Pulgarín J.; Varela, R. Development and use of lipidic nanoparticles loaded with edelfosine and ether phospholipids in antitumoral and antiparasitic therapy. **2011**. P201130433.

[7] Lasa-Saracibar, B.; Estella-Hermoso de Mendoza, A.; Mollinedo, F.; Odero, M. D.; Blanco-Prieto, M. J. Edelfosine lipid nanosystems overcome drug resistance in leukemic cell lines. Cancer Lett **2013**, *334*: 302-310.

[8] Mollinedo, F.; de la Iglesia-Vicente, J.; Gajate, C.; Estella-Hermoso de Mendoza, A.; Villa-Pulgarin, J. A.; Campanero, M. A.; Blanco-Prieto, M. J. Lipid raft-targeted therapy in multiple myeloma. Oncogene **2010**, *29*: 3748-3757.

[9] Mollinedo, F.; de la Iglesia-Vicente, J.; Gajate, C.; Estella-Hermoso de Mendoza, A.; Villa-Pulgarin, J. A.; de Frias, M.; Roue, G.; Gil, J.; Colomer, D.; Campanero, M. A.; Blanco-Prieto, M. J. In vitro and In vivo selective antitumor activity of Edelfosine against mantle cell lymphoma and chronic lymphocytic leukemia involving lipid rafts. Clin Cancer Res **2010**, *16*: 2046-2054.

[10] Qi, J.; Lu, Y.; Wu, W. Absorption, disposition and pharmacokinetics of solid lipid nanoparticles. Curr Drug Metab **2012**, *13*: 418-428.

[11] Debard, N.; Sierro, F.; Kraehenbuhl, J. P. Development of Peyer's patches, follicle-associated epithelium and M cell: lessons from immunodeficient and knockout mice. Semin Immunol **1999**, *11*: 183-191.

[12] Adachi, S.; Yoshida, H.; Honda, K.; Maki, K.; Saijo, K.; Ikuta, K.; Saito, T.; Nishikawa, S. I. Essential role of IL-7 receptor alpha in the formation of Peyer's patch anlage. Int Immunol **1998**, *10*: 1-6.

[13] Nishikawa, S.; Honda, K.; Vieira, P.; Yoshida, H. Organogenesis of peripheral lymphoid organs. Immunol Rev **2003**, *195*: 72-80.

[14] Chappaz, S.; Finke, D. The IL-7 signaling pathway regulates lymph node development independent of peripheral lymphocytes. J Immunol **2010**, *184*: 3562-3569.

[15] Hofer, U.; Baenziger, S.; Heikenwalder, M.; Schlaepfer, E.; Gehre, N.; Regenass, S.; Brunner, T.; Speck, R. F. RAG2-/- gamma(c)-/- mice transplanted with CD34+ cells from human cord blood show low levels of intestinal engraftment and are resistant to rectal transmission of human immunodeficiency virus. J Virol **2008**, *82*: 12145-12153.

[16] Estella-Hermoso de Mendoza, A.; Campanero, M. A.; Mollinedo, F.; Blanco-Prieto, M. J. Comparative study of A HPLC-MS assay versus an UHPLC-MS/MS for anti-tumoral alkyl lysophospholipid edelfosine determination in both biological samples and in lipid nanoparticulate systems. J Chromatogr B Analyt Technol Biomed Life Sci **2009**, *877*: 4035-4041.

[17] Harivardhan Reddy, L.; Sharma, R. K.; Chuttani, K.; Mishra, A. K.; Murthy, R. S. Influence of administration route on tumor uptake and biodistribution of etoposide loaded solid lipid nanoparticles in Dalton's lymphoma tumor bearing mice. J Control Release **2005**, *105*: 185-198.

[18] Agarwal, R.; Roy, K. Intracellular delivery of polymeric nanocarriers: a matter of size, shape, charge, elasticity and surface composition. Ther Deliv **2013**, *4*: 705-723.

[19] Beloqui, A.; Solinis, M. A.; Gascon, A. R.; del Pozo-Rodriguez, A.; des Rieux, A.; Preat, V. Mechanism of transport of saquinavir-loaded nanostructured lipid carriers across the intestinal barrier. J Control Release **2012**, *166*: 115-123.

GENERAL DISCUSSION

According to the World Health Organization, cancer is one of the leading causes of death worldwide, and cancer deaths are projected to continue rising to over 13.1 million in 2030. Among all cancer types, leukemia represents 3% of all cancer cases [1]. Leukemia is a cancer of the blood caused by the rapid production of abnormal white blood cells. These abnormal white blood cells are not able to fight infection and impair the ability of the bone marrow to produce red blood cells and platelets. Leukemia can be classified into acute or chronic. Chronic leukemia is developed over many years whereas acute leukemia develops in a very short time and can be lethal in a few weeks if left untreated. Leukemia is also classified into lymphocytic or myelogenous. Lymphocytic leukemia refers to abnormal cell growth in the marrow cells that become lymphocytes, whereas in myelogenous leukemia, abnormal cell growth occurs in the marrow cells that mature into red blood cells, white blood cells, and platelets. There are four broad classifications of leukemia: i) Acute lymphocytic leukemia (ALL); ii) Acute myeloid leukemia (AML); iii) Chronic lymphocytic leukemia (CLL) and iv) Chronic myelogenous leukemia (CML). Leukemia occurs in both adults and children, being ALL the most common form of childhood leukemia and AML the second one. The two most prevalent adult leukemias are AML and CLL [2]. Current leukemia treatment involves chemotherapy, biological therapy, targeted therapy, radiation and stem cell transplant. These treatments are generally associated to severe side-effects and, despite their effectiveness in children, relapse is frequent in adults [3].

Edelfosine (ET-18-OCH_3; ET) is the prototype of a family of antitumor drugs known as alkyl-lysophospholipids (ALPs). These antineoplastic agents were synthetized in the late 60s as metabolically stable analogues of lysophosphatidylcholine (LysoPC). Edelfosine structure was obtained by replacing the ester bond in LysoPC by an ether linkage and by adding another ether-linked methyl group at the C2 position [4]. The resulting molecule has demonstrated potent antitumor effects against several cancer types [5-7]. Moreover, it presents a great

advantage over the classic antitumor drugs because ET is selectively incorporated into tumor cells sparing healthy ones [8]. This selectivity seems to be related to the fact that ET targets lipid rafts of the cell membrane and the plasmatic membrane of cancer cells are enriched in cholesterol. However, the use of ET in clinic remains limited. In fact, it is only used to purge the bone marrow in acute leukemia transplantation [4]. This upsetting preclinical-clinical translation responds to ET side-effects, such as gastrointestinal toxicity and haemolytic toxicity [4, 9, 10].

Nanotechnology is aimed to work in the submicron size world and it is applied to many different work fields. Due to similitude in scale to biologic molecules, nanotechnology has achieved great success in the medicine field where it is known as “nanomedicine” and it is applied to the diagnosis and treatment of diseases. Nanomedicine is the daily basis of current pharmaceutical technology research and it comprises a wide number of vehicles such as liposomes, lipid nanoparticles (LN), polymeric nanoparticles, carbon nanotubes and fibre scaffolds, among others. Some of them are being studied in clinical trials or have been already approved by the FDA for their use in humans [11]. Among all nanomedicines, LN have been widely proposed as useful vehicles in cancer research [12]. LN were developed in the 1980s as an alternative vehicle to traditional liposomes [13]. LN are colloidal carriers composed by lipids that are solid at room and body temperature. These nanosystems have been widely used in cancer due to their benefits in therapy; they provide protection against drug toxic effects and better bioavailability profiles. Moreover, most of these LN are suitable for oral delivery of drugs, which turns into a clear benefit on the patient wellbeing [12]. In view of this background, our group previously synthesized and patented LN containing ET (ET-LN) [14] in order to overcome ET drawbacks through nanotechnology. ET-LN demonstrated improved oral bioavailability, decreased side-effects and showed high efficacy in animal models of glioma and lymphoma [15, 16].

Herein, based on the potent benefits of ET-LN in cancer treatment and on previous works showing ET effectiveness in leukemia [8], the present work hypothesized that ET-LN might be an effective therapy in leukemia. These

nanosystems could provide better efficacy and higher security profiles in the treatment of this blood cancer.

This general hypothesis comprised different partial objectives. The first objective was to evaluate the efficacy of free and nanoencapsulated ET after administration to sensitive and resistant leukemia cell lines. Secondly, we aimed to evaluate the uptake mechanisms of ET and ET-LN in leukemia cells as well as the molecular mechanisms implicated in cell death upon internalization of both the free and nanoencapsulated drug. The third objective of this work was to assess the permeability of LN across the intestinal barrier in *in vitro* models of enterocytes and Microfold cells. Next, we evaluated the *in vivo* oral toxicity profile of the drug unloaded nanosystem, the free drug and the ET-LN and the last objective was to study the biodistribution of ET-LN the therapeutic efficacy of the developed nanosystems in a xenogeneic mouse model of human lymphoblastic leukemia.

Previous studies demonstrated the efficacy of ET in leukemia [8, 17-20]. These studies stated that some leukemia cells are resistant to the antitumor action of ET [20]. Antitumor cell resistance to ALPs has been attributed to many causes, such as a lower entrance of drug into the cells [21] and/or different contributions to pro and antiapoptotic mediators [7, 20, 22]. Within this basis, we hypothesized that ET-LN might overcome the resistance of leukemic cells to edelfosine by means of increasing intracellular drug content or promoting a different intracellular delivery of the drug and, hence, inducing different apoptotic mechanism. The *in vitro* studies in leukemia cells included four AML cell lines (HL-60, HEL, OCI-AML-2 and MOLM-13) and one CML-BC cell line (K-562). Results of these studies are presented in Chapters 1 and 2 of the manuscript. These cells presented different sensitivity to the action of the free drug. In high sensitive cells, ET-LN were as effective as the free drug inducing cell death and, therefore, we can conclude that the antitumor effect of the drug is not affected by its encapsulation into LN. Interestingly, ET-LN were able to overcome drug resistance in case of cells that did not respond to the antitumor action of the free ET. These results led us to conclude that the overcoming of drug resistance might occur by an enhanced intracellular drug content mediated by the vehiculization of the ET or by the triggering of different mechanisms of action by the

free and the nanoencapsulated drug. In these sense, uptake studies in HL-60 (sensitive) and K-562 (resistant) cells were performed. Internalization studies of nanocarriers can follow different established strategies. The present work involves in first place, the use of Nile Red, a lipophilic fluorochrome, which is encapsulated into LN and, as a second strategy, the direct quantification of the internalized drug. The obtained results demonstrated that LN containing Nile Red followed a similar pattern of internalization in both cell lines. However, these studies offer very few information as it is not possible to compare this data with the internalization of the free drug. Therefore, further uptake studies developed in Chapter 2 were much more informative. In this chapter, the quantity of drug that was internalized in the cells was determined by UHPLC-MS/MS. These studies confirmed that LN were internalized in similar rates in both cell lines as it had been seen in Chapter 1. However, it could be also demonstrated that the use of LN did not enhance intracellular drug concentration of the drug in these cells. Therefore, we could conclude that overcoming of the resistance that K-562 cells present to free ET is not related to a higher intracellular content of drug when it is encapsulated into LN. These studies also revealed the involvement of different mechanism of entry in the cell when ET was nanoencapsulated. In sensitive cells (HL-60) free drug was internalized by clathrin and lipid rafts mediated endocytosis as well as by passive and facilitated diffusion, whereas in resistant cells (K-562) passive and facilitated diffusion seemed to be more predominant. In contrast, ET-LN uptake was not affected by endocytosis inhibitors, thus pointing towards the involvement of macropinocytosis, phagocytosis and passive diffusion as likely LN uptake mechanisms. The different mechanism of entry of ET and ET-LN in the cell might imply a different intracellular delivery location of the drug for both treatments. Furthermore, this different intracellular location might trigger different cell death mechanisms. In this regard, Chapters 1 and 2 describe these studies showing that ET and ET-LN promoted similar caspase-mediated apoptosis cell death in sensitive HL-60 cells, whereas the induction of this cell death mechanism was not observed in resistant K-562 cells. These results suggested the involvement of caspase independent apoptosis in K-562 cell death. Considering this, autophagy induction by both treatments was also evaluated. Interestingly, results showed that both treatments, ET and ET-LN, endorsed a high

induction of autophagic vesicles. As the induction of autophagy was demonstrated for both treatments, it is not possible to directly correlate K-562 sensitivity to ET-LN with autophagy cell death. Nevertheless, the present study only evaluated the forming of autophagic vacuoles (demonstrated by the recruitment of LC3 II) and these autophagosomes are part of a natural protective process in cells that, only in some occasions, impair cells coping with the stress due to accumulation of autophagic vacuoles and drive cells to death. Nevertheless, more experiments (i.e microscopy studies with LC3-GFP transfectants or characterization of the cell death response to ET and ET-LN in presence of autophagic flux inhibitors) should be performed in order to ascertain the role of the observed autophagic induction in cell death.

Taking into account the confirmed efficacy of ET-LN in leukemia cells *in vitro*, these nanosystems seemed to be a promising therapeutic alternative in leukemia; nonetheless, these results had to be confirmed by *in vivo* experiments. *In vivo* studies, however, imply a more complex system and many factors should be taking into consideration before efficacy studies. In this sense, route of administration, pharmacokinetics and biodistribution or toxicity are relevant aspects that should be studied in order to obtain optimal efficacy results with low toxicity effects. Therefore, as these nanosystems are designed for oral delivery, the next step on this work aimed to evaluate the intestinal absorption of ET and ET-LN after oral administration. This work (described in Chapter 3) involved the development of two *in vitro* intestinal models. When cultured under specific conditions, the human Caco-2 cell line simulates the enterocytes in the intestine [23]. Besides, a co-culture with Raji cells promotes the differentiation of Caco-2 cells into M cells [24]. These models are widely used because they promote cell polarization and differentiation and allow the quantification of the drug that is translocated from the apical to the basal face of the cells [25]. Although previous pharmacokinetics and biodistribution studies developed in our research group have already demonstrated the high oral bioavailability of ET-LN by the oral route [15], these studies were conducted in order to demonstrate the different absorption of free and nanoencapsulated ET at the intestinal level. Surprisingly, these results evidenced a likely metabolic process of ET in enterocytes.

The metabolization of ET by other cells is described in the literature [26] but, to our knowledge, this is the first time that it is suggested in enterocytes. This metabolic process might be involved in the low oral bioavailability of ET [15]. In case of ET-LN, this effect was not observed which means that ET might be protected from this metabolic process when it is encapsulated into LN. Besides, the developed Caco-2/Raji co-culture model did not show translocation of ET-LN from the apical to the basal compartment. These results are in disagreement with the high bioavailability of the nanoencapsulated drug after its oral administration [15]. At this point, these results could be explained as the limitations of *in vitro* experiments to describe *in vivo* behaviours of drugs. In fact, a minimal amount of drug is necessary in order to further detect the molecule by the analysing method and this might limit the lapse time of the experiment due to possible toxicity. In the present study, this required quantity of edelfosine was toxic for the cells if the experiment lasted for more than two hours and, consequently, all the experiments lasted two hours which could be limiting the LN translocation across the cells. On the other hand, several studies confirm a lymphatic absorption of LN [12], which would be simulated with the Caco-2/Raji *in vitro* model due to its capacity to mimic M cells in the Peyer´s patches of the intestine. Conversely, LN translocation was not visible either in this model. Other authors also refer a lack of transport increase in Caco-2/Raji co-cultures in comparison to Caco-2 monoculture [27]. Therefore, this *in vitro* model might be not simulating the complexity of these lymphatic regions of the intestine and more accurate models should be established. In this sense, some authors point towards the development of three-dimensional *in vitro* models [28].

Afterwards, and bearing in mind the poor safety of antitumor drugs, we aimed to confirm the benefits that LN might provide in the toxicological profile of ET. In this sense, Chapter 4 of the manuscript aimed to evaluate the *in vivo* toxicological profile by the oral route of the empty vehicle, the free ET and the ET-LN. Toxicological studies regarding the use of LN are very limited in the literature. Although LN are made by biodegradable lipids approved by the FDA, these lipids are approved for their use as excipients in classic pharmaceutical forms. In this regard, the use of these lipids to produce vehicles in the nanometric scale would completely change their

safety profile due to the specific interactions of LN with biological systems. Results confirm that LN provide a protective effect against toxicity of the free drug, as LN prevented from the severe acute toxicity of higher dose of ET which induced the death of the animals within the first 72 hours of the experiment. Besides, ET at the higher dose caused gastrointestinal toxicity and triggered an immunosuppressive effect. Free drug (30 mg/kg), blank-LN and ET-LN (30 and 120 mg/kg) did not induce any side-effects. These results were very interesting because they demonstrate not only that ET-LN are safe even at high doses but also that LN are a safe vehicle to administer other antitumor agents by the oral route.

Finally, a preliminary efficacy study was performed in a xenogeneic mouse model of human acute lymphoblastic leukemia [3]. This model was chosen based on its similarities with a real leukemia due to its capacity of blood, spleen and bone marrow engraftment. As it has been mentioned before, LN were design to be orally administered due to the benefits of this route for patients, the optimal oral bioavailability of ET-LN and the demonstrated safety of these systems by this administration route. However, the genetic characteristics of the mice in which the *in vivo* leukemia model was developed prevented oral administration. Mice employed to develop the disease present a genetic abnormality that produces abnormal development of the Peyer's patches in the gut [29-33]. As it is generally recognised that orally administered LN are absorbed via lymphatic system, this abnormality might influence ET-LN absorption and, therefore, might affect ET-LN efficacy. Taking this into consideration, alternative routes of administration were studied by evaluating the *in vivo* distribution of ET-LN labelled with ^{99m}Tc. Results of this work are described in Chapter 5. Radiolabeling studies led to the conclusion that intraperitoneal (i.p.) route might be more adequate to administer ET-LN due to an apparent capability of providing a sustained release of drug to the blood owing to an accumulation of the drug in a depot compartment. Besides, in comparison to the intravenous route, i.p. administration provided less accumulation of the drug in the RES organs, such as liver, spleen and lungs. In addition, it is remarkable that this labelling technique seems to be inadequate to study LN trafficking through the intestinal tract, as technetium labelled-LN tended to aggregate in contact with gastric

medium and, thus they might reach sizes larger than 300 nm which is the maximum size to ensure intestinal absorption [34]. In fact, radiolabeled ET-LN were mainly retained in the stomach and intestine, whereas previous studies state an improvement of ET absorption after oral administration when it is vehiculized in LN [15].

Therefore, efficacy studies were performed by i.p. route. Animals were administered a dose that is considered safe by the oral route; however, unfortunately, animals treated with ET, and ET-LN showed severe toxicity signs. In consequence, animals were sacrificed before the end of the experiment and, therefore, results from efficacy studies were not concluding. Nevertheless, efficacy studies were encouraging as both ET and ET-LN were able to decrease percentage of human leukemia cells in mice with respect to control group. This experiment should be optimized in terms of ET-dosing to confirm preliminary results.

To conclude, the general hypothesis of the work has been confirmed as *in vitro* results in leukemia cells showed similar o greater efficacy of the ET-LN over the free drug. Besides, even in the case of similar efficacy, LN would offer advantages over the free drug in terms of protection against ET toxicity. Regarding this subject, toxicity studies demonstrated that LN are a safe vehicle by the oral route and might be advantageous in encapsulating not only ET but other antitumor agents. Finally, *in vivo* efficacy studies should be optimized with the aim of confirming preliminary obtained results.

References

[1] WHO Cancer. Fact sheets. Available at: http://www.who.int/mediacentre /factsheets/fs297/en/ [Last accessed: 2 Oct 2013].

[2] Hematology, A. S. o. Blood cancers, leukemia. Available at: http://hematology.org/Patients/ Blood-Disorders/Blood-Cancers/5230.aspx [Last accessed: 2 Nov 2013].

[3] Vilas-Zornoza, A.; Agirre, X.; Abizanda, G.; Moreno, C.; Segura, V.; De Martino Rodriguez, A.; Jose-Eneriz, E. S.; Miranda, E.; Martin-Subero, J. I.; Garate, L.; Blanco-Prieto, M. J.; Garcia de Jalon, J. A.; Rio, P.; Rifon, J.; Cigudosa, J. C.; Martinez-Climent, J. A.; Roman-Gomez, J.; Calasanz, M. J.; Ribera, J. M.; Prosper, F. Preclinical activity of LBH589 alone or in combination with chemotherapy in a xenogeneic mouse model of human acute lymphoblastic leukemia. Leukemia **2012**, *26*: 1517-1526.

[4] van Blitterswijk, W. J.; Verheij, M. A. Biochim Biophys Acta **2013**, *1831*: 663-674.

[5] Gajate, C.; Matos-da-Silva, M.; Dakir el, H.; Fonteriz, R. I.; Alvarez, J.; Mollinedo, F. Antitumor alkyl-lysophospholipid analog edelfosine induces apoptosis in pancreatic cancer by targeting endoplasmic reticulum. Oncogene **2011**, *31*: 2627-2639.

[6] Gajate, C.; Santos-Beneit, A. M.; Macho, A.; Lazaro, M.; Hernandez-De Rojas, A.; Modolell, M.; Munoz, E.; Mollinedo, F. Involvement of mitochondria and caspase-3 in ET-18-OCH(3)-induced apoptosis of human leukemic cells. Int J Cancer **2000**, *86*: 208-218.

[7] Mollinedo, F.; Fernandez-Luna, J. L.; Gajate, C.; Martin-Martin, B.; Benito, A.; Martinez-Dalmau, R.; Modolell, M. Selective induction of apoptosis in cancer cells by the ether lipid ET-18-OCH3 (Edelfosine): molecular structure requirements, cellular uptake, and protection by Bcl-2 and Bcl-X(L). Cancer Res **1997**, *57*: 1320-1328.

[8] Mollinedo, F.; de la Iglesia-Vicente, J.; Gajate, C.; Estella-Hermoso de Mendoza, A.; Villa-Pulgarin, J. A.; de Frias, M.; Roue, G.; Gil, J.; Colomer, D.; Campanero, M. A.; Blanco-Prieto, M. J. In vitro and In vivo selective antitumor activity of Edelfosine against mantle cell lymphoma and chronic lymphocytic leukemia involving lipid rafts. Clin Cancer Res **2010**, *16*: 2046-2054.

[9] Gajate, C.; Mollinedo, F. Biological activities, mechanisms of action and biomedical prospect of the antitumor ether phospholipid ET-18-OCH(3) (edelfosine), a proapoptotic agent in tumor cells. Curr Drug Metab **2002**, *3*: 491-525.

[10] Vink, S. R.; van Blitterswijk, W. J.; Schellens, J. H.; Verheij, M. Rationale and clinical application of alkylphospholipid analogues in combination with radiotherapy. Cancer Treat Rev **2007** *33*: 191-202.

[11] Kim, B. Y.; Rutka, J. T.; Chan, W. C. Nanomedicine. N Engl J Med **2010**, *363*: 2434-2443.

[12] Lasa-Saracibar, B.; Estella-Hermoso de Mendoza, A.; Guada, M.; Dios-Vieitez, C.; Blanco-Prieto, M. J. Lipid nanoparticles for cancer therapy: state of the art and future prospects. Expert Opin Drug Deliv **2012**, *9*: 1245-1261.

[13] Speiser, P. Lipid nanopellets als tragersystem fur arzneimittel zur peroralen anwendung. . EP 0167825 (1990).

[14] Estella-Hermoso de Mendoza A., Blanco-Prieto M.J., Campanero M.A., Mollinedo F., Villa-Pulgarín J., Varela R. Development and use of lipidic nanoparticles loaded with edelfosine and ether phospholipids in antitumoral and antiparasitic therapy. P201130433. 2011.

[15] Estella-Hermoso de Mendoza, A.; Campanero, M. A.; Lana, H.; Villa-Pulgarin, J. A.; de la Iglesia-Vicente, J.; Mollinedo, F.; Blanco-Prieto, M. J. Complete inhibition of extranodal dissemination of lymphoma by edelfosine-loaded lipid nanoparticles. Nanomedicine (Lond) **2012**, *7*: 679-690.

[16] Estella-Hermoso de Mendoza, A.; Preat, V.; Mollinedo, F.; Blanco-Prieto, M. J. In vitro and in vivo efficacy of edelfosine-loaded lipid nanoparticles against glioma. J Control Release **2011**, *156*: 421-426.

[17] Gajate, C.; Gonzalez-Camacho, F.; Mollinedo, F. Involvement of raft aggregates enriched in Fas/CD95 death-inducing signaling complex in the antileukemic action of edelfosine in Jurkat cells. PLoS One **2009**, *4*: e5044.

[18] Nieto-Miguel, T.; Gajate, C.; Gonzalez-Camacho, F.; Mollinedo, F. Proapoptotic role of Hsp90 by its interaction with c-Jun N-terminal kinase in lipid rafts in edelfosine-mediated antileukemic therapy. Oncogene **2008**, *27*: 1779-1787.

[19] Chabot, M. C.; Wykle, R. L.; Modest, E. J.; Daniel, L. W. Correlation of ether lipid content of human leukemia cell lines and their susceptibility to 1-O-octadecyl-2-O-methyl-rac-glycero-3-phosphocholine. Cancer Res **1989**, *49*: 4441-4445.

[20] Wagner, B. A.; Buettner, G. R.; Oberley, L. W.; Burns, C. P. Sensitivity of K562 and HL-60 cells to edelfosine, an ether lipid drug, correlates with production of reactive oxygen species. Cancer Res **1998**, *58*: 2809-2816.

[21] Gajate, C.; Del Canto-Janez, E.; Acuna, A. U.; Amat-Guerri, F.; Geijo, E.; Santos-Beneit, A. M.; Veldman, R. J.; Mollinedo, F. Intracellular triggering of Fas aggregation and recruitment of apoptotic molecules into Fas-enriched rafts in selective tumor cell apoptosis. J Exp Med **2004**, *200*: 353-365.

[22] Fu, D.; Shi, Z.; Wang, Y. Bcl-2 plays a key role instead of mdr1 in the resistance to hexadecylphosphocholine in human epidermoid tumor cell line KB. Cancer Lett **1999**, *142*: 147-153.

[23] Sambuy, Y.; De Angelis, I.; Ranaldi, G.; Scarino, M. L.; Stammati, A.; Zucco, F. The Caco-2 cell line as a model of the intestinal barrier: influence of cell and culture-related factors on Caco-2 cell functional characteristics. Cell Biol Toxicol **2005**, *21*: 1-26.

[24] des Rieux, A.; Fievez, V.; Theate, I.; Mast, J.; Preat, V.; Schneider, Y. J. An improved in vitro model of human intestinal follicle-associated epithelium to study nanoparticle transport by M cells. Eur J Pharm Sci **2007**, *30*: 380-391.

[25] Sarmento, B.; Andrade, F.; da Silva, S. B.; Rodrigues, F.; das Neves, J.; Ferreira, D. Cell-based in vitro models for predicting drug permeability. Expert Opin Drug Metab Toxicol **2012**, *8*: 607-621.

[26] Magistrelli, A.; Villa, P.; Benfenati, E.; Modest, E. J.; Salmona, M.; Tacconi, M. T. Fate of 1-O-octadecyl-2-O-methyl-rac-glycero-3-phosphocholine (ET18-OME) in malignant cells, normal cells, and isolated and perfused rat liver. Drug Metab Dispos **1995**, *23*: 113-118.

[27] Beloqui, A.; Solinis, M. A.; Gascon, A. R.; del Pozo-Rodriguez, A.; des Rieux, A.; Preat, V. Mechanism of transport of saquinavir-loaded nanostructured lipid carriers across the intestinal barrier. J Control Release **2012**, *166*: 115-123.

[28] Pusch, J.; Votteler, M.; Gohler, S.; Engl, J.; Hampel, M.; Walles, H.; Schenke-Layland, K. The physiological performance of a three-dimensional model that mimics the microenvironment of the small intestine. Biomaterials **2011**, *32*: 7469-7478.

[29] Adachi, S.; Yoshida, H.; Honda, K.; Maki, K.; Saijo, K.; Ikuta, K.; Saito, T.; Nishikawa, S. I. Essential role of IL-7 receptor alpha in the formation of Peyer's patch anlage. Int Immunol **1998**, *10*: 1-6.

[30] Debard, N.; Sierro, F.; Kraehenbuhl, J. P. Development of Peyer's patches, follicle-associated epithelium and M cell: lessons from immunodeficient and knockout mice. Semin Immunol **1999**, *11*: 183-191.

[31] Nishikawa, S.; Honda, K.; Vieira, P.; Yoshida, H. Organogenesis of peripheral lymphoid organs. Immunol Rev **2003**, *195*: 72-80.

[32] Hofer, U.; Baenziger, S.; Heikenwalder, M.; Schlaepfer, E.; Gehre, N.; Regenass, S.; Brunner, T.; Speck, R. F. RAG2-/- gamma(c)-/- mice transplanted with CD34+ cells from human cord blood show low levels of intestinal engraftment and are resistant to rectal transmission of human immunodeficiency virus. J Virol **2008**, *82*: 12145-12153.

[33] Chappaz, S.; Finke, D. The IL-7 signaling pathway regulates lymph node development independent of peripheral lymphocytes. J Immunol **2010**, *184*: 3562-3569.

[34] Agarwal, R.; Roy, K. Intracellular delivery of polymeric nanocarriers: a matter of size, shape, charge, elasticity and surface composition. Ther Deliv **2013**, *4*: 705-723.

[33] Chappaz, S.; Finke, D. The IL-7 signaling pathway regulates lymph node development independent of peripheral lymphocytes. J Immunol **2010**, *184*: 3562-3569.

[34] Agarwal, R.; Roy, K. Intracellular delivery of polymeric nanocarriers: a matter of size, shape, charge, elasticity and surface composition. Ther Deliv **2013**, *4*: 705-723

CONCLUSIONS

1. Edelfosine lipid nanoparticles previously developed in our research group and optimized in the present work preserved the potent apoptotic effect that free edelfosine has in sensitive leukemia cells. These nanosystems are internalized in sensitive and resistant leukemia cells. Edelfosine lipid nanoparticles were able to induce cell death of resistant leukemia cells whereas the free drug was practically devoid of efficacy.

2. Edelfosine and edelfosine lipid nanoparticles intracellular incorporation was prompted by different uptake mechanisms. Facilitated and simple diffusion appeared to be major uptake mechanisms in free drug uptake in HL-60 cells (sensitive) and K-562 cells (resistant) while endocytosis was also visible in HL-60 cells (sensitive). In case of encapsulated edelfosine, passive diffusion, phagocytosis and macropinocytosis were the most likely uptake mechanisms. Lipid nanoparticles did not enhance the intracellular concentration of the drug in comparison to free drug.

3. Both treatments activated caspase-mediated cell death in the edelfosine sensitive cell line HL-60, whereas the absence of activation of this route in K-562 was confirmed. Moreover, an important increase of lipidated LC3 II was detected after both treatments, pointing towards an increase of autophagic vesicles in K-562 cells. Importantly, as edelfosine lipid nanoparticles overcomed the resistance of K-562 cells, autophagic cell death could be involved in the cell demise process caused by the toxic effects of edelfosine when it is incorporated in the nanoparticles to a subcellular location different from the free drug.

4. Edelfosine was internalized at a higher rate in its free form in both *in vitro* intestinal models (Caco-2 and Caco-2/Raji). This rapid drug internalization in the culture monolayers might be related to the lipidic nature of the drug, the elevated presence of lipid rafts in the apical surface of enterocytes and the saturation of the P-gp transporter. In addition, results suggested that

edelfosine might suffer some metabolic process upon being internalized in Caco-2 and Caco-2/Raji intestinal models. Edelfosine lipid nanoparticles were not translocated from luminal to basolateral side in any of the studied *in vitro* models. Bearing in mind that previous studies have demonstrated high oral bioavailability of the drug after oral administration in lipid nanoparticles, the results suggest that the microfold model is not a good model to study the absorption of these nanosystems across the intestinal barrier *in vitro*; thus more complex models should be developed.

5. Lipid nanoparticles showed a protective effect against the free drug toxicity. Edelfosine presented gastrointestinal toxicity and triggered an immunosuppressive effect at the higher dose whereas no toxic effect was observed with the encapsulated drug or the empty vehicle. The results of the *in vivo* toxicity study confirmed that lipid nanoparticles are a safe vehicle for the administration of antitumor drugs by the oral route.

6. Edelfosine lipid nanoparticles were successfully radiolabeled 99mTc. Moreover, the technetium was not dissociated. Radiolabeled nanoparticles were stable after incubation with serum, gastric or intestinal media; however large radiocomplexes were formed after incubation with all the different media. This undesirable event might alter nanoparticles biodistribution; indeed this might be the cause of impaired oral absorption. Intravenous administrations lead to accumulation of the lipid nanoparticles in the reticuloendothelial system organs such as liver, spleen and lungs. In contrast, intraperitoneal route showed a wider biodistribution with a lower accumulation in organs of the reticuloendothelial system. Besides, sustained blood and kidneys radioactive signal for 48 hours suggested the presence of a biphasic biodistribution due to an accumulation on the labelled nanosystems in a depot compartment.

7. Biodistribution studies led us to choose the intraperitoneal route for the administration of edelfosine lipid nanoparticles in the efficacy studies. The administered dose of edelfosine, although safe by the oral route, resulted to be toxic when administered intraperitoneally. Both treatments, edelfosine

and edelfosine lipid nanoparticles showed a slight decrease in human leukemia cells engraftment in the blood. Although this experiment requires optimization of the dose regime, preliminary results were favourable.

CONCLUSIONES

1. Las nanopartículas lipídicas, que contienen el antitumoral edelfosina, desarrolladas por nuestro grupo de investigación y que han sido optimizadas en el presente trabajo, mostraron un efecto antitumoral similar al que produce el fármaco libre en líneas de leucemia sensibles a la acción del mismo. Además, estas nanopartículas fueron capaces de inducir la muerte celular en una línea de leucemia resistente a la acción del fármaco libre.

2. Se encontró que la internalización de la edelfosina libre y nanoencapsulada era mediada por mecanismos diferentes. El fármaco libre se internaliza principalmente por difusión simple y difusión facilitada en las líneas de leucemia HL-60 (sensible a la edelfosina) y K-562 (resistente a la acción del fármaco). En el caso de la línea sensible a la edelfosina también se observó internalización de fármaco libre mediada por endocitosis, mientras que la internalización de las nanopartículas se producía por difusión pasiva, micropinocitosis y fagocitosis.

3. Ambos tratamientos (edelfosina y nanopartículas lipídicas de edelfosina) indujeron la apoptosis mediada por caspasas en la línea celular sensible al fármaco libre (HL-60); sin embargo, esta vía no se activó con ninguno de los tratamientos en la línea celular resistente a edelfosina (K-562). Además, ambos tratamientos mostraron un importante incremento de la proteína LC3 II en la línea K-562, lo que se traduce en una acumulación de autofagosomas, que en el caso del tratamiento con nanopartículas podría desencadenar la muerte celular por autofagia.

4. La edelfosina libre se internaliza en mayor proporción que las nanopartículas en los modelos intestinales *in vitro* (Caco-2 y Caco-2/Raji). Asimismo, los resultados sugieren que el fármaco libre podría ser metabolizado tras su internalización en las células intestinales. Además, no se observó translocación de nanopartículas a la cara basal de los cultivos lo que sugiere

5. que el modelo de Caco-2/Raji no es adecuado para estudiar la permeabilidad de las nanopartículas de edelfosina *in vitro.*

6. En un modelo murino, las nanopartículas lipídicas de edelfosina mostraron un efecto protector frente a la toxicidad producida por el fármaco libre. La edelfosina libre provocó toxicidad gastrointestinal así como un efecto inmunosupresor. Dichos efectos no se observaron ni con el vehículo vacío ni con las nanopartículas de edelfosina. Los resultados del estudio de toxicidad *in vivo* demostraron que las nanopartículas lipídicas desarrolladas son un vehículo seguro para la administración de fármacos antitumorales por vía oral.

7. Las nanopartículas de edelfosina fueron marcadas satisfactoriamente con ^{99m}Tc. El marcaje permaneció estable durante la incubación con suero y medios gástrico e intestinal. Sin embargo, la incubación con dichos medios produjo la formación de radiocomplejos de mayor tamaño lo que impidió la absorción de las nanopartículas por vía oral. La administración por vía intraperitoneal mostró una biodistribución amplia y niveles sostenidos de radioactividad en sangre.

8. Los resultados de biodistribución permitieron seleccionar la vía intraperitoneal para los estudios de eficacia. Sin embargo, a pesar de que la dosis administrada es segura por vía oral, ésta resultó ser excesiva para la vía intraperitoneal. Los resultados preliminares apuntan hacia un posible efecto beneficioso del fármaco aunque la dosis de edelfosina debe ser optimizada.

ANNEX I

Lipid nanoparticles in biomedicine

*Ander Estella-Hermoso de Mendoza[1], Beatriz Lasa-Saracíbar[1], Miguel Á. Campanero[2], Maria J. Blanco-Prieto[1]**

[1]Department of Pharmacy and Pharmaceutical Technology, School of Pharmacy, University of Navarra, Pamplona, Spain

[2]Clinical pharmacology service, University of Navarra Clinic, Pamplona, Spain

***Corresponding author**

Dr. María J. Blanco-Prieto, Department of Pharmaceutics and Pharmaceutical Technology, School of Pharmacy, University of Navarra, C/Irunlarrea 1, E-31080 Pamplona, Spain, Office phone: + 34 948 425 600 ext. 6519, Fax: + 34 948 425 649, e-mail: mjblanco@unav.es

Author Contributions

The manuscript was written through contributions of all authors. All authors have given approval to the final version of the manuscript.

Declaration of interest: The authors state no conflict of interest.

Encyclopedia of Nanoscience and Nanotechnology. Vol: 288. US: American Scientific Publishers, 2010. ISBN 1-58883-001-2

ENN Encyclopedia of Nanoscience and Nanotechnology
www.aspbs.com/enn

Lipid Nanoparticles in Biomedicine

A. Estella-Hermoso de Mendoza,[a] B. Lasa-Saracibar,[a] M. A. Campanero,[b] M. J. Blanco-Prieto[a]

[a]*Department of Pharmacy and Pharmaceutical Technology, School of Pharmacy, University of Navarra, E-31008, Spain*

[b]*Clinical Pharmacology Service, University of Navarra Clinic, E-31080 Pamplona, Spain*

CONTENTS

1. INTRODUCTION

Over the last two decades, nanotechnology has become a rapidly expanding field, encompassing the development of materials in the range of 5–1000 nm in size. Advances in colloidal drug delivery systems have lead to a revolution in the field of therapeutics, making early diagnosis of diseases and treatment for them as effective as possible. Nanotechnology has thus put into practice the concept of drug targeting, based on the idea of minimizing the risk-to-benefit ratio.

Liposomes were first described in the early 1910s [1], but it was not until the end of the 1960s that they were rediscovered by Bangham [2, 3] and were applied as the first delivery systems developed. Since then, increasingly sophisticated nanocarriers have been designed in order to improve their performance. Many research studies, as well as the successful development of liposomal products for intravenous (i.v.) administration such as liposomal doxorubicin (Doxyl®, Caelyx®) [4], daunorubicin (DaunoXome®) [5], and liposomal amphotericin B (AmBisome®), have shown that liposomes are advantageous lipid carriers. On the other hand, their limited physical stability, difficulty associated with manufacture, the scaling up of the manufacturing process, and the elevated cost of their formulation are some drawbacks that hamper the successful commercialization of liposomes [6].

Lipid nanoparticles (LNs) are the next step in colloidal carriers composed of biocompatible and biodegradable lipid matrices. They combine the advantages of liposomes, polymeric nanoparticles, and emulsions, while diminishing possible drawbacks associated with them [7, 8]. In the past, solid lipids were mainly employed for dermal and rectal applications, but in the mid-1980s, solid lipid micro- and nanoparticles (called nanopellets) were developed by Speiser and coworkers [9]. These nanopellets were obtained by dispersion of molten lipids with ultrasound or high-speed mixers.

Today, the great challenge in the development of drug delivery carriers is to overcome the limitations set by the physico-chemical properties of the drug, including high molecular weight, low permeability, poor solubility, or short half-life [10].

It has been shown that by using solid lipids instead of liquid lipids, it is possible to modify the control of the kinetics of encapsulated compounds, increasing the release and stability of encapsulated chemically sensitive lipophilic ingredients [11]. These effects are explained by several lipid state phase-related physicochemical phenomena. First, the chemical-degradation reactions are delayed, as the mobility of reactive agents in a solid matrix is rather lower than in a liquid matrix. Second, it is possible to control microphase separations of the active pharmaceutical ingredients and carrier lipid within individual liquid particles, and by doing so, the accumulation of active compounds at the surface of LNs is avoided, being this location where chemical-degradation reactions often happen [7, 10, 12–15]. Lastly, it has been shown that the biological absorption of poorly absorbed bioactive compounds is improved by their incorporation into LNs [16, 17]. Several studies have also revealed the decrease in the lipid digestion rate when a solid matrix is used instead of a liquid matrix, thus allowing for a more sustained release of the incorporated compound [18].

The aim of the current chapter will be to provide an overview of LNs and their potential biomedical applications.

ISBN: X-XXXXX-XXX-X

Encyclopedia of Nanoscience and Nanotechnology
Edited by H. S. Nalwa
Volume X: Pages (1–24)

2. TYPES OF LNs

There are several types of LNs. Recently, to overcome membrane stability and drug leakage problems associated with liposomes and conventional emulsions, new lipid delivery systems, such as solid lipid nanoparticles (SLNs®), nanostructured lipid carriers (NLCs®), and lipid drug conjugates (LDCs®), have been designed [19].

2.1. First-Generation LNs: SLNs®

Among the lipid nanocarriers, SLNs are a relatively new class of drug carriers. As stated before, the first solid lipid-based micro- and nanoparticles for oral delivery (named nanopellets) were developed by Speiser in the mid-1980s [9]. Since then, lipid materials have attracted the attention of many scientists interested in the preparation of drug-delivery systems. It was in the beginning of the 1990s that the first generation of lipid nanocarriers was produced. SLNs were developed almost in parallel by Müller and Lucks [20]; and Gasco [21]. The techniques employed by each group to prepare the SLNs were different. While Müller and Lucks produced the SLNs by high-pressure homogenization, Gasco developed a microemulsion technique. These preparation methods will be explained in detail later in this chapter.

SLNs are colloidal particles made of lipids that are generally recognized as safe (GRAS) or have an accepted regulatory status. These particles remain solid at room and body temperature and present sizes from 50 up to 1000 nm, depending on the method and materials employed for the manufacturing process. Advantages that SLNs present are the improvement of the bioavailability of poorly water-soluble molecules, the use of biodegradable physiological lipids, enhanced drug penetration into the skin after topical administration, and shelter of chemically labile agents from degradation in the gastrointestinal tract [8, 22–24]. On the other hand, limitations to these SLNs are the relatively low drug loading and the expected expulsion of the incorporated drug during storage. The expulsion phenomenon can be explained by the modification of the lipid crystallization pattern in which the drug is incorporated. This alteration is likely to occur along the time-dependent restructuring process that happens during storage of the SLNs. The transformation of the lipid pattern from a less perfect crystalline lattice to a more perfect lipid crystalline structure leads to drug expulsion [25–27]. Consequently, properties such as miscibility, solubility of the drug in the lipid melt, type of matrix material, and degree of crystallinity and polymorphic form of the lipid play an important role in the incorporation capability of drugs and do not only depend on physical-chemical properties of the drug [24, 28]. It may also be the case that drug molecules may adsorb onto the nanoparticle surface because they are not accommodated within the crystalline lattice. As a result, three different mechanisms of drug incorporation can be stated (Fig. 1(A)): the solid solution, the drug-enriched shell, and the drug-enriched core models. Major advances in this field were obtained by Mehnert and coworkers [23, 29]. The formation of either one type of SLN or another mainly depends on the greater solubility of the drug in either the lipid or the aqueous phase at the temperature along the production process. In the case of a solid solution, the particle matrix allows a uniform molecular dispersion of the drug. Diffusion from the solid lipid matrix is the main process for drug release, although further LN degradation may also take place [30]. The drug-enriched shell model can be explained as a function of the solubility of the drug in the water–surfactant mixture at increased temperature during the production process. During the SLN production, the drug escapes moderately from the particle and dissolves in the aqueous phase. Cooling of the formed oil–water nanoemulsion decreases the drug solubility in the aqueous phase, and if the particle core has already started to solidify, the drug tends to scatter into the particles. This fact eventually leads to enrichment of the particle shell with drug molecules. The drug-enriched core model is formed when the drug precipitates first after cooling of the hot o/w emulsion. Unlike the previous model, this is typical of lipid solutions with the drug dissolved at its saturation solubility in the lipid at production temperature. At some stage in cooling, super saturation and consequent drug precipitation are obtained.

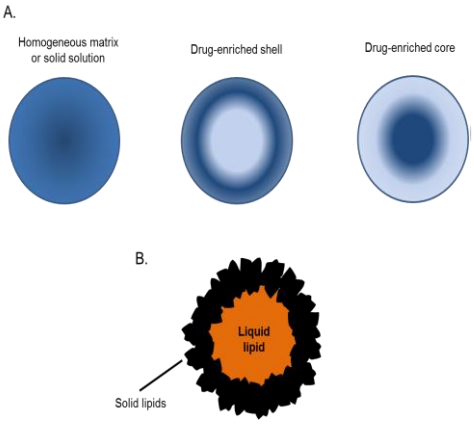

Figure 1. Representation of the proposed drug incorporation models for the three types of SLNs (A) and basic structure of NLCs (B).

2.2. Second-Generation Lipid Nanocarriers

2.2.1. NLCs®

With the beginning of the new century, a new generation of LNs was developed. These nanoparticles were named NLCs® and, like SLNs, they present a particle matrix that remains solid at temperatures up to 40°C. However, unlike SLNs, they are made of a blend of a solid lipid with a liquid lipid (oil) (Fig. 1(B)). These NLCs minimize the aforementioned problems of drug-loading capacity, potential of drug expulsion during storage, and high water content of aqueous SLN dispersions [31, 32]. This issue can be overcome by the accommodation of the active molecules inside an imperfect particle matrix. Owing to the physical-chemical characteristics of the components of the nanoparticles (solid–liquid), NLCs present considerable crystal disorder, which implies a higher drug loading and less drug expulsion during storage [33]. Nevertheless, this advantage can sometimes become a drawback as the diffusion length of the lipid matrix is decreased and, therefore, controlled release properties of the carrier may be compromised [34]. However, this effect can be minimized by regulating the proportions of liquid and solid lipids [24].

Inside the group of the NLCs, three types are proposed. First, the imperfect type of NLC, formed by spatially different lipids that cause imperfections in the lattice, creating more areas for the drugs to incorporate, for example, a mixture of glycerides composed of various fatty acids which leads to different longer or shorter distances among the fatty acid chains of the glycerides. It is possible to achieve high drug loading by the mixture of solid lipids with a small portion of oils or liquid lipids [31]. A second type, the multiple type of NLC, is an oil-in-solid lipid-in-water dispersion, which is therefore similar to a multiple emulsion (w/o/w). In this case, the liquid lipid is mixed with lipids in excess of its solubility, leading to a phase separation and, consequently, the formation of different oily nanocompartments within the solid lipid matrix [34, 35]. This method is appropriate for the encapsulation of drugs that show a greater solubility in liquid lipids than in solid lipids, as they can be dissolved in the liquid lipid and still be protected from degradation by the surrounding solid lipid. The last type of NLC is the structureless type, based on the production of solid but amorphous NLCs, as the crystallization process is a cause of expulsion of the drug. This can be achieved by using special mixtures of solid lipids and oils that become solid but do not crystallize when they are melted and cooled [34, 35].

2.2.2. LDCs®

SLNs and NLCs present a great advantage for highly efficient incorporation of hydrophobic drugs owing to their hydrophobic nature, but they present a moderate loading capacity for hydrophilic compounds [30]. In order to solve this problem, LDCs were developed. In this case, the hydrophilic drug is transformed into a more hydrophobic molecule by conjugation by esterification or amidation with a lipid compound. LDCs can be prepared either by covalent linkage to esters or ethers, or by salt formation with a fatty acid [36]. Most of the lipid conjugates melt around 50–100°C. In the covalent linking process, the drug and a fatty alcohol combine in the presence of a catalyst and the LDC bulk is recrystallized in order to purify the compound. As a final step, the LDC is then subjected to nanoparticle formulation with an aqueous surfactant solution by means of high-pressure homogenization [10]. In the salt-formation process, the free-drug base and the fatty acid are dissolved in an appropriate solvent that will be further evaporated under reduced pressure. These LDC suspensions could to some extent be considered as nanosuspensions of a prodrug. LDCs present advantages for oral and parenteral administration of hydrophilic drugs. After parenteral administration, the LDC nanoparticles offer improved possibilities for drug targeting and distribution through the organism according to the partition coefficient of the drug. Additionally, the bioavailability is enhanced in comparison to the administration of micronized conjugate powder after oral administration [10].

3. LN PRODUCTION PROCEDURES

3.1. Ingredients

General ingredients comprise lipids (either solid or liquid), surfactants, and water. The word lipid is used generally in a very extensive sense, including solid lipids such as triglycerides, fatty acids, steroids, partial glycerides, or waxes and liquid lipids such as oils. All surfactants and cosurfactants, such as poloxamers, polysorbates, bile acids, or lecithins, are used to stabilize the lipid dispersion. Besides, combinations of different emulsifiers are able to prevent particle agglomeration in a more efficient way [37].

3.1.1. Lipids

In general, the lipids used for LN preparation are fatty acids and their derivatives as well as substances functionally or biosynthetically related to these compounds [38]. These molecules usually present an amphiphilic structure, combining the lipophilic portion which consists of fatty acids and the hydrophilic portion to which the fatty acids are esterified. As main characteristics, it can be stated that the melting point of the lipids increases with the molecular weight of the lipids but decreases as the number of insaturations of the fatty acids increases.

The lipids used for LN formulation are summarized in Table 1.

3.1.2. Surfactants and Cosurfactants

Different surfactants or stabilizing agents give various interesting properties to the lipidic systems. For instance, it has been reported that Tween® 80, sodium dodecylsulfate, and Solutol® HS15 can make SLNs cross the blood–brain barrier

Table 1. Main components employed in the formulation of LNs.

Lipid matrix	Caprylic–capryc triglyceride (Myglol® 812)
	Glyceryl trilaurate (Dynasan® 112)
	Glyceryl trimyristate (Dynasan® 114)
	Glyceryl tripalmitate (Dynasan® 116)
	Glyceryl tristearate (Dynasan® 118)
	Glyceryl monostearate (Imwitor® 900)
	Glyceryl behenate (Compritol® 888 ATO)
	Glyceryl palmitostearate (Precirol® ATO 5)
	Triglycerides (Labrafac®)
	Cetylpalmitate
	Cholesterol
	Oleic acid
	Solid paraffin
	Stearic acid
Surfactants and cosurfactants	Phosphatidyl choline (Epikuron®)
	Lecithins (egg, soy)
	Pluronic® F68
	Polysorbate 80 (Tween® 80)
	Solutol® HS15
	Sodium glycocholate
	Sodium taurocholate
	Sodium tauroglycocholate
	Sodium taurodeoxycholate
	Cholesteryl hemisuccinate
Cryoprotectants	Trehalose
	Sucrose
	Sorbitol
	Maltose
	Glucose
	Mannose
Molecules on surface	PEG
	Folic acid
	Transferrin
	Antibodies

(BBB) and deliver drugs into the brain [39–42]. In another experiment, steric stabilizers such as polysorbates or poloxamers were able to hinder the binding of the lipase–colipase complexes in the gut and therefore, the degradation of the SLNs [43]. The main surfactants and cosurfactants employed in the formulation of SLNs are listed in Table 1.

3.1.3. Ligands for Active Targeting

Many studies have reported that the PEG (polyethylene glycol) modification of drug delivery systems can inhibit effectively the clearance in vivo by the reticuloendothelial system (RES) and achieve a longer plasma half-life [15, 44–46].

In the field of oncology, many tumors possess some unique pathophysiologic characteristics such us high vascular permeability or extensive angiogenesis, called enhanced permeability and retention (EPR) effect, which provide a passive target for nanocarriers [47]. However, active targeting on these tumors can also be achieved with LNs, as they can be conjugated with various smart therapeutic carriers in order to improve their efficacy and decrease the systemic toxicity. The goal of active targeting can be accomplished by the use of ligands that specifically bind to surface receptors on target sites [40, 48]. There are many receptors in cancer cells reported in the literature that seem to be overexpressed in neoplastic cells. Some examples are peptide receptors (growth factors, gastrin-related peptides, and vasoactive intestinal peptide) [49–51], receptors for LDL (in breast cancer and colon cancer) [52, 53], and folic acid or ferritin receptors (overexpressed in carcinomas) [48, 54–56]. It has been proven that the attachment of suitable ligands onto the surface of LN results in increased selectivity for tumor tissue compared to the ligand-free nanoparticle [57–61]. However, the antigen that allows molecular targeting must fulfill a number of requisites: it must be an integral part of an essential cellular function of the cancer cells, it must be expressed exclusively on cancer cells, and it should not easily mutate as the cancer cells multiply [62].

Molecules such as folic acid [57, 60, 63–66], ferritin [48], or monoclonal antibodies [67] can be used as a coating for SLNs. In the case of folic acid, this molecule has been exploited as a targeting agent attached to LNs in order to actively target tumor cells, especially in ovarian cancer and lung cancer cells [57, 60]. This can be achieved by enhancing the cellular uptake of SLNs, and thus, by the improved endocytosis mediated by folate receptor which results in significantly greater tumor growth inhibition and animal survival compared to treatment with nontargeted SLNs or free drugs [57, 60, 63]. Similarly, the administration of ferritin-coated LNs has also resulted in an effective reduction in tumor growth in MDA-MB-468 tumor-bearing mice as compared with free drug and plain SLNs [48]. Another approach for tumor targeting involves the use of intact antibodies or their fragments as highly specific targeting agents. As a result, it is possible to enhance the uptake of NLCs by tissues overexpressing transferrin receptors by the conjugation of a whole monoclonal antibody to these particles directed against these receptors [67].

Recently, the delivery of actives to different tissues has been improved by the combination of nanoparticulate drug carriers with novel targeting principles of "differential protein adsorption (PathFinder Technology)" [10, 42, 68]. The principle of this technology is to identify the naturally occurring mechanism for localization of material in different parts of the body via adsorbed blood proteins. Knowing the protein adsorption patterns of nanoparticles, the production of particles with suitable surface properties leads in vivo to preferential adsorption of the targeting protein and, therefore, to site-specific delivery [10].

3.2. Preparation Methods of LNs

As previously mentioned, the pioneers of SLN techniques are generally thought to be Müller and Lucks [20], with the high-pressure homogenization, and Gasco [21] in her work using the microemulsion technique. However, many other techniques and their variations have arisen over recent years. In order to obtain a wide variety of SLNs presenting different physical-chemical profiles, many materials (solid lipids, liquid lipids, and surfactants) and homogenizing techniques are now available to achieve the lipidic systems described above.

3.2.1. Microemulsion Technique

This method, patented by Gasco [21] in 1992, consists of the preparation of a warm microemulsion by stirring a certain amount of molten solid lipid, surfactants, and cosurfactants (containing typically around 10%, 15%, and up to 10% of these, respectively). This warm microemulsion is then dispersed using a thermostated syringe in excess cold water under stirring, in a typical ratio of 1:50. As a final step and in order to increase the particle concentration, the excess water is removed either by ultrafiltration or by lyophilization. Antineoplastic drugs such as cholesteryl butirate [69], tamoxifen [70], paclitaxel [69], idarubicin [71], and doxorubicin [17, 45, 46, 72] have been encapsulated by means of this technique and its variations. Interferon-α [73], various antioxidants such as β-carotene or α-tocopherol [74] and some antiviral drugs against human immunodeficiency virus (HIV) were also successfully loaded into these SLNs, namely, saquinavir, stavudine, and delavirdine [75, 76].

3.2.2. High-Pressure Homogenization

Along with the microemulsion technique, the high-pressure homogenization method patented by Müller and Lucks [20] in the mid-1990s has been employed to obtain SLNs with narrow distribution in size. This method presents two different approaches: hot and cold high-pressure homogenization. The main difference between these two techniques is the temperature achieved during the formulation process [8]. The choice is made depending on the type of drug to be encapsulated. For instance, hot high-pressure homogenization is not an appropriate technique to prepare SLN-containing thermolabile drugs.

1. *Hot high-pressure homogenization.* In this approach, drugs are dispersed in a molten solid lipid, usually from 5 to 10°C above the melting point of the lipid. In a following step, the drug–lipid melt is dispersed in a surfactant solution maintained at the same temperature by high-speed stirring, thus obtaining an aqueous o/w pre-emulsion. This primary emulsion is passed at the same temperature as the previous step through a

high-pressure homogenizer. Different homogenization parameters yield SLNs with different physical-chemical properties. The number of cycles of homogenization also influences the properties of the particles. Therefore, the more cycles that are performed, the greater the decrease in size and polydispersity index (P.I.) is obtained [8, 30]. However, on a regular basis, classic parameters for this method are from one to three homogenization cycles of 500 bar [8, 30]. All-trans retinoic acid [77], camptothecin [78], sodium diclofenac [79], etoposide [80, 81], fenofibrate [82], flurbiprofen [83], paclitaxel [84], and different opiod agents such as morphine hydrochloride, buprenorphine hydrochloride, hydromorphone hydrochloride and naloxone hydrochloride dihydrate, fentanyl citrate, and transforming growth factor-β1 [85] are some examples of drugs incorporated into lipid nanosystems by hot high-pressure homogenization.

2. *Cold high-pressure homogenization.* In the case of the cold-homogenization process, the first preparatory step is identical to the hot high-homogenization procedure. This step concerns the solubilization or dispersing of the drug in the melt of the bulk lipid. However, from this point, the steps that follow differ. After the drug is dissolved in the melted lipid, it is fast-cooled by means of dry ice or liquid nitrogen, which leads to the formation of a solid solution. This solution is then subjected to micronization by means of a mortar or a ball mill, and those solid lipid microparticles are then dispersed and emulsified in a cool aqueous phase containing surfactants. As mentioned, this method overcomes most formulation problems encountered with thermolabile drugs such as vinorelbine bitartrate [86] or DNA [87–89].

3.2.3. Hot Homogenization by High Shear Homogenization and/or Ultrasonication

The avoidance of organic solvents or large amounts of surfactants for the formulation of LNs is considered to be the main advantage of this method. Molten lipid is added and dispersed in an aqueous solution with the help of high shear homogenization or ultrasonication. The next step is to leave the formed emulsion to cool down to a temperature below the crystallization temperature of the carrier lipid in order to form solid particles. Then, ultrafiltration can be employed to concentrate the particle suspension.

The main disadvantages of this technique are low dispersion quality, which is often affected by the presence of a small percentage of microparticles, and metal contamination, presented by ultrasonication.

Drugs that have been successfully incorporated into lipid nanocarriers by this method are retinoic acid [90], β-elemene [91], camptothecin [33], chlorambucil [92], docetaxel [93], methotrexate [19], and nitrendipine [94].

3.2.4. Emulsion-Formation Solvent-Evaporation Method

This method is based on the one patented by Vanderhoff et al. [95], at the end of the 1970s for the preparation of pseudolatex. For a long period of time, it has been the most widely employed method for the formulation of polymeric nanoparticles. Nowadays, it can also be employed to formulate LNs. In the emulsion-formation solvent-evaporation method [26, 96], the lipid is completely dissolved in a water-immiscible organic solvent (e.g., chloroform or methylene chloride). This organic solution is then emulsified in an aqueous surfactant solution before evaporation of the solvent under reduced pressure. Once the solvent evaporates, the lipids precipitate forming SLNs. The avoidance of heating during nanoparticle preparation makes this method suitable for the incorporation of highly thermolabile drugs. On the other hand, some drawbacks might arise owing to solvent residues in the final suspension. These suspensions are often quite dilute, since the lipid presents a limited solubility in the organic material. Lipid concentrations in the final SLN dispersion range around 0.1 g l^{-1}, and therefore ultrafiltration or evaporation techniques are required in order to increase the particle concentration. Particle sizes around 100 nm can be achieved by this method with very narrow size distributions. Edelfosine [26] and DNA [97] are two examples of drugs that have been encapsulated via this method.

3.2.5. Emulsion-Formation Solvent-Diffusion Method

In this technique, partially water-miscible solvents (e.g., benzyl alcohol, ethyl formate) are used [98]. Initially, they are both saturated with water to make a certain initial thermodynamic balance of the two liquids. Later, the lipid is dissolved in the water-saturated solvent and subsequently emulsified with solvent-saturated aqueous surfactant solution at a raised temperature. After the addition of excess water (typical ratio: 1:5–1:10), the SLNs precipitate owing to diffusion of the organic solvent from the emulsion droplets to the continuous aqueous phase. As with the production of SLNs via microemulsions, the particle suspension needs to be concentrated by means of ultrafiltration or lyophilization. In an identical way to the previous method, small, narrow distribution particles (around 100 nm) can be obtained by this method. Paclitaxel [57], methotrexate [99], or actarit [100] are examples of drugs incorporated in SLNs via solvent diffusion method.

3.2.6. Solvent Injection Method

This technique, developed by Fessi et al. [101], to produce polymeric nanoparticles, is based on the previous solvent diffusion method. SLNs are prepared by rapidly injecting a solid lipid solution in water miscible solvents into water. The organic solvent diffuses from the emulsion droplets to the continuous aqueous phase causing the precipitation of the SLNs. The most widely used solvents in this method are ethanol, acetone, isopropanol, and methanol.

An example of drug successfully vectorized by this method is 5-fluorouracil [48].

3.2.7. Emulsification Dispersion Followed by Ultrasonication

The first step of this method consists of dissolving the components of the LNs (namely, drug, lipid, and emulsifier) in a common organic solvent, which is then evaporated under reduced pressure to obtain a drug-dispersed lipid phase free of solvent. The next step is to homogenize this

lipid phase with a hot aqueous surfactant solution by means of a homogenizer. Finally, this pre-emulsion is ultrasonicated to obtain the final nanoemulsion. In order to form the SLNs, the final nanoemulsion is left to cool at room temperature. Cisplatin [102] and mitoxantrone [96] have been encapsulated by means of this method.

3.2.8. Water-in-Oil-in-Water (w/o/w) Double-Emulsion Method

This method is based on obtaining a first warm w/o nanoemulsion by the emulsification of the lipid melt with an aqueous drug and surfactant solution at a high temperature (5–10°C above the melting point of the lipid) by high shear homogenization (e.g., Ultra Turrax®). This first emulsion will then be dispersed in an aqueous external phase of the final w/o/w emulsion containing a stabilizer under mechanical stirring at cold temperature (2–3°C). This surfactant should be capable of preventing the leakage of the drug to the external phase during solvent evaporation. The obtained SLN suspension is then concentrated and purified by diafiltration [26, 103, 104]. Pencyclovir [105] has been successfully entrapped into LNs by means of this method.

4. PHYSICAL-CHEMICAL CHARACTERIZATION OF LNs

The most important parameters of SLNs to be characterized include particle size and shape, the surface charge, the degree of crystallization, and the kind of lipid modification. All these physical-chemical properties must be well characterized because we have to bear in mind that any contact of the SLN dispersion with new surfaces might be able to induce changes in their structure, causing, for example, an alteration in the lipid crystallization or modification leading to the formation of a gel or to the drug expulsion [37].

4.1. Particle Size

The accurate determination of the particle size is crucial, as it will determine its fate through the organism. For instance, particle sizes below 300 nm are suitable for intestinal transport to the thoracic duct [106], while sizes no larger than 5 μm are required not to cause embolisms after parenteral administration of LNs owing to the blocking of the thin capillaries [107]. Besides, particle size also plays a very important role in the clearance of the LNs by the RES. The most established method for particle size measurement is photon correlation spectroscopy (PCS) and laser diffraction (LD) [108]. Nanoparticles are usually polydisperse in nature and P.I. gives a measure of size distribution of the nanoparticle population. Therefore, the lower the P.I. value, the more monodisperse an LN suspension is. Even if most researchers accept P.I. values below 0.3 as optimum values [26, 109–112], some authors affirm that the P.I. could be less than 0.5 for acceptable polydisperse systems [40, 113]. We have to take into account that these methods do not measure particle size, but detect light-scattering effects that are then employed to calculate particle sizes. Therefore, care must be taken because there might exist different particle sizes which may be a consequence of accidental microbial contamination, particle agglomerates, or dust in the analyzed samples which can sometimes lead to erroneous results. To avoid these incorrect data, it is always recommended to corroborate the results with additional methods or techniques such as light microscopy, electron microscopy, or atomic force microscopy (AFM).

4.2. Imaging Techniques

Light microscopy, even though it is not sensitive to the nanometer size range, gives a fast indication of the existence and the character of possible aggregates or microparticles in the formulation. Scanning electron microscopy, unlike PCS or LD, provides direct information on the particle shape [94, 114]. AFM is an advanced microscopic technique that allows the study of either nonconductive, hydrated, and solvent-containing particulate or biological samples, owing to its ability to image surfaces under liquids [28, 114–116]. This technique provides a 3D surface profile, whereas electron microscopy provides a 2D image of the sample. Currently, this is the only technique available that directly provides structural, mechanical, functional, and topographical information about surfaces with nanometer- to angstrom-scale resolution.

4.3. Zeta Potential

The zeta potential is the overall charge a particle gains in a specific medium, and its value is linked to the storage stability of colloidal dispersions. This value indicates the degree of repulsion between close and similarly charged particles in dispersion. For particles in colloidal range, a high zeta potential will confer stability, that is, the solution or dispersion will resist aggregation. However, when the potential is low, attraction exceeds repulsion and the dispersion will break and flocculate. Colloids with high zeta potential (negative or positive) are thus electrically stabilized, while colloids with low zeta potentials tend to coagulate or flocculate. In general, zeta potentials superior to –60 mV are essential for excellent electrostatic stabilization. Values of –30 mV have been found to be enough for good stabilization, hence indicating good physical stability [117].

4.4. Crystallinity

The polymorphic behavior of lipids, as well as their cristallinity, influences both drug incorporation and release rates to a high degree. Extensive work by Bunjes and coworkers [25, 118–120] reports on crystalline properties of lipids and their recrystallization patterns during nanoparticle preparation, and the influence of nanoparticle size on recrystallization pattern. It is known that crystalline lipids present an orderly display of units. However, the preparative methods, the presence of emulsifiers, the small particle size, as well as the high dispersity of these nanoparticulate systems influence the crystallinity of the lipids in the LNs. Among the problems that can be found in these systems upon crystallization, we encounter drug expulsion during storage

and change in zeta potential that may cause instability problems such as gelling [117].

Differential scanning calorimetry (DSC) and X-ray diffractometry (XRD) are two of the main tools employed to determine the crystallinity and polymorphic behavior of the components of the SLNs. DSC gives information on the melting and crystallization behavior of all liquid and solid constituents of the particles, while XRD is used to identify specific crystalline compounds, organic and mineral, based on their crystal structure. In XRD, a powder comprised of small crystals is irradiated with a monochromatic beam of X-rays assuming that the orientation of the crystallite is random. The beam is diffracted at angles determined by the spacing of the planes in the crystals and the type and arrangement of the atoms. A scanning detector records the diffracted beams as a pattern. The position and intensity of the diffractions are unique to each type of crystalline material. Even in complex mixtures, this pattern can be identified by comparison to reference spectra using a computerized database. XRD investigations have been particularly important in the elucidation of the manner of arrangement of lipid molecules, their multiple-melting phenomena, phase behavior, and the characterization and identification of the structure of lipid and drug molecules [25, 26]. Bearing in mind that the incorporated drug may undergo a polymorphic transition, the determination of the crystallinity of the components of the formulation is a very important issue. Lipid matrices can also change their polymorphic behavior leading to a possible undesirable drug expulsion during storage [27].

4.5. Storage and Stability

Most ingredients of SLNs and incorporated drugs are usually unstable, oxidizing, or hydrolyzing. Besides, since SLNs are thermodynamically unstable systems, it is very important to obtain a dry product in order to allow their long-term storage and to ensure their stability. Lyophilization is one of the most widely used techniques for producing dry powders from nanoparticulate suspensions [44, 121–124] and provides an increase in chemical and physical stability over extended periods of time. In addition, lyophilization also offers the possibility for SLNs to be incorporated in tablets, pellets, or capsules. However, the parameters employed in this procedure depend on the lipid used for the SLN formulation [107]. Consequently, the lyophilization process subjects the lipid nanosystems to freezing and drying, two important stresses that can affect their physical stability if suitable stabilizers or cryoprotectants (namely, saccharides) are not employed. In fact, the final SLN product commonly results in the aggregation of particles, which acquire a rubbery aspect when the LN suspension is lyophilized without cryoprotectants. The most generally employed cryoprotectants in the formulation of SLNs are trehalose, sucrose, sorbitol, maltose, glucose, and mannose. In a study of freeze-drying of SLNs, it was concluded that trehalose was the most effective cryoprotectant in preventing particle growth [125]. Along these lines, some researchers studied the short- and long-term stability of lyophilized DNA-containing Precirol-SLNs cryoprotected with glucose and trehalose [97], concluding that 5% glucose-cryprotected SLNs rendered a powdered product that became rubber after 48 h, while the use of other glucose concentrations led to rubbery samples from the beginning. In the case of trehalose, a concentration of 10% manifested the best results, yielding a powdered product that remained over time. This study also showed that the lyophilization process of the SLNs translated into an increase in the particle size of about 100 nm, whatever the trehalose concentration used. However, this size hardly varied along the first 9 months at room temperature.

An interesting alternative to lyophilization was suggested by Gasco's group in 2003. This technique is based on drying with a nitrogen stream at low temperatures of 3–10°C [126]. Compared to the lyophilization process, the avoidance of freezing and the energy efficiency resulting from the higher vapor pressure of water are the main advantages.

One of the main physical instabilities of SLNs is the formation of a gel, leading to a change in surface area. This gelation takes place by the SLNs building up a network and lipid bridges between them [117]. Examples that form gels at temperatures of 40°C can be found in lipid formulations with Imwitor 900 (glyceryl stearate) or Dynasan 118 (tristearin) [127]. More recently, some studies have shown that temperature plays an important role in the stability of SLNs, concluding that, in general, SLNs maintain their size at 4°C, while this size increases when these particles are kept at 25°C [99].

5. TISSUE DISTRIBUTION, PHARMACOKINETICS, AND SAFETY OF LNs

5.1. General Overview

Most therapeutic agents are extensively distributed among different tissues when they reach systemic circulation. Therefore, significantly larger doses of the therapeutic agent need to be administered to compensate the body distribution effect, and in some cases systemic toxicity can be observed. However, if the drug is encapsulated in nanocarriers such as LNs, which can be preferentially delivered to certain parts of the body, less body distribution effect is observed, and lower doses could be administered to achieve the same therapeutic benefit. Moreover, the favorable pharmacokinetic profile of the systemically administered nanocarriers can lead to improvements in therapeutic outcomes. It is important to point out that conjugation with lipids effectively alters the physicochemical properties of therapeutic molecules (size and charge), reduces the uptake by the organs of the RES, such as liver and spleen, prolongs the circulation time, and improves the overall pharmacokinetics and therapeutic index of the drug.

LNs have drawn increasing interest from every branch of medicine for their ability to overcome certain biological barriers, resulting in increased therapeutic efficacy of the encapsulated drug. The encapsulation of therapeutic agents in LNs increases the tumor accumulation of cytostatic drugs [128] or the antibacterial activity of antiparasitic and

antifungal drugs [129] and allows brain delivery of some drugs that are not able to cross the BBB when they are systemically administered [45]. The use of lipid nanoparticulate formulations also plays an important role to increase the bioavailability of therapeutic agents with poor biopharmaceutical properties, such as poor solubility, poor permeability across the intestinal epithelium, enzymatic or nonenzymatic degradation and metabolism, and intestinal efflux, and poor transport properties.

Compared to other nanocarriers, LNs seem to offer more advantages, such as higher physical stability, greater protection from degradation and better release profile of incorporated drugs, and good tolerability. The history of LNs is relatively short and there is still lack of clinical studies of the use of these nanoparticles. Nevertheless, the findings in the preclinical studies using cell culture systems or animal models have so far been very promising. They can be regarded as effective carriers for chemotherapeutic, gene therapy, anti-Parkinsonian, antiretroviral, antipsychotic, anti–rheumatoid arthritis, antiparasitic, antihypertensive, and antibiotic agents, as well as diagnostic tools in neurooncology [130].

The toxicity of the excipients is a major issue in the development and the use of nanoparticulate delivery systems. LNs are well tolerated since they are constituted of physiological systems, and therefore, no problems should be observed after administration to living systems. The good tolerability of LNs compared with polymeric nanoparticles has been confirmed in both in vitro and in vivo studies [131].

5.2. Administration Routes and in Vivo Fate

In general, the in vivo fate of the nanocarriers depends mainly on the selected administration route, and the distribution and enzymatic processes that the nanoparticulate systems undergo. LNs are composed of physiological or physiologically related lipids or waxes. Therefore, most of the metabolic pathways described for lipid transportation through biological barriers and catabolism are applicable.

LNs have been developed for various pharmaceutical applications and evaluated after their administration by different routes: parenteral [7], peroral [30], dermal [132], ocular [133], pulmonary [134], and rectal [135] administration.

5.2.1. Oral Administration

Oral delivery is the easiest and most convenient route for drug administration, but many drugs are not administered orally because they are not absorbed or are degraded in the gastrointestinal tract. The use of submicron-sized particular systems for oral drug delivery has attracted considerable pharmaceutical interest in the last years. It has been reported that the drug formulation in nanosized systems enables the bypass of gastric and intestinal degradation observed when the free drug is orally administered [136] as well as the uptake and transport through the intestinal mucosa of low bioavailability presenting drugs [137]. LNs were introduced as a novel drug carrier system for oral delivery in the mid 1990s. Although the oral administration of LNs has been easily performed, especially SLNs, the mechanism of oral absorption still needs to be revealed. Different mechanisms for particle absorption from the gastrointestinal tract have been described in the literature. Figure 2 shows a schematic representation of this absorption process. In vivo studies performed with orally administered LN-containing drugs such as cyclosporine A [138], camptothecin [139], idarubicin [71], tobramycin [129, 140], rifampicin, isoniazid, and pyrazinamide [141] and proteins [142] have shown a bioavailability enhancement of the encapsulated drug. Absorption of nanoparticles may occur through intestinal mucosa by several mechanisms, namely through the Peyer's patches (PP), by intracellular uptake, or by the paracellular pathway. Mediated transport by the M-cells has also been proposed as a possible mechanism. The main uptake pathway of SLNs described in rats is M-cells transport overlaying the PP [16]. Owing to their small particle size, LNs may enter in the intervillar spaces, thus increasing their residence time in the gastrointestinal tract resulting in enhanced bioavailability and reduced or minimized erratic absorption. As the colloidal species resulting from lipid digestion, LNs should be taken up through the enterocyte membrane by passive

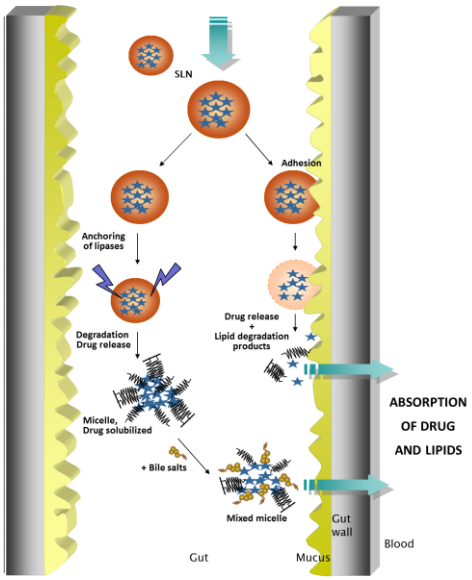

Figure 2. Mechanisms of absorption promoting effect of lipids formulated as an SLN. In a first moment, enzymes degrade the lipids in the gut allowing the formation of surface active mono- and diglycerides on the surface of the nanoparticle. The detachment of these molecules leads to the formation of micelles, a process in which the drug dissolved in the lipid is taken up in the micelle and solubilized. These micelles interact with bile salts present in the gut (e.g., sodium cholate) and "mixed micelles" are formed. In the following absorption process, the drug is simultaneously absorbed along with the lipid-degradation product. Reprinted with permission from [210], A. Estella-Hermoso de Mendoza et al., *J. Biomed. Nanotechnol.* 5, 323–343 (2009). © 2009, American Scientific Publishers.

diffusion, facilitated diffusion, and active transport. In the cytosol, a fatty acid–binding protein transports them from the apical to the basolateral membrane.

The majority of orally administered compounds access the systemic circulation by the portal blood. However, some extremely lipophilic compounds ($\log P > 5$) gain access to the systemic circulation via a lymphatic route, avoiding hepatic first-pass metabolism. Several experiments have been performed to assure the lymphatic uptake of LNs after duodenal administration. Transmission electron microscopy was used to observe the presence of SLNs in lymph and blood [16, 129, 140, 143]. In some recent research, SLN suspensions were administered by oral gavage to rats with and without thoracic lymph duct cannulation. Approximately 77.9% of absorbed SLNs were transported into systematic circulation via lymph, whereas the remaining 22.1% of SLNs were absorbed by nonlymphoid pathway [144].

There are some critical factors that have to be considered in the design of new and efficient lipid carrier systems for oral use. As we have previously mentioned, particle size is a critical determinant of the absorption of orally administered nanoparticles. Larger particles (greater than 300 nm) may be retained for longer periods in PP, while smaller particles are transported to the thoracic duct. Moreover, the environmental conditions of the gastrointestinal tract (acidic pH and high ionic strength) enhance particle aggregation, leading to a decrease in the interaction capability of LNs with the intestinal mucosa [145].

The composition of LNs can also play a role in relation to the uptake pathway. A wide variety of solid lipids derived from physiologically compatible lipids, such as highly purified triglycerides, complex glyceride mixtures, phospholipids, or even waxes, is employed to prepare LNs. Studies have shown that the fatty acid chain length plays a major role in the lymphatic drug transport of lipid compounds. In general, lipids with fatty acids of chain length of 12 carbons are absorbed primarily by means of the portal blood, whereas lipid compounds with chain lengths above 12 carbons are re-esterified and transported via intestinal lymph [146–148]. The surfactants used to stabilize the obtained drug-delivery formulation also contribute to an increase in the permeability of the intestinal membrane or improve the affinity between LNs and the intestinal membrane. In previous research [149], the absorption was greatly improved by increasing the amount of Pluronic® F68 and Tween® 80 on SLNs.

During the absorption phase, the drug molecules are usually exposed to the activity of the phase I drug metabolizing enzymes and extrusion transporters present at high concentrations in enterocytes located at the villus tip of the small intestine in humans, leading, in some cases, to a drug bioavailability decrease. However, the bioavailability of these drugs shows a significant increase when they are coadministered with lipids. The same effect is observed when certain drugs are encapsulated in LNs and administered by an oral route. In vitro studies on P-glycoprotein (P-gp) overexpressing human cancer cells using doxorubicin- and paclitaxel-loaded LNs have shown that this may overcome multidrug resistance (MDR) [150]. The exact mechanism behind this phenomenon is still unclear. Few researchers are of the opinion that the lipids attenuate the expression and activity of these enzymes, while others have proposed that the lipid shields the drug molecules from the enzymes [151].

The stability of LNs after contact with gastrointestinal fluids is a critical parameter that cannot be overlooked in the design of these nanocarriers for oral use. LNs are composed of biodegradable materials, and particle size in the nanometer range maximizes the surface area for enzymatic degradation. However, the influence of artificial gastrointestinal media on the physical stability of solid lipid formulations has been investigated in a few cases [152, 153]. The results obtained provide evidence that LNs show a certain physical stability in the gut lumen and lymph, ensuring a partial protection of the incorporated drugs. The physical stability of SLNs reduces the local adverse effect of some drugs on the gastrointestinal tract and protects biodegradable molecules, such as orally administered peptides and proteins [152, 153].

Various companies are interested in solid lipid nanotechnology for oral drug delivery. Pharmatec (Italy) developed a cyclosporine SLNs formulation for oral administration [154]. AlphaRx has also rifampicin-loaded SLNs under preclinical phase (Rifamsolin™).

5.2.2. Parenteral Administration

LNs are colloidal drug carriers very suitable for systemic delivery. In contrast to carriers prepared with synthetic polymers such as pluronic or polyacrylamide, they are composed of physiologically well-tolerated ingredients that are eliminated by the endogenous metabolic pathways. Moreover, they have good storage capabilities after lyophilization and/or sterilization. Upon administration of SLNs and NLCs via the parenteral route of administration, improved biodistribution profile, targeting, and enhanced cytotoxicity against multidrug resistant cancer cells have been observed [33, 155].

In general, parenteral application of SLNs reduces the possible side effects of drug incorporated with a substantially increase in drug bioavailability. LNs avoid the RES uptake since they are colloidal sized. Therefore, LNs circulate through the microvascular system without macrophage uptake and drugs show a lower clearance, a higher distribution volume, and a significantly higher area under the curve (AUC) when entrapped in LNs rather than when administered as free drug. The decreased uptake by RES tissues (kidney, spleen, and liver) of LNs also increased the drug bioavailability in non-RES tissue targeting such as brain and lung.

LNs are being widely investigated as carriers for parenteral delivery of macromolecules such as proteins, oligonucleotides, and DNA. Cationic solid nanoparticles were used and shown to be efficacious in transfecting COS-1 cells in vitro for the first time in 2001 [156], whereas therapeutically relevant peptides (calcitonin, cyclosporine A, insulin, LHRH, and somatostatin), protein antigens (hepatitis B and malaria antigens), and model protein drugs (e.g., bovine serum albumin and lysozyme) have been evaluated after loading into SLN particles [134]. SLN vehiculating different types of antineoplastic agents (conventional cytotoxic drugs such as doxorubicin and paclitaxel, the prodrug cholesteryl butyrate and antivasculoendothelial growth factor antisense

oligonucleotides) have been tested in experimental animal models of cerebral gliomas [157], mouse xenograft model [158], or Dalton's lymphoma tumor-bearing mice [159]. Cardiovascular drugs, antiparasitic agents, antipsychotics, antiparkinsonians, anti-ischemic drugs, and antibiotics have also been encapsulated in LNs either to modify the biodistribution or for brain targeting [42, 160–162].

Uptake of the nanoparticles in cells of the RES is different depending on the size and composition of the particles. Uptake of LNs can also be avoided by PEGylation leading to long-circulating particles, so-called stealth LNs. In general, an increase in particle size by coating nanoparticles with stabilizing hydrophilic molecules leads to extend blood circulation of LNs. The concentration and the physical-chemical properties of stealth agents affect in a high degree the rate of the phagocytic uptake. The hydrophobicity degree of the particle surface strongly affects the phagocytosis of colloidal particles by RES, with a reduced phagocytic recognition when LNs are coated with a high hydrophilic surface [45, 159, 161]. Hydrophilic coating of colloids improves the tissue distribution and the transport of these through the BBB. Some researchers have demonstrated that coated SLNs with hydrophilic molecules carrying anticancer drugs can reach cancer cells in solid tumors more effectively than healthy tissues [157–159].

The surface charge of a colloid can also alter the biodistribution and clearance rate of drugs. In general, the plasma half-life of negatively charged colloids was found to be higher than that of positively charged colloids, and a strong negative charge or a strong positive charge usually leads to more rapid phagocytic uptake than a weak negative or positive charge [145]. The presence of hydrophobic coating on the surface of LNs partially masks the native charge of the uncoated particles [163].

The great advantages and the lower drawbacks of LNs compared to polymeric nanoparticles make them attractive drug carrier systems for pharmaceutical companies. LN products made by several pharmaceutical companies can be listed as follows: cationic SLNs for gene transfer, namely TransoPlex®, were produced by PharmaSol DDS (Germany). AlphaRx (USA) is developing vancomycin and gentamicin products with Vansolin™ and Zysolin™ trade names. SkyePharma (UK) also has formulations of nanoparticulate technology which includes nanosuspensions and SLNs under preclinical development.

5.2.3. Nasal and Pulmonary Administration

The nebulization of LNs is a new and upcoming area of research. Inhalation nanoparticles are deposited in all regions of the respiratory tract. The respiratory tract can be divided into three regions: the nasopharyngeal, tracheobronchial, and alveolar regions. The distribution of LNs along the respiratory tract is size dependent. Ninety percent of nanoparticles of 1 nm in diameter deposit in the nasopharyngeal region, whereas only 10% of these nanoparticles deposit in the tracheobronchial region and almost none reach the alveolar region [164]. However, 15% of nanoparticles of 20 nm in diameter deposit in the nasopharyngeal region, 15% in the tracheobronchial region, and approximately 50% in the alveolar region [165].

The small size, biocompatible composition, and deep-lung deposition ability of LNs make them more suitable as carriers for pulmonary delivery. The lung offers a large surface area for drug absorption, and the alveolar epithelium allows rapid drug absorption. Nanoparticles can access the systemic vasculature directly or via lymphatic transfer by transcytosis, crossing the epithelia of the respiratory tract into the interstitium, phagocytosis, endocytosis, or some other transmembrane process [14]. Although metabolic enzymes can be found in the lungs, the metabolic activities are different from those observed in the gastrointestinal tract. These advantages make the pulmonary administration a very promising route for drugs that are rapidly degraded in the gastrointestinal tract, such as peptides and proteins. Moreover, pulmonary administration is an effective route to deliver drug containing LNs to the lymphatic system. Assessment of inhaled radio-labeled SLN biodistribution has been described and the data showed an important and significant uptake of the radio-labeled SLNs into the lymphatics after inhalation. In fact, few minutes after drug deposition, inhaled nanoparticles translocate to regional lymph nodules [166]. The nasal-associated lymphoid tissue is also capable of transporting nanosized carriers to extrarespiratory sites. However, it was demonstrated that the therapeutic outcome of nasally delivered antigen-containing colloidal carriers is highly dependent on the involvement of the lower respiratory tract [167]. The clearance mechanism is dependent on particle size and physicochemical characteristics of LNs, not on the lipids employed in the LN preparation. LNs must present a mean diameter within the submicron range to penetrate in the alveolar interstitium [168]. Particle clearance from lungs generally shows a rapid initial elimination phase followed by an equilibrium phase prolonged for a longer period. In recent research, a relative bioavailability of 22.33% was obtained after inhalation of insulin-SLNs, which was almost fourfold higher than the control.

Various research groups have proposed SLNs as nasal and pulmonary delivery systems of macromolecular therapeutic agents and diagnostic agents. Proteins, genes, and antibacterial agents are the LN-encapsulated drugs in these applications [10, 134, 167–170]. Hydrophilic coating of LNs may permit the interaction and transport of LNs through the nasal mucosa and, therefore, bring great benefits and compliance as nasal drug carriers, especially for vaccines [171].

Nebulization of SLN-carrying antitubercular drugs was observed to be successful in improving drug bioavailability and reducing the dosing frequency for better management of pulmonary tuberculosis after pulmonary administration [141, 172].

5.2.4. Topical Administration

SLNs are considered to be the latest generation of colloidal drug carriers for topical use. SLNs and NLCs are very attractive colloidal carrier systems for skin applications owing to their various desirable effects on skin, apart from their characteristics of a colloidal carrier system. Compared with other vehicles, such as creams, tinctures, emulsions, and other delivery systems such as the liposomes and microparticles, they combine such advantages as local tolerance, good adhesive properties, the protection of the

encapsulated drugs against chemical decomposition, and the possibility to modulate the drug release [22].

The bioavailability of nanoparticulate carrier drugs may be increased by the close contact between the small particle size of nanoparticles and stratum corneum. However, the limited voids in the lipid bilayers of stratum corneum make the diffusion of intact particles into the skin impossible. LNs have a more favorable occlusive effect than other pharmaceutical preparations and drug delivery effects, increasing the particle permeation through the skin. LNs form adhesive films of densely packed spheres on the surface of the skin increasing skin hydration. Following the evaporation of water from the lipid nanodispersion, LNs form an adhesive layer occluding the skin surface [173]. The increase of the hydration of the stratum corneum facilitates drug penetration into deeper skin strata. Occlusive effects appear to be strongly related to particle size. As a result, nanoparticles have turned out to be 15-fold more occlusive than microparticles [174].

Improved dermal absorption of active pharmaceutical compounds loaded into lipid carriers may result in increased contact surface of entrapped compounds with corneocytes, skin occlusion, rapid and steady release, and surfactant effects. The small size of the particles allows close contact of the lipid carriers with superficial junctions of corneocyte clusters and furrows between corneocyte islands, favoring accumulation for several hours in the application site. LNs are made of lipids that are solid at room temperature. Application of an LN dispersion or LN-loaded cream or gel to the skin surface, whose temperature is 32–35°C, induces structural changes of particle structure. Water evaporation results in a transition of the lipid matrix to a more highly ordered structure, leading to drug expulsion. The supersaturated solution enhances the penetration into the tissue [32].

The enhanced skin permeation of LNs was probably owing to the additives included in the formulation. Nonionic surfactants, which are used for lipid nanoparticulate stabilization, are reported to enhance drug-loaded penetration into human skin [22].

During the last few years, SLNs and NLCs with active compounds such as vitamin E [175], tocopherol acetate [176], retinol [177], ascorbyl palmitate [178, 179], clotrimazole [180], triptolide [181], podophyllotoxin [173], and a nonsteroidal antiandrogen RU 58841 [182] have been developed and evaluated for topical application.

5.2.5. Other Administration Routes

Ocular administration of drugs is often difficult because the poor bioavailability of drugs from ocular dosage forms is mainly owing to precorneal loss factors [183, 184]. Therefore, the development of a substitute for the solution-type eyedrop that would offer sustained delivery of an active compound presents a major challenge. In general, colloidal drug delivery systems enhance the ocular bioavailability of drugs. Biocompatibility and mucoadhesive properties of LNs improve their interaction with ocular mucosa and prolong the corneal residence time of the drug. The ocular drug administration of SLNs has been reported several times in the literature. Some researchers evaluated the carrier effect of SLNs of tobramycin for ocular delivery in rabbit eyes. Tobramycin bioavalability in the aqueous humor was significantly enhanced when it was entrapped in SLNs [185]. They also studied pilocarpine delivery in SLNs. They reported very similar results concerning enhancement of the ocular bioavailability of drug [186]. In another study, cyclosporine A was successfully incorporated into cationic SLNs for ocular administration. Cyclosporine A could be detected in both aqueous and vitreous humor samples for 48 h showing the ocular penetration of formulation with an increased release profile [187]. The administration of diclofenac-loaded SLNs combining the homolipid from goat (goat fat) and a phospholipid in bioengineered human cornea yielded a sustained release of the analgesic drug [188].

Few reports are available in the literature on the rectal administration of drugs entrapped in SLNs. This administration route seems very open to research, especially when the benefits of the rectal route are taken into consideration. The plasma levels and therapeutic efficacy of rectally administered drugs were reported to be higher compared with those given orally or intramuscularly at the same dose [135]. The feasibility of the inclusion of diazepam in SLN-based suppositories with rapid onset and prolonged release of the drug has been recently investigated. Sznitowska et al. [135] incorporated diazepam into SLNs in order to provide a rapid action after rectal administration. They found that the use of these diazepam-loaded SLNs is not an advantageous system for a rapid diazepam rectal delivery. However, the developed formulation is a promising delivery system for the prolongation of diazepam release through the rectal route [189].

5.3. Pharmacokinetics and Tissue Distribution

In general, once a therapeutic agent achieves the circulatory system, it is distributed systemically via the vascular and lymphatic systems. The tissues and organs with high blood flow, such as the brain, liver, heart, intestines, lungs, kidneys, and spleen, are exposed to higher concentrations of the administered drug. Therefore, the therapeutic agents are extensively and nonspecifically distributed to highly irrigated organs and tissues when they are administered in free form, whereas lower concentrations are obtained in less irrigated tissues.

Administration of drugs incorporated in LNs leads to different pharmacokinetic profiles from those obtained after free-drug administration. When the drugs are encapsulated in LNs, they are protected from chemical degradation in the gastrointestinal tract, bypass the effect of extrusion membrane proteins, reduce the drug exposure to hepatic metabolizing enzyme activity, and avoid the renal clearance owing to decreased size. The body normally clears waste and distributes nutrients and drugs via the vascular and lymphatic systems after systemic administration. Intravenously injected particles are scavenged and cleared from circulation by the RES in a process that is facilitated by surface deposition of opsonic factors and complement proteins on the nanoparticles themselves [190]. The size and surface characteristics of injected nanoparticles influence the clearance and opsonization. Particles greater than 200 nm in diameter activate the complement system more efficiently and are cleared more rapidly than very small nanoparticles.

The reduced liver metabolism and renal clearance of drugs encapsulated in LNs often result in prolonged blood circulation with an increased chance of accumulation in the target tissue. A threefold to fivefold enhancement of plasma concentrations of the encapsulated drug is observed when SLNs are administered by i.v. route. The plasma concentration–time profile of the loaded drug generally showed a biexponential curve with high AUC, a lower rate of clearance, and a smaller volume of distribution in comparison to the free drug [16, 71, 140, 144]. The biphasic behavior is explained as being probably owing to the slow distribution of SLNs to organs and tissues. It is interesting to note that sometimes two peaks are observed in the concentration–time profile of encapsulated drug after SLN administration, whatever the administration route is. The first peak takes place immediately after i.v. administration of the nanocarrier system and during 1–2 h after oral administration. Then, the concentrations of the entrapped drug begin to decrease, which may be related to the uptake of LNs by the macrophages or the distribution among particular organs, and the release of encapsulated drug as happened with polymeric nanoparticles [191, 192]. The second peak appears at about 6–8 h, and the maximum concentrations of the entrapped drug are lower than those of the first peak. The second peak may be caused by the redistribution of LNs which could be released from those particular organs into systemic circulation [144].

The interaction of LNs with the major circulatory protein, serum albumin, has been investigated in the present decade. Albumin adsorption forms a capping layer of 17 nm on the particle surface of SLNs. The SLNs are protected by this layer against flattening on surfaces of *p*-dodecanoylcalix[4]arene. At physiological albumin concentrations (35–50 g l^{-1}) the increased size was not found to be important enough to explain blood cell aggregation [193]. In general, distinct types of LNs have distinct affinities to red blood cells. The affinity is directly correlated with the type of surfactant used. Olbrich et al. [136] showed that a solid lipid nanoparticulate formulation prepared with Compritol® as matrix material and the surfactants Tween® 80 and poloxamer 188 showed no binding to erythrocytes (SLNs binding lower than 10.0%). In contrast, when Span® 85 was used, the blood cell affinity of the labeled nanocarrier was increased, leading to significant aggregation of red blood cells (75.3%).

The bioavailability of the encapsulated drug increased considerably after oral administration of LNs. The AUC values obtained after administration of idarubicin-SLNs to rats were higher (around 21-fold) than that of idarubicin-free solution [71]. The administration route affects heavily the bioavailability of lipid nanoparticulate-encapsulated drugs. The AUC of idarubicin after administration of SLNs into the duodenum was higher than that obtained after i.v. administration [71]. These results confirm the conclusions of a previous study where tobramycin-loaded SLNs were administered duodenally and intravenously to rats [140]. The difference between the two administration routes for the most part lies in the predominant transmucosal transport of LNs to the lymph; lymphatic transport chiefly contributes to the absorption of LNs, which could affect the drug bioavailability.

The tissue distribution profiles of LN-encapsulated drug differ significantly from the observed profile after administration of the free drug. With the exception of the brain, concentrations of encapsulated drugs are lower after LN administration than with that obtained after drug-free administration, especially for the liver, spleen, kidneys, heart, and lungs. They could be related to slower distribution of LNs through biological barriers and/or the slow release of entrapped drug in the targeted organs. In contrast to polymeric nanoparticles, LNs are widely distributed in slowly irrigated tissues such as muscles, bones, and fatty tissues [78, 129, 139, 194]. The major limiting factor for the systemic use of colloidal carriers is their rapid clearance from the blood circulation by the RES. However, LNs, particularly those in the range of 120–200 nm, are not taken up readily by the cells of the RES, and thus bypass liver and spleen filtration.

Drug targeting within the brain is mainly hampered, among other factors, by the weak permeability of the BBB separating the blood vessels from the cerebral parenchyma [195]. Furthermore, BBB active drug efflux transporters are widely present in the cerebral endothelium and play an important role in the efflux mechanism of a wide variety of drugs [196]. LNs are promising systems for the delivery of drugs to tumors of the central nervous system as they are able to bypass these drawbacks [39]. Various mechanisms for nanoparticle-mediated drug uptake by the brain have been outlined over the years. These include the enhancement of drug carrier retention in the brain–blood capillaries, by adsorption onto the capillary walls, resulting in a high concentration gradient across the BBB; the opening of tight junctions owing to the presence of nanoparticles; the transcytosis of nanoparticles through the endothelium; solubilization of endothelial cell membrane lipids and membrane fluidization, owing to surfactant effects of polysorbates present in the drug carrier; or inhibition of efflux system of BBB, especially P-gp [39]. However, the mechanism for LN uptake by brain is not completely understood. Depending on the LN composition, P-gp efflux pump inhibition and stealth properties can be conferred to LNs. For instance, Solutol® HS15- and Tween® 80-loaded LNs resulted in a negative regulation of the ATPase activity, by the interaction with P-gp [196, 197]. Figure 3 depicts the most generally accepted method by which Tween 80-coated LNs are able to cross the BBB. Briefly, apolipoproteins (especially E) adsorb onto the surface of the LNs and after being recognized by the LDL receptors present in the BBB, they are internalized. After this, the drug may be freed inside these cells and diffuse into the inner brain or the particles may be transcytosed. Some other processes such as P-gp inhibition or tight junction modulation can also happen [198].

LNs were first proposed for brain drug targeting application by two research groups in the late 1990s [139, 143]. They undertook scientific research to study the pharmacokinetics of two anticancer agents, namely camptothecin and doxorubicin, after free and SLN-drug-encapsulated administration to rats, and observed drug accumulation in the brain after both oral and i.v. administration. The administration of camptothecin entrapped in SLNs increased by 180% the achieved maximum drug concentration (C_{max})

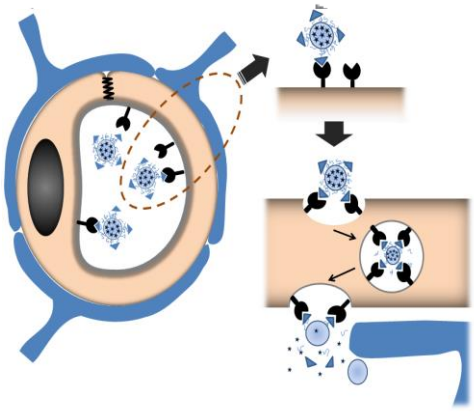

Figure 3. Schematic representation of the mechanism of brain uptake of SLNs formulated with Tween 80. In a first step, Apo-E is adsorbed onto the surface of SLNs. Then, nanoparticles bind to the BBB LDL receptors and they are endocytosed and transcytosed. Finally, the drug is released from LNs through the BBB endothelial cells.

with regard to the C_{max} of the drug solution. The AUC–dose and the mean residence time (MRT) were 10.4- and 4-fold higher, respectively, after administration of camptothecin in SLNs [139]. In other independent research, stealth SLNs of doxorubicin (stearic acid–PEG 2000 as stealth agent) were found in rat cerebrospinal fluid (CSF) 20 min after i.v. administration [46]. The bioavailability and brain uptake of nitrendipine was also improved when it was administered in SLNs by i.v. route. Nitrendipine-SLNs were made using different triglycerides (tripalmitin, trimyristin, and tristearin), emulsifiers (soy lecithin), poloxamer 188, and charge modifiers (dicetyl phosphate, DCP and stearylamine, SA). The C_{max} of 3.2, 7.3, and 9.1 times was achieved with nitrendipine tripalmitin, nitrendipine tripalmitin DCP, and nitrendipine tripalmitin SA SLNs when compared with a nitrendipine suspension [160]. A 10-fold increase in brain was observed after an i.v. injection of 1.3 mg kg^{-1} of the anticancer drug camptothecin into mice when it was entrapped on stearic acid SLNs compared with a free-drug solution [139]. The antiparkinson activity of bromocriptine encapsulated in NLCs was studied in a model of Parkinson's disease, 6-hydroxydopamine hemilesioned rats. The results indirectly demonstrated that higher brain levels of bromocriptine were achieved after administration as NLCs. The antiparkinsonian bromocriptin NLCs have rapid onset of action as compared to that of solution and were retained for a longer duration [199].

The brain concentration of the encapsulated drug is higher when stealth LNs are used. Zara et al. [46] evaluated the effect of the stealth agent concentration in the brain uptake of doxorubicin SLNs. They observed an increase in the brain concentration of doxorubicin, as the amount of stealthing agent employed was increased. The amount of drug present in the rabbit brain ranged from 27.5 ng g^{-1} for nonstealth SLNs to 242.0 ng g^{-1} for stealth SLNs preparation loaded with 0.45% PEG after 30 min.

The surface charge of LNs also plays a significant role in order to achieve brain targeting. The brain uptake of etoposide entrapped in positively (surface charge: +5 mV) and negatively (surface charge: −47 mV) charged tripalmitin SLNs were evaluated and compared to that of free-labeled drug in mice after i.v. administration. Positively charged SLNs showed a higher brain accumulation compared with both negatively charged SLN and free-labeled drug. The etoposide concentration, achieved using positively charged SLNs, was 10- and 14-fold higher with respect to the negatively charged SLNs at 1 and 4 h after administration, respectively [81]. Unfortunately, the strategy of using surface-charged SLNs to cross the BBB has been found to have some important drawbacks which limit its usefulness. High concentrations of anionic nanoparticles and cationic nanoparticles disrupted the BBB, whereas neutral nanoparticles lack effect on BBB permeability [41].

The coating of SLNs increases the nanoparticle brain uptake. The coating of clozapine-SLNs with sterylamine results in significantly higher amount of clozapine in brain (as a measure of AUC) as compared to that of clozapine SLNs without sterylamine and clozapine suspension [200]. The brain uptake of the SLNs was increased when they were coated with thiamine, as it can be seen in a study using in situ rat brain perfusion technique with and without thiamine [201].

Several improvements in tumor drug accumulation have been observed when anticancer drugs are administered in LNs. Elevated etoposide concentrations were found in tumor when SLNs were intravenously administered to Dalton's lymphoma tumor-bearing mice (67% increase 1 h postinjection and 30% increase 24 h postinjection), compared to free drug [159]. The accumulation of docetaxel in tumors was also 1.7–2.4 times higher in female nude mice bearing hepatoma 6 h after i.v. injection of SLNs [93]. Tumor AUC values of chlorambucil after i.v. administration of SLNs to C57 BL/6 male mice subcutaneously inoculated with colon-38 tumor fragments from donor mice were significantly higher ($p < 0.01$) than those obtained after i.v. administration of the free drug [92]. The higher accumulation of the anticancer drugs loaded in SLNs could be attributed to the following reasons: first, encapsulation of anticancer drugs into SLNs resulted in higher accumulation in both the liver and the tumor. In general, LNs can increase drug concentration in tumor via the previously explained EPR effect. Nanoparticles with a diameter below 200 nm can significantly accumulate in tumors by this mechanism [202]. Second, the internalization of LNs was further enhanced by the modification of the particle surface with a ligand that can bind to specific receptor of a type of carcinoma cells. The requirements of the antigen that will allow molecular targeting are: exclusive expression in cancer cells, to be an integral part of an essential cellular function of the cancer cells, and not to easily mutate as the cancer cells proliferate [62]. Docetaxel incorporated in galactosylated LNs showed a tumor-increased accumulation in the treatment of hepatocellular carcinomas expressing the asialoglycoprotein receptor compared with unmodified LNs [93]. On the

other hand, a folate receptor–targeted LN system significantly improved in vivo tumor growth inhibition and tumor-bearing animal survival compared to nontargeted LNs [60].

Significant improvements in tumor drug accumulation were observed when the etoposide formulations were injected intraperitoneally or subcutaneously rather than when intravenously administered [159]. The slower and progressive penetration of the nanoparticles (and hence the loaded drug) from the peritoneum or the subcutaneous injection site into the tumor may result in more favorable patterns of drug distribution. The route of administration of a LN formulation will be a key aspect to consider when designing animal or clinical studies using LNs for anticancer drug delivery.

5.4. Safety

So far, little extensive research has been conducted to analyze the toxicity of LNs. The field of nanotoxicology is still in its early life, with very limited literature regarding the potential toxic effects of the nanosystems. The possible mechanisms of toxicity for nanoparticles have recently been hypothesized [203]. First, nanomaterials can create and/or scavenge reactive oxygen species and free radicals. The toxicity of LNs may also be linked to their size and their propensity to agglomerate. Moreover, there is a growing concern about the role of LNs in possible allergic reactions. However, the toxicology of bulk materials is relatively well defined.

Unlike some nanosized systems, LNs are well tolerated in living systems because they are made from excipients that are chemically similar to physiological compounds, and therefore metabolic pathways exist to eliminate them. The results of cytotoxicity studies (MTT tests) indicated that SLNs are less toxic than polymeric nanoparticles [204]. The viability of human granulocytes was 84% after incubation with 2.5% poloxamer 188–cetyl palmitate SLNs and 72% after incubation with 5% poloxamer 188–Compritol® SLNs. Poloxamer-stabilized polylactide–polyglycolide (PLGA) particles reduced the cell viability to 50% at a concentration of 0.1%. Higher concentrations (0.5%) led to complete cell death [131]. Similarly, low cytotoxicity was observed in a comparable study on poloxamine 908- and poloxamer 407-stabilized SLNs [161]. The experimental data of the toxicity studies on cells in vitro confirm the expected low toxicity of the carrier. Glyceride SLNs showed nearly 10 times lower cytotoxicity when compared to that of PLGA nanoparticles in another study [205].

SLNs made from lipids consisting of stearic acid or dimethyl-dioctadecylammonium bromide were assayed in vitro using murine macrophages in the presence of different concentrations and different sizes of nanoparticles [206]. It was concluded that the nanoparticles were cytotoxic at the concentration of 0.01%, independently of the size of the SLNs. However, SLNs made from lipids consisting of triglycerides, paraffin, or cetylpalmitate were found to be harmless at the same concentration. These data are consistent with the results obtained by Weyhers et al. [207], who in an in vivo study provided a better understanding of the toxicity of two types of SLNs, one made from Compritol® and the other made from cetyl palmitate (which is less physiological), intravenously administered six times within a period of 20 days. The hepatic and splenic tissues were analyzed histopathologically. For the less physiological lipid cetyl palmitate containing SLNs no pathological results were obtained, whereas Compritol®-containing formulations led to a partially reversible accumulation of the lipid in liver and spleen and subsequently to pathological alterations. This accumulation was attributed to the slow degradation of the Compritol® matrix compared to the faster degradation of cetyl palmitate. In contrast, a lower dose of Compritol® SLNs (2.5%, w/w) was well tolerated.

In general, the tolerability of LNs depends in the first line on the surfactant used and secondarily on the lipid. The biocompatibility and cytotoxicity of the surfactants used in the preparation of different types of LNs have also been investigated. To formulate parenteral SLNs, surfactant of GRAS status must be employed, such as lecithin, Tween® 80, poloxamer 188, Span® 85, or sodium glycocholate. Many authors have studied the toxicity of different stabilizing agents on cells and their capability to reverse MDR, suggesting as one of the possible mechanism(s) that MDR reversal by polyoxyethylene surfactants involves alterations of the lipids physical state of the plasma membrane in resistant cells [208, 209]. Two-third of the R100 cells (MDR derivative of human leukaemia cell line) were lysed when they were incubated for only 1 h with the polyethoxylated solubilising agent employed in the formulation of lipid nanocapsules, Solutol® HS15, at concentrations equivalent to 1:100 (w/v), and 100% were lysed by 1:10 (w/v) [209]. LNs have diverse affinities to erythrocytes depending on the surfactant used. Solid lipid nanosized formulations made of Compritol® as matrix material and Tween® 80 and poloxamer 188 as surfactants exhibit a binding to erythrocytes below 10.0%. In contrast, when Span® 85 was employed, blood cell affinity of SLNs was increased, which translated into a significant aggregation of red blood cells (75.3%) [136].

Mammalian systems have been used as the main in vivo model to test the toxicity of nanocarrier systems; in particular, several studies describe the exposure of the respiratory system. Other exposure routes, such as skin and gastrointestinal tract, have not been considered as extensively as the respiratory tract. Further studies are needed to investigate the toxic effects and fate of nanoparticles after their deposition in the respiratory tract or following oral ingestion. LNs were originally designed for the controlled release of drugs after i.v. injection. The solid state of the lipid is a serious hurdle for i.v. injection of the LNs dispersions in the clinical practice. Some lipid nanosized carriers such as SLNs are not deformable, and therefore, in contrast to nanoemulsions, capillary blockage will occur if the particle size exceeds the size of the diameter of the blood vessel. Moreover, gelation of the low-viscosity LN dispersion in the syringe needle might occur, which will immediately form a viscous suspension and provide difficulties in administration [8].

6. APPLICATION OF LNs

LNs combine the advantages of the colloidal drug carrier systems such as liposomes, polymeric nanoparticles, and emulsions, but at the same time minimize the drawbacks

associated with their use. LNs are easily prepared using a rapid and effective production process, show a good tolerability since they include physiological components in their composition, and are site-specific targeting nanocarrier systems that, as it has been previously explained in this chapter, can accumulate, in tumor and brain tissues, depending on the molecules on their surface, in a higher extent than the surface-unmodified LNs. Table 2

Table 2. Active compounds incorporated in LNs.

Drug	Disease	Type of LNs	Route of administration	References
3′,5′-Dioctanoyl-5-fluoro-2′-deoxyuridine	Cancer	SLNs	IV	[217]
5-FU	Cancer	SLNs	IV	[256]
99mTc/188Re	Imaging agent	SLNs, nanocapsules	IV	[257, 258]
Actarit	Rheumatoid arthritis	SLNs	IV	[100]
α-Lipoic acid	Antioxidant	SLNs	Topical	[259]
All trans retinoic acid	Cancer	SLNs	IV	[77, 260]
Ascorbyl palmitate	Antioxidant	SLNs, NLCs	Topical	[178]
Bromocriptine	Anti-parkinsonism	SLNs	IP	[199]
Camptothecin	Cancer	SLNs	IV	[78]
CdSEe–ZnS	Imaging agent	QDs encapsulated in SLNs	IV	[261]
Clozapine	Antipsychotic	SLNs	ID	[200]
Ciclosporine A	Immunosupresant	SLNs	OR	[138, 262]
Coenzyme Q10	Mitochondrial disorders, cancer	NLCs	Topical	[263]
Dexamethasone acetate	Pulmonary disease	SLNs	IV	[264]
Diminazene	Antitrypanosomal	LDCs	n.t.	[223]
DNA	Cancer	Cationic SLNs	n.t.	[156, 235, 236]
Doxorubicin	Cancer	Stealth and nonstealth SLNs, SLNs	IV	[45, 46, 155].
Etoposide	Cancer	SLNs	IV–SC–IP	[80, 81, 159]
Idarubicin	Cancer	SLNs	IV–OR	[71]
Isotretinoin	Acne	SLNs	Topical	[226]
Ferulic acid	Antioxidant	SLNs	Topical	[265]
Iron oxide	Imaging agent	SLNs	n.t.	[239]
Magnetite	Imaging agent	SLNs	n.t.	[204]
Methotrexate	Cancer	LMBVs	IV	[19, 266]
Mitoxantrone	Cancer	SLNs	Local injection	[96]
Nicotinamide	Anti-inflammatory, anxyolitic	SLNs, NLCs	Topical	[267]
Nitrendipine	Antihypertensive	SLNs	IV, ID, Topical	[94, 152, 160]
N,N-Diethyl-*m*-toluamide (DEET)	Insect repellent	SLNs	Topical	[268, 269]
Paclitaxel	Cancer	SLN–Wax NP–sterically stabilized SLNs	IV, OR	[44, 60, 84, 270, 271]
Paclitaxel and doxorubicin	Cancer	SLNs	n.t.	[69, 150]
Podophyllotoxin	Cancer	SLNs	Topical	[173, 272]
Quinine dihydrochloride	Malaria	Transferrin conjugated SLNs	IV	[68, 162]
Retinoids	Anti-inflammatory, cancer, photoaging	SLNs	Topical	[226, 260, 273, 274]
Sunscreens	UV filters	SLNs, NLCs	Topical	[227, 275, 276]
Tamoxifen	Cancer	SLNs	IV	[70, 277]
Tashinone II A	Vasodialator	SLNs	IV	[249, 250]
Temozolomide	Cancer	SLNs	IV	[219]
Testosterone ^{125}I radiolabeled	Imaging agent	SLNs	IV	[240]
Tobramycin	Antibiotic	SLNs	IV or ID	[129, 140]
Tocopherol	Antioxidant	SLNs	Topical	[227, 278]
Vinorelbine bitartate	Cancer	PEG-modified SLNs	n.t.	[214]

IV, intravenous; ID, intraduodenum; IP, intraperitoneum; SC, subcutaneous; OR, oral; and n.t., not tested.

summarizes the number of active compounds that have been incorporated into LNs over the years.

6.1. Cancer

Cancer is the most widely studied application for SLNs in recent years [210]. The formulation of cytotoxic drugs in LNs has been shown to improve the treatment efficacy with a concomitant reduction in the side effects associated with the antineoplastic treatment. The features of SLNs which make them a suitable carrier for antitumor drug delivery are their ability to encapsulate antitumor agents of diverse physicochemical properties as well as the improved stability of the drug, less in vitro toxicity, enhanced drug efficacy, and improved pharmacokinetics [130]. The in vitro and in vivo efficacy of cytotoxic drugs loaded into LNs has been evaluated by suitable studies. The reviews by Estella-Hermoso de Mendoza et al. [210], Shenoy et al. [211], and Wong et al. [212] summarize the major studies reported in the literature.

Yang et al. [139] performed the first in vivo biodistribution studies of an anticancer agent encapsulated in LNs. They investigated the body distribution of camptothecin-loaded SLNs administered intravenously to mice. The average particle size of the SLNs was 197 nm. The concentration of camptothecin at different time intervals after i.v. administration of camptothecin-loaded SLNs was measured and compared to the data obtained after administration of free camptothecin solution. Camptothecin demonstrated higher AUC and MRT (18-fold enhancement) and body distribution (especially in brain, heart, and reticuloendothelial cell–containing organs) when it was administered as camptothecin-loaded SLNs, compared to camptothecin solution. A higher concentration of camptothecin was also measured in the brain after administration of camptothecin-loaded SLNs.

The cytotoxic drug paclitaxel has been selected by some researchers to evaluate the potential of LNs. Long-circulating SLNs were made from bioacceptable and biodegradable lipids with two types of stealth agents: for example, F68 (particle size 220 ± 98 nm) and Brij78 (particle size 103.5 ± 29.2 nm), using the emulsion-formation and solvent-evaporation method. KM mice were injected with these SLNs. The results revealed marked differences in pharmacokinetic parameters, especially in $t_{1/2\beta}$ (elimination half-life) and AUC, in comparison with the data obtained after administration of the paclitaxel solution in Cremophor EL. This was attributed to the reduced clearance rate and, hence, to the reduced uptake of SLNs by RES [128].

The potential of paclitaxel-SLNs in the treatment of brain tumors was evaluated in vitro by Koziara et al. [213]. Paclitaxel SLNs were prepared by the microemulsion technique, showing a particle size lower than 100 nm, and were tested in vivo using an in situ rat brain perfusion model. They tested the cytotoxicity of paclitaxel entrapped in novel cetyl alcohol–polysorbate SLNs on the U-118 human glioblastoma cell line and in the HCT-15 human adenocarcinoma cell line. Their results indicate that the loading of paclitaxel into SLNs increases the drug uptake in the brain and its cytotoxicity toward P-gp expressing tumor cells.

Paclitaxel loaded in SLNs has been demonstrated to overcome the in vitro drug resistance in HCT-15 cells and in vivo HCT-15 mouse xenograft model when injected intratumorally. Paclitaxel SLNs were prepared using emulsifying wax and were tested in vivo in an HCT-15 mouse xenograft model. A significant increase in the cytotoxic activity efficacy was achieved in the endothelial cell differentiation assays for paclitaxel SLNs. The results of the in vivo assay showed a significant inhibition in the paclitaxel-loaded SLNs treated group from the Taxol treated group on day 19 [158]. The in vitro cytotoxicities against human ovarian and breast cancer cells of sterically stabilized SLNs with trimyristin and egg phosphotidylcholine and pegylated phospholipids as stabilizers were comparable to those of a commercially available cremophor EL-based paclitaxel formulation [84]. In another study, the cytotoxic activity of NLCs with paclitaxel and doxorubicin was tested against different cell lines. Doxorubicin or paclitaxel was taken up by human promyelocytic leukemia (HL60) and human breast carcinoma (MCF-7) cells when they were entrapped in SLNs, and more cytotoxicity was observed when they were formulated in the lipid nanocarriers [58]. Similar results have been reported with HT-29 colorectal cancer cells [17] and in P-gp overexpressing cells where the IC_{50} value of paclitaxel nanoparticles was over ninefold lower than that obtained with Taxol [150].

The potential of stealth and nonstealth SLNs to improve the biodistribution of entrapped drugs has been extensively investigated. In one study [45], nonstealth and stealth SLNs containing doxorubicin with an average particle size of 80 ± 5 nm (stealth) and 90 ± 5 nm (nonstealth) were prepared by the microemulsion technique. These particles were administered intravenously to rats. The results obtained were compared with the corresponding to the commercial solution of doxorubicin. There was a significant increase ($p < 0.001$) in $t_{1/2\beta}$, C_{max} (fivefold with nonstealth and sevenfold with stealth SLNs), and AUC values in stealth and nonstealth SLNs loaded with doxorubicin as compared to commercial doxorubicin solution. Significant amounts of doxorubicin were detectable in the brain of rats treated with SLNs. However, a lower concentration of doxorubicin was found in heart and in RES tissues, indicating lower cardiotoxicity compared to commercial doxorubicin solution, which is one of the effects limiting the usefulness of doxorubicin. In another study [46], the pharmacokinetics and tissue distribution of nonstealth and stealth SLNs with increasing concentration of stearic acid–PEG 2000 encapsulating doxorubicin (58−95.5 nm), formulated by the microemulsion technique, were studied in rabbits. Doxorubicin was detected in blood 6 h postinjection from both nonstealth and stealth SLNs, while no doxorubicin was detectable after i.v. injection of the doxorubicin solution. The AUC of doxorubicin increased as a function of the amount of stealth agent present in the SLNs.

Other anticancer agents that have been formulated as LNs are tamoxifen [70], etoposide [81], mitroxantone [96], vinorelbine bitartrate [214], gadolinium [215], idarubicin [71], 4′-*O*-tetrahydropyranyl adriamycin [216], 3′,5′-dioctanoyl-5-fluoro-2′-deoxyuridine [217], oridonin [218], temozolomide [219], and docetaxel [93, 220]. The local or systemic chemotherapeutic response of these drugs may be improved by incorporation of anticancer agents in different types of LNs. The mean survival time of mice bearing Dalton's lymphoma was

increased by 5–8 days after treatment with etoposide-loaded SLNs made of glycerol monostearate, glycerol distearate, and tripalmitin [81]. Mitoxantrone-loaded SLNs also showed better efficacy in the treatment of lymph node metastases. The treatment with SLNs gave a mean size of lymph node three times smaller than that of the mitoxantrone solution [96]. The antitumor activity of vinorelbine bitartrate was found to be enhanced significantly when it is entrapped in SLNs and in pegylated SLNs. The pegylation of SLNs makes a significant improvement in the uptake by cancer cells (MCF-7 and A549).

The administration of docetaxel loaded to PEG-SLNs improves the accumulation of the docetaxel in tumors in vivo. After i.v. administration to C57BL/6 mice with pre-established TC-1 tumors, the amount of docetaxel recovered from the tumors was 4.5-fold higher than that in mice injected with the free docetaxel [220]. Higher amounts of folate-coated SLNs of gadolinium were retained in the tumor tissue in comparison to PEG-coated SLNs [215]. The study of tissue distribution and transport across the BBB of drug-free stealth and nonstealth SLNs labeled using a radioactive marker, prepared by the microemulsion technique, was evaluated in rats after i.v. injection. The average size of these SLNs was below 100 nm. The results again confirmed localization of SLNs in the brain and in the CSF.

The second generation of LNs, NLCs, and polymer-LNs has not been extensively studied for the controlled release of anticancer agents. 9-nitrocamptothecin was mainly found in the lung, liver, pancreas, ovaries, and uterus after the in vivo administration of 9-nitrocamptothecin NLCs. The AUC of 9-nitrocamptothecin-loaded NLCs was higher than that of the solution [221]. In another study, two synthetic derivatives of antitumor drug temozolomide were encapsulated into NLCs. An enhancement of the cytotoxic effects of citotoxic compounds on human prostate cancer (PC-3) and human hepatocellular carcinoma (HuH-6, HuH-7) cell lines with respect to free drug was observed [222].

6.2. Infectious Diseases

LNs have been of great interest in the area of anti-infectious drugs, mainly owing to their versatile nature and attractive advantages. Considering the nature of infections, ideally the strategy developed for delivering controlled release formulations of anti-infectious drugs is expected to possess the following properties:

1. It should allow oral administration.
2. It should allow low toxicity and immunogenicity, and protect the drug from extracellular degradation.
3. It should shorten the duration of the treatment by improving pharmacokinetic or pharmacodynamic profile of the anti-infectious agent.
4. It should be versatile enough to allow delivery of combination of anti-infectious agents, which is a normal practice in the current situation
5. It should have the ability to selectively transport the anti-infectious agent to the infective agent to render maximum efficacy and minimum adverse effects.

The potential and applications of the loading of anti-infectious agents in LNs have been studied in the last years. The potential of SLNs in the treatment of tuberculosis has been evaluated in an experimental tuberculosis model. Mycobacterium is an intracellularly residing microorganism which is not easy to treat. Antitubercular combination therapy, though effective in complete eradication, suffers from numerous disadvantages from the patient's perspective. The major limiting factor is daily dosing of antitubercular drugs which must be continued for a very long period of time. Following a single oral administration to mice of pyrazinamide, rifampicin, and isoniazid incorporated in SLNs, therapeutic drug concentrations were maintained in plasma for 8 days and in organs (lungs, liver, and spleen) for 10 days, whereas free drugs were cleared in 1–2 days. Furthermore, no tubercular bacilli were detected in the lungs–spleen after five oral doses of drug-loaded SLNs administered at every 10th day in *Mycobacterium tuberculosis* H37Rv–infected mice, whereas 46 daily oral doses of unencapsulated drugs were required to obtain an equivalent therapeutic benefit [141].

SLNs have also been explored as antiparasitic drug carriers. β-Artemether, a potent and rapidly acting antimalarial agent listed as one of the essential drugs for the treatment of severe multiresistant malaria by the World Health Organization (WHO), has been loaded in NLCs in order to hasten its uptake and prolong its release [162]. Enhanced uptake in brain tissue of transferrin-conjugated SLNs of quinine dihydrochloride was observed in fluorescence studies after i.v. administration of these SLNs. This study confirmed again the utility of SLNs for the management of cerebral malaria [68]. LDCs are another type of LN which have been studied for the delivery of antiparasitic agents. The hydrophilic antitrypanosomal drug diminazene was conjugated with stearic acid and oleic acid and incubated with human serum in order to incorporate apolipoprotein E. This is a key lipoprotein responsible for the delivery of nanoparticles to the brain, where the parasites *Trypanosoma brucei*, *Trypanosoma brucei gambiense*. and *Trypanosoma brucei rhodiense* reside [223].

Examples with other anti-infectious agents such as antivirals or immune stimulants formulated in LNs have been described in the literature, even though their in vitro or in vivo application has not been completely evaluated. Saquinavir-entrapping cationic SLNs composed of nonionic Compritol® ATO 888 and cacao butter in the center of the lipid core and cationic SA and dioctadecyldimethyl ammonium bromide in the periphery of the lipid core should be applied to the study of transport behavior across the BBB [75]. Recently, IFN-α-loaded SLNs have been proposed as a useful formulation for controlled release in the treatment of hepatitis B and C, and infectious diseases in patients with leukemia, multiple myeloma, and some other carcinomas. SLNs preserved the bioactivity of yak IFN-α after encapsulation and release processes and at the same time provided a controlled release of IFN-α. Additionally, the formulation had no toxicity to cell lines [73].

6.3. Skin Diseases

Topical administration has some advantages compared to oral or parenteral drug administration. High drug levels can be achieved at the site of the disease, and systemic side

effects can be reduced. NLCs and SLNs have many features that are advantageous for topical application. Over the last decade, the dermal application of NLCs and SLNs has been studied intensively, in both pharmaceutical and cosmetic uses.

LNs have been investigated to improve the treatment of inflammatory skin diseases such as atopic eczema and psoriasis with glucocorticoids and T-cell inhibitors. An improved extent of prednicarbate uptake by human skin in vitro was observed when an SLNs dispersion or cream containing prednicarbate-loaded SLNs was topically administered [224]. A clinical study on clobetasol propionate–loaded SLNs in patients with eczema has demonstrated the expected improved efficacy of pertinent glucocorticoid treatment over the conventional cream [225].

The loading of retinoids and antiandrogenic agents in SLNs is an adequate drug-delivery system to improve topical antiacne therapy. Retinol incorporated into Compritol®-based SLNs has been found to be released more rapidly and to a greater extent as compared to conventional vehicles after topical administration. This effect appears to result from a burst release from the solid particles following water evaporation on the skin surface [177]. The application of cyproterone acetate–loaded SLNs increased the skin penetration at least fourfold over the data obtained after the application of a cream and an emulsion of free drug, whereas the drug amount found in the dermis was low for all preparations. Moreover, the topical administration of cyproterone acetate entrapped on SLNs avoided the systemic side effects (loss of libido, gynecomastia, and vasomotor flushing) observed after the oral administration of the drug [110]. The penetration through the skin surface and the permeation between skin layers of isotretinoin was investigated after its entrapment in SLNs and compared with the observed penetration after topical administration of an isotretinoin ethanolic solution. No penetration through rat skin was found for isotretinoin-loaded SLNs, avoiding the side effects observed after the systemic uptake of the drug. Moreover, a high accumulative amount of isotretinoin was found in the skin for the isotretinoin-loaded SLN treatment, showing a skin targeting effect [226].

Unloaded and loaded SLNs have already been investigated in the search for a possible use in the application of UV absorbers. Cetyl palmitate nanodispersions act both as particulate UV blockers themselves and as carriers for UV-absorbing agents such as 2-hydroxy-4-methoxy benzophenone. This results in a 3-fold increase in UV protection which allows a reduction of the concentration of the UV absorber [32]. Recently, similar effects have been described when testing 3,4,5-trimethoxybenzoylchitin-loaded SLNs [227].

NLC-based delivery systems have been evaluated for the topical application of the nonsteroidal anti-inflammatory drugs celecoxib and valecoxib. The pharmacodynamic efficiency of an NLC-based gel of celecoxib with a micellar gel with the same composition in an Aerosil-induced rat paw edema has been recently studied. The in vivo comparison of the percentage of edema inhibition produced by NLCs and the micellar gel showed significantly greater inhibition after application of the NLC-based gel than that observed after the application of the micellar gel [228]. Valdecoxib-loaded NLCs incorporated into Carbopol® showed better skin tolerability and longer activity than the marketed formulation [229]. In another comparative study, the anti-inflammatory effect following the topical application of indomethacin, measured in UV-B induced erythrema model animals, was more prolonged for indomethacin-loaded NLCs treatment than for the free indomethacin gel [230]. The same effect was observed in a similar study with etoprofen-, flurbiprofen-, and naproxen-loaded NLCs incorporated into a gel [231, 232]. In all the cases, NLCs were able to reduce the drug penetration through excised human skin, while the drug permeation and drug accumulation in the horny layer increased.

SLNs and NLCs have been developed for topical delivery of antifungals such as clotrimazole and ketoconazol [233]. Nevertheless, further investigations regarding the skin permeation, skin penetration, and reduction of adverse effects need to be carried out.

One of the major disadvantages associated with the topical application is local skin irritation. Topical administration of SLN-based formulations resulted in marked fewer erythemic episodes compared to the currently marketed cream. Tretinoin, a metabolite of vitamin A, is used for topical treatment of various proliferateive and inflammatory skin diseases such as psoriasis, acne, photoaging, epidermotropic T-cell lymphomas, and epithelial skin cancer. After topical administration of a tretinoin-free cream, moderate side effects may be observed, such as erythema, peeling and burning, as well as increased sensitivity to sunlight. To overcome these problems tretinoin was incorporated into SLNs with a better benefit–risk ratio [234].

6.4. Gene Therapy

Lipid-based colloidal particles have been extensively studied as systemic gene-delivery carriers. Cationic liposomes have been classified among the more efficient synthetic gene delivery agents in vitro. The utilization of lipid-based systems for DNA transfection has also been documented in the literature. These systems have been used extensively to deliver therapeutic genes in animal models. Although there are many publications about cationic liposomes and cationic lipid emulsions for gene therapy, only few reports about the use of SLNs for gene delivery have appeared.

Olbrich et al. [156] were the first authors to report that cationic SLNs could efficiently bind and transfect plasmid DNA. Cationic SLNs have proven to be efficacious in transfecting African green monkey kidney fibroblast-like cells (COS-1) [88] and human bronchoepithelial cells (16HBE14o-) [170]. The DNA-binding efficacy and transfection were found to be comparable to that obtained with liposomes.

The transfection efficiency of SLNs has also been investigated by Mumper and coworkers [235]. Emulsifying wax-based nanoparticles stabilized by cationic detergent cetyltrimethylammonium bromide were prepared by the microemulsion technique, and coated with plasmid DNA and a ligand to target dendritic cells (mannan) on the surface. SLNs resulted in 300% increase in cytokine

production in vitro and 16-fold higher IgG titre and T-helper cells in comparison with the naked DNA after subcutaneous injection to mice [235]. In another study, two types of cationic surfactants, viz. DOTAP and DDAB, were used to complex the plasmid DNA and encapsulated in the SLNs prepared from emulsifying wax using the microemulsion technique and coated with pullulan, a hepatocyte targeting ligand. The in vivo studies carried out in mice demonstrated 40% transfection efficiency in the case of SLNs, which was significantly higher than that obtained with DNA (16%) [236].

Another formulation of cationic SLNs for gene delivery, composed by tricaprin as a core, 3b[*N*-(*N*0, *N*0-dimethylaminoethane) carbamoyl] cholesterol, dioleoylphosphatidylethanolamine, and Tween® 80 in various ratios and produced by a slight modification of the melt homogenization method, has been evaluated as nonviral vector-mediated p53 gene delivery in lung cancer. The developed SLNs show higher transfection efficiency in human lung cancer cells compared with commercially available Lipofectin reagent. The higher transfection efficiency of plasmid DNA has been attributed by the authors to the enhanced stability of the plasmid DNA–SLN complexes [237].

Recently, stable SLN–DNA complexes prepared with a new single-tailed cationic lipid, 6-lauroxyhexyl lysinate, showed higher gene transfection efficiency than the naked DNA, and equal transfection efficiency to that of lipofectamine–DNA complexes, with lower cytotoxicity. The novel cationic SLNs might overcome some drawbacks of the conventional cationic nanocarriers in vivo and may become a promising nonviral gene therapy vector [238].

6.5. Imaging Agents

Lipid-based nanocarriers have been found to be successful in the delivery of mainly chemotherapeutic agents. The development of image-guided drug nanocarriers containing therapeutic and imaging agents may certainly be of importance, since they should allow the development of an online monitoring of tumor location and intratumor distribution, and achieve tumor targeting levels with a determined drug release kinetics during chemotherapeutic treatment. Molecular imaging by use of nanoparticles has been explored on a wide range of different nanoparticle formulations. However, the experience with solid lipid nanoparticulate formulations or NLCs is limited.

Magnetite was the first imaging agent which was incorporated in LNs [204]. The magnetite-loaded SLNs were found to be less cytotoxic than magnetite-loaded PLGA particles after i.v. formulation for magnetic resonance imaging and as potential carrier for drug targeting.

In another study, iron oxide–loaded SLNs demonstrated similar relaxometric properties to those of contrast medium Endorem® on magnetic resonance imaging of the central nervous system. Endorem® is a colloid of superparamagnetic iron oxide associated with dextran for i.v. administration usually used in magnetic resonance imaging. Superparamagnetic SLNs have also shown slower blood clearance than Endorem® [239]. ^{125}I or luminescent lipophilic CdSe–ZnS core–shell quantum dots (QDs) were also encapsulated into SLNs and intravenously injected. It was found that they remained in the blood for higher time in comparison to many colloidal carriers [240]. The fluorescence properties of QDs were retained even after encapsulation. The fluorescence signal and the signal to background ratio were also found to be enhanced.

6.6. Other Applications

6.6.1. Vaccination

Recently, many polymeric nanoparticulate carrier systems have been studied for their adjuvant properties, with antigens entrapped within the polymer matrix or adsorbed on their surface [241–243]. However, the main problems associated with polymers such as polylactic acid (PLA) or PLGA are the costs and the potentially toxic organic solvents employed for particle production [244]. SLNs have arisen as an alternative to these systems. Besides, optimizing the conditions of the production steps, it is possible to incorporate both lipophilic or hydrophilic proteins and thermolabile antigenic molecules [134]. Olbrich et al. [245] have demonstrated that biodegradable glycerides–based SLNs containing *Mycoplasma bovis* antigen and immunoglobulin G (IgG) would be a promising alternative to Freud's complete adjuvant. Researchers showed that particles greater than 100 nm exhibited higher adjuvant activity as compared to the particles lower than 100 nm in the first study, which showed that the adjuvant activity of SLNs is dependent on their particle size.

In another study by Mumper and Cui [246, 247], anionic LNs were employed to coat a catonized model protein antigen. It was found that the LNs enhanced both T-helper type 1 and type 2 immune responses. These authors have also studied the effect of coadministration of adjuvants with LN-based genetic vaccine delivery system on the immune response. Significant enhancement was observed in immunization over naked plasmid DNA, e.g., 300-fold for cholera toxin (100 lg) and 250-fold for lipid A (50 lg) by subcutaneous route.

6.6.2. Rheumatoid Arthritis

Treatment options for arthritis vary depending on the type of arthritis and include physical therapy, lifestyle changes (including exercise and weight control), orthopedic bracing, dietary supplements, and medications. Actarit is a drug employed for the treatment of rheumatoid arthritis. SLNs were prepared to reduce the potential acute and chronic toxicity that this molecule presents after its oral administration, such as gastrointestinal disorders [248]. Upon i.v. injection, an in vivo study with New Zealand rabbits revealed a threefold increase in targeting efficiency, 1.88 times higher AUC, and an MRT around 10 times higher with actarit-loaded SLNs as compared to that of the actarit solution.

6.6.3. Cardiovascular Diseases

Tashinone IIA is a natural lipophilic drug that presents the ability to dilate coronary arteries and increase myocardial contractility. In order to improve the delivery of

this cardiovascular drug, Liu and coworkers studied the possibility of entrapping it in SLNs [249, 250]. In an in vitro study, poloxamer 188-coated SLNs were prepared, and the macrophage uptake of these SLNs was studied in comparison to SLNs without surfactant. The poloxamer 188-coated SLNs showed significantly lower macrophage uptake as compared to SLNs without poloxamer coating [249]. As we have previously mentioned, different coatings are used to escape from the RES. The RES evading ability of these poloxamer-coated SLNs was evaluated by carrying out pharmacokinetic studies in rabbits. The pharmacokinetic studies [250] revealed that the AUC and the MRT of the poloxamer-coated tashinone SLNs were 3.3 and 3.9 times higher than those of tashinone IIA control solution, respectively.

In another study with the antihypertensive nitrendipine, the pharmacokinetics of SLNs loaded with this drug, a calcium channel blocker used in the treatment of hypertension, were studied in male Wistar rats after i.v. and intraduodenal injection [160]. Effective bioavailability of nitrendipine-loaded SLNs was from around 3- to almost 5.5-fold greater after intraduodenal administration.

6.6.4. Antiviral Treatment

SLNs have attracted increasing interest in the treatment of many viral agents, such as HIV [76, 251], Herpesvirus [252], or hepatitis B virus (HBV) [253].

The latest statistics on the world epidemic of HIV and acquired immunodeficiency syndrome (AIDS) were published by the United Nations Joint Programme on HIV/AIDS and the WHO in July 2008, and refer to the end of 2007. More than 33 million people were estimated to be living with HIV–AIDS in 2007 [254]. SLNs can also be used in this context. Some research studies have shown that SLNs were effective carriers of stavudine, delavirdine, and saquinavir to improve BBB permeability by threefold to 16-fold, indicating the clinical potential of SLN formulations for the treatment of AIDS, because it has been stated that for the therapy of the AIDS, drug transport across the BBB is an essential issue as HIV can migrate to and multiply in CNS, yielding several neurological disorders. Furthermore, HIV can accumulate in the brain, as suggested by the high amount of unintegrated HIV-1 DNA in brain tissue of the AIDS patients [76, 255].

The antiherpetic activity of *Artemisia arborescens* essential oil has been investigated by Lai et al. [252]. The antiviral activity of free and SLN-loaded essential oil was tested in vitro against herpes simplex virus-1 by MTT. In vitro skin permeation experiments demonstrated the ability of SLNs to greatly improve the accumulation of the oil into the skin, whereas oil accumulation was reduced when the oil was delivered from the control solution.

Chronic HBV infection is a major global public health problem. In order to treat this disease, Zhang et al. [253] studied the in vitro activity of adefovir dipivoxil (ADV) loaded in SLNs, which was found to enhance the inhibitory effect not only on HBV DNA replication but also on HBV antigen expression.

7. CONCLUSIONS

LNs have been demonstrated to offer many advantages for the delivery of drugs through every route of administration. They have emerged as effective alternatives to other drug delivery systems such as liposomes or polymeric nanoparticles, not only because of the relative ease with which they can be scaled up but also because they present a better stability profile. After this overview of the LN-based drug delivery vehicles, it is apparent that these systems have been found not only to improve the efficacy of the drugs, but also to reduce their toxicity, achieving better pharmacokinetics and drug biodistribution profiles when the drug is incorporated in them.

ACKNOWLEDGMENTS

We gratefully acknowledge the support from the Spanish Ministry of Science and Innovation (SAF2007-61261, PCT-090100-2007-27) and Caja Navarra Foundation. Ander Estella-Hermoso de Mendoza is supported by the research grant from the Department of Education of the Basque Government (BFI06.37).

REFERENCES

1. O. Lehmann, "Carl Winters Universitätsbuchhandlung Heidelberg," 1912.
2. A. D. Bangham and D. A. Haydon, *Br. Med. Bull.* 24, 124–126 (1968).
3. A. D. Bangham, *Chem. Phys. Lipids* 64, 275–285 (1993).
4. D. D. Lasic, *Nature* 380, 561–562 (1996).
5. P. S. Gill, B. M. Espina, F. Muggia, S. Cabriales, A. Tulpule, J. A. Esplin, H. A. Liebman, E. Forssen, M. E. Ross, and A. M. Levine, *J. Clin. Oncol.* 13, 996–1003 (1995).
6. H. Bunjes and B. Siekmann, in "Nanoparticulate Drug Delivery Systems" (M. Deleers, Y. Pathak, and D. Thassu, Eds.), Informa Healthcare, , pp. 213–268, 2007.
7. S. A. Wissing, O. Kayser, and R. H. Muller, *Adv. Drug Deliv. Rev.* 56, 1257–1272 (2004).
8. R. H. Muller, K. Mader, and S. Gohla, *Eur. J. Pharm. Biopharm.* 50, 161–177 (2000).
9. P. Speiser, European Patent Application, EP 0,167,825, 1986.
10. R. H. Muller and C. M. Keck, *J. Biotechnol.* 113, 151–170 (2004).
11. T. Helgason, T. S. Awad, K. Kristbergsson, D. J. McClements, and J. Weiss, *J. Coll. Interf. Sci.* 334, 75–81 (2009).
12. Y. Yang, J. F. Feng, H. Zhang, and J. Y. Luo, *Zhongguo Zhong Yao Za Zhi* 31, 650–653 (2006).
13. R. Sivaramakrishnan, C. Nakamura, W. Mehnert, H. C. Korting, K. D. Kramer, and M. Schafer-Korting, *J. Cont. Rel.* 97, 493–502 (2004).
14. M. A. Videira, M. F. Botelho, A. C. Santos, L. F. Gouveia, J. J. de Lima, and A. J. Almeida, *J. Drug Target.* 10, 607–613 (2002).
15. Y. Wang and W. Wu, *Drug Deliv.* 13, 189–192 (2006).
16. A. Bargoni, R. Cavalli, O. Caputo, A. Fundaro, M. R. Gasco, and G. P. Zara, *Pharm. Res.* 15, 745–750 (1998).
17. A. Miglietta, R. Cavalli, C. Bocca, L. Gabriel, and M. R. Gasco, *Int. J. Pharm.* 210, 61–67 (2000).
18. L. Bonnaire, S. Sandra, T. Helgason, E. A. Decker, J. Weiss, and D. J. McClements, *J. Agric. Food Chem.* 56, 3791–3797 (2008).

19. K. Ruckmani, M. Sivakumar, and P. A. Ganeshkumar, *J. Nanosci. Nanotechnol.* 6, 2991–2995 (2006).
20. R. H. Müller and J. S. Lucks, European Patent Application, EP 0605497, 1996.
21. M. R. Gasco, U.S. Patent Application, US 5,250,236, 1993.
22. J. Y. Fang, C. L. Fang, C. H. Liu, and Y. H. Su, *Eur. J. Pharm. Biopharm.* 70, 633–640 (2008).
23. W. Mehnert and K. Mader, *Adv. Drug Deliv. Rev.* 47, 165–196 (2001).
24. S. S. Shidhaye, R. Vaidya, S. Sutar, A. Patwardhan, and V. J. Kadam, *Curr. Drug Deliv.* 5, 324–331 (2008).
25. H. Bunjes, F. Steiniger, and W. Richter, *Langmuir* 23, 4005–4011 (2007).
26. A. Estella-Hermoso de Mendoza, M. Rayo, F. Mollinedo, and M. J. Blanco-Prieto, *Eur. J. Pharm. Biopharm.* 68, 207–213 (2008).
27. E. B. Souto, W. Mehnert, and R. H. Muller, *J. Microencapsul.* 23, 417–433 (2006).
28. K. Manjunath, J. S. Reddy, and V. Venkateswarlu, *Meth. Find. Exp. Clin. Pharmacol.* 27, 127–144 (2005).
29. A. zur Muhlen, C. Schwarz, and W. Mehnert, *Eur. J. Pharm. Biopharm.* 45, 149–155 (1998).
30. M. Muchow, P. Maincent, and R. H. Muller, *Drug Dev. Ind. Pharm.* 34, 1394–1405 (2008).
31. R. H. Muller, M. Radtke, and S. A. Wissing, *Int. J. Pharm.* 242, 121–128 (2002).
32. R. H. Muller, M. Radtke, and S. A. Wissing, *Adv. Drug Deliv. Rev.* 54 Suppl 1, 131–155 (2002).
33. Z. R. Huang, S. C. Hua, Y. L. Yang, and J. Y. Fang, *Acta Pharmacol. Sin.* 29, 1094–1102 (2008).
34. V. Jenning, K. Mader, and S. H. Gohla, *Int. J. Pharm.* 205, 15–21 (2000).
35. V. Jenning, A. F. Thunemann, and S. H. Gohla, *Int. J. Pharm.* 199, 167–177 (2000).
36. K. K. Sawant and S. S. Dodiya, *Recent Pat. Drug Deliv. Formul.* 2, 120–135 (2008).
37. K. Mader, in "Nanoparticulates as Drug Carriers" (V. P. Torchilin), Imperial College Press, 2006.
38. V. Jannin, J. Musakhanian, and D. Marchaud, *Adv. Drug Deliv. Rev.* 60, 734–746 (2008).
39. Y. Chen, G. Dalwadi, and H. A. Benson, *Curr. Drug Deliv.* 1, 361–376 (2004).
40. I. P. Kaur, R. Bhandari, S. Bhandari, and V. Kakkar, *J. Cont. Rel.* 127, 97–109 (2008).
41. P. R. Lockman, J. M. Koziara, R. J. Mumper, and D. D. Allen, *J. Drug Target.* 12, 635–641 (2004).
42. R. H. Muller and C. M. Keck, *J. Nanosci. Nanotechnol.* 4, 471–483 (2004).
43. C. Olbrich and R. H. Muller, *Int. J. Pharm.* 180, 31–39 (1999).
44. R. Cavalli, O. Caputo, and M. R. Gasco, *Eur. J. Pharm. Sci.* 10, 305–309 (2000).
45. A. Fundaro, R. Cavalli, A. Bargoni, D. Vighetto, G. P. Zara, and M. R. Gasco, *Pharmacol. Res.* 42, 337–343 (2000).
46. G. P. Zara, R. Cavalli, A. Bargoni, A. Fundaro, D. Vighetto, and M. R. Gasco, *J. Drug Target.* 10, 327–335 (2002).
47. H. Maeda, J. Wu, T. Sawa, Y. Matsumura, and K. Hori, *J. Cont. Rel.* 65, 271–284 (2000).
48. S. K. Jain, A. Chaurasiya, Y. Gupta, A. Jain, P. Dagur, B. Joshi, and V. M. Katoch, *J. Microencapsul.* 25, 289–297 (2008).
49. C. L. Denholt, P. R. Hansen, N. Pedersen, H. S. Poulsen, N. Gillings, and A. Kjaer, *Biopolymers* 91, 201–206 (2009).
50. D. B. Cornelio, L. Meurer, R. Roesler, and G. Schwartsmann, *Oncology* 73, 340–345 (2007).
51. K. Zhang, M. R. Aruva, N. Shanthly, C. A. Cardi, C. A. Patel, S. Rattan, G. Cesarone, E. Wickstrom, and M. L. Thakur, *Regul. Pept.* 144, 91–100 (2007).
52. M. G. Caruso, C. Messa, A. Orlando, B. D'Attoma, and M. Notarnicola, *Fitoterapia* 79, 524–528 (2008).
53. C. Peterson, S. Vitols, M. Rudling, H. Blomgren, F. Edsmyr, and L. Skoog, *Med. Oncol. Tumor Pharmacother.* 2, 143–147 (1985).
54. S. Markert, S. Lassmann, B. Gabriel, M. Klar, M. Werner, G. Gitsch, F. Kratz, and A. Hasenburg, *Anticancer Res.* 28, 3567–3572 (2008).
55. C. O. Evans, C. Yao, D. Laborde, and N. M. Oyesiku, *Vitam. Horm.* 79, 235–266 (2008).
56. Y. Lu, E. Sega, and P. S. Low, *Int. J. Cancer* 116, 710–719 (2005).
57. H. Yuan, J. Miao, Y. Z. Du, J. You, F. Q. Hu, and S. Zeng, *Int. J. Pharm.* 348, 137–145 (2008).
58. X. G. Zhang, J. Miao, Y. Q. Dai, Y. Z. Du, H. Yuan, and F. Q. Hu, *Int. J. Pharm.* 361, 239–244 (2008).
59. S. M. Stephenson, P. S. Low, and R. J. Lee, *Methods Enzymol.* 387, 33–50 (2004).
60. P. J. Stevens, M. Sekido, and R. J. Lee, *Pharm. Res.* 21, 2153–2157 (2004).
61. M. N. Khalid, P. Simard, D. Hoarau, A. Dragomir, and J. C. Leroux, *Pharm. Res.* 23, 752–758 (2006).
62. R. Abou-Jawde, T. Choueiri, C. Alemany, and T. Mekhail, *Clin. Ther.* 25, 2121–2137 (2003).
63. B. Stella, S. Arpicco, M. T. Peracchia, D. Desmaele, J. Hoebeke, M. Renoir, J. D'Angelo, L. Cattel, and P. Couvreur, *J. Pharm. Sci.* 89, 1452–1464 (2000).
64. Z. Liu, Z. Zhong, G. Peng, S. Wang, X. Du, D. Yan, Z. Zhang, Q. He, and J. Liu, *Drug Deliv.* 16, 341–347 (2009).
65. R. R. Patlolla and V. Vobalaboina, *J. Drug Target.* 16, 269–275 (2008).
66. P. J. Stevens, M. Sekido, and R. J. Lee, *Anticancer Res.* 24, 161–165 (2004).
67. A. Beduneau, P. Saulnier, F. Hindre, A. Clavreul, J. C. Leroux, and J. P. Benoit, *Biomaterials* 28, 4978–4990 (2007).
68. Y. Gupta, A. Jain, and S. K. Jain, *J. Pharm. Pharmacol.* 59, 935–940 (2007).
69. L. Serpe, M. G. Catalano, R. Cavalli, E. Ugazio, O. Bosco, R. Canaparo, E. Muntoni, et al., *Eur. J. Pharm. Biopharm.* 58, 673–680 (2004).
70. G. Fontana, L. Maniscalco, D. Schillaci, G. Cavallaro, and G. Giammona, *Drug Deliv.* 12, 385–392 (2005).
71. G. P. Zara, A. Bargoni, R. Cavalli, A. Fundaro, D. Vighetto, and M. R. Gasco, *J. Pharm. Sci.* 91, 1324–1333 (2002).
72. L. Serpe, M. Guido, R. Canaparo, E. Muntoni, R. Cavalli, P. Panzanelli, C. Della Pepal, et al., *J. Nanosci. Nanotechnol.* 6, 3062–3069 (2006).
73. S. Li, B. Zhao, F. Wang, M. Wang, S. Xie, S. Wang, C. Han, L. Zhu, and W. Zhou, *Res. Vet. Sci.* (in press).
74. S. Trombino, R. Cassano, R. Muzzalupo, A. Pingitore, E. Cione, and N. Picci, *Coll. Surf. B: Biointerfaces* 72, 181–187 (2009).
75. Y. C. Kuo and H. H. Chen, *Int. J. Pharm.* 365, 206–213 (2009).
76. Y. C. Kuo and F. L. Su, *Int. J. Pharm.* 340, 143–152 (2007).
77. S. J. Lim and C. K. Kim, *Int. J. Pharm.* 243, 135–146 (2002).
78. S. C. Yang, L. F. Lu, Y. Cai, J. B. Zhu, B. W. Liang, and C. Z. Yang, *J. Cont. Rel.* 59, 299–307 (1999).
79. A. A. Attama, S. Reichl, and C. C. Muller-Goymann, *Int. J. Pharm.* 355, 307–313 (2008).
80. L. H. Reddy, J. S. Adhikari, B. S. Dwarakanath, R. K. Sharma, and R. R. Murthy, *AAPS J.* 8, 254–262 (2006).
81. L. H. Reddy, R. K. Sharma, K. Chuttani, A. K. Mishra, and R. R. Murthy, *AAPS J.* 6, article 23 (2004).
82. A. Hanafy, H. Spahn-Langguth, G. Vergnault, P. Grenier, M. Tubic Grozdanis, T. Lenhardt, and P. Langguth, *Adv. Drug Deliv. Rev.* 59, 419–426 (2007).
83. K. Bhaskar, J. Anbu, V. Ravichandiran, V. Venkateswarlu, and Y. M. Rao, *Lipids Health Dis.* (in press).
84. M. K. Lee, S. J. Lim, and C. K. Kim, *Biomaterials* 28, 2137–2146 (2007).

85. S. Kuchler, M. R. Radowski, T. Blaschke, M. Dathe, J. Plendl, R. Haag, M. Schafer-Korting, and K. D. Kramer, *Eur. J. Pharm. Biopharm.* 71, 243–250 (2009).
86. J. You, F. Wan, F. de Cui, Y. Sun, Y. Z. Du, and F. Q. Hu, *Int. J. Pharm.* 343, 270–276 (2007).
87. Y. Hattori and Y. Maitani, *Curr. Drug Deliv.* 2, 243–252 (2005).
88. K. Tabatt, C. Kneuer, M. Sameti, C. Olbrich, R. H. Muller, C. M. Lehr, and U. Bakowsky, *J. Cont. Rel.* 97, 321–332 (2004).
89. K. Tabatt, M. Sameti, C. Olbrich, R. H. Muller, and C. M. Lehr, *Eur. J. Pharm. Biopharm.* 57, 155–162 (2004).
90. G. A. Castro, A. L. Coelho, C. A. Oliveira, G. A. Mahecha, R. L. Orefice, and L. A. Ferreira, *Int. J. Pharm.* (in press).
91. Y. Wang, Y. Deng, S. Mao, S. Jin, J. Wang, and D. Bi, *Drug Dev. Ind. Pharm.* 31, 769–778 (2005).
92. P. Sharma, S. Ganta, W. A. Denny, and S. Garg, *Int. J. Pharm.* 367, 187–194 (2008).
93. Z. Xu, L. Chen, W. Gu, Y. Gao, L. Lin, Z. Zhang, Y. Xi, and Y. Li, *Biomaterials* 30, 226–232 (2009).
94. K. Bhaskar, C. Krishna Mohan, M. Lingam, S. Jagan Mohan, V. Venkateswarlu, Y. Madhusudan Rao, J. Anbu, and V. Ravichandran, *Drug Dev. Ind. Pharm.* 35, 98–113 (2009).
95. J. W. Vanderhoff, M. S. El-Aaser, and J. Ugelstad, US Patent Application, US 4 177 177, 1979.
96. B. Lu, S. B. Xiong, H. Yang, X. D. Yin, and R. B. Chao, *Eur. J. Pharm. Sci.* 28, 86–95 (2006).
97. A. Del Pozo-Rodriguez, M. A. Solinis, A. R. Gascon, and J. L. Pedraz, *Eur. J. Pharm. Biopharm.* 71, 181–189 (2008).
98. M. Trotta, F. Debernardi, and O. Caputo, *Int. J. Pharm.* 257, 153–160 (2003).
99. R. Paliwal, S. Rai, B. Vaidya, K. Khatri, A. K. Goyal, N. Mishra, A. Mehta, and S. P. Vyas, *Nanomed.: Nanotechnol. Biol. Med.* 5, 184–191 (2008).
100. J. Ye, Q. Wang, X. Zhou, and N. Zhang, *Int. J. Pharm.* 352, 273–279 (2008).
101. H. Fessi, F. Puisieux, J. P. Devissaguet, N. Ammoury, and S. Benita, *Int. J. Pharm.* 55, R1–R4 (1989).
102. J. Tian, X. Pang, K. Yu, L. Liu, and J. Zhou, *Pharmazie* 63, 593–597 (2008).
103. R. Cortesi, E. Esposito, G. Luca, and C. Nastruzzi, *Biomaterials* 23, 2283–2294 (2002).
104. M. Uner, *Pharmazie* 61, 375–386 (2006).
105. Q. Lv, A. Yu, Y. Xi, H. Li, Z. Song, J. Cui, F. Cao, and G. Zhai, *Int. J. Pharm.* 372, 191–198 (2009).
106. W. N. Charman and V. J. Stella, "Lymphatic Transport of Drugs," Boca Raton, FL: CRC Press, 1992.
107. E. Zimmermann, R. H. Muller, and K. Mader, *Int. J. Pharm.* 196, 211–213 (2000).
108. J. Kreuter, *Int. J. Pharm.* 14, 43–58 (1983).
109. P. Ahlin, J. Kristl, A. Kristl, and F. Vrecer, *Int. J. Pharm.* 239, 113–120 (2002).
110. J. Stecova, W. Mehnert, T. Blaschke, B. Kleuser, R. Sivaramakrishnan, C. C. Zouboulis, H. Seltmann, H. C. Korting, K. D. Kramer, and M. Schafer-Korting, *Pharm. Res.* 24, 991–1000 (2007).
111. J. Zhang, Y. Fan, and E. Smith, *J. Pharm. Sci.* 98, 1813–1819 (2008).
112. N. Anton, J. P. Benoit, and P. Saulnier, *J. Cont. Rel.* 128, 185–199 (2008).
113. M. Nidhin, R. Indumathy, K. J. Sreeram, and B. U. Nair, *Bull. Mater. Sci.* 31, 93–96 (2008).
114. A. Dubes, H. Parrot-Lopez, W. Abdelwahed, G. Degobert, H. Fessi, P. Shahgaldian, and A. W. Coleman, *Eur. J. Pharm. Biopharm.* 55, 279–282 (2003).
115. N. Gadegaard, *Biotech. Histochem.* 81, 87–97 (2006).
116. P. Shahgaldian, L. Quattrocchi, J. Gualbert, A. W. Coleman, and P. Goreloff, *Eur. J. Pharm. Biopharm.* 55, 107–113 (2003).
117. C. Freitas and R. H. Muller, *Int. J. Pharm.* 168, 221–229 (1998).
118. H. Bunjes and M. H. Koch, *J. Cont. Rel.* 107, 229–243 (2005).
119. H. Bunjes, M. H. Koch, and K. Westesen, *Prog. Coll. Polym. Sci.* 121, 7–10 (2002).
120. H. Bunjes, M. H. Koch, and K. Westesen, *J. Pharm. Sci.* 92, 1509–1520 (2003).
121. T. Kramer, D. M. Kremer, M. J. Pikal, W. J. Petre, E. Y. Shalaev, and L. A. Gatlin, *J. Pharm. Sci.* 98, 307–318 (2009).
122. P. Yadava, M. Gibbs, C. Castro, and J. A. Hughes, *AAPS Pharm. Sci. Tech.* 9, 335–341 (2008).
123. Y. Bensouda and A. Laatiris, *Drug Dev. Ind. Pharm.* 32, 941–945 (2006).
124. R. Seetharam, Y. Wada, S. Ramachandran, H. Hess, and P. Satir, *Lab. Chip.* 6, 1239–1242 (2006).
125. C. Schwarz and W. Mehnert, *Int. J. Pharm.* 157, 171–179 (1997).
126. E. Marengo, R. Cavalli, G. Rovero, and M. R. Gasco, *Pharm. Dev. Technol.* 8, 299–309 (2003).
127. A. Radomska-Soukharev, *Adv. Drug Deliv. Rev.* 59, 411–418 (2007).
128. D. B. Chen, T. Z. Yang, W. L. Lu, and Q. Zhang, *Chem. Pharm. Bull. (Tokyo)* 49, 1444–1447 (2001).
129. A. Bargoni, R. Cavalli, G. P. Zara, A. Fundaro, O. Caputo, and M. R. Gasco, *Pharmacol. Res.* 43, 497–502 (2001).
130. M. D. Joshi and R. H. Muller, *Eur. J. Pharm. Biopharm.* 71, 161–172 (2009).
131. S. Maassen, C. Schwarz, W. Mehnert, J. S. Lucks, F. Yunis-Specht, B. W. Muller, and R. H. Muller, in "Int. Symp. Control. Release Bioact. Mater.," pp. 490–491, 1993.
132. J. Pardeike, A. Hommoss, and R. H. Muller, *Int. J. Pharm.* 366, 170–184 (2009).
133. P. Gershkovich, K. M. Wasan, and C. A. Barta, *Crit. Rev. Ther. Drug Carrier Syst.* 25, 545–584 (2008).
134. A. J. Almeida and E. Souto, *Adv. Drug Deliv. Rev.* 59, 478–490 (2007).
135. M. Sznitowska, M. Gajewska, S. Janicki, A. Radwanska, and G. Lukowski, *Eur. J. Pharm. Biopharm.* 52, 159–163 (2001).
136. C. Olbrich, O. Kayser, and R. H. Muller, *Int. J. Pharm.* 237, 119–128 (2002).
137. B. Sarmento, S. Martins, D. Ferreira, and E. B. Souto, *Int. J. Nanomed.* 2, 743–749 (2007).
138. E. Ugazio, R. Cavalli, and M. R. Gasco, *Int. J. Pharm.* 241, 341–344 (2002).
139. S. Yang, J. Zhu, Y. Lu, B. Liang, and C. Yang, *Pharm. Res.* 16, 751–757 (1999).
140. R. Cavalli, G. P. Zara, O. Caputo, A. Bargoni, A. Fundaro, and M. R. Gasco, *Pharmacol. Res.* 42, 541–545 (2000).
141. R. Pandey, S. Sharma, and G. K. Khuller, *Tuberculosis (Edinb)* 85, 415–420 (2005).
142. N. Zhang, Q. Ping, G. Huang, W. Xu, Y. Cheng, and X. Han, *Int. J. Pharm.* 327, 153–159 (2006).
143. G. P. Zara, R. Cavalli, A. Fundaro, A. Bargoni, O. Caputo, and M. R. Gasco, *Pharmacol. Res.* 40, 281–286 (1999).
144. H. Yuan, J. Chen, Y. Z. Du, F. Q. Hu, S. Zeng, and H. L. Zhao, *Coll. Surf. B: Biointerfaces* 58, 157–164 (2007).
145. M. Uner and G. Yener, *Int. J. Nanomed.* 2, 289–300 (2007).
146. P. H. Green and R. M. Glickman, *J. Lipid Res.* 22, 1153–1173 (1981).
147. M. Cheema, K. J. Palin, and S. S. Davis, *J. Pharm. Pharmacol.* 39, 55–56 (1987).
148. R. K. Ockner, J. P. Pittman, and J. L. Yager, *Gastroenterology* 62, 981–992 (1972).
149. L. D. Hu, X. Tang, and F. D. Cui, *J. Pharm. Pharmacol.* 56, 1527–1535 (2004).
150. X. Dong, C. A. Mattingly, M. T. Tseng, M. J. Cho, Y. Liu, V. R. Adams, and R. J. Mumper, *Cancer Res.* 69, 3918–3926 (2009).
151. S. Chakraborty, D. Shukla, B. Mishra, and S. Singh, *Eur. J. Pharm. Biopharm.* 73, 1–15 (2009).

152. V. V. Kumar, D. Chandrasekar, S. Ramakrishna, V. Kishan, Y. M. Rao, and P. V. Diwan, *Int. J. Pharm.* 335, 167–175 (2007).
153. E. Zimmermann and R. H. Muller, *Eur. J. Pharm. Biopharm.* 52, 203–210 (2001).
154. R. H. Muller, S. A. Runge, and V. Ravelli, German Patent Application, DE 19819273A1, 1998.
155. H. L. Wong, A. M. Rauth, R. Bendayan, J. L. Manias, M. Ramaswamy, Z. Liu, S. Z. Erhan, and X. Y. Wu, *Pharm. Res.* 23, 1574–1585 (2006).
156. C. Olbrich, U. Bakowsky, C. M. Lehr, R. H. Muller, and C. Kneuer, *J. Cont. Rel.* 77, 345–355 (2001).
157. A. Brioschi, F. Zenga, G. P. Zara, M. R. Gasco, A. Ducati, and A. Mauro, *Neurol. Res.* 29, 324–330 (2007).
158. J. M. Koziara, T. R. Whisman, M. T. Tseng, and R. J. Mumper, *J. Cont. Rel.* 112, 312–319 (2006).
159. L. H. Reddy, R. K. Sharma, K. Chuttani, A. K. Mishrah, and R. S. R. Murth, *J. Cont. Rel.* 105, 185–198 (2005).
160. K. Manjunath and V. Venkateswarlu, *J. Drug Target.* 14, 632–645 (2006).
161. R. H. Muller, S. Maassen, H. Weyhers, and W. Mehnert, *J. Drug Target.* 4, 161–170 (1996).
162. A. A. Date, M. D. Joshi, and V. B. Patravale, *Adv. Drug Deliv. Rev.* 59, 505–521 (2007).
163. C. Bocca, O. Caputo, R. Cavalli, L. Gabriel, A. Miglietta, and M. R. Gasco, *Int. J. Pharm.* 175, 185–193 (1998).
164. S. M. Moghimi, *Adv. Drug Deliv. Rev.* 16, 183–193 (1995).
165. W. I. Hagens, A. G. Oomen, W. H. de Jong, F. R. Cassee, and A. J. Sips, *Regul. Toxicol. Pharmacol.* 49, 217–229 (2007).
166. M. A. Videira, A. J. Almeida, M. F. Botelho, A. C. Santos, C. Gomes, and J. J. P. de Lima, *Eur. J. Nucl. Med.* 26, 1168 (1999).
167. S. Saraf, D. Mishra, A. Asthana, R. Jain, S. Singh, and N. K. Jain, *Vaccine* 24, 45–56 (2006).
168. J. Liu, T. Gong, H. Fu, C. Wang, X. Wang, Q. Chen, Q. Zhang, Q. He, and Z. Zhang, *Int. J. Pharm.* 356, 333–344 (2008).
169. C. Prego, M. Garcia, D. Torres, and M. J. Alonso, *J. Cont. Rel.* 101, 151–162 (2005).
170. C. Rudolph, U. Schillinger, A. Ortiz, K. Tabatt, C. Plank, R. H. Muller, and J. Rosenecker, *Pharm. Res.* 21, 1662–1669 (2004).
171. A. Vila, H. Gill, O. McCallion, and M. J. Alonso, *J. Cont. Rel.* 98, 231–244 (2004).
172. R. Pandey and G. K. Khuller, *Tuberculosis (Edinb)* 85, 227–234 (2005).
173. H. Chen, X. Chang, D. Du, W. Liu, J. Liu, T. Weng, Y. Yang, H. Xu, and X. Yang, *J. Cont. Rel.* 110, 296–306 (2006).
174. S. A. Wissing and R. H. Muller, *Pharmazie* 56, 783–786 (2001).
175. A. Dingler, R. P. Blum, H. Niehus, R. H. Muller, and S. Gohla, *J. Microencapsul.* 16, 751–767 (1999).
176. S. A. Wissing and R. H. Muller, *Int. J. Cosmet. Sci.* 23, 233–243 (2001).
177. V. Jenning, A. Gysler, M. Schafer-Korting, and S. H. Gohla, *Eur. J. Pharm. Biopharm.* 49, 211–218 (2000).
178. M. Uner, S. A. Wissing, G. Yener, and R. H. Muller, *Pharmazie* 60, 577–582 (2005).
179. M. Uner, S. A. Wissing, G. Yener, and R. H. Muller, *Pharmazie* 60, 751–755 (2005).
180. E. B. Souto, S. A. Wissing, C. M. Barbosa, and R. H. Muller, *Int. J. Pharm.* 278, 71–77 (2004).
181. Z. Mei, H. Chen, T. Weng, Y. Yang, and X. Yang, *Eur. J. Pharm. Biopharm.* 56, 189–196 (2003).
182. U. Munster, C. Nakamura, A. Haberland, K. Jores, W. Mehnert, S. Rummel, M. Schaller, et al., *Pharmazie* 60, 8–12 (2005).
183. I. P. Kaur, A. Garg, A. K. Singla, and D. Aggarwal, *Int. J. Pharm.* 269, 1–14 (2004).
184. R. T. Pijls, T. Sonderkamp, G. W. Daube, R. Krebber, H. H. Hanssen, R. M. Nuijts, and L. H. Koole, *Eur. J. Pharm. Biopharm.* 59, 283–288 (2005).
185. R. Cavalli, M. R. Gasco, P. Chetoni, S. Burgalassi, and M. F. Saettone, *Int. J. Pharm.* 238, 241–245 (2002).
186. R. Cavalli, S. Morel, M. R. Gasco, P. Chetoni, and m. F. Saettone, *Int. J. Pharm.* 117, 243–246 (1995).
187. E. Basaran, M. Demirel, B. Sirmagul, and Y. Yazan, *J. Microencapsul.* [in press].
188. A. A. Attama, S. Reichl, and C. C. Muller-Goymann, *Int. J. Pharm.* 355, 307–313 (2008).
189. G. Abdelbary and R. H. Fahmy, *AAPS Pharm. Sci. Tech.* 10, 211–219 (2009).
190. S. M. Moghimi and J. Szebeni, *Prog. Lipid Res.* 42, 463–478 (2003).
191. D. E. Owens, 3rd and N. A. Peppas, *Int. J. Pharm.* 307, 93–102 (2006).
192. C. E. Soma, C. Dubernet, G. Barratt, F. Nemati, M. Appel, S. Benita, and P. Couvreur, *Pharm. Res.* 16, 1710–1716 (1999).
193. J. Gualbert, P. Shahgaldian, and A. W. Coleman, *Int. J. Pharm.* 257, 69–73 (2003).
194. N. L. Trevaskis, W. N. Charman, and C. J. Porter, *Adv. Drug Deliv. Rev.* 60, 702–716 (2008).
195. S. Gururangan and H. S. Friedman, *Neuroimag. Clin. N. Am.* 12, 583–597 (2002).
196. W. Loscher and H. Potschka, *NeuroRx* 2, 86–98 (2005).
197. A. Beduneau, F. Hindre, A. Clavreul, J. C. Leroux, P. Saulnier, and J. P. Benoit, *J. Cont. Rel.* 126, 44–49 (2008).
198. J. Kreuter, *Adv. Drug Deliv. Rev.* 47, 65–81 (2001).
199. E. Esposito, M. Fantin, M. Marti, M. Drechsler, L. Paccamiccio, P. Mariani, E. Sivieri, et al., *Pharm. Res.* 25, 1521–1530 (2008).
200. K. Manjunath and V. Venkateswarlu, *J. Cont. Rel.* 107, 215–228 (2005).
201. P. R. Lockman, M. O. Oyewumi, J. M. Koziara, K. E. Roder, R. J. Mumper, and D. D. Allen, *J. Cont. Rel.* 93, 271–282 (2003).
202. N. Iodoshima, C. Udagawa, T. Ando, H. Fukuyasu, T. Watanabe, and S. Nakabayashi, *Int. J. Pharm.* 146, 81–92 (1997).
203. J. Curtis, M. Greenberg, J. Kester, S. Phillips, and G. Krieger, *Toxicol. Rev.* 25, 245–260 (2006).
204. R. H. Muller, S. Maaszen, H. Weyhers, F. Specht, and J. S. Lucks, *Int. J. Pharm.* 138, 85–94 (1996).
205. R. H. Müller, S. Maassen, C. Schwarz, and W. Mehnert, *J. Cont. Rel.* 47, 261–269 (1997).
206. N. Scholer, H. Hahn, R. H. Muller, and O. Liesenfeld, *Int. J. Pharm.* 231, 167–176 (2002).
207. H. Weyhers, S. Ehlers, H. Hahn, E. B. Souto, and R. H. Muller, *Pharmazie* 61, 539–544 (2006).
208. P. K. Dudeja, K. M. Anderson, J. S. Harris, L. Buckingham, and J. S. Coon, *Arch. Biochem. Biophys.* 319, 309–315 (1995).
209. D. M. Woodcock, M. E. Linsenmeyer, G. Chojnowski, A. B. Kriegler, V. Nink, L. K. Webster, and W. H. Sawyer, *Br. J. Cancer* 66, 62–68 (1992).
210. A. Estella-Hermoso de Mendoza, M. A. Campanero, F. Mollinedo, and M. J. Blanco-Prieto, *J. Biomed. Nanotechnol.* 5, 323–343 (2009).
211. V. S. Shenoy, I. K. Vijay, and R. S. Murthy, *J. Pharm. Pharmacol.* 57, 411–422 (2005).
212. H. L. Wong, Y. Li, R. Bendayan, A. M. Rauth, and X. Y. Wu, in "Nanotechnology for Cancer Therapy" (M. M. Amiji, Ed.), pp. 714–776, Boca Raton, FL: CRC Press, 2006.
213. J. M. Koziara, P. R. Lockman, D. D. Allen, and R. J. Mumper, *J. Cont. Rel.* 99, 259–269 (2004).
214. F. Wan, J. You, Y. Sun, X. G. Zhang, F. D. Cui, Y. Z. Du, H. Yuan, and F. Q. Hu, *Int. J. Pharm.* 359, 104–110 (2008).
215. M. O. Oyewumi, R. A. Yokel, M. Jay, T. Coakley, and R. J. Mumper, *J. Cont. Rel.* 95, 613–626 (2004).
216. N. Hodoshima, C. Udagawa, T. Ando, H. Fukuyasu, H. Watanabe, and S. Nakabayashi, *Int. J. Pharm.* 146, 81–92 (1997).
217. J. X. Wang, X. Sun, and Z. R. Zhang, *Eur. J. Pharm. Biopharm.* 54, 285–290 (2002).

218. D. R. Zhang, T. C. Ren, H. X. Lou, and J. Xing, *Yao Xue Xue Bao* 40, 573–576 (2005).
219. G. Huang, N. Zhang, X. Bi, and M. Dou, *Int. J. Pharm.* 355, 314–320 (2008).
220. N. Yanasarn, B. R. Sloat, and Z. Cui, *Int. J. Pharm.* 379, 174–180 (2009).
221. J. C. Li, X. Y. Sha, L. J. Zhang, and X. L. Fang, *Yao Xue Xue Bao* 40, 970–975 (2005).
222. M. L. Bondi, E. F. Craparo, G. Giammona, M. Cervello, A. Azzolina, P. Diana, A. Martorana, and G. Cirrincione, *Drug Deliv.* 14, 61–67 (2007).
223. C. Olbrich, A. Gessner, W. Schroder, O. Kayser, and R. H. Muller, *J. Cont. Rel.* 96, 425–435 (2004).
224. C. S. Maia, W. Mehnert, and M. Schafer-Korting, *Int. J. Pharm.* 196, 165–167 (2000).
225. M. Kalariya, B. K. Padhi, M. Chougule, and A. Misra, *Ind. J. Exp. Biol.* 43, 233–240 (2005).
226. J. Liu, W. Hu, H. Chen, Q. Ni, H. Xu, and X. Yang, *Int. J. Pharm.* 328, 191–195 (2007).
227. C. Song and S. Liu, *Int. J. Biol. Macromol.* 36, 116–119 (2005).
228. M. Joshi and V. Patravale, *Int. J. Pharm.* 346, 124–132 (2008).
229. M. Joshi and V. Patravale, *Drug Dev. Ind. Pharm.* 32, 911–918 (2006).
230. M. Ricci, C. Puglia, F. Bonina, C. Di Giovanni, S. Giovagnoli, and C. Rossi, *J. Pharm. Sci.* 94, 1149–1159 (2005).
231. F. Han, S. Li, R. Yin, X. Shi, and Q. Jia, *Drug Dev. Ind. Pharm.* 34, 453–458 (2008).
232. C. Puglia, P. Blasi, L. Rizza, A. Schoubben, F. Bonina, C. Rossi, and M. Ricci, *Int. J. Pharm.* 357, 295–304 (2008).
233. E. B. Souto and R. H. Muller, *J. Microencapsul.* 22, 501–510 (2005).
234. K. A. Shah, A. A. Date, M. D. Joshi, and V. B. Patravale, *Int. J. Pharm.* 345, 163–171 (2007).
235. Z. Cui and R. J. Mumper, *Pharm. Res.* 19, 939–946 (2002).
236. Z. Cui and R. J. Mumper, *Bioconjug. Chem.* 13, 1319–1327 (2002).
237. S. H. Choi, S. E. Jin, M. K. Lee, S. J. Lim, J. S. Park, B. G. Kim, W. S. Ahn, and C. K. Kim, *Eur. J. Pharm. Biopharm.* 68, 545–554 (2008).
238. W. Yu, C. Liu, J. Ye, W. Zou, N. Zhang, and W. Xu, *Nanotechnology* 20, 215102 (2009).
239. E. Peira, P. Marzola, V. Podio, S. Aime, A. Sbarbati, and M. R. Gasco, *J. Drug Target.* 11, 19–24 (2003).
240. H. Weyhers, R. Lobenberg, W. Mehnert, E. Souto, J. Kreuter, and R. H. Muller, *Pharm. Indust.* 68, 889–894 (2006).
241. C. S. Chong, M. Cao, W. W. Wong, K. P. Fischer, W. R. Addison, G. S. Kwon, D. L. Tyrrell, and J. Samuel, *J. Cont. Rel.* 102, 85–99 (2005).
242. M. Diwan, P. Elamanchili, M. Cao, and J. Samuel, *Curr. Drug Deliv.* 1, 405–412 (2004).
243. S. Y. Kim, H. J. Doh, M. H. Jang, Y. J. Ha, S. I. Chung, and H. J. Park, *Helicobacter* 4, 33–39 (1999).
244. J. H. Park, M. Ye, and K. Park, *Molecules* 10, 146–161 (2005).
245. C. Olbrich, R. H. Muller, K. Tabatt, O. Kayser, C. Schulze, and R. Schade, *Altern. Lab. Anim.* 30, 443–458 (2002).
246. Z. Cui and R. J. Mumper, *Int. J. Pharm.* 238, 229–239 (2002).
247. R. J. Mumper and Z. Cui, US Patent Application, US 2008124350, 2008.
248. T. Matsubara, *Rheumatology* 22, 81–97 (1999).
249. W. Zhang, J. Liu, S. Li, M. Chen, and H. Liu, *J. Microencapsul.* 25, 203–209 (2008).
250. J. Liu, J. Zhu, Z. Du, and B. Qin, *Drug Dev. Ind. Pharm.* 31, 551–556 (2005).
251. Y. C. Kuo and C. W. Lin, *Coll. Surf. B: Biointerfaces* 72, 201–207 (2009).
252. F. Lai, C. Sinico, A. De Logu, M. Zaru, R. H. Muller, and A. M. Fadda, *Int. J. Nanomed.* 2, 419–425 (2007).
253. X. G. Zhang, J. Miao, M. W. Li, S. P. Jiang, F. Q. Hu, and Y. Z. Du, *J. Zhejiang Univ. Sci. B* 9, 506–510 (2008).
254. 2008 Report on the global AIDS epidemic, by UNAIDS, 2008.
255. S. Pang, Y. Koyanagi, S. Miles, C. Wiley, H. V. Vinters, and I. S. Chen, *Nature* 343, 85–89 (1990).
256. B. T. Yu, Z. R. Zhang, and R. J. Zeng, *Yao Xue Xue Bao* 35, 704–705 (2000).
257. M. A. Videira, L. Gano, C. Santos, M. Neves, and A. J. Almeida, *J. Microencapsul.* 23, 855–862 (2006).
258. E. Allard, F. Hindre, C. Passirani, L. Lemaire, N. Lepareur, N. Noiret, P. Menei, and J. P. Benoit, *Eur. J. Nucl. Med. Mol. Imag.* 35, 1838–1846 (2008).
259. E. B. Souto, R. H. Muller, and S. Gohla, *J. Microencapsul.* 22, 581–592 (2005).
260. L. D. Hu, X. Tang, and F. D. Cui, *Yao Xue Xue Bao* 40, 71–75 (2005).
261. W. Liu, Z. He, J. Liang, Y. Zhu, H. Xu, and X. Yang, *J. Biomed. Mater. Res. A* 84, 1018–1025 (2008).
262. R. H. Muller, S. A. Runge, V. Ravelli, A. F. Thunemann, W. Mehnert, and E. B. Souto, *Eur. J. Pharm. Biopharm.* 68, 535–544 (2008).
263. V. Teeranachaideekul, E. B. Souto, V. B. Junyaprasert, and R. H. Muller, *Eur. J. Pharm. Biopharm.* 67, 141–148 (2007).
264. Q. Y. Xiang, M. T. Wang, F. Chen, T. Gong, Y. L. Jian, Z. R. Zhang, and Y. Huang, *Arch. Pharm. Res.* 30, 519–525 (2007).
265. E. B. Souto, C. Anselmi, M. Centini, and R. H. Muller, *Int. J. Pharm.* 295, 261–268 (2005).
266. S. Utreja, A. J. Khopade, and N. K. Jain, *Pharm. Acta Helv.* 73, 275–279 (1999).
267. E. B. Souto, V. Teeranachaideekul, V. B. Junyaprasert, and R. H. Muller, in "15th International Symposium on Microencapsulation," Parma, Italy, 2005.
268. Y. Iscan, S. Hekimoglu, M. F. Sargon, and A. A. Hincal, *J. Microencapsul.* 23, 315–327 (2006).
269. Y. Iscan, S. A. Wissing, S. Hekimoglu, and R. H. Muller, *Pharmazie* 60, 905–909 (2005).
270. F. Lacoeuille, F. Hindre, F. Moal, J. Roux, C. Passirani, O. Couturier, P. Cales, J. J. Le Jeune, A. Lamprecht, and J. P. Benoit, *Int. J. Pharm.* 344, 143–149 (2007).
271. D. Pandita, A. Ahuja, T. Velpandian, V. Lather, T. Dutta, and R. K. Khar, *Pharmazie* 64, 301–310 (2009).
272. R. R. Zhu, L. L. Qin, M. Wang, S. M. Wu, S. L. Wang, R. Zhang, Z. X. Liu, X. Y. Sun, and S. D. Yao, *Nanotechnology* 20, 55702 (2009).
273. G. A. Castro, R. L. Orefice, J. M. Vilela, M. S. Andrade, and L. A. Ferreira, *J. Microencapsul.* 24, 395–407 (2007).
274. P. V. Pople and K. K. Singh, *AAPS Pharm. Sci. Tech.* 7, 91 (2006).
275. J. R. Villalobos-Hernandez and C. C. Muller-Goymann, *Eur. J. Pharm. Biopharm.* 60, 113–122 (2005).
276. G. Yener, T. Incegul, and N. Yener, *Int. J. Pharm.* 258, 203–207 (2003).
277. L. H. Reddy, K. Vivek, N. Bakshi, and R. S. Murthy, *Pharm. Dev. Technol.* 11, 167–177 (2006).
278. A. Dingler, G. Hildebrand, H. Niehus, and R. H. Muller, in "Proc. Intern. Symp. Control. Rel. Bioact. Mater.," pp. 433–434, 1998.

ANNEX II

Efficacy of edelfosine lipid nanoparticles in breast cancer cells

*María Ángela Aznar, Beatriz Lasa-Saracíbar, Ander Estella-Hermoso de Mendoza, ,Maria J. Blanco-Prieto**

[1]*Department of Pharmacy and Pharmaceutical Technology, School of Pharmacy, University of Navarra, Pamplona, Spain*

***Corresponding author**

Dr. María J. Blanco-Prieto, Department of Pharmaceutics and Pharmaceutical Technology, School of Pharmacy, University of Navarra, C/Irunlarrea 1, E-31080 Pamplona, Spain, Office phone: + 34 948 425 600 ext. 6519, Fax: + 34 948 425 649, e-mail: mjblanco@unav.es

Author Contributions

The manuscript was written through contributions of all authors. All authors have given approval to the final version of the manuscript.

Declaration of interest: The authors state no conflict of interest.

International Journal of Pharmaceutics. 2013 Oct 1;454(2):720-6

International Journal of Pharmaceutics 454 (2013) 720–726

Contents lists available at SciVerse ScienceDirect

International Journal of Pharmaceutics

journal homepage: www.elsevier.com/locate/ijpharm

Efficacy of edelfosine lipid nanoparticles in breast cancer cells

María Ángela Aznar, Beatriz Lasa-Saracíbar, Ander Estella-Hermoso de Mendoza [1], María José Blanco-Prieto *

Department of Pharmacy and Pharmaceutical Technology, School of Pharmacy, University of Navarra, C/Irunlarrea no. 1, 31008 Pamplona, Spain

ARTICLE INFO

Article history:
Received 1 February 2013
Received in revised form 27 March 2013
Accepted 15 April 2013
Available online 30 April 2013

Keywords:
Breast cancer
MCF7
Lipid nanoparticles
Edelfosine
Alkylphospholipids

ABSTRACT

Breast cancer is a heterogeneous group of neoplasms predominantly originating in the terminal duct lobular units. It represents the leading cause of cancer death in women and the survival frequencies for patients at advanced stages of the disease remain low. New treatment options need to be researched to improve these rates. The anti-tumor ether lipid edelfosine (ET) is the prototype of a novel generation of promising anticancer drugs. However, it presents several drawbacks for its use in cancer therapy, including gastrointestinal and hemolytic toxicity and low oral bioavailability. To overcome these obstacles, ET was encapsulated in Precirol ATO 5 lipid nanoparticles (ET-LN), and its anti-tumor potential was in vitro tested in breast cancer. The formulated ET-LN were more effective in inhibiting cell proliferation and notably decreased cell viability, showing that the cytotoxic effect of ET was considerably enhanced when ET was encapsulated. In addition, ET and ET-LN were able to promote cell cycle arrest at G1 phase. Moreover, although both treatments provoked an apoptotic effect in a time-dependent manner, such anti-tumor effects were noticeably improved with ET-LN treatment. Therefore, our results indicate that encapsulating ET in LN played an essential role in improving the efficacy of the drug.

1. Introduction

Breast cancer is a heterogeneous group of neoplasms, predominantly originating in the terminal duct lobular units, regardless of histological type (Weigelt and Reis-Filho, 2009; Wellings and Jensen, 1973; Wellings et al., 1975). It represents the fifth most common cancer worldwide, the second most common cause of cancer death and the leading cause of cancer death in women (Siegel et al., 2013). The global burden of breast cancer exceeds all other cancers and the incidence rates of breast cancer are increasing. The ability of breast cancer cells to metastasize to distant organs makes this disease refractory and incurable and is the key factor in the treatment and prognosis of breast cancer (Lu and Kang, 2007). Current treatment approaches usually involve intrusive processes, chemotherapy to shrink any cancer present, surgery to then remove the tumor if possible, followed by more chemotherapy and radiation. However, the survival rates for patients at advanced stages of the disease remain low (Siegel et al., 2013). Consequently, new treatment options have to be studied to improve these rates. Current research areas include, on the one hand, the development of carriers that allow alternative dosing routes and reduce toxicity; and on the other, new therapeutic targets such as blood vessels fueling tumor growth and targeted therapeutics that are more specific in their activity (Brannon-Peppas and Blanchette, 2004).

The anti-tumor ether lipid edelfosine (ET-18-OCH3, ET) has been shown as an effective anti-tumor agent in different malignancies (Estella-Hermoso de Mendoza et al., 2009a; Mollinedo et al., 2010a; Na and Surh, 2008; Shafer and Williams, 2003). However, when it is administered in its free form, it presents several drawbacks such as dose-dependent hemolytic toxicity after intravenous administration (Ahmad et al., 1997), poor oral bioavailability and gastrointestinal irritation when administered orally (Estella-Hermoso de Mendoza et al., 2009a, 2012; Houlihan et al., 1995; Munder and Westphal, 1990).

Owing to the drawbacks of this molecule, new drug delivery systems have been designed (Estella-Hermoso de Mendoza et al., 2012). Lipid nanoparticles (LN) are colloidal transporters composed of a biocompatible and biodegradable lipid matrix. They are passively targeted at the tumor tissue due to the well-known enhanced permeability and retention effect (EPR), resulting in an increased concentration of drug in tumor cells and in lower side effects (Peer

Abbreviations: ET, edelfosine; ALPs, alkylphospholipids; LN, lipid nanoparticles; EPR effect, enhanced permeability and retention effect; ET-LN, edelfosine-loaded lipid nanoparticles; MCL, mantle cell lymphoma; PDI, polydispersity index; B-LN, blank (unloaded) nanoparticles; PI, propidium iodide; IC_{50}, inhibitory concentration 50.

* Corresponding author at: Department of Pharmacy and Pharmaceutical Technology, School of Pharmacy, University of Navarra, Irunlarrea 1, E-31080 Pamplona, Spain. Tel.: +34 948 425600x6519; fax: +34 948 425649.
E-mail addresses: mjblanco@unav.es, maria.blanco@nanomedicinas.es (M.J. Blanco-Prieto).
[1] Present address: ETH Zürich, HCI J392.4, Wolfgang-Pauli-Str. 10, 8093 Zürich, Switzerland.

0378-5173/$ – see front matter © 2013 Elsevier B.V. All rights reserved.
http://dx.doi.org/10.1016/j.ijpharm.2013.04.068

et al., 2007; Torchilin, 2011). Besides, LN can be administered orally and are mainly absorbed via the lymphatic system, circumventing first-pass hepatic metabolism, and thereby opening a new window in the treatment of cancer metastases (Estella-Hermoso de Mendoza et al., 2012; Lasa-Saracíbar et al., 2012). Moreover, LN may modify the entrance mechanism of the ET into cancer cells and this might overcome the resistance that some cell lines show to the free drug, (Wagner et al., 1998). In this context, the potential of ET-LN in overcoming the resistance of cancer cells has recently been proved in leukemic cell lines (Lasa-Saracíbar et al., 2013).

The purpose of this study was to develop LN loaded with ET to enhance its therapeutic activity against breast cancer cells. We formulated ET-LN and we characterized their physicochemical properties. The cytotoxicity of ET-LN, their effects in cell cycle and the cell death induction mechanisms in breast cancer were also investigated.

2. Material and methods

2.1. Chemicals

ET was from Apointech (Salamanca, Spain). Precirol ATO 5 was a gift from Gattefossé (Lyon, France). Tween® 80 was obtained from Roig Farma (Barcelona, Spain). Phosphate-buffered saline (PBS; 10 mM phosphate, 0.9% NaCl), 3-(4,5-dimethylthiazol-2-yl)-2,5-diphenyl tetrazolium bromide (MTT), Trypan Blue, RNase and Propidium iodide (PI) were obtained from Sigma-Aldrich (Madrid, Spain). Chloroform was purchased from Panreac (Madrid, Spain) and methanol was obtained from Merck (Barcelona, Spain). Ultrapurified water was used throughout and all other chemicals were of analytical grade.

2.2. Cell culture

MCF7 breast cancer cells were purchased from ATCC (American Type Culture Collection, Manassas, VA, USA). Dubelcco's modified Eagle's medium (DMEM), heat-inactivated fetal bovine serum (FBS), trypsin–EDTA and penicillin–streptomycin mixtures were purchased from Gibco® BRL (Carlsbad, CA, USA).

MCF7 breast cancer cell line was grown in DMEM supplemented with 50 U/mL penicillin, 50 U/mL streptomycin and 10% FBS at 37 °C in a humidified incubator supplemented with 5% carbon dioxide.

2.3. Preparation of LN

ET-LN formulations were prepared by the hot homogenization method followed by high shear homogenization and ultrasonication as previously described (Estella-Hermoso de Mendoza et al., 2012). The lipid phase consisted of 300 mg of Precirol ATO 5 with 30 mg ET, while the aqueous phase consisted of 10 mL of a 2% (w/v) Tween® 80 aqueous solution. The nanoparticle suspension obtained was subsequently cooled in an ice bath and washed twice with filtered water by diafiltration with Amicon Ultra-15 filters of 10,000 Da molecular weight cut-off membranes (Millipore®, Cork, Ireland) to remove the excess of surfactant and non-incorporated drug. LN were then resuspended in 3% trehalose (75% of the Precirol ATO 5 weigh) and the suspension was kept at −80 °C and freeze-dried to preserve the formulation for further studies. Blank (unloaded) nanoparticles (B-LN) were formulated as empty control of LN for in vitro experiments using an identical procedure.

2.4. Nanoparticle characterization

2.4.1. Particle size and Zeta potential

Nanoparticle size and polydispersity index (PDI) of LN were determined in triplicate by photon correlation spectroscopy and zeta potential by laser doppler anemometry, using a Zetasizer Nano (Malvern, UK). Each sample was diluted 30-fold in distilled water until the appropriate concentration of particles was achieved to avoid multiscattering events. Similarly, the zeta potential was measured using the same equipment with a combination of laser doppler electrophoresis (Clogston and Patri, 2011; Kaszuba et al., 2010). Each experiment was performed in triplicate. All data are expressed as a mean value ± standard deviation.

2.4.2. Encapsulation efficiency and loading capacity

Encapsulated ET was quantified by a previously validated ultra-high performance liquid chromatography–tandem mass spectrometry method as previously validated (Estella-Hermoso de Mendoza et al., 2009b). The drug was extracted from a sample of 5 mg of lyophilized LN, to which 1 mL of chloroform was added in order to dissolve them and subsequently 3 ml of methanol were added to the mixture. After vortex mixing for 1 min at room temperature and centrifuging at 20,000 × *g* for 10 min, 2 µl aliquots of the supernatant were injected into the chromatographic system.

2.5. Cytotoxicity studies

The cytotoxic potential of ET-LN was evaluated with the MTT assay. 21,000 cells/cm^2 were grown in 96-well plates in the presence of increasing amounts of ET or equivalent concentrations of ET-LN for 72 h. B-LN were also tested as control. Then, MTT solution was added directly to the culture media at a final concentration of 0.5 mg/mL and then incubated for 3 h at 37 °C. Afterwards, MTT containing medium was removed from all wells and the remaining cells containing formazan crystals were dissolved in DMSO. Optical density was determined with a BioRad microplate reader at 570 nm after background correction at 690 nm. Average cell viability of treated cells was expressed as a percentage of the absorbance of control cells. Untreated cells were taken as control with 100% viability and cells grown in presence of 10% DMSO were used as positive control of cytotoxicity. All experiments were performed in triplicate.

Cell number and viability, as denoted by Trypan Blue exclusion, were calculated by cell counting with a Bright-Line Hemacytometer (Sigma–Aldrich, Madrid, Spain). Cell counts were performed in triplicate.

Images of the morphological changes induced by ET and LN were obtained using a Nikon Eclipse TS100 microscope.

2.6. Cell cycle analysis

For cell cycle evaluation, 21,000 cells/cm^2 were seeded in 6-well plates and incubated with 20 µg/mL of ET or equivalent concentrations of ET-LN. B-LN were also tested as control. Cells were trypsinized, collected by centrifugation, washed with PBS and fixed with 70% ethanol at 4 °C for 1 h. Next, cells were incubated with 0.45 U/mL RNase and stained with 10 µg/mL of propidium bromide. Cell fluorescence was detected on a FACSCalibur flow cytometer (BD Biosciences, Madrid, Spain) and analyzed with CellQuest Pro (BD Biosciences) and FlowJo data analysis software package (TreeStar, USA). All experiments were performed in triplicate after 48 and 72 h of incubation with the corresponding treatments.

2.7. Assessment of apoptosis by Annexin-V FITC staining

For evaluation of apoptosis in MCF7 cells after ET and LN treatments, 21,000 cells/cm^2 were seeded in 6-well plates and incubated with 20 µg/mL of ET or equivalent concentrations of ET-LN. B-LN were also tested as control. After 24, 48 or 72 h of incubation, cells were collected and washed twice with PBS and subsequently

labeled. Two different approaches were used for the assessment of apoptosis induction of MCF7 cells.

On the one hand, apoptosis was determined by flow cytometry as the percentage of cells in the sub-G1 region (hypodiploidy) in cell cycle analysis as previously described (Gajate et al., 2000).

On the other hand, an Annexin V-FLUOS Apoptosis Detection Kit (Roche Molecular Biochemicals, Barcelona, Spain) was used according to the manufacturer's protocol. The percentage of cells that underwent apoptosis was quantified by flow cytometry on a FACSCalibur flow cytometer using CellQuest software and analyzed with FlowJo software. All experiments were performed in triplicate.

2.8. Statistical analysis

Data are presented as a mean of three or more independent experiments, with error bars indicating the standard deviation. The inhibitory concentration 50 (IC_{50}) values were calculated with GraphPad Prism software using the sigmoidal dose–response function (variable slope). Statistical comparisons were performed by analysis of variance, and further post hoc testing was conducted using the statistical software GraphPad Prism 5 (GraphPad Software, Inc., San Diego, CA, USA). Non-parametric statistics (Kruskal–Wallis test followed by Dunn's Post Hoc test) were used for the analysis of Sub-G1 data. Cell viability, cell cycle and apoptosis statistical analyses were performed with two-way Anova and Bonferroni post hoc tests. Groups that are significantly different are indicated in the figures as $^{*}p < 0.05$, $^{**}p < 0.01$ and $^{***}p < 0.001$.

3. Results and discussion

ET is an anti-tumor drug belonging to the ALPs family that has been employed for the treatment of various malignancies with promising results (Estella-Hermoso de Mendoza et al., 2009a; Mollinedo et al., 2010a; Na and Surh, 2008; Shafer and Williams, 2003). However, due to its nature, ET presents several drawbacks that have to be overcome by protecting the molecule. Nanotechnology applications in medicine have successfully enhanced the therapeutic efficacy of many anti-cancer drugs. In fact, the nanoencapsulation approach of ET has yielded promising results (Estella-Hermoso de Mendoza et al., 2012; Lasa-Saracibar et al., 2013), demonstrating that the vehiculization strategy is essential to ensure the effectiveness of ET (Estella-Hermoso de Mendoza et al., 2012). Such hopeful results prompted us to develop ET-loaded LN for studying its in vitro anti-tumor effect compared to the free drug in breast cancer.

3.1. Nanoparticle characterization

ET-loaded LNs were produced by a solvent-free hot homogenization method followed by high shear homogenization and ultrasonication, and were freeze-dried afterwards. LN were characterized in terms of size, zeta potential, encapsulation efficiency and drug loading. As shown in Table 1, we were able to obtain submicron-sized LN with homogeneous diameter. All data are expressed as mean value ± standard deviation. Both drug-free LN and ET-LN mean diameters were below 150 nm, indicating that LN developed are suitable for both gastrointestinal and intravenous administration without entailing embolism risks (Charman and Stella, 1992; Estella-Hermoso de Mendoza et al., 2009c; Varshosaz et al., 2010; Zimmermann et al., 2000). Furthermore, the incorporation of edelfosine into LN proved to significantly decrease the hemolytic toxicity of the free drug in a previous work published by our group (Estella-Hermoso de Mendoza et al., 2012). PDI was below 0.3, proving that the developed particles were monodisperse (Anton et al., 2008; Estella-Hermoso de Mendoza et al., 2008). Zeta potential of LN, a parameter that indicates the stability of colloid dispersions, was not affected by the incorporation of edelfosine (−28.46 for B-LN and −27.07 mV for ET-LN). In general, zeta potential values of −30 mV are enough for suitable stabilization (Estella-Hermoso de Mendoza et al., 2009c). Therefore, in our case the zeta-potential values obtained indicate that the formulations presented a good physical stability and that the LN generated would not induce cell membrane instability (Estella-Hermoso de Mendoza et al., 2009c; Müller, 1996). The LN obtained showed good encapsulation efficiency of 58.80%, presenting a drug loading of 30 μg ET per mg of formulation.

3.2. ET anti-tumor effect is enhanced when drug is encapsulated in LN

As the encapsulation procedure may modify the anti-tumor potential of ET, we analyzed the effectiveness of the ET-LN in MCF7 breast cancer cells. In order to evaluate the cytotoxic potential of the encapsulated drug, MCF7 cells were cultured for 72 h in the presence of growing concentrations of ET or equivalent concentrations of ET-LN. B-LN were also tested as control. Cytotoxicity was assessed by the comparison of IC_{50} values. The optimized ET-LN were effective in inhibiting the proliferation of MCF7 breast cancer

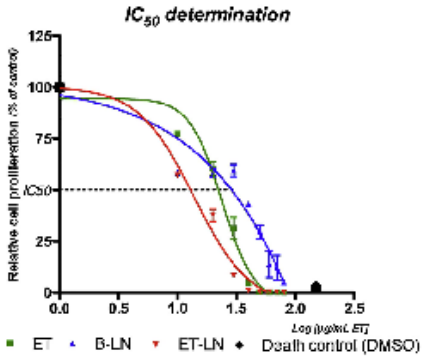

Fig. 1. MTT assay was used to determine the dose–response curve in MCF7 cells at 72 h of incubation with different doses of free edelfosine (ET), unloaded (B-LN) or drug-loaded (ET-LN). IC_{50} values were calculated using the sigmoidal dose–response function. DMSO-treated cells were included as positive control of cell death.

Table 1
Physicochemical characteristics (mean particle size, polydispersity index, zeta potential, encapsulation efficiency and drug loading) of solid lipid nanoparticle formulations prepared by the hot homogenization method followed by high shear homogenization and ultrasonication.

Lipid nanoparticle[a]	Size ± SD (nm)	Polydispersity index ± SD	Zeta potential	Encapsulation efficiency ± SD (%)	Drug loading ± SD ([μg edelfosine]/[mg formulation])
B-LN (n = 17)	112.74 ± 2.98	0.251 ± 0.017	−28.46 ± 6.62	–	–
ET-LN (n = 16)	133.787 ± 17.65	0.246 ± 0.017	−27.07 ± 3.32	58.803 ± 10.948	27.53 ± 4.56

[a] BLN, unloaded nanoparticles; ET-LN, edelfosine-loaded nanoparticles.

cell line at an IC_{50} concentration of 12.9 (±2.23) μg/mL, whereas the corresponding IC_{50} values of the free drug and B-LN were 17.8 (±4.06) and 28.7 (±8.08) μg/mL, respectively (Fig. 1).

The efficacy of the drug may also be assessed by visualizing changes in the appearance and size of cells after being incubated with the different treatments. Optical inspection of the MCF7 cell cultures by light microscopy revealed morphological changes in MCF7 after the treatment with either ET or ET-LN. Compared with untreated controls and with cells incubated with B-LN, treated cell cultures showed expression of intracellular vesicles (indicated with arrows in Fig. 2A) and presented distorted and detached rounded cells that had shrunk. These signs are indicative of cell death (Kroemer et al., 2009). In fact, the percentage of viable cells was dramatically diminished in ET-LN-treated cultures in comparison to cells treated with B-LN. Moreover, the observed decrease was significantly higher than that of the cells treated with the free drug, confirming that the encapsulation strategy increased the cytotoxic potential of ET (Fig. 2B). This effect was time-dependent and reached statistical significance after 72 h of incubation.

Hence the developed ET-LN formulation maintained the antitumor activity of ET; moreover, ET-LN were 1.37 times more effective in inducing cell death in MCF7 cells than the free drug, and produced a remarkable decrease in cell viability.

Our results are in accordance with previously reported work, in which the cytotoxic effect of ET against other tumor types was found to be significantly improved when encapsulated in LN (Estella-Hermoso de Mendoza et al., 2009b, 2011; Lasa-Saracibar et al., 2013), thereby giving additional support to the usefulness of encapsulating the ET in LN.

3.3. Cell cycle arrest and induction of apoptotic mechanisms by ET and ET-LN in MCF7 breast cancer cells

The aforementioned decrease in cell viability may be caused by an abnormality in the cell cycle or in the cell growth. Therefore, MCF7 cells were stained with PI and subsequently cell cycle status was examined by flow cytometry (Fig. 3A). In cells grown either with ET or ET-LN, a cell accumulation in G1 stage, with a concomitant reduction of cells in S phase, was detected (Fig. 3B). It has been reported that ET-treated cells may accumulate in the G0/G1 and G2/M phases of the cell cycle, due to an inhibition of cytokinesis (Mollinedo et al., 2004; Pushkareva et al., 1999),

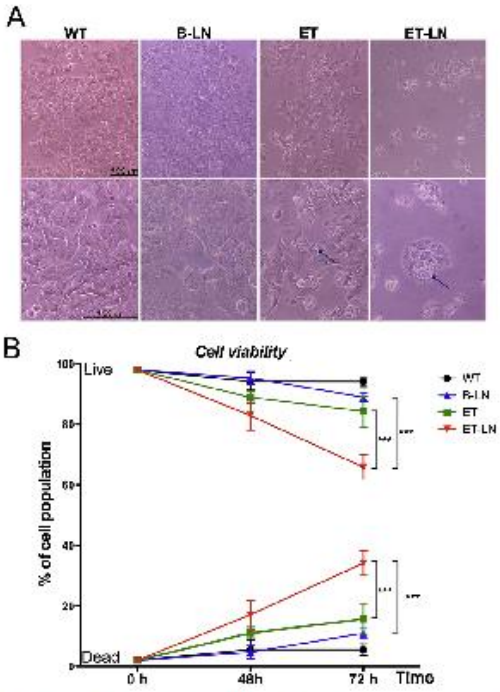

Fig. 2. Cytotoxic effects in MCF-7 cells after treatment with 20 μg/mL of edelfosine (ET) or equivalent concentrations ET-loaded nanoparticles (ET-LN). B-LN were also tested as control. (A) Light microscope images revealed that at 48 h treated groups showed unattached and distorted cells and the expression of intracellular vesicles (indicated with arrows). (B) Trypan blue assay was used to determine cell viability of treated cells at 48 and 72 h. Untreated (WT) cells were included as control. ***$p < 0.001$ vs. corresponding ET group by two-way ANOVA (Bonferroni post-test).

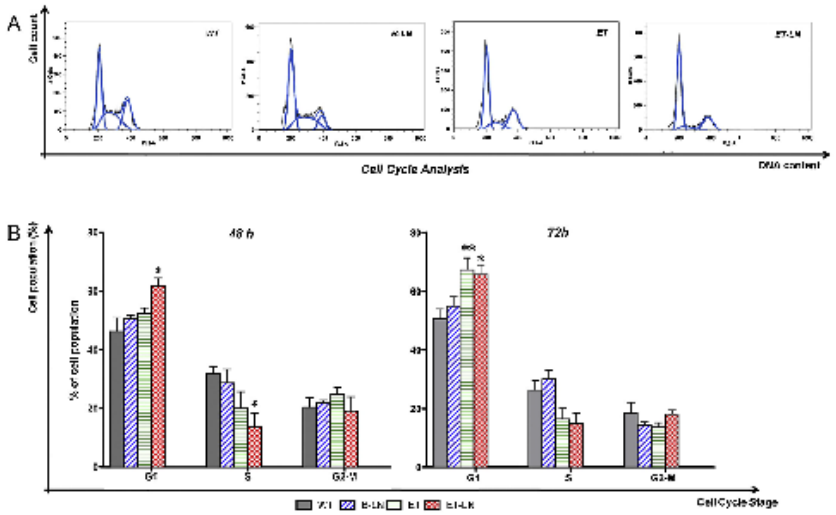

Fig. 3. Free and nanoencapsulated drug effect in cell cycle after 48 and 72 h of incubation. Cells were treated with medium, blank-LN, free ET and drug-loaded LN at a dose equivalent to 20 μg/mL of edelfosine (ET). (A) Cell cytometry images of treated cells. (B) Quantification of cell cycle peaks.
*$p < 0.05$; **$p < 0.01$ vs. control by two-way ANOVA (Bonferroni post-test).

although the cell cycle blockage induced by ET has more commonly been detected at the G2/M stage (Lasa-Saracíbar et al., 2013; Mollinedo et al., 2004; Nieto-Miguel et al., 2007). This suggests that ET may provoke cell cycle arrest by influencing diverse molecular pathways, and the phase where the cell cycle is blocked would depend on the cell signaling routes characteristic of each cancer cell type.

On the other hand, the aforementioned cell cycle arrest may reflect defective cell growth or an induction of cell death mechanisms caused by the effects that ET exerts in tumor cells. Moreover, the disturbance of phospholipid metabolism and the interference in the membrane interactions with signaling molecules caused by ET may induce cellular stress, deregulation of apoptotic pathways, growth inhibition and cell cycle arrest and apoptosis (Mollinedo et al., 2010b; Van Blitterswijk and Verheij, 2008; Van der Luit et al., 2007). In addition, ET has been described to induce apoptosis through the aggregation of Fas/CD95 in clustered rafts (Gajate et al., 2009; Gajate and Mollinedo, 2007). Accordingly, we analyzed the apoptotic status of treated-MCF7 cultures. Firstly, the percentage of cells in the sub-G1 region (hypodiploidy) in cell cycle analysis was determined by staining the cells with PI. As shown in Fig. 4A, the sub-G1 subset of MCF7 cells exhibited a strong increase in cells treated with either ET or ET-LN after 72 h of treatment. Along the lines of previous reported analyses of sub-G1 of ET-LN in several cancer malignancies (Mollinedo et al., 2010b), our data indicate that MCF7 undergoes apoptosis in the presence of ET in the culture media. However, the extensive DNA fragmentation and loss of DNA fragments is not exclusive to apoptotic death. Besides, the sub-G1 peak may represent apoptotic cells, as well as nuclear fragments, clusters of chromosomes, micronuclei or nuclei with normal DNA content but altered chromatin structure and diminished accessibility of fluorochrome to DNA (Darzynkiewicz et al., 2001; Riccardi and Nicoletti, 2006).

The aforementioned effect may dim the DNA degradation caused by apoptosis. Consequently, to further characterize this cell death mechanism, cells were treated in identical conditions, stained with annexin V-FITC and PI dyes and subsequently analyzed by flow cytometry to determine the percentage of viable, early apoptotic, and late apoptotic/necrotic sub-populations in MCF7-treated cultures (Fig. 4B and C). As is shown in Fig. 4C, the early apoptosis and the late apoptosis/necrosis/death cell subsets were increased in treated cells in comparison to their corresponding control. This induction was detected even with lower concentrations of the treatments (data not shown), and was statistically significant after 48 and 72 h of incubation with 20 μg/mL of ET or equivalent concentrations of ET-LN. Interestingly, the induction of cell death was stronger in ET-LN than in cells grown in the presence of the free drug, compared to their equivalent B-LN controls. In particular, the cell late apoptosis/necrosis/death subset was highly increased in cells grown in the presence of 20 μg/mL of ET-LN for 72 h. The results are in agreement with those recently reported by Lasa-Saracíbar et al. in leukemic cells when treated with the free drug and ET-LN (Lasa-Saracíbar et al., 2013). Accordingly, our results show that both ET and ET-LN displayed a pro-apoptotic activity against MCF7 breast cancer cells in a time- and dose-dependent manner. This effect was probably caused by the characteristic controlled drug release of LN. In addition, there was a substantial increment in the population of cells that underwent apoptosis in the presence of ET-LN in comparison to the free drug treatment.

The results presented indicate that the cytotoxic effect of ET on MCF7 was considerably enhanced when the drug was entrapped in LN. Moreover, although ET was able to promote both an apoptotic

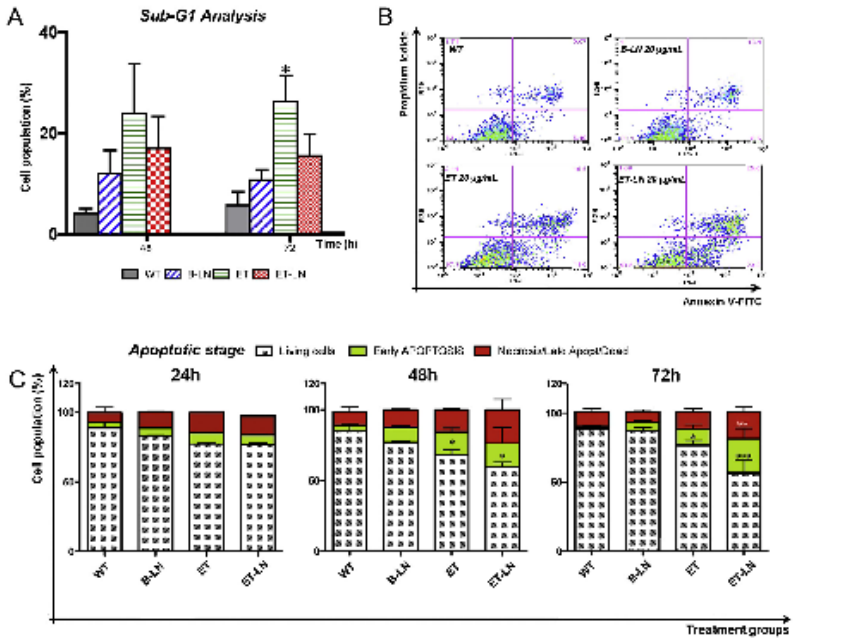

Fig. 4. Apoptosis analysis of MCF7 after incubation with medium (WT), blank-LN (B-LN), free edelfosine (ET) and drug-loaded LN (ET-LN) at a dose equivalent of 20 μg/mL of edelfosine. Apoptosis was firstly assessed with quantification of DNA content in cells and determination of sub-G1 cell subset (A) and subsequently analyzed with flow cytometry (B). *$p < 0.05$ vs. control with Kruskall–Wallis test (Dunns post hoc test) for sub-G1 analysis, *$p < 0.05$; **$p < 0.01$; ***$p < 0.001$ vs. B-LN control by two-way ANOVA (Bonferroni post-test).

and a cytostatic effect in MCF7, such anti-tumor effects were considerably enhanced in ET-LN-treated cells.

4. Conclusions

The data presented in this paper provide evidence that entrapping ET in LN entails an improvement in its efficacy when treating MCF7 breast cancer cells, leading to a moderate cell cycle arrest. Besides, ET-LN induced apoptosis in a time- and dose-dependent manner to a greater extent in comparison with the treatment using the free drug, suggesting that encapsulating ET in LN is essential to improve the efficacy of the drug. Molecular cell death mechanisms must be studied in greater depth in order to further characterize the induction process by which ET-LN exert their anti-tumor effect.

Conflict of interest

The authors have no other relevant affiliations or financial involvement with any organization or entity with a financial interest in or financial conflict with the subject matter or materials discussed in the manuscript apart from those disclosed.

Acknowledgements

Caja Navarra Foundation, Ibercaja, University of Navarra (FUN), the Government of Navarra, Department of Health (ref: 63/09, "Ortiz de Landázuri" fellowship) and the Spanish Ministry of Science and Innovation (SAF2010-15547). This work has been carried out in the framework of the COST Action TD1004.

References

Ahmad, I., Filep, J.J., Franklin, J.C., Janoff, A.S., Masters, G.R., Pattassery, J., Peters, A., Schupsky, J.J., Zha, Y., Mayhew, E., 1997. Enhanced therapeutic effects of liposome-associated 1-O-octadecyl-2-O-methyl-sn-glycero-3-phosphocholine. Cancer Res. 57, 1915–1921.

Anton, N., Benoit, J.P., Saulnier, P., 2008. Design and production of nanoparticles formulated from nano-emulsion templates—a review. J. Control. Release 128, 185–199.

Brannon-Peppas, L., Blanchette, J.O., 2004. Nanoparticle and targeted systems for cancer therapy. Adv. Drug Deliv. Rev. 56, 1649–1659.

Charman, W.N., Stella, V.J. (Eds.), 1992. Lymphatic Transport of Drugs. CRC Press, Boca Raton.

Clogston, J.D., Patri, A.K., 2011. Zeta potential measurement. Methods Mol. Biol. 697, 63–70.

Darzynkiewicz, Z., Bedner, E., Smolewski, P., 2001. Flow cytometry in analysis of cell cycle and apoptosis. Semin. Hematol. 38, 179–193.

Estella-Hermoso de Mendoza, A., Campanero, M.A., de la Iglesia-Vicente, J., Gajate, C., Mollinedo, F., Blanco-Prieto, M.J., 2009a. Antitumor alkyl ether lipid edelfosine: tissue distribution and pharmacokinetic behavior in healthy and tumor-bearing immunosuppressed mice. Clin. Cancer Res. 15, 858–864.

Estella-Hermoso de Mendoza, A., Campanero, M.A., Lana, H., Villa-Pulgarin, J.A., de la Iglesia-Vicente, J., Mollinedo, F., Blanco-Prieto, M.J., 2012. Complete inhibition of extranodal dissemination of lymphoma by edelfosine-loaded lipid nanoparticles. Nanomedicine (Lond) 7, 679–690.

Estella-Hermoso de Mendoza, A., Campanero, M.A., Mollinedo, F., Blanco-Prieto, M.J., 2009b. Comparative study of A HPLC–MS assay versus an UHPLC-MS/MS for anti-tumoral alkyl lysophospholipid edelfosine determination in both biological samples and in lipid nanoparticulate systems. J. Chromatogr. B: Analyt. Technol. Biomed. Life Sci. 877, 4035–4041.

Estella-Hermoso de Mendoza, A., Campanero, M.A., Mollinedo, F., Blanco-Prieto, M.J., 2009c. Lipid nanomedicines for anticancer drug therapy. J. Biomed. Nanotechnol. 5, 323–343.

Estella-Hermoso de Mendoza, A., Preat, V., Mollinedo, F., Blanco-Prieto, M.J., 2011. In vitro and in vivo efficacy of edelfosine-loaded lipid nanoparticles against glioma. J. Control. Release 156, 421–426.

Estella-Hermoso de Mendoza, A., Rayo, M., Mollinedo, F., Blanco-Prieto, M.J., 2008. Lipid nanoparticles for alkyl lysophospholipid edelfosine encapsulation: development and in vitro characterization. Eur. J. Pharm. Biopharm. 68, 207–213.

Gajate, C., Gonzalez-Camacho, F., Mollinedo, F., 2009. Involvement of raft aggregates enriched in Fas/CD95 death-inducing signaling complex in the antileukemic action of edelfosine in Jurkat cells. PLoS ONE 4, e5044.

Gajate, C., Mollinedo, F., 2007. Edelfosine and perifosine induce selective apoptosis in multiple myeloma by recruitment of death receptors and downstream signaling molecules into lipid rafts. Blood 109, 711–719.

Gajate, C., Santos-Beneit, A.M., Macho, A., Lazaro, M., Hernandez-De Rojas, A., Modolell, M., Munoz, E., Mollinedo, F., 2000. Involvement of mitochondria and caspase-3 in ET-18-OCH(3)-induced apoptosis of human leukemic cells. Int. J. Cancer 86, 208–218.

Houlihan, W.J., Lohmeyer, M., Workman, P., Cheon, S.H., 1995. Phospholipid antitumor agents. Med. Res. Rev. 15, 157–223.

Kaszuba, M., Corbett, J., Watson, F.M., Jones, A., 2010. High-concentration zeta potential measurements using light-scattering techniques. Philos. Transact. A Math. Phys. Eng. Sci. 368, 4439–4451.

Kroemer, G., Galluzzi, L., Vandenabeele, P., Abrams, J., Alnemri, E.S., Baehrecke, E.H., Blagosklonny, M.V., El-Deiry, W.S., Golstein, P., Green, D.R., Hengartner, M., Knight, R.A., Kumar, S., Lipton, S.A., Malorni, W., Nunez, G., Peter, M.E., Tschopp, J., Yuan, J., Piacentini, M., Zhivotovsky, B., Melino, G., 2009. Classification of cell death: recommendations of the nomenclature committee on cell death 2009. Cell Death Differ. 16, 3–11.

Lasa-Saracibar, B., Estella-Hermoso de Mendoza, A., Guada, M., Dios-Vieitez, C., Blanco-Prieto, M.J., 2012. Lipid nanoparticles for cancer therapy: state of the art and future prospects. Expert Opin. Drug Deliv. 9, 1245–1261.

Lasa-Saracibar, B., Mendoza, A.E., Mollinedo, F., Odero, M.D., Blanco-Prieto, M.J., 2013. Edelfosine lipid nanosystems overcome drug resistance in leukemic cell lines. Cancer Lett., http://dx.doi.org/10.1016/j.canlet.2013.01.018 (in press), [Epub ahead of print].

Lu, X., Kang, Y., 2007. Organotropism of breast cancer metastasis. J. Mammary Gland Biol. Neoplasia 12, 153–162.

Mollinedo, F., de la Iglesia-Vicente, J., Gajate, C., Estella-Hermoso de Mendoza, A., Villa-Pulgarin, J.A., Campanero, M.A., Blanco-Prieto, M.J., 2010a. Lipid raft-targeted therapy in multiple myeloma. Oncogene 29, 3748–3757.

Mollinedo, F., de la Iglesia-Vicente, J., Gajate, C., Estella-Hermoso de Mendoza, A., Villa-Pulgarin, J.A., de Frias, M., Roue, G., Gil, J., Colomer, D., Campanero, M.A., Blanco-Prieto, M.J., 2010b. In vitro and in vivo selective antitumor activity of Edelfosine against mantle cell lymphoma and chronic lymphocytic leukemia involving lipid rafts. Clin. Cancer Res. 16, 2046–2054.

Mollinedo, F., Gajate, C., Martin-Santamaria, S., Gago, F., 2004. ET-18-OCH3 (edelfosine): a selective antitumour lipid targeting apoptosis through intracellular activation of Fas/CD95 death receptor. Curr. Med. Chem. 11, 3163–3184.

Müller, R.H., 1996. Zetapotential und Partikelladung in der Laborpraxis-Einführung in die Theorie, praktische Meßdurchführung. Dateninterpretation. Wissenschaftliche, Verlagsgesellschaft, Stuttgart, pp. 37.

Munder, P.G., Westphal, O., 1990. Antitumoral and other biomedical activities of synthetic ether lysophospholipids. Chem. Immunol. 49, 206–235.

Na, H.K., Surh, Y.J., 2008. The antitumor ether lipid edelfosine (ET-18-O-CH3) induces apoptosis in H-ras transformed human breast epithelial cells: by blocking ERK1/2 and p38 mitogen-activated protein kinases as potential targets. Asia Pac. J. Clin. Nutr. 17, 204–207.

Nieto-Miguel, T., Fonteriz, R.I., Vay, L., Gajate, C., Lopez-Hernandez, S., Mollinedo, F., 2007. Endoplasmic reticulum stress in the proapoptotic action of edelfosine in solid tumor cells. Cancer Res. 67, 10368–10378.

Peer, D., Karp, J.M., Hong, S., Farokhzad, O.C., Margalit, R., Langer, R., 2007. Nanocarriers as an emerging platform for cancer therapy. Nat. Nanotechnol. 2, 751–760.

Pushkareva, M.Y., Janoff, A.S., Mayhew, E., 1999. Inhibition of cell division but not nuclear division by 1-O-octadecyl-2-O-methyl-Sn-glycero-3-phosphocholine. Cell Biol. Int. 23, 817–828.

Riccardi, C., Nicoletti, I., 2006. Analysis of apoptosis by propidium iodide staining and flow cytometry. Nat. Protoc. 1, 1458–1461.

Shaffer, S.H., Williams, C.L., 2003. Non-small and small cell lung carcinoma cell lines exhibit cell type-specific sensitivity to edelfosine-induced cell death and different cell line-specific responses to edelfosine treatment. Int. J. Oncol. 23, 389–400.

Siegel, R., Naishadham, D., Jemal, A., 2013. Cancer statistics, 2013. CA Cancer J. Clin. 63, 11–30.

Torchilin, V., 2011. Tumor delivery of macromolecular drugs based on the EPR effect. Adv. Drug Deliv. Rev. 63, 131–135.

Van Blitterswijk, W.J., Verheij, M., 2008. Anticancer alkylphospholipids: mechanisms of action, cellular sensitivity and resistance, and clinical prospects. Curr. Pharm. Des. 14, 2061–2074.

Van der Luit, A.H., Vink, S.R., Klarenbeek, J.B., Perrissoud, D., Solary, E., Verheij, M., van Blitterswijk, W.J., 2007. A new class of anticancer alkylphospholipids uses lipid rafts as membrane gateways to induce apoptosis in lymphoma cells. Mol. Cancer Ther. 6, 2337–2345.

Varshosaz, J., Minayian, M., Mozaen, E., 2010. Enhancement of oral bioavailability of pentoxifylline by solid lipid nanoparticles. J. Liposome Res. 20, 115–123.

Wagner, B.A., Buettner, G.R., Oberley, L.W., Burns, C.P., 1998. Sensitivity of K562 and HL-60 cells to edelfosine, an ether lipid drug, correlates with production of reactive oxygen species. Cancer Res. 58, 2809–2816.

Weigelt, B., Reis-Filho, J.S., 2009. Histological and molecular types of breast cancer: is there a unifying taxonomy? Nat. Rev. Clin. Oncol. 6, 718–730.

Wellings, S.R., Jensen, H.M., 1973. On the origin and progression of ductal carcinoma in the human breast. J. Natl. Cancer Inst. 50, 1111–1118.

Wellings, S.R., Jensen, H.M., Marcum, R.G., 1975. An atlas of subgross pathology of the human breast with special reference to possible precancerous lesions. J. Natl. Cancer Inst. 55, 231–273.

Zimmermann, E., Muller, R.H., Mader, K., 2000. Influence of different parameters on reconstitution of lyophilized SLN. Int. J. Pharm. 196, 211–213.